

LONDON
SCHOOL of
HYGIENE
& TROPICAL
MEDICINE



Mathematical Modelling of Cross-protection Between Respiratory Viruses

Naomi Ruth Waterlow

Thesis submitted in accordance with the requirements for the degree of
Doctor of Philosophy
of the
University of London
SEPTEMBER 2021

Department of Infectious Disease Epidemiology

Faculty of Epidemiology and Population Health

LONDON SCHOOL OF HYGIENE & TROPICAL MEDICINE

Funded by the Medical Research Council (grant number MR/N013638/1)

Research group affiliation(s):
Centre for the Mathematical Modelling of Infectious Diseases

Declaration

Statement of Own Work

I, Naomi Waterlow, confirm that the work presented in this thesis is my own. Where information has been derived from other sources, this has been indicated in the thesis. I have read and understood the school's definition of plagiarism and cheating given in the Research Degrees Handbook.

Naomi Waterlow,



September 2021

Abstract

Respiratory viruses cause substantial health and economic burdens. These viruses circulate concurrently, and changes in host susceptibility brought about by infection by one virus has the potential to change the transmission dynamics of another. Understanding the effects of such cross-protection between viruses at a population level can inform public health policies. Current evidence for cross-protection between these viruses mainly comes from population level shifts in dynamics, which cannot assess causation, and from small-scale biological experiments. I use mathematical modelling to research cross-protection between respiratory viruses, as these methods allow for testing of the mechanism.

Initially, I develop a two-pathogen interaction model parameterised to simulate influenza and RSV epidemiology in the UK. Using a surveillance-like stochastic observation process I generate a range of possible trajectories, and then back-infer the parameters using Markov Chain Monte Carlo. I found that the strength and duration of influenza and RSV interaction could be estimated well; however, the robustness of inference does decline towards the extremes of the plausible parameter ranges, with misleading results.

Next, I use parallel tempering to fit an adapted two-pathogen model to a unique dataset from Vietnam. I show that the population level-dynamics of influenza and RSV circulation support either moderate or no cross-protection. However, I add evidence that co-infection increases the rate of reporting. The benefits of limiting severe co-infection by vaccination in this setting may therefore outweigh the increased transmission that occurs due to cross-protection between the viruses.

Finally, I use coronavirus surveillance data from England and Wales to estimate key seasonal coronavirus (HCoV) parameters, and I use these estimates to investigate age-specific susceptibility to SARS-CoV-2, varying the interaction assumption. I show that while cross-protection between HCoV and SARS-CoV-2 may contribute to the age distribution, it is insufficient to explain the observed reduced susceptibility of children.

Collectively, the research in this thesis demonstrates that surveillance data and mathematical models can be used to study respiratory viral interactions. It implies that while models can be used to study this phenomenon, stochasticity can obscure results. The research also alleviates concerns that vaccination against influenza or RSV may have a detrimental impact on the other virus, due to interaction, although this must be investigated further to understand the generalisability of the results to other settings. Finally, the research implies that other factors must influence susceptibility

to coronaviruses, and the observed shifting of epidemic peaks that has been hypothesised to be a result of respiratory viral interaction.

Acknowledgments

I have been supported a great deal throughout this PhD by many people. Firstly, I thank my supervisors Dr Rosalind M Eggo and Dr Stefan Flasche, for being the best supervisory team imaginable. They have provided constant support (even during the pandemic), insightful discussions, and amazing opportunities. I would also like to thank the collaborators I have had during the work in this thesis. Dr Richard Pebody for his support at Public Health England, Dr Edwin van Leewuen for his help during projects that went ahead, as well as those that had to be stopped. Dr Lay-Myint Yoshida and his team, for the great data they provided. Dr Amanda Minter for her help during her time at LSHTM. Dr Adam Kucharski for organising my placement for me, and the collaborators in the Dominican Republic for hosting me, despite the unfortunate timings. Dr Punam Mangtani for being on the advisory board. Thank you also to the MRC London Intercollegiate Doctoral Training Partnership Studentship for funding this project, and to Lara, Jenny, and Lauren for dealing with the administration that has made this research possible.

I am inordinately grateful to have been able to study for this PhD at the Centre for Mathematical Modelling of Infectious Diseases (CMMID) at LSHTM. I would like to thank everyone involved with the centre, who makes / has made it an exciting, compelling, and supportive place to work. For the countless people who are always on hand to provide coding help (especially Carl), the multitudes of people up for a coffee and conversation and the inspiring science and seminars that members contribute to.

I also have had the great fortune to have been in LG22, an office full of talented students who have helped me endlessly along the way. Thank you Ali, for the statistical and emotional support, never-ending snacks, squash games and general nonsense that comes with sharing an office with you. Thank you Alexis, for being such a great ECR co-lead, scintillating conversation and R brilliance! To Richard, for challenging me; to Charlotte for the cheerful attitude and cake; to Ellie for listening to me grumble, to Chris, James, Akira, Sophie, Isobel, Rebecca... to every single person who contributed to the great office environment – thank you.

I have been extremely lucky to have been surrounded and supported by my friends throughout this PhD. Thank you Orlagh, for the constant tea breaks, stats help and for ‘surviving’ with me. Thank you Kelly and Emily, for the drinks, fun and dog chats. To the Newnham girls, Aria, Emilia and Lior who have helped me develop my passion for science over these 10 years and always been on hand with a glass of wine. To ‘dinner clan’ for the food and relaxation, Vicki and Georgia for the games nights,

Laura for Tuesday walks and great breakfast chat and everyone else who has supported me and helped me relax and laugh.

I have had the opportunity to do this PhD because of the amazing support of my family. To Mum and Dad, thank you for supporting me, giving me opportunities, trusting me and always being there for me. Thank you Sam, for helping me develop as a better human. To my wider family for their guidance and love, especially Grandpa B for sponsoring my masters and being such a great inspiration (getting a PhD in your seventies!). To Pauline, for your care (and food!) over the years. Thanks also to Oscar for giving me playful breaks, and not eating my laptop!

And finally, thank you Jack, for your blind faith that I can do anything, no matter the challenge.

Table of Contents

Declaration	2
Abstract	3
Acknowledgments	5
List of Figures	11
List of Tables	13
Acronyms	14
1 Introduction	16
1.1 Background	16
1.1.1 Motivation for study.....	16
1.1.2 Case study viruses.....	17
1.1.2.1 Influenza	17
1.1.2.2 RSV	20
1.1.2.3 Coronaviruses	21
1.1.3 Viral Interaction	23
1.1.4 Short term, non-specific interaction.....	23
1.1.5 Long term, specific interaction	28
1.1.6 Mathematical Modelling approaches.....	30
1.1.7 Fitting models	35
1.1.8 Summary Motivation	38
1.2 Aims	38
1.3 Thesis Structure	39
1.4 References	41
2 Chapter 2: Competition between RSV and influenza: Limits of modelling inference from surveillance data	56
2.1 Research Paper cover sheet	56
2.2 Bridging section	58
2.3 Abstract and Author Summary	60
2.4 Introduction	61
2.5 Methods	62
2.5.1 Model Structure.....	62
2.5.2 Simulated data.....	64
2.5.3 Parameter estimation.....	66
2.6 Results	67
2.6.1 Epidemic profiles	67
2.6.2 Correlation Analysis.....	68
2.6.3 Inferring the strength of cross-protection (σ)	69
2.6.4 Inferring the duration of cross-protection ($1/\rho$).....	69

2.6.5	Variation between replicates.....	70
2.7	Discussion.....	71
2.8	Acknowledgments.....	75
2.9	References.....	76
3	<i>Chapter 3 - Evidence for Influenza and RSV interaction from 10 years of enhanced surveillance in Nha Trang, Vietnam, a modelling study.....</i>	81
3.1	Research Paper Cover Sheet.....	81
3.2	Bridging Section.....	83
3.3	Title page and abstract.....	84
3.4	Introduction.....	85
3.5	Methods.....	86
3.5.1	Study population.....	86
3.5.2	Data analysis.....	87
3.5.3	Model.....	88
3.5.4	Likelihood.....	90
3.5.5	Inference.....	90
3.5.6	Vaccination.....	91
3.5.7	Sensitivity analyses.....	91
3.5.8	Ethics.....	91
3.6	Results.....	91
3.6.1	Descriptive Analysis.....	91
3.6.2	Model inference.....	93
3.6.3	Sensitivity.....	95
3.7	Discussion.....	95
3.8	References.....	98
4	<i>Chapter 4 - How immunity from and interaction with seasonal coronaviruses can shape SARS-CoV-2 epidemiology.....</i>	103
4.1	Research Paper Cover Sheet.....	103
4.2	Bridging Section.....	105
4.3	Title page and abstract.....	106
4.4	Introduction.....	107
4.5	Results.....	108
4.5.1	Seasonal HCoV and SARS-CoV-2 epidemic data.....	108
4.5.2	Seasonal HCoVs have an R_0 of 5.9.....	109
4.5.3	Cross-protection from seasonal HCoVs is not sufficient to explain age-specific patterns of SARS-CoV-2 infection.....	110
4.5.4	Future SARS-CoV2 epidemiology could be shaped by coronavirus interactions.....	112

4.6	Discussion	113
4.7	Materials and Methods	118
4.7.1	Data	118
4.7.2	Cross-protection Model.....	119
4.7.3	Inferring seasonal HCoV parameters.....	121
4.7.4	Simulating SARS-CoV-2 with a range of strengths of cross-protection	122
4.7.5	Projecting future dynamics of SARS-CoV-2 and Seasonal HCoVs	123
4.8	References	124
5	Discussion	131
5.1	Summary of Findings	131
5.1.1	Competition between RSV and influenza: Limits of modelling inference from surveillance data	131
5.1.2	How cross-protection between Influenza and Respiratory Syncytial virus shapes paediatric hospital admissions in Nha Trang, Vietnam.....	132
5.1.3	How immunity from and interaction with seasonal coronaviruses can shape SARS-CoV-2 epidemiology	133
5.2	Strengths and Limitations	133
5.2.1	Strengths.....	133
5.2.2	Limitations	136
5.3	Implications and future work	140
5.4	Concluding Remarks	143
5.5	References	144
6	Appendices	149
	Appendix A Supplementary material for Chapter 2	149
A.1	Model equations	150
A.2	Full model Diagram	152
A.3	R_0 calculation.....	152
A.4	Susceptibility to RSV.....	153
A.5	Generating simulations	153
A.6	Sensitivity of introductions	155
A.7	Priors and parameter limits	157
A.8	Simulated data total case numbers	158
A.9	Individuals within infectious compartments.....	159
A.10	Parameter correlations	162
A.11	Convergence	170
A.12	Individual Simulation Analysis.....	171
A.13	Varying the R_0	199
A.14	References	204
	Appendix B Supplementary material for Chapter 3	205
B.1	Estimated influenza attack rate	206

B.2	Data.....	206
B.3	Model equations.....	207
B.4	R_0 equations.....	209
B.5	Susceptibility to RSV.....	210
B.6	Susceptibility to Influenza.....	210
B.7	Parallel tempering.....	211
B.8	Attack Rates.....	213
B.9	Sensitivity to severity of dual infected cases.....	213
B.10	Prior Sensitivity.....	214
B.11	Modelled correlation.....	215
B.12	References.....	217
Appendix C	Supplementary material for Chapter 4.....	218
C.1	Data.....	219
C.2	Model equations.....	220
C.3	R_0 calculations.....	223
C.4	Parallel Tempering.....	226
C.5	Attack Rates.....	229
C.6	Simulating lockdown.....	230
C.7	SARS-CoV-2 death simulations.....	231
C.8	Sensitivity - Duration of immunity.....	231
C.9	Sensitivity - Excluding 2014 season.....	232
C.10	Sensitivity - Only beta-coronaviruses.....	234
C.11	Comparison with existing estimates.....	236
C.12	References.....	238
Appendix D	LSHTM Ethics for influenza and RSV.....	239
Appendix E	Local Nha Trang Ethics.....	240
Appendix F	LSHTM Ethics for coronaviruses.....	241

List of Figures

Excludes Appendices

Figure 1-1: Reports of coronavirus (excluding SARS-CoV-2), influenza and Respiratory Syncytial Virus (RSV) reported by Public Health England (PHE) from mid 2014 to early 2020. Data extracted from PHE laboratory reports ⁴³	19
Figure 1-2: Simplified schema depicting different potential mechanisms of interaction between viruses.....	25
Figure 1-3: Susceptible (S) – Infectious (I) – Recovered (R) compartmental model. Parameters are the transmission rate (β) and the infectious period ($1/\omega$)	31
Figure 1-4: Pseudocode for an MCMC sampler with a symmetrical proposal distribution.....	37
Figure 2-1. Model diagram for RSV and Influenza (INF). Individuals could be either Susceptible (S), Infected, (I), Protected (P) or Recovered (R) to either virus. Following infection, (which occurred at rate $\lambda_{RSV, i}$ and $\lambda_{INF, i}$), recovery occurred at a constant rate (γ_{RSV} and γ_{INF}), and the population entered the P state. Here they are immune to the virus they were infected by and protected to a varying extent (σ) against infection from the second virus. This protection waned at rate ρ , and the population entered the R compartment. In the R compartment the population was immune to the virus it was infected by, but not the other virus. We ran the model for one season and compartments $I_{RSV, i}P_{INF, i}$ and $I_{RSV, i}R_{INF, i}$, were combined, and $P_{RSV, i}I_{INF, i}$ and $R_{RSV, i}I_{INF, i}$ were combined, because they are effectively identical. Parameters were: age susceptibility to RSV infection (τ_i). For clarity, age structure is given only by the subscript (i), for further details see supplement section 2.63	
Figure 2-2: Mean weekly incidence of observed cases in under 5s (sum of age groups 0-1 and 2-4) from simulations with A) varying σ values and a fixed protection duration of 10 days ($\rho=0.1$), and B) varying ρ values, and a fixed σ of 0.5. Simulations were run and sampled 1000 times for each parameter set and the shaded windows are the 95% quantiles for each week. In both A and B the top panel shows the observed cases for RSV, and the lower panel the cases for Influenza.	67
Figure 2-3. A) Mean Pearson correlation coefficient between parameters. B) Correlation coefficient between σ (strength of cross-protection) and Δ_{INF} (start day of influenza). This is shown for 1 simulation, but the patterns were similar for all (Supplementary Section 12)	68
Figure 2-4. A) Estimated σ values for simulations with different σ and ρ values. Median value and 95% CI are shown. The black line is the simulated (true) value of σ in each case. B) Imprecision of σ estimates calculated as the 95% quantile range. C) Inaccuracy of the σ estimates, calculated as the difference between the posterior median and the true value.	69
Figure 2-5. A) Estimated $1/\rho$ values for simulations with different σ and ρ . Lines represent 95% quantiles of the posterior sample and the circle represents the median value. The black line shows the true $1/\rho$ value in each case. B) Imprecision of ρ estimates calculated as the 95% quantile range. C) Inaccuracy of the ρ estimates, calculated as the difference between the posterior median and the true value.....	70
Figure 2-6: Proportion of simulations where the true value of σ (A) and ρ (B) was included in the 95% CI of the posterior estimate.....	71

Figure 3-1: Data. A) Weekly reported infections of children under 5 years old infected with influenza and RSV over the study period. B) Total number of cases reported over the entire study period by age group and virus. C) Percentage of reported cases by week of the year for RSV and Influenza. The numerator is the weekly number of either influenza or RSV cases reported and the denominator the total number of influenza or RSV cases reported over the relevant year. The thick lines show the combined total reported across all years, the semi-transparent lines show the 4-week moving average per year. 92

Figure 3-2: Model Fit: Black lines are the data, coloured lines are the 95% CrI posterior predictive interval. Panels show the fit by age group and Virus. 93

Figure 3-3 A) Posterior estimates for parameters sigma and rho, and the corresponding likelihood values. Colour is split by sigma value of 0.2. B) Goodness of Fit: Observed cases by season against Modelled cases by season by virus and age group. The black line indicates the same value 94

Figure 3-4: Vaccination scenarios: Number of cases modelled over all seasons, with different vaccination assumptions. Dots represent the median and lines the 95% CrI..... 95

Figure 4-1: Seasonal HCoV Fit. A) Model fit for seasonal HCoV by age. Black dots show reported HCoV cases, blue are 100 random samples from the posterior. B) Posterior distributions for the duration of waning and the R_0 of seasonal HCoV. C) Mean annual attack rate for each age group from 100 samples of the posterior and the last 5 years of the fit. 110

Figure 4-2: SARS-CoV-2 simulations A) Estimated R_0 values for SARS-CoV-2 with different strengths of cross-protection. Points display the $R_{0, C19}$ and lines show the range of $R_{eff, C19}$ during the simulation. B) Simulated age-specific serology rates for SARS-CoV-2 by the end of May 2020. Sources are Blood and Transplant donors (BT)³¹ and the ‘What’s the STORY’ study (STORY)³²..... 111

Figure 4-3: 10-year forward projections of seasonal HCoV and SARS-CoV-2 epidemics. Red indicates SARS-CoV-2, blue indicates Seasonal HCoVs. The dashed vertical line indicates a change in axis scale due to the much larger SARS-CoV-2 pandemic wave, with that to the left of the dashed line marked by the left axis and that to the right by the right axis. Cross-protection strength and estimated SARS-CoV-2 R_0 for the scenario are shown to the left of the figure. A has cross-protection from seasonal HCoV to SARS-CoV-2, and B has bidirectional cross-protection. No control measures were included. Different linetypes show different samples from the posterior of the seasonal HCoV fit. 113

Figure 5-1: Six major respiratory viruses (positive numbers) reported from PHE and NHS laboratories (SGSS) in England and Wales between week 1, 2011 and week 29, 2021 (3-week moving average). Extracted from www.gov.uk⁵⁵ 142

List of Tables

Excludes Appendices

Table 3-1: Parameter values used for generating simulations.	65
Table 3-2: Demography and susceptibility input used for model simulations	65
Table 4-1: Parameter definitions, values and priors.....	89
Table 5-1: Model Parameters	120

Acronyms

AR	Attack Rate
ARI	Acute Respiratory Infection
BT	Blood and Transplant Donors
CI	Confidence Interval
CrI	Credible Interval
E	Exposed
FOI	Force of Infection
H	Hemagglutinin
HCoV	Human Coronavirus
I	Infected
ILI	Influenza-like illness
INF	Influenza
INF	Interferon
KHGH	Khanh Hoa General Hospital
LAIV	Live Attenuated Influenza Vaccine
MCMC	Markov Chain Monte Carlo
MERS-CoV	Middle Easter Respiratory Syndrome Coronavirus
MH	Metropolis – Hastings
N	Neuraminidase
NHS	National Health Service
NP	Nasopharyngeal
NREVSS	National Respiratory and Enteric Virus Surveillance System
ONS	Office for National Statistics
P	Protected
PAMP	Pathogen Associated Molecular Patterns

PCR	Polymerase Chain Reaction
PHE	Public Health England
PNAS	Proceedings of the National Academy of Sciences of the United States of America
Pnd	Pandemic
PRR	Pattern Recognition Receptor
R	Recovered
R_0	Basic Reproduction Number
RIG-I	Retinoic acid-inducible gene I
RSV	Respiratory Syncytial Virus
RSV	Respiratory Syncytial Virus
S	Susceptible
SARS-CoV-1	Severe Acute Respiratory Syndrome Coronavirus 1
SARS-CoV-2	Severe Acute Respiratory Syndrome Coronavirus 2
SEU	SeroEpidemiological Unit
SIR	Susceptible-Infected-Recovered model
SIRS	Susceptible-Infected-Recovered-Susceptible Model
SMC	Sequential Monte Carlo
STORY	What's the Story study
TLR	Toll-like Receptor
USA	United States of America
WHO	World Health Organisation

1 Introduction

1.1 Background

1.1.1 Motivation for study

Respiratory viruses are a global burden

Respiratory viruses result in a large global burden; the World Health Organisation (WHO) estimates that in 2015 respiratory infections resulted in 3,199,000 deaths worldwide, totalling 5.7% of all-cause mortality that year¹. In addition to the symptoms and deaths they cause, they also exacerbate chronic pulmonary conditions such as asthma and chronic obstructive pulmonary disease^{2,3}. The health and economic burden of respiratory illness and of days of work lost is therefore substantial. Even small changes in the circulation of these viruses can have large impacts.

They exist within a complex ecosystem

There are many factors that influence viral transmission, ranging from environmental factors, such as temperature and rainfall⁴, to viral adaptation to host immunity⁵, host behaviour changes⁶ and host susceptibility⁷. Previous scientific evidence has suggested that viruses may interact, resulting in a reduction in host susceptibility to secondary infection. As respiratory viruses do not exist in isolation, but instead circulate concurrently, any changes in host susceptibility brought about by infection with one virus has the potential to change the transmission dynamics of another. This may be either through temporary non-specific cross-protection to a distinct virus or specific and longer-term cross-protection with related viruses.

There is evidence suggesting interaction

Current evidence for interaction comes from a few main sources: shifts in viral incidence epidemics⁸⁻¹², experimental studies both *in vivo* and *in vitro*¹³⁻¹⁷ and sampling of human sera¹⁸⁻²². While these studies give indications of interaction, they are unable to test the links between biological mechanisms and population level impacts. However, mathematical modelling can address this gap as specific mechanisms can be included.

Motivation

Understanding the extent of interaction among these viruses and the effects interaction can have on transmission dynamics can help prepare for outbreaks, make informed policy decisions, and evaluate different public health interventions. This is particularly relevant for viruses where multiple vaccines are available, e.g. influenza²³, and new vaccines are being developed, e.g. Respiratory Syncytial Virus (RSV)²⁴ because vaccinating against one virus may change the dynamics of the other, potentially causing higher morbidity. The Severe Acute Respiratory Syndrome Coronavirus 2 (SARS-CoV-2) pandemic has shown the devastating impact a virus can have in terms of loss of life, livelihoods and freedoms. Developing mathematical models to increase our understanding of the dynamics of susceptibility to interacting viral infections can help inform public policy decisions, and potentially save many lives.

What is in the thesis?

In this thesis I use case studies to investigate the interactions between respiratory viruses and the extent to which mathematical modelling can help us understand these interactions. I use RSV and Influenza as case studies for short term, non-specific interaction, and coronaviruses as a case study for specific, long-term interaction. These viruses were chosen due to their large healthcare burdens, availability of protective interventions and time relevance. This introduction covers the background on these viruses, why they were chosen as case studies, current evidence for interactions, and how mathematical models can be used in this context.

1.1.2 Case study viruses

1.1.2.1 *Influenza*

Influenza transmission is associated with a large health and economic burden which cause 870'000 hospitalisations in under five-year-olds globally per year²⁵. In the UK there are 8 vaccines marketed for the 2020/21 influenza season: 1 Live Attenuated Influenza Vaccine (LAIV), 4 split virion inactivated vaccines, 3 surface antigen vaccines, and 1 recombinant vaccine²³. Public Health policies vary by country, for example in England LAIV is recommended for children aged 2 to 16 and inactivated vaccines are recommend for those 18 or over²⁶. Children have been included in the vaccination programme in England and Wales because of both the considerable health burden imposed on them by influenza and their role as primary drivers of transmission²⁷ — even though the

majority of severe illness and death occurs in older adults^{28,29}. In other countries, such as Vietnam, there is little to no seasonal influenza vaccination³⁰. As well as preventative vaccination, antivirals such as oseltamivir and zanamivir are available for post-exposure prophylaxis in high risk individuals and treatment³¹.

Influenza is a segmented single-stranded RNA virus that evolves through the accumulation of mutations (antigenic drift) and reassortment of the segments between strains (antigenic shift)³². There are three human influenza subtypes: A, B and C, and strains are identified by the Hemagglutinin (H) and Neuraminidase (N) proteins on the surface of the influenza virus particle. Two major strains of each of A and B have circulated in recent years: A (H1N1) and A (H3N2) and B Yamagata and B Victoria. Influenza C causes only mild disease and does not result in epidemics³³.

Symptoms caused by influenza are not specific as other circulating respiratory viruses cause similar symptoms. This set of symptoms is known as Influenza-like-illness (ILI), defined by the WHO as an Acute Respiratory Infection (ARI) with a measured fever of over 38 degrees Celsius and cough, with onset within the last 10 days³⁴. Because of this lack of specificity of symptoms, syndromic surveillance is often followed up by laboratory confirmation of the virus³⁵. Influenza can, however, also be detected in the nasopharynx of individuals who are not suffering from respiratory disease³⁶.

Influenza is highly seasonal in temperate climates, but is present for longer and less likely to show seasonal peaks in the tropics³⁷. In the UK, the influenza season begins between October and November^{38,39}, with incidence usually peaking between December and March (Figure 1-1). There is substantial annual variation in peak timing and size, and there is evidence for the impact of climatic factors on influenza transmission, particularly ambient temperature and absolute humidity⁴⁰⁻⁴². Novel variants can result in pandemic influenza, such as Influenza A(H1N1) 'swine flu' in 2009 and Influenza A(H1N1) 'Spanish flu' in 1918/1919.

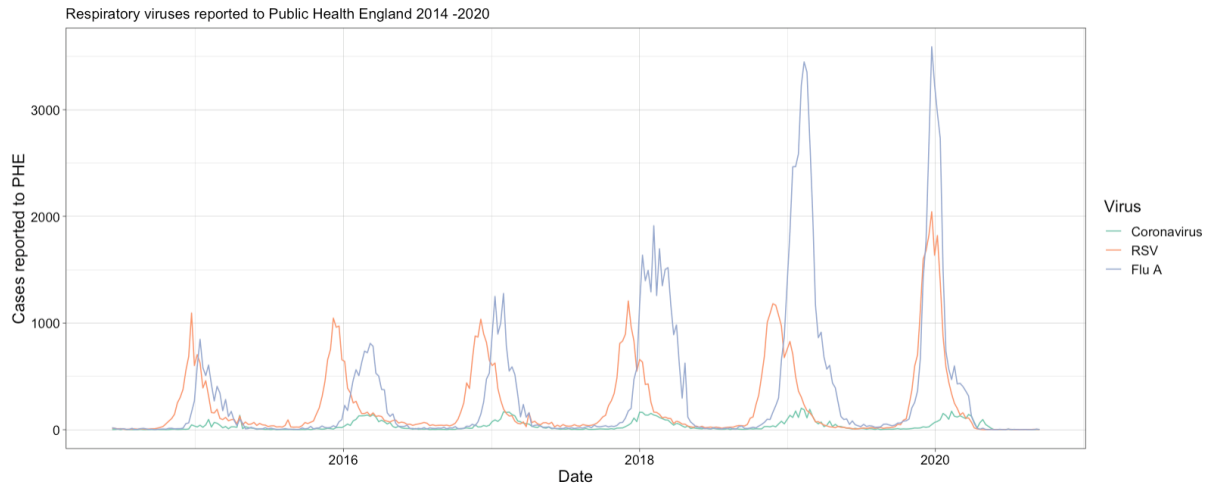


Figure 1-1: Reports of coronavirus (excluding SARS-CoV-2), influenza and Respiratory Syncytial Virus (RSV) reported by Public Health England (PHE) from mid 2014 to early 2020. Data extracted from PHE laboratory reports⁴³.

Briefly, the innate immune system is activated upon influenza infection through the detection of Pathogen Associated Molecular Patterns (PAMPS) by Pattern Recognition Receptors (PRRs), such as the double-stranded and tri-phosphorylated RNA. These are detected by a range of receptors, such as retinoic acid-inducible gene I (RIG-I) and Toll-like Receptor 3 (TLR3)⁴⁴. Upon activation of the receptors, signalling pathways are initiated, leading to expression of interferons (INFs) and other cytokines. The downstream effects of these signalling pathways result in the activation of an antiviral innate immune response, and the development of a subsequent adaptive response. Influenza is unusual for RNA viruses, in that it replicates within the nucleus of the host cell⁴⁵, so activates slightly different PRRs than other RNA viruses.

There is evidence of cross-immunity between influenza strains due to cross-reactive antibodies and T-cells. Cross-reactive antibodies in ferrets, as a result of sequential infection with H1N1, protected against novel pandemic influenza (H1N1pnd09)^{46,47}, as well as resulting in a boost of pre-existing antibody levels.⁴⁶ However, one influenza infection may not be sufficient to induce cross-protection⁴⁸. Cross-reactive antibodies targeted the Hemagglutinin stalk proteins, and have also been shown to induce antibodies that have broad reactivity and neutralising properties in mice and humans⁴⁹. Other studies have found T-cells to be a correlate of cross-protection against symptomatic pandemic influenza; for example, the presence of A(H3N2) Nucleoprotein reactive T-cells resulted in reduced symptomatic and PCR-confirmed pandemic influenza (odds ratio 0.27)⁵⁰. Another study showed that higher pre-existing frequencies of T-cells as compared to conserved epitopes resulted in less severe illness ($r = -0.39$ overall symptom score compared with pre-existing cytokine secreting T-cells), and correlated with cross-protection against symptomatic pandemic

influenza⁵¹. Such cross-protection has also been observed between seasonal strains⁵²⁻⁵⁴, and not just with pandemic influenza, but the extent of cross-protection from each strain does appear to vary⁵⁵. Future immune responses may also be determined by the first influenza virus encountered, a phenomenon known as original antigenic sin⁵⁶.

1.1.2.2 RSV

RSV infections results in 3.2 million hospital admissions in under 5-year-olds globally per year⁵⁷. There are currently no treatments or vaccines, and only limited preventative therapy: a monoclonal antibody, Palivizumab, which is recommended for high-risk infants in England⁵⁸ and elsewhere^{59,60}. In addition, Nirsevimab, also a monoclonal antibody, is close to licensure⁶¹. The antibody is given to at-risk infants to prevent severe lower respiratory tract disease through passive immunity⁶². As of February 2020, there were 19 vaccine candidates being evaluated in clinical trials across phases 1-3²⁴. RSV vaccines may therefore be introduced soon, affecting RSV transmission and thus potentially the transmission of other viruses.

In the UK, RSV has a consistent December annual peak in incidence, falling in the last few weeks of the year⁶³. However, some countries experience longer transmission seasons (e.g. Malaysia and Mozambique up to 10 months)⁶⁴, and others such as Finland observe more complicated dynamics, such as 2-year cycles⁶⁵. RSV circulation could be impacted by climatic factors, such as rainfall and temperature, and research from different regions shows different relationships: a positive relationship to maximum temperature in Mexico (correlation coefficient 0.25)⁶⁶, a negative relationship with mean temperature in Thailand⁶⁷ and China⁶⁸ (correlation coefficient -0.27 and -0.77 respectively), and a bimodal relationship with mean temperature in various locations⁶⁹. While differing results are expected in different climates, due to, for example, different temperature ranges, the combined evidence available does not indicate an important role of such climatic factors. Differences between regions may also occur due to differing population immunity, demography, and behaviour.

In high income, temperate countries the majority of children (80% in the UK) become infected with RSV before their second birthday^{12,63}. The disease incidence is twice as high in developing countries for children under 5⁷⁰. Maternal antibodies are present in infants for up to 7 months⁷¹. After infection, the average duration of immunity to RSV is estimated to be 200 days⁷² before return to a susceptible state. However, as infection in very young children is much more severe than subsequent infections⁶³ some longer-lasting protection against disease may be gained. Despite this,

older adults can experience severe RSV infection; there are a similar number of deaths in the over 65s attributed to RSV as to influenza (13900 RSV deaths compared to 15500 influenza deaths during an 8 year study in the Netherlands) ⁷³.

RSV is a paramyxovirus containing single-stranded RNA. There are two subtypes (A and B), which circulate at the same time, one of which often predominates each year ^{8,74}. The subtypes are clinically indistinguishable, and rarely tested for during routine surveillance. Studies on differing severity between the subtypes have had mixed results, with some concluding A is more severe ⁷⁵⁻⁷⁷, others finding no difference ^{78,79}, and one concluding that B is more severe ⁸⁰.

While the activation in immune response against RSV infection is very similar to that of influenza infection, there are some differences. RSV is detected by many of the same PRRs, however some of the TLRs are different, and there are other differences such as potential lower importance of RIG-I⁴⁴. In addition, while both viruses result in the innate IFN expression in epithelial cells, RSV's primary source of IFN is alveolar macrophages, whereas influenza's derive from plasmacytoid dendritic cells ⁴⁴.

1.1.2.3 *Coronaviruses*

SARS-CoV-2 emerged in 2019, and, as of February 2021, over 100 million cases have been reported globally, resulting in over 2.3 million reported deaths⁸¹. Combined with the health, economic and educational impacts of Non-Pharmaceutical Interventions (NPIs), the worldwide impact of SARS-CoV-2 is colossal. The novel coronavirus emerged against a backdrop of circulating seasonal coronaviruses, and is the third emergent coronavirus in the 21st century⁸², following Severe Acute Respiratory Syndrome Coronavirus 1 (SARS-CoV-1) and Middle Eastern Respiratory Syndrome Coronavirus (MERS-CoV)⁸³. Due to pandemic preparedness activities and intensive research in the area, there are now multiple vaccines available as well as proven effective NPIs.

There are four seasonal human coronaviruses (HCoVs): two alpha coronaviruses (HCoV-229E, HCoV-NL63) and two beta coronaviruses (HCoV-HKU1, HCoV-OC43). Whilst all four of these viruses result in respiratory infection, cases are often mild or asymptomatic⁸⁴, and frequently co-detected with other respiratory viral infections⁸⁵. These viruses are seasonal in temperate sites (excluding China), but less seasonal in tropical sites (and China), and associated with lower temperatures and higher humidity⁸⁶. In the UK, cases peak in February, and have consistent seasonal patterns (Figure 1-1). First infection with all four seasonal coronaviruses occurs in childhood⁸⁷. There is evidence from

observational studies suggesting that reinfection with homologous seasonal coronaviruses can occur within a year^{88,89}. Experimental infections with HCoV-229E have also shown that reinfection (albeit symptomless) can occur within a year, despite the presence of specific antibody to a homologous virus⁹⁰. There are indications, however, that the average duration of immunity is longer, with few reinfections in a 3-year cohort study⁹¹, sterilising immunity to HCoV-229E following challenge one year after experimental infection and an average reinfection time ranging from 30-55 months in a study of 10 individuals^{92 93}. It has also been shown that T-cells can neutralise new strains up to 8-17 years after infection⁹⁴.

As well as SARS-CoV-2, other coronaviruses have recently emerged: SARS-CoV-1 (discovered February 2003⁹⁵) and MERS-CoV (discovered September 2012⁹⁶). These may also stimulate lasting immunity; SARS-CoV-1 reactive T-cells are detectable up to 11 years post-infection⁹⁷. Current evidence for the duration of immunity to SARS-CoV-2 suggests it lasts 6 to 8 months, with one study showing a protective immune response for 5 to 7 months⁹⁸, and other studies observing an immune duration of around 8 months^{99,100}, as well as relatively few re-infections^{101,102}.

During the SARS-CoV-2 pandemic, lower infection rates were observed in children¹⁰³⁻¹⁰⁷, and it has been hypothesised that this could be due to cross-reaction between seasonal coronaviruses and SARS-CoV-2. This is because children have higher contact rates¹⁰⁸ and therefore higher rates of infection, which could translate to protection against SARS-CoV-2.

As coronaviruses are also RNA viruses, host detection thereof acts similarly to the host detection of influenza and RSV viruses, activating a selection of PRRs such as TLR-3 and TLR-7. This leads to downstream responses via the interferon pathway. For seasonal coronaviruses, such as HCoV-229E, robust interferon responses have been recorded¹⁰⁹; however, SARS-CoV-2 and the other pandemic coronaviruses have been shown to impede this pathway¹⁰⁹. In a simplistic view, to activate the adaptative pathway, immune cells such as dendritic cells phagocytose the virus and present antigens to T-cells in the lymph nodes. These differentiate and use feedback from the antigen presenting cells: T-cells specific for the viral antigens are selected for. These then evolve down two major pathways: effector CD4+ T-cells that stimulate B-cells to make antibodies, and cytotoxic CD8 cells that kill infected host cells¹¹⁰. After infection, immune memory cells persist, making the response following subsequent infection much quicker, as specific T-cells and antibodies are already present.

1.1.3 Viral Interaction

Pathogen interaction can be competitive or synergistic. Opatowski *et al.* (2017) reviewed evidence of influenza interaction with other pathogens. They defined interaction as “any process by which infection caused by one pathogen affects the probability, timing, or natural history of infection by another”, and they concluded that influenza interaction with other viruses is most likely competitive¹¹¹. This interaction could be within-host or at population level and could be during co-infection, or for a period after infection.

It should be noted however, that the respiratory tract is full of microorganisms, collectively known as the microbiome¹¹². This microbiome is constantly evolving, and collectively shapes our response to incoming infections.¹¹³ However, some parts of the microbiome are more important than others, and I therefore focus specifically on interaction between respiratory viruses in this thesis, despite the further complexities in reality.

In the upcoming sections I discuss the two types of interaction: short-term, non-specific interaction and long-term, specific interaction. Each section discusses the relevant mechanisms of interaction. For short-term interaction these are: behavioural responses, competition for resources, changes in severity, innate immune system activation and short-term immune memory. For long-term interaction the mechanisms are antibody-derived immune responses and T-cell derived immune responses.

1.1.4 Short term, non-specific interaction

Short-term immunity involves non-specific immunity between the different respiratory viruses, where infection from one virus reduces the likelihood of being infected with a second virus during or for a period after the primary infection. The reduction in susceptibility to the second virus may come about through changes in human behaviour, or through activation of the human immune system. This is more likely to occur between similar viruses, as they use similar transmission pathways and activate a similar immune response. While this could occur between any respiratory viruses, I focus on influenza and RSV as most of the evidence for such short-term, non-specific interactions comes from these two viruses.

Observations of time series data have provided indications of interaction between RSV and Influenza. Insights are especially noticeable after the 2009 influenza pandemic; 4 studies have shown

a delay in the RSV epidemic following the influenza pandemic (Israel^{8,9}, Germany¹¹⁴ and France¹⁰) and in Hong Kong the annual RSV epidemic appeared to be completely absent after the influenza pandemic¹¹.

Observation in other years has shown that the peaks of influenza and RSV rarely coincide (USA, Norway)^{115,116}. In a study from the Netherlands, data from 9 years concluded that on the three occasions when the influenza A season began earlier, the RSV peak was decreased once and shifted later twice¹¹⁷. This was done by visually categorising influenza epidemics as early or late and generating correlation coefficients. In Japan, a study between 1999 and 2002 observed possible interference in the second two years, with the number of patients with RSV decreasing after the start of the influenza epidemic, but recovering to some extent after the influenza peak¹¹⁸.

Assessing the rate of observed co-infections compared to the expected rate has also given indications of cross-protection, with one study showing 6-7 fold fewer RSV and influenza coinfections than expected¹¹⁹, taking into account their circulation at the time.

While such observational studies give indications that interaction between influenza and RSV may occur, they are unable to determine the mechanisms behind the hypothesised interaction, and are therefore limited in their ability to determine whether interaction is the causal factor behind the observations. Multiple mechanisms by which interaction may occur have been hypothesised (Figure 1-2) which I describe in turn. These mechanisms are incorporated to varying extents in the different chapters, with Chapters 2 and 3 incorporating concurrent and both types of subsequent infection. As the model does not have the ability to distinguish between these types a “duration of cross-protection” parameter is fit, which gives indications of the likely mechanism. In Chapter four the model incorporates longer term interaction, although it cannot specify whether it is antibody or T cell derived. In addition, behavioural changes before infection are incorporated into the model in Chapter 4, by modelling changes in contact patterns.

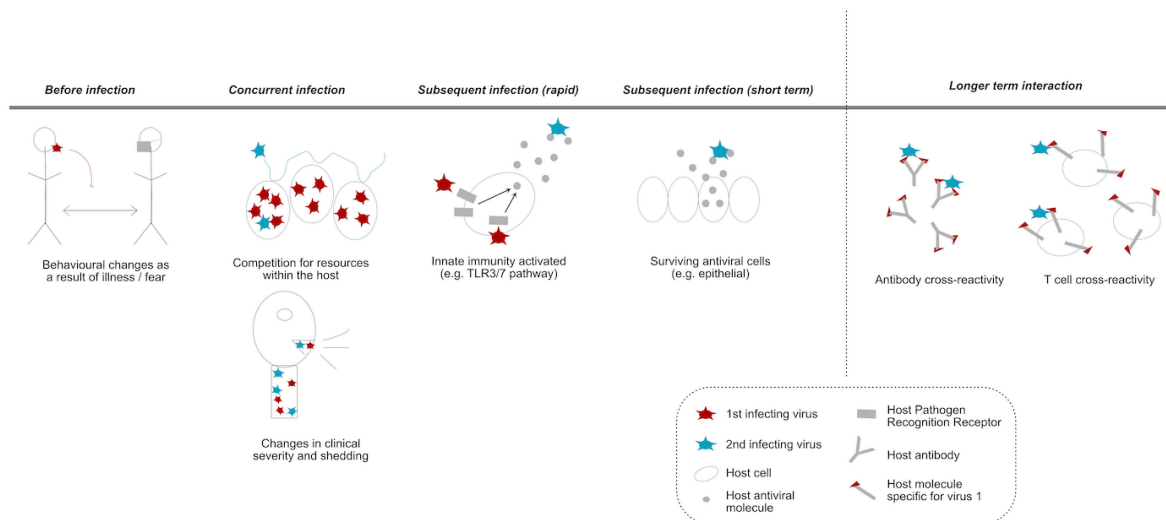


Figure 1-2: Simplified schema depicting different potential mechanisms of interaction between viruses.

Mechanism - Behavioural responses

Viral interaction may occur because of behavioural changes by the host in response to an infection. If an individual becomes symptomatic, they may be more likely to remain at home or implement other preventative measures, such as face masks, reducing the chance of them acquiring other viruses. Fear of becoming infected during an epidemic can also result in individuals reducing their daily contacts, which will equally effect the transmission of other respiratory pathogens with the same transmission routes⁶. Pathogens with similar transmission routes may also be impacted by the same public health interventions, such as school closures and lockdowns^{120,121}.

Mechanism - Competition for resources

During infection, viruses may compete directly for host cell resources. Pinky *et al.* (2016) developed a model to look at within-host competition between respiratory viruses, which concluded that, for viruses with the same preference of host cells, the virus with the highest growth rate would dominate. However timing of infection had an impact, with earlier virus infection allowing the otherwise weaker virus to dominate¹²². There are also *in vitro* experiments that look at viral growth. One experiment found that, when infecting cells 12 hours apart, influenza followed by RSV did not alter the growth of RSV in cell culture, whereas initial infection with RSV reduced the growth of influenza¹²³. While these studies are good indications of interaction, they don't allow for the complexity seen within a human host.

Mechanism - Changes in severity

Damage to host cells from viral infection may also change the rate of colonisation of other pathogens, which could have impacts on severity of infections. Yoshida *et al.* (2013)¹²⁴ ran a prospective surveillance and case-control study looking at severity of respiratory virus mono- and co-infections in humans. Although presence of two viruses in the samples resulted in increased severity for some viruses, this was not observed for influenza and RSV. These dual infections were no more severe than infection with RSV alone¹²⁴. It was postulated that this may be due to the viruses activating different immune pathways, resulting in neutralisation of their respective immunopathology. Other studies have shown varied results: one Brazilian study, for instance, found no difference in co-infection severity of hospitalised infants in Brazil¹²⁵. A separate Brazilian study showed a longer hospital stay (14.3 ± 7.7 days compared to 7.4 ± 4.3 days) for RSV coinfections with other respiratory viruses, compared to RSV mono-infections in preterm infants followed for a year¹²⁶. A Japanese hospital based paediatric study showed shedding of RSV was 65% (95% CrI 49% – 77%) longer when co-infected with coronaviruses, rhinoviruses or adenoviruses¹²⁷. In addition, studies on other respiratory pathogens have shown that co-infection can increase severity, such as influenza infection increasing the risk of invasive pneumococcal disease in adults¹²⁸. It seems that pneumococcus may also affect RSV severity, with the introduction of pneumococcus vaccination reducing RSV-associated hospitalisations¹²⁹. Evidence is therefore unclear as to what effects RSV and influenza co-infections may have, as coinfections between these two viruses were not specifically analysed in most of the above studies, often due to a lack of co-infection numbers.

Mechanism - Innate immune system activation

The innate immune system is activated after viral infection in the respiratory tract through PRRs. Among these are TLRs, of which TLR-3 detects double-stranded RNA from viral replication, and TLR-7 recognises single-stranded RNA, which are both activated upon influenza and RSV infection^{44,130}. Along with other PRRs (Nod-like receptors, RIG-I-like receptors), this releases cytokines and chemokines that activate a signalling pathway which results in the initial innate antiviral response^{44,130}. Once activated, the following immune response may impair infection by a second, different virus. Cross-protection by this mechanism would be relatively short-lived, lasting as long as the downstream responses after viral clearance. An example is the upregulation of RNA-binding proteins after infection with influenza A, which inhibits subsequent growth of RSV, which was shown

in vivo and *in vitro*¹³. In this study mice were infected with RSV following influenza infection, and then the presence of the virus in the lungs was surveyed 4 days later. When RSV infection occurred 1 or 2 days after influenza infection, no RSV was observed. As the time between infections increased so did the amount of RSV, reaching just under 60% of RSV compared to the control group with a 12-day gap¹³. Further evidence for this comes from mouse studies, in which prior vaccination with cold-adapted, LAIV reduced the replication of subsequent RSV infection, if the challenge was within 6 days of vaccination. This effect was not observed in Knockout mice missing the TLR-3/7 receptors¹⁴. Another mouse study showed that previous influenza infection of mice protects against weight loss, illness and lung eosinophilia, attenuates recruitment of inflammatory cells, and reduces cytokine secretion caused by RSV attachment proteins 2 to 3 weeks later¹³¹. It did not affect RSV clearance. This study also showed that splenocytes from previously influenza infected mice could confer this immunity to naïve mice, if transferred. Experimental infection of ferrets suggested that complete protection lasted less than 2 weeks, although virus challenges after this period were cleared faster¹⁵. Overall, this combines to compelling evidence that activation of the innate immune system following infection from influenza does impact the response upon infection with RSV in mice. However, the extent and impacts of this cross-protection is unclear, as is its applicability to human hosts.

Mechanism - Short term immune memory

Others have suggested mechanisms of extended interaction; for example, Hamilton *et al.* (2016) showed that cells forming the respiratory epithelium in mice can survive influenza A infection and will remain in a state of heightened antiviral activation for 3 to 12 weeks, with waning of the conferred protection against influenza observable at 6 weeks¹⁶. This extended duration agrees with Kelly *et al.* (2010) who stipulate that the conferred protection could be a mean of 3 months¹⁷. For this study they looked at potential interactions between seasonal and pandemic influenza, and assumed that vaccination against seasonal influenza did not bestow the immunity conferred by natural infection of seasonal influenza.

Evidence for short-term non-specific cross-protection also comes from studying the evolution of the influenza genome. Ferguson *et al.* (2003) suggest that, after a viral infection is cleared, there is a continued period of time where the individual is less susceptible to new viral infections from any influenza strain, due to the heightened state of the immune system¹³². This was determined by modelling the evolution of influenza strains to generate ladder-like phylogenetic trees. It was

determined that “short-lived strain-transcending immunity is essential to restrict viral diversity in the host population”.

The evidence for this extended non-specific immunity comes from a range of disciplines: wet lab, population dynamics, and phylogenetic analysis. While this gives credibility to the hypothesis, all of the above-mentioned studies focus on non-specific cross-protection between different types of influenza, so they may not be as applicable to cross-protection against RSV.

1.1.5 Long term, specific interaction

Long-term immunity involves identifying specific pathogen features, and storing a memory of the response against pathogens with these features. However, these features may have similarities with related pathogens (e.g., different coronavirus species), resulting in activation of the immune response to the similar pathogen. This can lead to partial immunity towards similar, yet previously unseen, pathogens. While the adaptive immune system is extremely complicated, two main features have been studied when looking at cross-reactive and/or cross-protective immune responses: Antibodies and T-cells.

Antibody-derived immune responses

Cross-protective responses have been noted both between and within seasonal and pandemic coronaviruses. A study following the SARS-CoV-1 pandemic showed that 12 out of 20 SARS patients displayed an increase in antibody titre against HCoV-OC43 and/or HCoV-229E seasonal coronaviruses following SARS infection¹⁹, and similar results were found in an *in vitro* study¹³³. While an increase in antibody titre does not necessarily result in an effective immune response, SARS-CoV-1 patients have also shown substantial neutralising antibody titres against MERS-CoV¹³⁴.

Similar cross-protection has also been observed in relation to SARS-CoV-2; uninfected individuals' serum were seen to neutralise SARS-CoV-2, although less well than serum from SARS-CoV-2 patients¹³⁵. There was a strong indication that these cross-reactive antibodies were targeting a much smaller range of viral targets than those from COVID-19 patients¹³⁵. Another study looking at beta-coronaviruses (HCoV-OC43, HCoV-HKU1, SARS-CoV-1, MERS-CoV and SARS-CoV-2) detected potential cross-reactive antibodies to SARS-CoV-2 from all four other viruses. The strongest cross-recognition was that of SARS/MERS-CoV and SARS-CoV-2 — hypothesised to be due to their closer homology¹³⁶. Cross-reactive responses, however, do not necessarily translate into cross-protection;

there are indications that seasonal coronavirus antibodies may be boosted by SARS-CoV-2 infection, but they do not correlate with protection against infection or hospitalisation¹³⁷.

Cross-reactive antibodies have also been identified in influenza infection: between 13% and 68% of individuals (children and adults) had cross-reactive antibodies to strains that they had not been exposed to in one Israeli study¹⁸. Some responses have been shown to be cross-protective as well as cross-reactive, such as between H1N1 and H3N2 subtypes in mice¹³⁸.

Coronavirus antibody responses, including those against SARS-CoV-2, are, however, complicated by the varied and rapid decrease in antibody titres after infection¹³⁹. Yet, T-cells can also have cross-reactive and potentially cross-protective responses across pathogens¹⁴⁰.

T-cell-derived immune responses

There is evidence of this phenomenon in coronaviruses, for example, a mouse study showed very strong cross-reactive T-cell responses between MERS-CoV and HCoV-HKU1 (targeted at N-protein)¹⁴¹. Evidence is emerging that this could be the case for SARS-CoV-2 as well. In one study, 50% of healthy pre-pandemic donor samples (collected for unrelated studies) had reactive T-cells (non-spike) to SARS-CoV-2²⁰. These were all also seropositive for HCoV-OC43, suggesting that immune responses to some seasonal coronaviruses are cross-protective. Another study looking at healthy donors from unrelated studies prior to the pandemic also found that half of the unexposed donors possessed T-cells targeting SARS-CoV-2¹⁴². Interestingly, they found that whilst SARS-CoV-2 patients had T-cell responses that reacted to both ends of the S-protein, in the SARS-CoV-2 non-exposed individuals the target was almost exclusively just one end of the S-protein. This end does not contain the receptor binding region, but does have higher homology with seasonal coronaviruses. Further studies found cross-reactive T-cells in 20%¹⁴³, 24%²¹ and 35%²² of SARS-CoV-2 unexposed individuals. There is evidence that these cross-reactive T-cells are present at a higher frequency in younger adults¹⁴⁴, and that these responses can be protective. For example, SARS-CoV-1 and MERS-CoV T-cell epitopes were protective in mice against other human and bat coronaviruses¹⁴¹.

Cross-reactive T-cell responses have been more widely studied in the context of influenza, and human T-cells have been shown to be reactive to different influenza variants¹⁴⁵, and across influenza

A, B and C viruses¹⁴⁶. Cross-protection has also been shown, with a correlation between pre-existing influenza T-cells and reduced symptoms during the 2009 influenza pandemic^{50,51}.

Overall, there is strong evidence for cross-reactive immune responses between coronaviruses, in terms of both antibodies and T-cells, backed up by evidence of this phenomenon in other respiratory virus species. However, despite isolated studies, the extent to which this cross-reaction results in cross-protection is unclear, especially when considering a reduction in susceptibility to infection, rather than to symptomatic disease.

1.1.6 Mathematical Modelling approaches

By creating models, one simplifies complex systems. Modelling transmission dynamics can be particularly useful in epidemics because mechanistic models can be used to test alternative hypotheses. Mathematical models have been used to test drivers of seasonality^{147,148} and vaccination strategies^{149,150}, among other things. They offer an ideal opportunity to investigate pathogen interaction because features that influence the dynamics of interaction, such as susceptibility over time and age assortative mixing, can be included. This allows the researcher to test the influence of mechanisms, including pathogen interaction, which cannot be achieved using non-dynamic approaches.

Compartmental Models

Compartmental models split the population into different categories based on different characteristics or infectious states. These were first developed by Ross¹⁵¹, Ross and Hudson^{152,153} and Kermack and McKenzie¹⁵⁴ in the 19th century. One of the most basic versions is the ‘Susceptible – Infectious – Recovered’ (SIR) model (Figure 1-3), in which the population is split into compartments based on their infectious state. These models are often deterministic: flow between the compartments is defined by differential equations, shown below for the simple SIR model. The modelled population can be further divided into more compartments, such as by age, susceptibility level, vaccine status, etc., allowing the development of detailed pathogen-specific models. In addition, external factors such as seasonal forcing can be included, for example, by adding a cosine function to the Force of Infection (FOI).

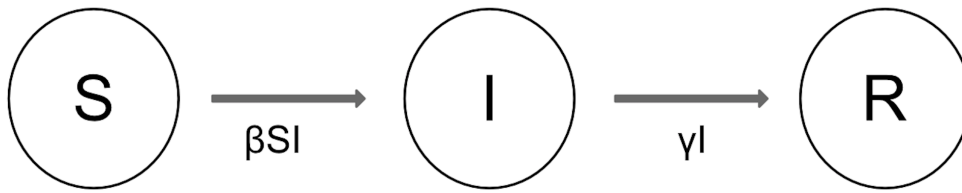


Figure 1-3: Susceptible (S) – Infectious (I) – Recovered (R) compartmental model. Parameters are the transmission rate (β) and the infectious period ($1/\gamma$)

$$\frac{dS}{dt} = -\beta SI \quad (1)$$

$$\frac{dI}{dt} = \beta SI - \gamma I \quad (2)$$

$$\frac{dR}{dt} = \gamma I \quad (3)$$

Where the states are Susceptible (S), Infectious (I) and Recovered (R). Parameters are the transmission rate (β) and the infectious period ($1/\gamma$).

To model interactions between viruses, the characteristics of each relevant virus must be incorporated into the model, as must a mechanism of interaction. I will, therefore, discuss the important characteristics of each virus that must be included in each of their individual models, before summarising methods for modelling interaction between pathogens.

Influenza

There is vast variety in influenza modelling approaches, which is largely because of the complex nature of influenza immunity. Types of compartmental models can be split in to two groups: those that take account of strain dynamics and those that do not. Kucharski *et al.* (2016) grouped the methods used as history-based (i.e. previous exposure) and status-based (i.e. current immune status)¹⁵⁵. These models can become very complex and are used when specifically focusing on strain dynamics.

Other influenza models assume that the strain dynamics can be encompassed in an annual waning rate, which takes antigenic drift and cross-immunity between subtypes into account. These can either model circulating subtypes^{150,156} or allow one generic influenza virus^{148,157,158}. They often include seasonal forcing to simulate seasonal climatic and behavioural factors that impact disease transmission, without having to specify each individual factor. In some models, specific parameters are also allowed to vary each year to further take into account annual differences in strains^{148,158}.

Another commonly used method for modelling influenza dynamics is to simulate each influenza season separately. Waning immunity and cross-immunity do not therefore need to be explicitly included in the model; instead, susceptibility at the beginning of the season is inputted, for example, as in Baguelin *et al.* (2013)²⁷. This is a convenient method that accounts for differing immunity between different strains, without explicitly modelling them, and it also incorporates immunity by vaccination.

RSV

Despite there being two subtypes, most RSV transmission models usually simulate only one circulating virus, as they are clinically indistinguishable and not routinely tested for. An exception to this is a model by White *et al.* (2005) that looks at cross protection between subtypes¹⁵⁹, in which they found low levels of cross-protection. Many models separate primary infection with RSV from secondary infections, the primary being the more severe^{147,160–162}, or allow for a build-up of partial immunity following infections^{163,164}. Unlike differentiating between subtypes, modelling the build-up of immunity is crucial for understanding the interaction dynamics of RSV, either with infection number, or with age (as in the absence of interventions these are correlated). Including age assortative mixing in models is crucial because of this variance in immunity by age. As with influenza, many models that look at the transmission of RSV over multiple years use seasonal forcing to simulate climatic and behavioural factors^{148,150,157,158}. While this can be useful to get repeated dynamics, seasonal forcing does not describe specific biological mechanisms, and therefore should be interpreted with caution.

Coronavirus

Models on coronaviruses have been developed quite irregularly: very few models have looked at seasonal coronaviruses, but large flurries of models have been published after coronavirus pandemics (e.g. 14 models on SARS-CoV-1 in the first 18 months since its emergence¹⁶⁵, 100's since the emergence of SARS-CoV-2). In general, models of pandemic viruses tend to be focused on estimating the impact of control measures^{166–170}, or on estimating key parameter values^{171,172}, such as the basic reproduction number (R_0). Many of these models include an “Exposed” (E) compartment, as the duration of this can have large impacts on the effectiveness of control measures, and it is biologically plausible. As contact dynamics are very important during the early

stages of a pandemic, network models have also been used, which place a greater emphasis on contact networks^{173,174}. However, many of these models make different assumptions about the immune dynamics, for example, they might have multiple susceptibility levels¹⁷⁵, or multiple strains of the virus¹⁷⁶. Super-spreading events have also been modelled^{168,177,178}, as these can be important factors in the initial phase of an epidemic. Further models have also been developed that look at the impacts the SARS-CoV-2 pandemic, and the associated social restrictions, have had on other pathogens, such as Tuberculosis co-infections¹⁷⁹. They also vary in looking at specific, enclosed populations, such as cruise ships¹⁸⁰, or a wider geographic spread. As with influenza and RSV, to understand coronavirus interactions it is important to model the level of immunity against coronaviruses in the population. In addition, as public health interventions often affect different age groups to a different extent (such as school closures), it is important to include age assortative mixing when dynamically modelling these.

Interaction models

Most infection interaction models simulate different strains rather than different pathogens. Frequently modelled pathogens with multiple strains are Influenza, *Streptococcus pneumoniae* and Dengue. These models can be individual-based, history-based or status-based as discussed by Kucharski *et al.* (2016)¹⁵⁵. Individual-based models track each individual separately, rather than combining them into groups based on infection status, history or other characteristics. While individual-based¹⁸¹ models therefore allow the capturing of both previous infections and immunity profiles for individuals, they are extremely computationally intensive and hard to parameterise. Compartmental models reduce this complexity, such as history-based ones¹⁸², which contain compartments for each combination of prior infections. Although this works well when there are only 2 interacting pathogens, it can become increasingly complex with more strains. These can however be reduced through symmetry of strain space¹⁸³ or age structure¹⁵⁵. Status based models^{184,185}, on the other hand, keep track of current immune status but not the combination of past infections that generated this immunity. This allows for easy incorporation of partial immunity, where, upon infection with a pathogen, individuals immunity levels against it and other pathogens differ. Such models do not, however, allow tracking of the strains which have resulted in the current immune status, which may be a substantial disadvantage for many questions regarding pathogens with many strains.

There are few models that simulate multiple respiratory pathologies. Influenza and pneumonia models are one example¹⁸⁶, but here it is important to note that it is the disease, and not the prevalence of bacteria, that is of interest for pneumonia. In these models, influenza is often included as a covariate of the model, where the prevalence of influenza over time is an input value that influences the propensity for progression to disease upon infection.

In terms of RSV and influenza models, there is one published within-host model, and one at the population level. Pinky *et al.* (2016)¹²² developed a model to look at within-host competition between respiratory viruses, which concluded that for viruses with the same preference of host cells, the virus with the highest growth rate would dominate. However, timing of infection had an impact, with earlier virus infection allowing the otherwise weaker virus to dominate. This is a relatively simple model, with no inclusion of immune responses to the virus, and with strong assumptions about host cell preference and a lack of superinfection. It does however provide evidence for the specific mechanism of interaction that the authors were looking at.

There is also a dynamic transmission model looking at co-infection between influenza and RSV on the population level. This model by Velasco-Hernandez *et al.* (2015)¹⁸⁷ allowed superinfection, i.e., once infected by one virus, individuals were less susceptible to a second. They assumed that RSV was the dominant virus, due to its higher mortality and its all-year presence in Mexico City. The model incorporated reduced susceptibility during infection, with no allowance for an increase in transmissibility. In the paper they did not discuss the sensitivity of the results to some major assumptions; for example, that RSV superinfects influenza, and not the other way around. Nor did they fit the model to data, so while it replicates the rough transmission patterns, the accuracy of the fit is not defined.

In terms of coronaviruses, Pinky *et al.* (2020)¹⁸⁸ looked at the growth rate of respiratory viruses and modelled the impact of these growth rates dependent on when infections occurred. They concluded that as SARS-CoV-2 has a lower growth rate, it will be outcompeted by respiratory viruses that had been infected at the same time or earlier¹⁸⁸. Kissler *et al.* (2020) developed an interaction model looking at the cross-protection between beta-coronaviruses (HCoV-HKU1 and HCoV-OC43), and at the impact cross-protection could have on the future dynamics of SARS-CoV-2¹⁸⁹. Using data from the USA they estimated relatively strong cross-protection between HCoV-HKU1 and HCoV-OC43, using a compartmental model with seasonal forcing. Whilst the model assumed no interaction with alpha-coronaviruses, and explored a relatively narrow parameter range, they used Bayesian

Methods to fit to 5 seasons of data, obtaining values for the extent of interaction, and were therefore able to test the impact of any cross-protection on SARS-CoV-2 transmission. They estimated that the average duration of immunity was 45 weeks, and that there was strong but unequal cross-protection between subtypes (0.51 and 0.78).

1.1.7 Fitting models

Most pathogen interaction modelling papers do not include fitting the model to data. There were four categories of methods used to evaluate the models:

A. Simulation to investigate behaviour – no data used.

There are many theoretical papers that look at how interacting pathogens/strains can be modelled, without comparing the simulation results to data. One example of this is a paper by Gog and Swinton (2012)¹⁹⁰, in which they develop a status-based approach to multiple strain dynamics, allowing for the incorporation of different forms of partial immunity. Instead of comparing their results to data, they compare the behaviour of their model to other models in the literature. This allows the investigation of impacts from different assumptions, but does not evaluate to what extent these assumptions apply in different settings.

B. Simulations that are compared to data visually.

The Influenza-RSV model by Velasco-Hernandez *et al.* (2015)¹⁸⁷ is an example of a model that compares simulations with data, but does not quantitatively fit them to it. This allows the authors to evaluate their hypothesis, but does not provide quantitative assessment as it is based on a visual comparison. While such visual comparison may be a reasonable method for looking at overall patterns, it is less good at identifying smaller differences, such as those that might be seen due to pathogen interaction. This may also be true when different sets of parameters fit equally well, and it is therefore less robust.

C. Inference validation through simulated data.

Shrestha *et al.* (2011)¹⁹¹ developed a model of pathogen interaction that was not restricted to a specific pathogen. They aimed to investigate whether it was possible to determine the level of interaction from surveillance data. To do this, they generated simulated data of monthly cases over

40 years for each parameter set, and the parameters approximated dengue transmission with different levels of interaction between strains. Subsequently, they fitted the model to this simulated data to investigate what accuracy of parameter values related to interaction could be determined by using Sequential Monte Carlo (SMC). They determined that in most cases it was possible to back-infer the parameters relating to interaction, and that it was easier when the interaction was stronger or longer in duration. In addition, when the initial conditions for the model were unknown (as opposed to their tested scenarios where they knew the initial conditions of the population) the precision of the parameter estimates was reduced despite still being identifiable. Analysis of the capabilities of a model done in this way gives confidence to subsequent analysis of observational data using the same model; however, such validation is also time consuming. It can also be used to determine the quality and quantity of data required to be able to fit to real time series data, which can be useful for planning study designs.

D. Fit the model to data.

Fitting to data provides empirical evidence for parameter estimates, and should therefore be used wherever possible. An example of fitting of an interaction model to data is assessing pneumococcal incidence in the presence of influenza. Shrestha *et al.* (2015)¹⁸⁶ used an SIRS model of pneumonia, where influenza was included as a covariate rather than as part of the transmission model. In this case, the authors used a partially observed Markov process. There are also papers that model both pathogens (or strains) dynamically. Pneumococcal strain models are one example of this; strains are often modelled as vaccine-type or non-vaccine-type¹⁹². Studies here have shown that transmission dynamics are sensitive to the competition between serotypes, and that introducing an intervention (in this case vaccination), allowed for the estimation of the competition parameter^{193,194}. In addition, information on which strains an individual is infected with (i.e. coinfections) resulted in more detailed estimates for competition between the strains¹⁹⁵.

Bayesian fitting methods

In this thesis I use Bayesian Methods to fit models to data. This includes fitting methods such as Markov Chain Monte Carlo (MCMC) and parallel tempering. The basis of these methods is to sample from an unknown posterior distribution. To sample the posterior distribution, $p(\theta|data)$, of parameters, $\theta = \{\alpha, \beta, \dots\}$, the likelihood, $p(data|\theta)$, and the prior on the parameters, $p(\theta)$, must

be calculated. Using Bayes theorem (Equation 4) a distribution that is proportional to the posterior can be estimated. This framework allows the inclusion of prior information, and gives a distribution that is proportional to the posterior parameters.

$$p(\theta|data) \propto p(data|\theta)p(\theta) \quad (4)$$

MCMC is a standard tool within the field to efficiently sample the posterior distribution, generating estimates of the parameter distributions. This typically involves proposing parameter values, and accepting or rejecting these proposed parameters based on the Metropolis-Hastings (MH) ratio. Pseudocode for an MH algorithm with symmetrical proposal distributions is shown in Figure 1-4. The Monte Carlo chains must reach convergence at the stationary distribution, thereby describing the posterior distribution. While various diagnostics can be used to show a lack of convergence¹⁹⁶, it is not possible to prove convergence, and this is a major limitation of many related methods, including MCMC. This is because one can never be sure that 100% of the parameter space has been explored. This is particularly true for more complicated posterior distributions, as chains can get stuck in local areas of high density. MCMC can, therefore, be further expanded to include more complex sampling and acceptance regimes, such as parallel tempering.

- a) Initialise sampler: Define initial parameter values θ_t and proposal densities
- b) For each iteration
 - Generate proposed parameters using θ_t and the proposal densities
 - Calculate prior of proposed parameters $p(\theta')$
 - Calculate likelihood of the data, given the proposed parameters $p(data|\theta')$
 - Calculate the acceptance ratio $\alpha = \frac{p(\theta')p(data|\theta')}{p(\theta_t)p(data|\theta_t)}$
 - Accept or reject
 - o Generate a uniform number u between 0 and 1
 - o If $u \leq \alpha$ accept the proposed parameters by setting $\theta_{t+1} = \theta'$
 - o If $u > \alpha$ reject the proposed parameters by setting $\theta_{t+1} = \theta_t$

Figure 1-4: Pseudocode for an MCMC sampler with a symmetrical proposal distribution

For parallel tempering, multiple chains are run at different temperatures, where higher temperatures accept lower likelihoods. After a given number of iterations, swaps between neighbouring chains are proposed. These swaps are accepted dependent on the likelihood and temperature difference between the chains, as shown in equation 5.

$$A_{i,j} = \min\left\{e^{\left(\frac{LL(i) - LL(j)}{\tau_j - \tau_i}\right)}, 1\right\} \quad (5)$$

Where $A_{i,j}$ is the acceptance probability between chains i and j , τ_i is the inverse of temperature of chain i , and $LL(i)$ is the log likelihood of chain i . This method allows the higher temperature chains explore a boarder range of the parameter spaces, while the lower temperature chains allow precision within the local minima. It is however a more computationally expensive fitting algorithm, as only the samples from the chain at temperature = 1 can be used as the posterior, despite multiple chains being run.

1.1.8 Summary Motivation

There are many gaps in our understanding of pathogen interactions. For influenza and RSV interactions it is still unclear whether biological indications of interaction, influence population level dynamics. In other words, the causal link between interaction within an individual host and the shifts in observed peaks is as yet untested. Regarding coronaviruses, there are many gaps in the knowledge of seasonal coronavirus circulation, including uncertainty in the duration of immunity, the R_0 , and the interactions with other coronaviruses. Specifically, after the initial waves of the SARS-CoV-2, it was hypothesised that cross-protection could have resulted in the reduced susceptibility of children to SARS-CoV-2; however, this could also have resulted from age-assortative mixing patterns or innate susceptibility differences between age groups. In this thesis I aim to address these gaps in what is known.

The key features of the pathogens that govern these interactions are manifold, including the basic viral dynamics, the complicated build-up of immunity within a population due to prior infections and vaccination, and the age assortative mixing patterns and interventions. These elements are all crucial to modelling interactions as they strongly influence pathogen dynamics.

Mathematical modelling is therefore a key tool in the study of pathogen interactions as it allows for the inclusion of such complexities. This is because the researcher can include these attributes of transmission into the mechanisms of the model. Combined with Bayesian fitting methods to match the model to the data, and to include prior information, this set of tools creates a unique opportunity with which to approach the questions of pathogen interactions.

1.2 Aims

The overall aim of this thesis is to infer the strength and duration of cross-protection between respiratory viruses by rigorously fitting mathematical models to surveillance data.

This aim will be met by the following objectives:

- A) Understand whether one can in principle recover interaction parameters from simulated RSV and influenza surveillance data in a modelling framework.
- B) Infer the extent of cross-protection between RSV and influenza using data from 11 years of enhanced surveillance in a Vietnamese hospital, and assess the potential impact of vaccination.
- C) Assess whether cross-protection between seasonal coronaviruses and SARS-CoV-2 can explain the observed age susceptibility profile to SARS-CoV-2 during the first wave of the epidemic in England and Wales, and evaluate the impacts this cross-protection could have on future circulation of SARS-CoV-2.

1.3 Thesis Structure

This thesis is written in a *research paper style*, where each analysis chapter takes the form of a scientific paper that has been / will be published or submitted to a journal, preceded by a bridging section. This introductory chapter provides background on the relevant respiratory viruses, evidence of interaction between them, and mathematical models used to evaluate them. The thesis then contains three analysis chapters, followed by a discussion. The analysis chapters are as follows:

- **Chapter 2: Competition between RSV and influenza: Limits of modelling inference from surveillance data.** This chapter was published in the journal *Epidemics* in 2021. It includes the development of an interaction model between influenza and RSV, and evaluates the accuracy and precision of parameter estimates that can be inferred using data simulated based on the UK surveillance system. This chapter covers the thesis objective A.
- **Chapter 3: Evidence for Influenza and RSV interaction from 10 years of enhanced surveillance in Nha Trang, Vietnam, a modelling study.** This paper is currently being prepared for submission, and infers the strength and duration of cross-protection between RSV and influenza by fitting to positive viral samples from a hospital study in under 5-year-olds in Nha Trang, Vietnam. This covers the thesis objective B.
- **Chapter 4: How immunity from and interaction with seasonal coronaviruses can shape SARS-CoV-2 epidemiology.** This paper was published on *medrxiv* in 2021, and is currently

undergoing review following revision at the *Proceedings of the National Academy of Sciences of the United States of America (PNAS)*. It infers estimates for key seasonal coronavirus parameters, such as the duration of immunity and the basic reproduction number. Using these, it assesses the feasibility of existence of cross-protection from seasonal coronaviruses to SARS-CoV-2, and evaluates whether this cross-protection can explain the reduced susceptibility of children that was observed in the first wave of the pandemic. It also projects the long-term dynamics of both SARS-CoV-2 and seasonal coronaviruses at different levels of cross-protection. This chapter uses England and Wales as a case study, and covers thesis objective C.

1.4 References

1. WHO | Estimates for 2000–2015. *WHO* (2017).
2. Murray, C. S. *et al.* Study of modifiable risk factors for asthma exacerbations: virus infection and allergen exposure increase the risk of asthma hospital admissions in children. *Thorax* **61**, 376–82 (2006).
3. SEEMUNGAL, T. *et al.* Respiratory Viruses, Symptoms, and Inflammatory Markers in Acute Exacerbations and Stable Chronic Obstructive Pulmonary Disease. *American Journal of Respiratory and Critical Care Medicine* **164**, 1618–1623 (2001).
4. Pica, N. & Bouvier, N. M. Environmental factors affecting the transmission of respiratory viruses. *Curr Opin Virol* **2**, 90–95 (2012).
5. Kikkert, M. Innate Immune Evasion by Human Respiratory RNA Viruses. *JIN* **12**, 4–20 (2020).
6. Funk, S., Salathé, M. & Jansen, V. A. A. Modelling the influence of human behaviour on the spread of infectious diseases: a review. *Journal of the Royal Society, Interface* **7**, 1247–56 (2010).
7. Newton, A. H., Cardani, A. & Braciale, T. J. The host immune response in respiratory virus infection: balancing virus clearance and immunopathology. *Semin Immunopathol* **38**, 471–482 (2016).
8. Hirsh, S. *et al.* Epidemiological changes of Respiratory Syncytial Virus (RSV) infections in Israel. *PLoS ONE* **9**, (2014).
9. Meningher, T. *et al.* Relationships between A(H1N1)pdm09 influenza infection and infections with other respiratory viruses. *Influenza and other Respiratory Viruses* **8**, 422–430 (2014).
10. Casalegno, J. S. *et al.* Impact of the 2009 influenza a(H1N1) pandemic wave on the pattern of hibernal respiratory virus epidemics, France, 2009. *Eurosurveillance* **15**, 2 (2010).
11. Mak, G. C., Wong, A. H., Ho, W. Y. Y. & Lim, W. The impact of pandemic influenza A (H1N1) 2009 on the circulation of respiratory viruses 2009-2011. *Influenza and other Respiratory Viruses* **6**, e6-10 (2012).
12. Glezen, W. P., Taber, L. H., Frank, A. L. & Kasel, J. A. Risk of primary infection and reinfection with respiratory syncytial virus. *American journal of diseases of children (1960)* **140**, 543–6 (1986).
13. Drori, Y. *et al.* Influenza virus inhibits respiratory syncytial virus (RSV) infection via a two-wave expression of interferon-induced protein with tetratricopeptide (IFIT) proteins. *bioRxiv* 2020.08.17.253708-2020.08.17.253708 (2020) doi:10.1101/2020.08.17.253708.

14. Lee, Y. J. *et al.* Non-specific Effect of Vaccines: Immediate Protection against Respiratory Syncytial Virus Infection by a Live Attenuated Influenza Vaccine. *Frontiers in Microbiology* **9**, 83 (2018).
15. Laurie, K. L. *et al.* Interval Between Infections and Viral Hierarchy Are Determinants of Viral Interference Following Influenza Virus Infection in a Ferret Model. *Journal of Infectious Diseases* **212**, 1701–1710 (2015).
16. Hamilton, J. Club cells surviving influenza A virus infection induce temporary nonspecific antiviral immunity.
17. Kelly, H., Barry, S., Laurie, K. & Mercer, G. Seasonal influenza vaccination and the risk of infection with pandemic influenza: A possible illustration of nonspecific temporary immunity following infection. *Eurosurveillance* **15**, 19722 (2010).
18. Mandelboim, M. *et al.* Significant cross reactive antibodies to influenza virus in adults and children during a period of marked antigenic drift. *BMC Infectious Diseases* **14**, 346 (2014).
19. Chan, K. H. *et al.* Serological responses in patients with severe acute respiratory syndrome coronavirus infection and cross-reactivity with human coronaviruses 229E, OC43, and NL63. *Clinical and Diagnostic Laboratory Immunology* **12**, 1317–1321 (2005).
20. Grifoni, A. *et al.* Targets of T Cell Responses to SARS-CoV-2 Coronavirus in Humans with COVID-19 Disease and Unexposed Individuals. *Cell* (2020) doi:10.1016/j.cell.2020.05.015.
21. Mateus, J. *et al.* Selective and cross-reactive SARS-CoV-2 T cell epitopes in unexposed humans. *Science* eabd3871–eabd3871 (2020) doi:10.1126/science.abd3871.
22. Braun, J. *et al.* Presence of SARS-CoV-2 reactive T cells in COVID-19 patients and healthy donors. *medRxiv* 2020.04.17.20061440 (2020) doi:10.1101/2020.04.17.20061440.
23. Influenza vaccines: 2020 to 2021 flu season - GOV.UK. <https://www.gov.uk/government/publications/influenza-vaccine-ovalbumin-content/influenza-vaccines-2020-to-2021-flu-season>.
24. WHO | WHO vaccine pipeline tracker. *WHO* (2016).
25. Lafond, K. E. *et al.* Global Role and Burden of Influenza in Pediatric Respiratory Hospitalizations, 1982–2012: A Systematic Analysis. *PLOS Medicine* **13**, e1001977 (2016).
26. JCVI. The national flu immunisation programme 2017 / 18. 1–29 (2017).
27. Baguelin, M. *et al.* Assessing Optimal Target Populations for Influenza Vaccination Programmes: An Evidence Synthesis and Modelling Study. *PLoS Medicine* **10**, (2013).
28. Cromer, D. *et al.* The burden of influenza in England by age and clinical risk group: A statistical analysis to inform vaccine policy. *Journal of Infection* **68**, 363–371 (2014).
29. Annual flu reports - GOV.UK. <https://www.gov.uk/government/statistics/annual-flu-reports>.

30. de Boer, P. T. *et al.* The cost-effectiveness of trivalent and quadrivalent influenza vaccination in communities in South Africa, Vietnam and Australia. *Vaccine* vol. 36 997–1007 (2018).
31. Influenza | Treatment summary | BNF content published by NICE.
<https://bnf.nice.org.uk/treatment-summary/influenza.html>.
32. Centers for Disease Control and Prevention. How the flu virus can change: “Drift” and “shift”. 1600 Clifton Road Atlanta, GA 30329-4027 USA 2014 (2014).
33. Types of Influenza Viruses | CDC. <https://www.cdc.gov/flu/about/viruses/types.htm>.
34. WHO | WHO surveillance case definitions for ILI and SARI. *WHO* (2018).
35. Public Health Data. <https://www.rcgp.org.uk/clinical-and-research/our-programmes/research-and-surveillance-centre/public-health-data.aspx>.
36. Melchior, T. B., Perosa, A. H., Camargo, C. N., Granato, C. & Bellei, N. Influenza virus prevalence in asymptomatic and symptomatic subjects during pandemic and postpandemic periods. *American Journal of Infection Control* **43**, 460–464 (2015).
37. Caini, S. *et al.* Temporal patterns of influenza A and B in tropical and temperate countries: What are the lessons for influenza vaccination? *PLoS ONE* **11**, (2016).
38. Public Health England. *Surveillance of influenza and other respiratory viruses in the UK: Winter 2016 to 2017*. (2017).
39. Phe. *Surveillance of influenza and other respiratory viruses in the United Kingdom: winter 2014 to 2015*. (2015).
40. Shaman, J. *et al.* Absolute Humidity and the Seasonal Onset of Influenza in the Continental United States. **8**, e1000316 (2010).
41. Shaman, J. & Kohn, M. Absolute humidity modulates influenza survival, transmission, and seasonality. *Proceedings of the National Academy of Sciences of the United States of America* **106**, 3243–8 (2009).
42. Lowen, A. C. & Steel, J. Roles of humidity and temperature in shaping influenza seasonality. *Journal of virology* **88**, 7692–5 (2014).
43. Respiratory infections: laboratory reports 2019 - GOV.UK.
44. Ascough, S., Paterson, S. & Chiu, C. Induction and Subversion of Human Protective Immunity: Contrasting Influenza and Respiratory Syncytial Virus. *Frontiers in Immunology* **9**, 323 (2018).
45. Dou, D., Revol, R., Östbye, H., Wang, H. & Daniels, R. Influenza A Virus Cell Entry, Replication, Virion Assembly and Movement. *Front. Immunol.* **0**, (2018).
46. Kirchenbaum, G. A., Carter, D. M. & Ross, T. M. Sequential Infection in Ferrets with Antigenically Distinct Seasonal H1N1 Influenza Viruses Boosts Hemagglutinin Stalk-Specific Antibodies. *Journal of Virology* **90**, 1116–1128 (2016).

47. Laurie, K. L. *et al.* Multiple Infections with Seasonal Influenza A Virus Induce Cross-Protective Immunity against A(H1N1) Pandemic Influenza Virus in a Ferret Model. *The Journal of Infectious Diseases* **202**, 1011–1020 (2010).
48. Carter, D. M. *et al.* Sequential Seasonal H1N1 Influenza Virus Infections Protect Ferrets against Novel 2009 H1N1 Influenza Virus. *Journal of Virology* **87**, 1400–1410 (2013).
49. Margine, I. *et al.* H3N2 Influenza Virus Infection Induces Broadly Reactive Hemagglutinin Stalk Antibodies in Humans and Mice. *Journal of Virology* **87**, 4728–4737 (2013).
50. Hayward, A. C. *et al.* Natural T Cell–mediated Protection against Seasonal and Pandemic Influenza. Results of the Flu Watch Cohort Study. *Am J Respir Crit Care Med* **191**, 1422–1431 (2015).
51. Sridhar, S. *et al.* Cellular immune correlates of protection against symptomatic pandemic influenza. *Nature Medicine* **19**, 1305–1312 (2013).
52. Gill, P. W. & Murphy, A. M. NATURALLY ACQUIRED IMMUNITY TO INFLUENZA TYPE A: A FURTHER PROSPECTIVE STUDY. *Medical Journal of Australia* **2**, 761–765 (1977).
53. FRANK, A. L., TABER, L. H. & PORTER, C. M. INFLUENZA B VIRUS REINFECTION. *American Journal of Epidemiology* **125**, 576–586 (1987).
54. Sonoguchi, T., Naito, H., Hara, M., Takeuchi, Y. & Fukumi, H. Cross-Subtype Protection in Humans During Sequential, Overlapping, and/or Concurrent Epidemics Caused by H3N2 and H1N1 Influenza Viruses. *Journal of Infectious Diseases* **151**, 81–88 (1985).
55. Frank, A. L. & Taber, L. H. Variation in frequency of natural reinfection with influenza A viruses. *Journal of Medical Virology* **12**, 17–23 (1983).
56. Zhang, A., Stacey, H. D., Mullarkey, C. E. & Miller, M. S. Original Antigenic Sin: How First Exposure Shapes Lifelong Anti–Influenza Virus Immune Responses. *The Journal of Immunology* **202**, 335–340 (2019).
57. Shi, T. *et al.* Global, regional, and national disease burden estimates of acute lower respiratory infections due to respiratory syncytial virus in young children in 2015: a systematic review and modelling study. *Lancet (London, England)* **390**, 946–958 (2017).
58. British Medical Association and Royal Pharmaceutical Society of Great Britain. *BNF for Children: British National Formulary - NICE*. (NICE, 2017).
59. Simon, A., Gehrmann, S., Wagenpfeil, G. & Wagenpfeil, S. Use of Palivizumab in Germany – Report from the German Synagis™ Registry 2009 – 2016. *Klinische Pädiatrie* **230**, 263–269 (2018).
60. American Academy of Pediatrics Committee on Infectious Diseases, C. O. I. D. A. B. G. & American Academy of Pediatrics Bronchiolitis Guidelines Committee. Updated guidance for

- palivizumab prophylaxis among infants and young children at increased risk of hospitalization for respiratory syncytial virus infection. *Pediatrics* **134**, 415–20 (2014).
61. Nirsevimab reduced respiratory syncytial virus infections and hospitalisations in preterm infants in Phase IIb trial. <https://www.astrazeneca.com/media-centre/press-releases/2020/nirsevimab-reduced-respiratory-syncytial-virus-infections-and-hospitalisations-in-preterm-infants-in-phase-iib-trial.html>.
 62. Wang, D., Bayliss, S. & Meads, C. Palivizumab for immunoprophylaxis of respiratory syncytial virus (RSV) bronchiolitis in high-risk infants and young children: A systematic review and additional economic modelling of subgroup analyses. *Health Technology Assessment* vol. 15 iii–iv, 1–124 (2011).
 63. [www.gov.uk. Respiratory syncytial virus \(RSV\): symptoms, transmission, prevention, treatment - GOV.UK. https://www.gov.uk/government/publications/respiratory-syncytial-virus-rsv-symptoms-transmission-prevention-treatment/respiratory-syncytial-virus-rsv-symptoms-transmission-prevention-treatment.](https://www.gov.uk/government/publications/respiratory-syncytial-virus-rsv-symptoms-transmission-prevention-treatment/respiratory-syncytial-virus-rsv-symptoms-transmission-prevention-treatment)
 64. Obando-Pacheco, P. *et al.* Respiratory Syncytial Virus Seasonality: A Global Overview. *The Journal of Infectious Diseases* **217**, 1356–1364 (2018).
 65. Waris, M. Pattern of Respiratory Syncytial Virus Epidemics in Finland: Two-Year Cycles with Alternating Prevalence of Groups A and B. *The Journal of Infectious Diseases* **163**, 464–469 (1991).
 66. NOYOLA, D. E. & MANDEVILLE, P. B. Effect of climatological factors on respiratory syncytial virus epidemics. *Epidemiol Infect* **136**, 1328–1332 (2008).
 67. Thongpan, I., Vongpunsawad, S. & Poovorawan, Y. Respiratory syncytial virus infection trend is associated with meteorological factors. *Sci Rep* **10**, 10931 (2020).
 68. Tian, D. D., Jiang, R., Chen, X. J. & Ye, Q. Meteorological factors on the incidence of MP and RSV pneumonia in children. *PLoS ONE* **12**, (2017).
 69. YUSUF, S. *et al.* The relationship of meteorological conditions to the epidemic activity of respiratory syncytial virus. *Epidemiol Infect* **135**, 1077–1090 (2007).
 70. Nair, H. *et al.* Global burden of acute lower respiratory infections due to respiratory syncytial virus in young children: a systematic review and meta-analysis. *Lancet (London, England)* **375**, 1545–55 (2010).
 71. Domachowske, J. B. & Rosenberg, H. F. Respiratory syncytial virus infection: immune response, immunopathogenesis, and treatment. *Clinical microbiology reviews* **12**, 298–309 (1999).

72. Acedo, L., Díez-Domingo, J., Morano, J. A. & Villanueva, R. J. Mathematical modelling of respiratory syncytial virus (RSV): Vaccination strategies and budget applications. *Epidemiology and Infection* **138**, 853–860 (2010).
73. van Asten, L. *et al.* Mortality Attributable to 9 Common Infections: Significant Effect of Influenza A, Respiratory Syncytial Virus, Influenza B, Norovirus, and Parainfluenza in Elderly Persons. *The Journal of Infectious Diseases* **206**, 628–639 (2012).
74. Borchers, A. T., Chang, C., Gershwin, M. E. & Gershwin, L. J. Respiratory syncytial virus - A comprehensive review. *Clinical Reviews in Allergy and Immunology* vol. 45 331–379 (2013).
75. Imaz, M. S. *et al.* Clinical and epidemiologic characteristics of respiratory syncytial virus subgroups A and B infections in Santa Fe, Argentina. *Journal of Medical Virology* **61**, 76–80 (2000).
76. Walsh, E. E., McConnochie, K. M., Long, C. E. & Hall, C. B. Severity of Respiratory Syncytial Virus Infection Is Related to Virus Strain.
77. De Paulis, M. *et al.* Severity of viral coinfection in hospitalized infants with respiratory syncytial virus infection. *Jornal de pediatria* **87**, 307–313 (2011).
78. Kaplan, N. M. *et al.* Molecular epidemiology and disease severity of respiratory syncytial virus in relation to other potential pathogens in children hospitalized with acute respiratory infection in Jordan. *Journal of Medical Virology* **80**, 168–174 (2008).
79. Kneyber, M. C. *et al.* Relationship between clinical severity of respiratory syncytial virus infection and subtype. *Arch Dis Child* **75**, 137–140 (1996).
80. Hornsleth, A. *et al.* Severity of respiratory syncytial virus disease related to type and genotype of virus and to cytokine values in nasopharyngeal secretions. *Pediatric Infectious Disease Journal* **17**, 1114–1121 (1998).
81. WHO Coronavirus Disease (COVID-19) Dashboard | WHO Coronavirus Disease (COVID-19) Dashboard. <https://covid19.who.int/>.
82. Nickbakhsh, S. *et al.* Epidemiology of Seasonal Coronaviruses: Establishing the Context for the Emergence of Coronavirus Disease 2019. *The Journal of Infectious Diseases* **222**, 17–25 (2020).
83. de Wit, E., van Doremalen, N., Falzarano, D. & Munster, V. J. SARS and MERS: recent insights into emerging coronaviruses. *Nat Rev Microbiol* **14**, 523–534 (2016).
84. Monto, A. S. *et al.* Coronavirus Occurrence and Transmission Over 8 Years in the HIVE Cohort of Households in Michigan. *The Journal of infectious diseases* **222**, 9–16 (2020).
85. Gaunt, E. R., Hardie, A., Claas, E. C. J., Simmonds, P. & Templeton, K. E. Epidemiology and clinical presentations of the four human coronaviruses 229E, HKU1, NL63, and OC43

- detected over 3 years using a novel multiplex real-time PCR method. *Journal of Clinical Microbiology* **48**, 2940–2947 (2010).
86. Li, Y., Wang, X. & Nair, H. Global Seasonality of Human Seasonal Coronaviruses: A Clue for Postpandemic Circulating Season of Severe Acute Respiratory Syndrome Coronavirus 2? *The Journal of Infectious Diseases* (2020) doi:10.1093/infdis/jiaa436.
 87. Dijkman, R. *et al.* Human coronavirus NL63 and 229E seroconversion in children. *J Clin Microbiol* **46**, 2368–2373 (2008).
 88. Edridge, A. W. *et al.* Coronavirus protective immunity is short-lasting. *medRxiv* 2020.05.11.20086439 (2020) doi:10.1101/2020.05.11.20086439.
 89. Galanti, M. & Shaman, J. *Direct observation of repeated infections with endemic coronaviruses*. 2020.04.27.20082032 (Oxford University Press (OUP), 2020).
 90. Callow, K. A., Parry, H. F., Sergeant, M. & Tyrrell, D. A. J. The time course of the immune response to experimental coronavirus infection of man. *Epidemiology and Infection* **105**, 435–446 (1990).
 91. Aldridge, R. W. *et al.* Seasonality and immunity to laboratory-confirmed seasonal coronaviruses (HCoV-NL63, HCoV-OC43, and HCoV-229E): results from the Flu Watch cohort study. *Wellcome Open Res* **5**, 52 (2020).
 92. Reed, S. E. The behaviour of recent isolates of human respiratory coronavirus in vitro and in volunteers: evidence of heterogeneity among 229E-related strains. *J Med Virol* **13**, 179–192 (1984).
 93. Edridge, A. W. *et al.* Coronavirus protective immunity is short-lasting. *medRxiv* 2020.05.11.20086439-2020.05.11.20086439 (2020) doi:10.1101/2020.05.11.20086439.
 94. Eguia, R. *et al.* A human coronavirus evolves antigenically to escape antibody immunity. *bioRxiv* 2020.12.17.423313-2020.12.17.423313 (2020) doi:10.1101/2020.12.17.423313.
 95. CDC SARS Response Timeline | About | CDC. <https://www.cdc.gov/about/history/sars/timeline.htm> (2021).
 96. CDC. About MERS. *Centers for Disease Control and Prevention* <https://www.cdc.gov/coronavirus/mers/about/index.html> (2019).
 97. Ng, O.-W. *et al.* Memory T cell responses targeting the SARS coronavirus persist up to 11 years post-infection. *Vaccine* **34**, 2008–2014 (2016).
 98. Immune responses and immunity to SARS-CoV-2. *European Centre for Disease Prevention and Control* <https://www.ecdc.europa.eu/en/covid-19/latest-evidence/immune-responses>.

99. Engl, P. H. Past COVID-19 infection provides some immunity but people may still carry and transmit virus. *GOV.UK* <https://www.gov.uk/government/news/past-covid-19-infection-provides-some-immunity-but-people-may-still-carry-and-transmit-virus>.
100. Dan, J. M. *et al.* Immunological memory to SARS-CoV-2 assessed for up to 8 months after infection. *Science* **371**, (2021).
101. Tillett, R. L. *et al.* Genomic evidence for reinfection with SARS-CoV-2: a case study. *The Lancet Infectious Diseases* **0**, (2020).
102. Stokel-Walker, C. What we know about covid-19 reinfection so far. *BMJ* **372**, n99 (2021).
103. Viner, R. M. *et al.* Susceptibility to SARS-CoV-2 Infection Among Children and Adolescents Compared With Adults. *JAMA Pediatrics* (2020) doi:10.1001/jamapediatrics.2020.4573.
104. Davies, N. G. *et al.* Age-dependent effects in the transmission and control of COVID-19 epidemics. *Nature medicine* 1–7 (2020) doi:10.1038/s41591-020-0962-9.
105. Gaskell, K. M. *et al.* Extremely high SARS-CoV-2 seroprevalence in a strictly-Orthodox Jewish community in the UK. *medRxiv* 2021.02.01.21250839 (2021) doi:10.1101/2021.02.01.21250839.
106. Li, X. *et al.* The role of children in transmission of SARS-CoV-2: A rapid review. *J Glob Health* **10**, 011101 (2020).
107. Lai, C.-C., Wang, J.-H. & Hsueh, P.-R. Population-based seroprevalence surveys of anti-SARS-CoV-2 antibody: An up-to-date review. *Int J Infect Dis* **101**, 314–322 (2020).
108. Mossong, J. *et al.* Social contacts and mixing patterns relevant to the spread of infectious diseases. *PLoS Medicine* **5**, 0381–0391 (2008).
109. Kasuga, Y., Zhu, B., Jang, K.-J. & Yoo, J.-S. Innate immune sensing of coronavirus and viral evasion strategies. *Exp Mol Med* **53**, 723–736 (2021).
110. Vafaeinezhad, A., Atashzar, M. R. & Baharlou, R. The Immune Responses against Coronavirus Infections: Friend or Foe? *IAA* **182**, 863–876 (2021).
111. Opatowski, L., Baguelin, M. & Eggo, R. M. REVIEW Influenza Interaction with Cocirculating Pathogens, and Its Impact on Surveillance, Pathogenesis and Epidemic Profile: A Key Role for Mathematical Modeling. *PLOS Pathogens* **14**, e1006770 (2017).
112. Watson, R. L., Koff, E. M. de & Bogaert, D. Characterising the respiratory microbiome. *European Respiratory Journal* **53**, (2019).
113. Santacrose, L. *et al.* The Human Respiratory System and its Microbiome at a Glimpse. *Biology (Basel)* **9**, E318 (2020).

114. Gröndahl, B. *et al.* The 2009 pandemic influenza A(H1N1) coincides with changes in the epidemiology of other viral pathogens causing acute respiratory tract infections in children. *Infection* **42**, 303–308 (2014).
115. Glezen, W. P., Paredes, A. & Taber, L. H. Influenza in Children. *JAMA* **243**, 1345 (1980).
116. Anestad, G. & Nordbo, S. A. Interference between outbreaks of respiratory viruses. *Euro surveillance : bulletin européen sur les maladies transmissibles = European communicable disease bulletin* vol. 14 19359 (2009).
117. van Asten, L. *et al.* Early occurrence of influenza A epidemics coincided with changes in occurrence of other respiratory virus infections. *Influenza and Other Respiratory Viruses* **10**, 14–26 (2016).
118. Nishimura, N., Nishio, H., Lee, M. J. & Uemura, K. The clinical features of respiratory syncytial virus: Lower respiratory tract infection after upper respiratory tract infection due to influenza virus. *Pediatrics International* **47**, 412–416 (2005).
119. Meskill, S. D., Revell, P. A., Chandramohan, L. & Cruz, A. T. Prevalence of co-infection between respiratory syncytial virus and influenza in children. *The American journal of emergency medicine* **35**, 495–498 (/03//).
120. Gomez, G. B., Mahé, C. & Chaves, S. S. Uncertain effects of the pandemic on respiratory viruses. *Science* **372**, 1043–1044 (2021).
121. McNab, S. *et al.* Changing Epidemiology of Respiratory Syncytial Virus in Australia - delayed re-emergence in Victoria compared to WA/NSW after prolonged lock-down for COVID-19. *Clinical Infectious Diseases* (2021) doi:10.1093/cid/ciab240.
122. Pinky, L. & Dobrovolny, H. M. Coinfections of the respiratory tract: Viral competition for resources. *PLoS ONE* **11**, (2016).
123. Shinjoh, M., Omoe, K., Saito, N., Matsuo, N. & Nerome, K. In vitro growth profiles of respiratory syncytial virus in the presence of influenza virus. *Acta virologica* **44**, 91–7 (2000).
124. Yoshida, L.-M. *et al.* Respiratory syncytial virus: co-infection and paediatric lower respiratory tract infections. *The European respiratory journal* **42**, 461–469 (2013).
125. De Paulis, M. *et al.* Severity of viral coinfection in hospitalized infants with respiratory syncytial virus infection. *Jornal de pediatria* **87**, 307–313 (2011).
126. Arruda, E. *et al.* The burden of single virus and viral coinfections on severe lower respiratory tract infections among preterm infants: a prospective birth cohort study in Brazil. *The Pediatric infectious disease journal* **33**, 997–1003 (2014).

127. Harada, Y. *et al.* Does respiratory virus coinfection increase the clinical severity of acute respiratory infection among children infected with respiratory syncytial virus? *The Pediatric infectious disease journal* **32**, 441–445 (2013).
128. Weinberger, D. M. *et al.* Pneumococcal disease seasonality: incidence, severity and the role of influenza activity. *European Respiratory Journal* **43**, 833–841 (2014).
129. Weinberger, D. M., Klugman, K. P., Steiner, C. A., Simonsen, L. & Viboud, C. Association between Respiratory Syncytial Virus Activity and Pneumococcal Disease in Infants: A Time Series Analysis of US Hospitalization Data. *PLOS Medicine* **12**, e1001776 (2015).
130. Valkenburg, S. A. *et al.* Immunity to seasonal and pandemic influenza A viruses. *Microbes and infection* **13**, 489–501 (2011).
131. Walzl, G., Tafuro, S., Moss, P., Openshaw, P. J. & Hussell, T. Influenza virus lung infection protects from respiratory syncytial virus-induced immunopathology. *The Journal of experimental medicine* **192**, 1317–26 (2000).
132. Ferguson, N. M., Galvani, A. P. & Bush, R. M. Ecological and immunological determinants of influenza evolution. *Nature* **422**, 428–433 (2003).
133. Che, X. *et al.* Antigenic Cross-Reactivity between Severe Acute Respiratory Syndrome–Associated Coronavirus and Human Coronaviruses 229E and OC43. *The Journal of Infectious Diseases* **191**, 2033–2037 (2005).
134. Chan, K. H. *et al.* Cross-reactive antibodies in convalescent SARS patients' sera against the emerging novel human coronavirus EMC (2012) by both immunofluorescent and neutralizing antibody tests. *Journal of Infection* **67**, 130–140 (2013).
135. Ng, K. *et al.* Pre-existing and de novo humoral immunity to SARS-CoV-2 in humans. *bioRxiv* 2020.05.14.095414 (2020) doi:10.1101/2020.05.14.095414.
136. Hicks, J. *et al.* Serologic Cross-Reactivity of SARS-CoV-2 with Endemic and Seasonal Betacoronaviruses. *J Clin Immunol* (2021) doi:10.1007/s10875-021-00997-6.
137. Anderson, E. M. *et al.* Seasonal human coronavirus antibodies are boosted upon SARS-CoV-2 infection but not associated with protection. *medRxiv* 2020.11.06.20227215-2020.11.06.20227215 (2020) doi:10.1101/2020.11.06.20227215.
138. Chen, Y. *et al.* Influenza infection in humans induces broadly cross-reactive and protective neuraminidase-reactive antibodies. *Cell* **173**, 417–429.e10 (2018).
139. Seow, J. *et al.* Longitudinal evaluation and decline of antibody responses in SARS-CoV-2 infection. *medRxiv* 2020.07.09.20148429 (2020) doi:10.1101/2020.07.09.20148429.
140. Welsh, R. M. & Selin, L. K. No one is naive: The significance of heterologous T-cell immunity. *Nature Reviews Immunology* vol. 2 417–426 (2002).

141. Zhao, J. *et al.* Airway Memory CD4+ T Cells Mediate Protective Immunity against Emerging Respiratory Coronaviruses. *Immunity* **44**, 1379–1391 (2016).
142. Bert, N. Le *et al.* Different pattern of pre-existing SARS-COV-2 specific T cell immunity in SARS-recovered and uninfected individuals. *bioRxiv* 2020.05.26.115832 (2020)
doi:10.1101/2020.05.26.115832.
143. Weiskopf, D. *et al.* Phenotype of SARS-CoV-2-specific T-cells in COVID-19 patients with acute respiratory distress syndrome. *medRxiv* 2020.04.11.20062349 (2020)
doi:10.1101/2020.04.11.20062349.
144. Saletti, G. *et al.* Older adults lack SARS CoV-2 cross-reactive T lymphocytes directed to human coronaviruses OC43 and NL63. *Scientific Reports* **10**, 21447 (2020).
145. Grant, E. J. *et al.* Broad CD8+ T cell cross-recognition of distinct influenza A strains in humans. *Nat Commun* **9**, 5427 (2018).
146. Koutsakos, M. *et al.* Human CD8+ T cell cross-reactivity across influenza A, B and C viruses. *Nat Immunol* **20**, 613–625 (2019).
147. Paynter, S. *et al.* Using Mathematical Transmission Modelling to Investigate Drivers of Respiratory Syncytial Virus Seasonality in Children in the Philippines. *PLoS ONE* **9**, e90094 (2014).
148. Bock Axelsen, J., Yaari, R., Grenfell, B. T. & Stone, L. Multiannual forecasting of seasonal influenza dynamics reveals climatic and evolutionary drivers. doi:10.1073/pnas.1321656111.
149. Hogan, A. *et al.* Potential impact of a maternal vaccine for RSV: A mathematical modelling study.
150. Vynnycky, E., Pitman, R., Siddiqui, R., Gay, N. & Edmunds, W. J. Estimating the impact of childhood influenza vaccination programmes in England and Wales. *Vaccine* **26**, 5328–5337 (2008).
151. Ross, R. An application of the theory of probabilities to the study of a priori pathometry.—Part I. *Proceedings of the Royal Society of London. Series A, Containing Papers of a Mathematical and Physical Character* **92**, 204–230 (1916).
152. Ross, R. & Hudson, H. P. An application of the theory of probabilities to the study of a priori pathometry.—Part II. *Proceedings of the Royal Society of London. Series A, Containing Papers of a Mathematical and Physical Character* **93**, 212–225 (1917).
153. Ross, R. & Hudson, H. P. An application of the theory of probabilities to the study of a priori pathometry.—Part III. *Proceedings of the Royal Society of London. Series A, Containing Papers of a Mathematical and Physical Character* **93**, 225–240 (1917).

154. Kermack, W. O., McKendrick, A. G. & Walker, G. T. A contribution to the mathematical theory of epidemics. *Proceedings of the Royal Society of London. Series A, Containing Papers of a Mathematical and Physical Character* **115**, 700–721 (1927).
155. Kucharski, A. J., Andreasen, V. & Gog, J. R. Capturing the dynamics of pathogens with many strains. *Journal of Mathematical Biology* **72**, 1–24 (2016).
156. Pitman, R., White, L. & Sculpher, M. Estimating the clinical impact of introducing paediatric vaccination in England and Wales. *Vaccine* (2011).
157. Finkenstt Adt, B. F., Morton, A. & Rand, D. A. Modelling antigenic drift in weekly influenza incidence. *STATISTICS IN MEDICINE Statist. Med* **24**, 3447–3461 (2005).
158. Goeyvaerts, N. *et al.* Estimating dynamic transmission model parameters for seasonal influenza by fitting to age and season-specific influenza-like illness incidence. *Epidemics* **13**, 1–9 (2015).
159. White, L. J. *et al.* The transmission dynamics of groups A and B human respiratory syncytial virus (hRSV) in England & Wales and Finland: seasonality and cross-protection. *Epidemiology and Infection* **133**, 279–289 (2005).
160. Yamin, D. *et al.* Vaccination strategies against respiratory syncytial virus. doi:10.1073/pnas.1522597113.
161. Kinyanjui, T. M. *et al.* Vaccine Induced Herd Immunity for Control of Respiratory Syncytial Virus Disease in a Low-Income Country Setting. *PloS one* **10**, e0138018 (2015).
162. Moore, H. C., Jacoby, P., Hogan, A. B., Blyth, C. C. & Mercer, G. N. Modelling the Seasonal Epidemics of Respiratory Syncytial Virus in Young Children. *PloS one* **9**, e100422 (2014).
163. Pitzer, V. E. *et al.* Environmental drivers of the spatiotemporal dynamics of respiratory syncytial virus in the United States. **11**, e1004591 (2015).
164. Pan-Ngum, W. *et al.* Predicting the relative impacts of maternal and neonatal respiratory syncytial virus (RSV) vaccine target product profiles: A consensus modelling approach. *Vaccine* **35**, 403–409 (2017).
165. Bauch, C. T., Lloyd-Smith, J. O., Coffee, M. P. & Galvani, A. P. Dynamically modeling SARS and other newly emerging respiratory illnesses: past, present, and future. *Epidemiology* **16**, 791–801 (2005).
166. Wang, W. & Ruan, S. Simulating the SARS outbreak in Beijing with limited data. *J Theor Biol* **227**, 369–379 (2004).
167. Gumel, A. B. *et al.* Modelling strategies for controlling SARS outbreaks. *Proc Biol Sci* **271**, 2223–2232 (2004).

168. Riley, S. *et al.* Transmission dynamics of the etiological agent of SARS in Hong Kong: impact of public health interventions. *Science* **300**, 1961–1966 (2003).
169. Lloyd-Smith, J. O., Galvani, A. P. & Getz, W. M. Curtailing transmission of severe acute respiratory syndrome within a community and its hospital. *Proc Biol Sci* **270**, 1979–1989 (2003).
170. Panovska-Griffiths, J. *et al.* Determining the optimal strategy for reopening schools, the impact of test and trace interventions, and the risk of occurrence of a second COVID-19 epidemic wave in the UK: a modelling study. *Lancet Child Adolesc Health* **4**, 817–827 (2020).
171. Choi, B. C. K. & Pak, A. W. P. A simple approximate mathematical model to predict the number of severe acute respiratory syndrome cases and deaths. *J Epidemiol Community Health* **57**, 831–835 (2003).
172. Xia, Z.-Q., Zhang, J., Xue, Y.-K., Sun, G.-Q. & Jin, Z. Modeling the Transmission of Middle East Respirator Syndrome Corona Virus in the Republic of Korea. *PLoS One* **10**, e0144778 (2015).
173. Masuda, N., Konno, N. & Aihara, K. Transmission of severe acute respiratory syndrome in dynamical small-world networks. *Phys. Rev. E* **69**, 031917 (2004).
174. Meyers, L. A., Pourbohloul, B., Newman, M. E. J., Skowronski, D. M. & Brunham, R. C. Network theory and SARS: predicting outbreak diversity. *J Theor Biol* **232**, 71–81 (2005).
175. Chowell, G., Fenimore, P. W., Castillo-Garsow, M. A. & Castillo-Chavez, C. SARS outbreaks in Ontario, Hong Kong and Singapore: the role of diagnosis and isolation as a control mechanism. *J Theor Biol* **224**, 1–8 (2003).
176. Ng, T. W., Turinici, G. & Danchin, A. A double epidemic model for the SARS propagation. *BMC Infectious Diseases* **3**, 19 (2003).
177. Kim, Y., Ryu, H. & Lee, S. Agent-Based Modeling for Super-Spreading Events: A Case Study of MERS-CoV Transmission Dynamics in the Republic of Korea. *Int J Environ Res Public Health* **15**, E2369 (2018).
178. Lee, J., Chowell, G. & Jung, E. A dynamic compartmental model for the Middle East respiratory syndrome outbreak in the Republic of Korea: A retrospective analysis on control interventions and superspreading events. *J Theor Biol* **408**, 118–126 (2016).
179. Marimuthu, Y., Nagappa, B., Sharma, N., Basu, S. & Chopra, K. K. COVID-19 and tuberculosis: A mathematical model based forecasting in Delhi, India. *Indian J Tuberc* **67**, 177–181 (2020).
180. Russell, T. W. *et al.* Estimating the infection and case fatality ratio for coronavirus disease (COVID-19) using age-adjusted data from the outbreak on the Diamond Princess cruise ship, February 2020. *Euro Surveill* **25**, (2020).

181. Bedford, T., Rambaut, A. & Pascual, M. Canalization of the evolutionary trajectory of the human influenza virus. *BMC Biology* **10**, 38 (2012).
182. Kucharski, A. J. & Gog, J. R. Age profile of immunity to influenza: Effect of original antigenic sin. *Theoretical Population Biology* **81**, 102–112 (2012).
183. Lin, J., Andreasen, V. & Levin, S. A. Dynamics of influenza A drift: the linear three-strain model. *Mathematical Biosciences* **162**, 33–51 (1999).
184. Gog, J. R. & Grenfell, B. T. Dynamics and selection of many-strain pathogens. *Proceedings of the National Academy of Sciences* **99**, 17209–17214 (2002).
185. Kryazhimskiy, S., Dieckmann, U., Levin, S. A. & Dushoff, J. On state-space reduction in multi-strain pathogen models, with an application to antigenic drift in influenza A. *PLoS Computational Biology* **3**, 1513–1525 (2007).
186. Shrestha, S. *et al.* The role of influenza in the epidemiology of pneumonia. *Scientific Reports* **5**, 15314 (2015).
187. Velasco-Hernández, J. X., Núñez-López, M., Comas-García, A., Cherpitel, D. E. N. & Ocampo, M. C. Superinfection between Influenza and RSV alternating patterns in San Luis Potosí State, México. *PLoS ONE* **10**, (2015).
188. Pinky, L. & Dobrovolny, H. M. SARS-CoV-2 coinfections: Could influenza and the common cold be beneficial? *J Med Virol* 10.1002/jmv.26098 (2020) doi:10.1002/jmv.26098.
189. Kissler, S. M. Projecting the transmission dynamics of SARS-CoV-2 through the postpandemic period | Science. <https://science.sciencemag.org/content/368/6493/860>.
190. Gog, J. R. & Swinton, J. A status-based approach to multiple strain dynamics. *Journal of Mathematical Biology* **44**, 169–184 (2002).
191. Shrestha, S., King, A. A. & Rohani, P. Statistical Inference for Multi-Pathogen Systems. *PLoS Computational Biology* **7**, e1002135 (2011).
192. Bottomley, C., Roca, A., Hill, P. C., Greenwood, B. & Isham, V. A mathematical model of serotype replacement in pneumococcal carriage following vaccination. *J R Soc Interface* **10**, 20130786 (2013).
193. Melegaro, A. *et al.* Dynamic models of pneumococcal carriage and the impact of the Heptavalent Pneumococcal Conjugate Vaccine on invasive pneumococcal disease. *BMC Infect Dis* **10**, 90 (2010).
194. Choi, Y. H. *et al.* 7-Valent Pneumococcal Conjugate Vaccination in England and Wales: Is It Still Beneficial Despite High Levels of Serotype Replacement? *PLoS One* **6**, e26190 (2011).

195. Melegaro, A., Choi, Y., Pebody, R. & Gay, N. Pneumococcal Carriage in United Kingdom Families: Estimating Serotype-specific Transmission Parameters from Longitudinal Data. *American Journal of Epidemiology* **166**, 228–235 (2007).
196. Convergence Diagnostics for Markov Chain Monte Carlo | Annual Review of Statistics and Its Application. <https://www.annualreviews.org/doi/full/10.1146/annurev-statistics-031219-041300>.

2 Chapter 2: Competition between RSV and influenza: Limits of modelling inference from surveillance data

2.1 Research Paper cover sheet



London School of Hygiene & Tropical Medicine
Keppel Street, London WC1E 7HT

T: +44 (0)20 7299 4646
F: +44 (0)20 7299 4656
www.lshtm.ac.uk

RESEARCH PAPER COVER SHEET

Please note that a cover sheet must be completed for each research paper included within a thesis.

SECTION A – Student Details

Student ID Number	1402815	Title	Mrs
First Name(s)	Naomi Ruth		
Surname/Family Name	Waterlow		
Thesis Title	Mathematical Modelling of Cross-protection between Respiratory Viruses		
Primary Supervisor	Dr. Rosalind M Eggo		

If the Research Paper has previously been published please complete Section B, if not please move to Section C.

SECTION B – Paper already published

Where was the work published?	Epidemics		
When was the work published?	Available online 26 March 2021, published in Volume 35, June 2021		
If the work was published prior to registration for your research degree, give a brief rationale for its inclusion	NA		
Have you retained the copyright for the work?*	Yes	Was the work subject to academic peer review?	Yes

*If yes, please attach evidence of retention. If no, or if the work is being included in its published format, please attach evidence of permission from the copyright holder (publisher or other author) to include this work.

SECTION C – Prepared for publication, but not yet published

Where is the work intended to be published?	
Please list the paper's authors in the intended authorship order:	
Stage of publication	Choose an item.

Improving health worldwide


www.lshtm.ac.uk

SECTION D – Multi-authored work

For multi-authored work, give full details of your role in the research included in the paper and in the preparation of the paper. (Attach a further sheet if necessary)	I worked on: Conceptualisation, Methodology, Software, Validation, Formal Analysis, Writing – Original Draft, Visualization.
--	--

SECTION E

Student Signature	
Date	30/06/2021

Supervisor Signature	
Date	24 Aug 21

Paper and copyright available here:
<https://www.sciencedirect.com/science/article/pii/S1755436521000190?via%3Dihub>
© 2021 The Authors. Published by Elsevier B.V.

2.2 Bridging section

This paper was published in *Epidemics* in Volume 35, June 2021¹. It presents a transmission model that allows for interaction between RSV and influenza and tests its robustness on simulated data based on the UK surveillance system.

Cross-protection of RSV and influenza can be mechanistically included in dynamic models, allowing the estimation of the extent of cross-protection. However, it is unclear if the impacts of this are significant enough to be detectable at the population level, which is of particular concern if there is weak cross-protection, or if the duration is very short. Shrestha et al. (2011)² developed a pathogen non-specific model to investigate the identifiability of cross-protection, simulating monthly infections for 40 years and looking at three different scenarios with different types of interaction. However, this wealth of data is rarely available, and the peculiarities of each pathogen and setting will have an impact on the identifiability of the parameters. In this paper I set up a model that is specific for RSV and influenza, mimicking surveillance data collected in the UK³. I chose the UK as it has a consistent and reliable surveillance system for respiratory pathogens. In addition, I had permission to use the data and fitting the model to this was the original plan for Chapter 3. Unfortunately, this did not end up being possible due to accessibility issues because of the SARS-CoV-2 pandemic.

This Chapter validates the model used and sets the scene for fitting to real surveillance data. It demonstrates areas of parameter space where results are less trust-worthy, as well as showing the importance of fitting to multiple seasons. I take these lessons learned forward into the following chapters. As mentioned, I planned but was unable to use data from Public Health England in the next chapter. Instead, I adapt this model to fit data from Vietnam in Chapter 4. This model is also the base from which the model in Chapter 5 was developed from.

I developed the model, wrote all the code, and performed the fitting analysis. I also wrote the paper and made the figures. Throughout the process I received input/suggestions/edits from both my supervisors. After comments from review at a journal from which it was rejected, I made significant edits based on the reviewer comments, and a colleague (Dr. Amanda Minter, an author on the paper) also provided guidance at this stage. The version shown in this chapter is the final accepted version by the journal.

The Supplementary material of the original paper covers extra details on the methods and additional simulation results. This is included as Appendix A in this thesis, so any references to supplementary material can be found there.

2.3 Abstract and Author Summary

Competition between RSV and influenza: limits of modelling inference from surveillance data

Naomi R Waterlow^{1*}, Stefan Flasche¹, Amanda Minter¹, Rosalind M Eggo¹

¹Department of Infectious Disease Epidemiology, London School of Hygiene & Tropical Medicine, UK

Abstract

Respiratory Syncytial Virus (RSV) and Influenza cause a large burden of disease. Evidence of their interaction via temporary cross-protection implies that prevention of one could inadvertently lead to an increase in the burden of the other. However, evidence for the public health impact of such interaction is sparse and largely derives from ecological analyses of peak shifts in surveillance data. To test the robustness of estimates of interaction parameters between RSV and Influenza from surveillance data we conducted a simulation and back-inference study. We developed a two-pathogen interaction model, parameterised to simulate RSV and Influenza epidemiology in the UK. Using the infection model in combination with a surveillance-like stochastic observation process we generated a range of possible RSV and Influenza trajectories and then used Markov Chain Monte Carlo (MCMC) methods to back-infer parameters including those describing competition. We find that in most scenarios both the strength and duration of RSV and Influenza interaction could be estimated from the simulated surveillance data reasonably well. However, the robustness of inference declined towards the extremes of the plausible parameter ranges, with misleading results. It was for instance not possible to tell the difference between low/moderate interaction and no interaction. In conclusion, our results illustrate that in a plausible parameter range, the strength of RSV and Influenza interaction can be estimated from a single season of high-quality surveillance data but also highlights the importance to test parameter identifiability *a priori* in such situations.

Author Summary

Influenza and Respiratory Syncytial Virus (RSV) cause a large disease burden. Rather than acting independently these viruses may interact, meaning that infection with one decreases the likelihood of infection with the other. While this could have important implications for control strategies, the evidence for the strength of the interaction and its importance for public health is largely based on ecological studies, and it is not clear that surveillance data are sufficient to determine if interaction exists, and if so, how long the effect last. To test this assumption we used a mathematical model to simulate RSV and Influenza surveillance data and back-infer the strength and duration of interaction

used to generate the data. We found that in the majority of cases it was possible to determine the strength and duration of interaction from even a single season of high-quality surveillance. However, we also showed that for extreme parameter values, model estimates may be unreliable despite a seemingly good fit to the data and hence highlight the importance of *a priori* model validation for similar analyses.

2.4 Introduction

Respiratory Syncytial Viruses (RSV) and seasonal influenza viruses cause large burdens of respiratory disease, including in young children^{4,5}. RSV was recently identified as the primary cause of hospitalisation for severe paediatric pneumonia⁶, particularly in the neonatal period. In the northern hemisphere both viruses cause pronounced annual winter epidemics peaking between October and March⁷.

Evidence from epidemiological and biological studies implies there is competitive interaction between influenza and RSV⁸⁻¹³. The biological mechanism for competition is activation of the innate “antiviral response” by infection that can inhibit further or subsequent infection¹³⁻¹⁵, resulting in a period of cross-protection during and after infection. Mouse studies have shown this effect, where following influenza infection or live attenuated influenza vaccination (LAIV), RSV replication/severity was decreased^{13,15}. Within-host animal studies, both *in vitro* and modelling, have shown that the growth rates of the viruses can be affected by other viruses present^{16,17}. The duration of this cross-reactive response is debated, varying from “short-term”¹⁸, less than two weeks¹⁹ or up to 3 months²⁰. Influenza epidemics caused by different strains are thought to exhibit competitive exclusion^{8,21,22}, and for RSV and influenza syndromic surveillance has shown shifts in the seasonal incidence peaks of RSV following abnormal (pandemic or early) influenza seasons^{10,23-27}, which suggest this mechanism may not only occur but can substantially alter the epidemiology of influenza and RSV. There is, however, little evidence that links the strength of competition between RSV and influenza within a host to observed population dynamics. Understanding the dynamics is critical for predicting the effects of alteration of their ecological balance, for example through vaccination programs, and is the motivation for this study.

Influenza vaccination rates, especially in key transmission groups could disrupt transmission, potentially leading to effects on interacting viruses. In the UK, the RSV epidemic usually precedes the influenza epidemic by one or two months, so reduced influenza transmission as a result of childhood influenza vaccination may not affect RSV transmission dynamics. However, the competitive pressure

exhibited by RSV on influenza may become highly relevant soon. The only RSV vaccine candidate yet that completed Phase 3 trials, the maternal vaccine, Novavax, demonstrated only partial efficacy that the Advisory Committee for Immunization Practices in the US deemed insufficient to warrant licensure²⁸. However, the RSV vaccine pipeline contains a number of Phase 1 and 2 candidates that aim to protect children in part by limiting RSV circulation. As such, these future RSV vaccines have the potential to decrease the competitive pressure on influenza and thereby increase influenza as an unintended consequence, both in children and other age groups, as children are a key driver of transmission. These impacts will need to be considered as part of their cost benefit proposition preceding routine use.

Mathematical modelling is an important tool for testing mechanisms and hypotheses of epidemiologically significant RSV and influenza competition, such as the hypothesis that they competitively interact. Models offer an opportunity to mechanistically combine observations from surveillance data and extrapolate beyond the observed. However, in the case of RSV and influenza competition the identifiability of model parameters from viral surveillance data is uncertain. Hence, we conducted a simulation study to test whether parameters can be back-inferred from a range of realistic model-generated scenarios that include only partial observation of the infection dynamics from surveillance-like data.

2.5 Methods

2.5.1 Model Structure

We developed an age-stratified deterministic compartmental transmission model for RSV and Influenza with interactions (Figure 2-1 and Supplement Section 2). The population could be Susceptible (*S*), Infectious (*I*), Protected (*P*) or Recovered (*R*) for each of RSV and influenza viruses. We simulated one season so we did not consider potential loss of immunity, and current estimates for RSV immunity lasts less than a year²⁹, and we take influenza immunity into account by fitting the percentage susceptible at the start of the season (see below). There were separate transmission and recovery rates for each virus (subscripts RSV and INF), and *i* and *j* denote age groups. Susceptible individuals were infected at rates $\lambda_{INF,i}$ and $\lambda_{RSV,i}$ and enter the *I* compartment. They recovered at rates γ_{INF} and γ_{RSV} , and entered the *P* compartment where they were no longer infectious. In *P*, individuals were fully protected against homologous re-infection and also had some cross protection against the second virus. Loss of cross-protection occurred at rate ρ . Infection with a second virus was less likely in the *I* and *P* classes and occurred at a rate reduced by σ . The key parameters

determining interaction are therefore the strength of competition (σ) and the rate of loss of cross-protection (ρ). Compartments $I_{RSV,i}P_{INF,i}$ and $I_{RSV,i}R_{INF,i}$, as well as $P_{RSV,i}I_{INF,i}$ and $R_{RSV,i}I_{INF,i}$ were combined as they were effectively identical when modelling only one season.

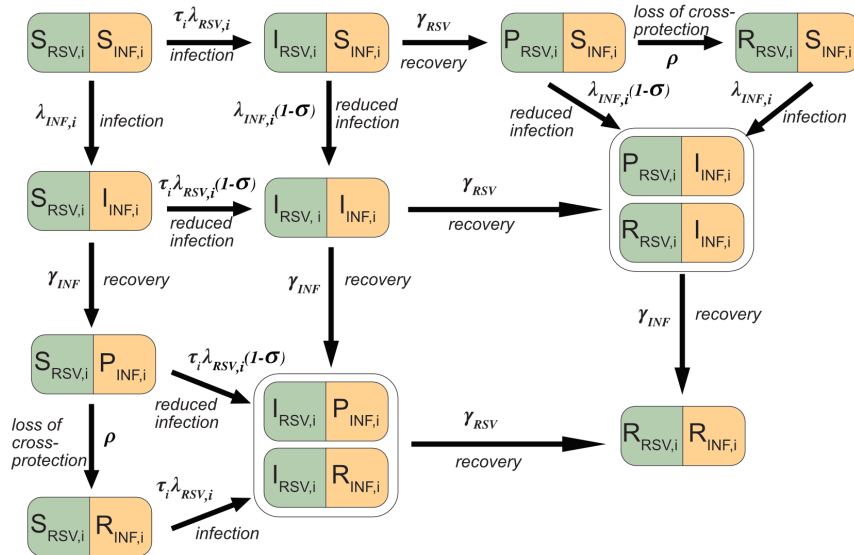


Figure 2-1. Model diagram for RSV and Influenza (INF). Individuals could be either Susceptible (S), Infected (I), Protected (P) or Recovered (R) to either virus. Following infection, (which occurred at rate $\lambda_{RSV,i}$ and $\lambda_{INF,i}$), recovery occurred at a constant rate (γ_{RSV} and γ_{INF}), and the population entered the P state. Here they are immune to the virus they were infected by and protected to a varying extent (σ) against infection from the second virus. This protection waned at rate ρ , and the population entered the R compartment. In the R compartment the population was immune to the virus it was infected by, but not the other virus. We ran the model for one season and compartments $I_{RSV,i}P_{INF,i}$ and $I_{RSV,i}R_{INF,i}$ were combined, and $P_{RSV,i}I_{INF,i}$ and $R_{RSV,i}I_{INF,i}$ were combined, because they are effectively identical. Parameters were: age susceptibility to RSV infection (τ_i), For clarity, age structure is given only by the subscript (i), for further details see supplement section 2.

The model was stratified into 5 age categories: infants: 0-1 years, pre-school-aged children: 2-4 years, school-aged children: 5-15 years, adults: 16-64 years, and older adults: aged 65+. Age-dependent contact patterns relevant to the transmission of infections are highly age heterogenous³⁰, and we used social contact patterns (including both physical and verbal contacts) in England from POLYMOD³⁰, a European wide contact study in 2005/6, and in the socialmixr R package³¹. We calculated forces of Infection, $\lambda_{RSV,i}$ and $\lambda_{INF,i}$, from the baseline transmission rates β_{INF} and β_{RSV} and the mixing parameters as:

$$\lambda_{RSV,i} = \sum_{j=1}^5 \beta_{RSV} \alpha_{ij} I_{RSV,j} \quad (1)$$

$$\lambda_{INF,i} = \sum_{j=1}^5 \beta_{INF} \alpha_{ij} I_{INF,j} \quad (2)$$

where α_{ij} is the contact rate between groups i and j and $I_{INF,j}$ and $I_{RSV,j}$ are the proportion infected with Influenza and RSV in age group j . See Supplement Section 1 for model equations.

We modelled one year from the start of the respiratory virus season, and initiated the model with a proportion of each age group susceptible to influenza set from serological data³² (Table 2-2) and the rest in $S_{RSV}R_{INF}$. RSV immunity to re-infection may last less than a year²⁹, therefore we considered the population to be susceptible to RSV at the start of the season. However, RSV susceptibility differs with age³³, and therefore we reduced the susceptibility to the same range as in other models³⁴ by decreasing the infection rate by a susceptibility parameter, τ_i (Table 2-2).

RSV was seeded at time η_{RSV} when one individual from the fully Susceptible class ($S_{RSV}S_{INF}$) becomes infected ($I_{RSV}S_{INF}$). Influenza infections are introduced at a rate of 0.1 cases per day from $S_{RSV}S_{INF}$ to $S_{RSV}I_{INF}$, starting on day η_{INF} . Influenza introduction assumptions differ from those of RSV as with a single introduction the influenza epidemic was suppressed for the whole season at certain parameter values, which is not seen in UK surveillance. See Supplementary section 6 for further details.

An observation process layer converted infections to detected cases using a binomial distribution. The number of detected cases is assumed to follow a binomial distribution as follows:

$$P(x_{virus,i,t} = X) = \binom{n_{virus,i}}{X_{virus,i}} \Delta_{virus,i}^X (1 - \Delta_{virus,i})^{(n_{virus,i} - X_{virus,i})} \quad (3)$$

where X is the number of detected cases in n infections and $x_{virus,i,t}$ is the cases detected for each virus, age group, and timestep. The proportion detected was different for each age group and virus (Table 2-2).

We implemented the model in R³⁵ and C++ using the Rcpp³⁶ and deSolve³⁷ packages.

2.5.2 Simulated data

We generated simulations to resemble data collected through surveillance systems in the UK³⁸, such as the Respiratory Datamart System in England and Wales³ and other Public Health England surveillance systems^{39,40}. This provides laboratory test results from routinely tested clinical respiratory samples from a range of respiratory viruses. The proportion detected varies by age-group for RSV (Table 2-1), as younger infants are more likely to present with severe symptoms⁴¹. Output from the model is weekly number of positive tests in the under-five population for RSV and influenza.

Table 2-1: Parameter values used for generating simulations.

Parameter	Symbol	Value used in simulations	Source	Status in inference
Duration of infectiousness for RSV	$1/\gamma_{RSV}$	9 days	Weber <i>et al</i> (2001) ²⁹ Range from published papers: 6.7-12 days ^{29,34,42}	Fixed
Transmission parameter for RSV	β_{RSV}	0.043	Calibrated to observed values. Equates to an R_0 and $R_{effective}$ of 2.5. See Supplementary section 3 for details	Estimated Log scale
Time of first infection for RSV	η_{RSV}	Day 1	Calibrated to observed pattern. See Supplementary section 6 for details.	Estimated
Age susceptibility to RSV infection (0-1, 2-4, 5-15, 16-64, 65+)	τ_i	1, 0.75, 0.65, 0.65, 0.65	Henderson <i>et al.</i> (1979) ³³ see supplement section 4.	Fixed
Proportion of RSV infections in ages 0-1 detected	Δ_{RSV1}	0.004	Calibrated to observed values. See Supplementary section 5 for details.	Estimated Log odds scale
Proportion of RSV infections in ages 2-4 detected	Δ_{RSV2}	0.001	Calibrated to observed values. See Supplementary section 5 for details	Estimated Log odds scale
Duration of infectiousness for influenza	$1/\gamma_{INF}$	3.8 days	Cauchemez <i>et al</i> (2004) ⁴³ Range from published papers: 1-4.5 days ⁴³⁻⁴⁶	Fixed
Transmission parameter for Influenza	β_{INF}	0.063	Calibrated to observed values. Equates to an R_0 of 2.91, $R_{effective}$ of 1.55. See Supplementary section 3 for details.	Estimated Log scale
Time of first infection for Influenza	η_{INF}	Day 10	Calibrated to observed pattern. See Supplementary section 6 for details.	Estimated
Proportion susceptible to influenza (<2, 2-4, 5+)	ω_i	1, 0.688, 0.525	Assuming born susceptible ⁴⁷ , then values from Baguelin <i>et al</i> from serology data from 2003/4 ⁴⁸	Fixed
Proportion of Influenza infections in ages 0-4 detected	Δ_{INF}	0.002	Calibrated to observed values. See Supplementary section 5.	Estimated Log odds scale
Strength of interaction	σ	0.01, 0.1, 0.2, 0.3, 0.4, 0.5, 0.6, 0.7, 0.8, 0.9, 0.99	Range of values tested	Estimated
Rate of loss of protection	ρ	0.025, 0.05, 0.1, 0.2, 0.5 per day	Range of values tested	Estimated Log scale

Table 2-2: Demography and susceptibility input used for model simulations

Demography	Value used	References/Comments
------------	------------	---------------------

Population size	56 758 452	UK. Demography from POLYMOD ³⁰
Population 2-4 years	2070936	UK. Demography from POLYMOD ³⁰
Population <2 years	1380624	UK. Demography from POLYMOD ³⁰

We generated simulations with parameter values from the literature and if unavailable we calibrated the values to realistic ranges (Table 2-1). Across simulations we varied σ (strength of interaction), for which we used 11 different values, and ρ (the rate of loss of cross-protection), for which we used 5 different values. This resulted in 55 combinations of σ and ρ and we simulated 5 replicates of each.

2.5.3 Parameter estimation

We assumed that the observed cases followed a Poisson distribution with likelihood:

$$L(\theta|x_1, \dots, x_n) = \sum_{j=1}^n e^{-\theta} \frac{\theta^{x_j}}{x_j!} \quad (4)$$

where θ is the modelled detected cases of RSV and influenza in the two youngest age groups, x_j is the observation and n is the total number of observations. We fitted only to the lowest 2 age groups to represent where the majority of samples for RSV are taken from and detected. We fitted the model to simulated data using Metropolis Hastings Markov Chain Monte Carlo (MCMC) sampling. Estimated parameters were transmission rates (β_{RSV}, β_{INF}) detection probabilities ($\Delta_{RSV2}, \Delta_{INF}$) interaction parameters (ρ, σ) and season start times (η_{RSV}, η_{INF}). For each scenario, we ran two chains with 450 000 iterations as burn in followed by a further 250 000 iterations. For chains that did not converge, we extended the chains for a further 250 000 iterations iteratively until convergence was reached or a total of 1 200 000 iterations were run. We used weak priors, and the priors for β_{RSV} and β_{INF} were calculated from R_0 values, assuming no interaction (see Supplement Section 3). We adapted the shape of the proposal distribution during burn in, from 5000 accepted proposals to a further 300000 proposals, to take correlation between parameters into account by allowing the covariance matrix for proposal distributions to change. Parameter limits are defined in Supplement Section 7 and $\beta_{RSV}, \beta_{INF}, \Delta_{RSV1}, \Delta_{RSV2}, \Delta_{INF}$ and ρ were sampled on a log scale to improve mixing where the parameter values were very low.

We assessed MCMC convergence via the Gelman-Rubin statistic, which compares the within-chain variance to the between-chain variance for each parameter. Scenarios with a statistic greater than 1.1 we deemed as practically unidentifiable from simulated data. We also calculated the Pearson correlation coefficient between each two estimated parameters and assessed how these changed

with the values of the interaction parameters (σ and ρ), in order to further understand difficulties with parameter estimation.

We compared the inferred parameter estimates to the simulated parameter values to determine inaccuracy and imprecision of the fit, where inaccuracy is defined as the difference between the median value of the posterior distribution and the true value, and imprecision is the range between the 95% credible intervals (95% CI). We present results from one replicate set of simulations in Results and others are given in the supplement.

2.6 Results

2.6.1 Epidemic profiles

Altering the strength or duration of cross-protection did not notably affect the timing or shape of the RSV epidemic (Figure 2-2), due to the higher transmission rate and earlier start of RSV in our scenarios. However, increasing the strength or duration of interaction delayed the influenza peak. The total number of influenza infections in the youngest two age groups did not change (percentage difference $<1\%$ between $\sigma = 1$ and $\sigma = 0$) with the strength of interaction (Supplement Section 8). Increasing the duration of cross-protection resulted in an 11% lower total number of infections from the shortest (2 days) to longest (40 days) duration of cross-protection (Supplement Section 8). Plots showing the epidemic curves for each infectious compartment are shown in Supplement Section 9.

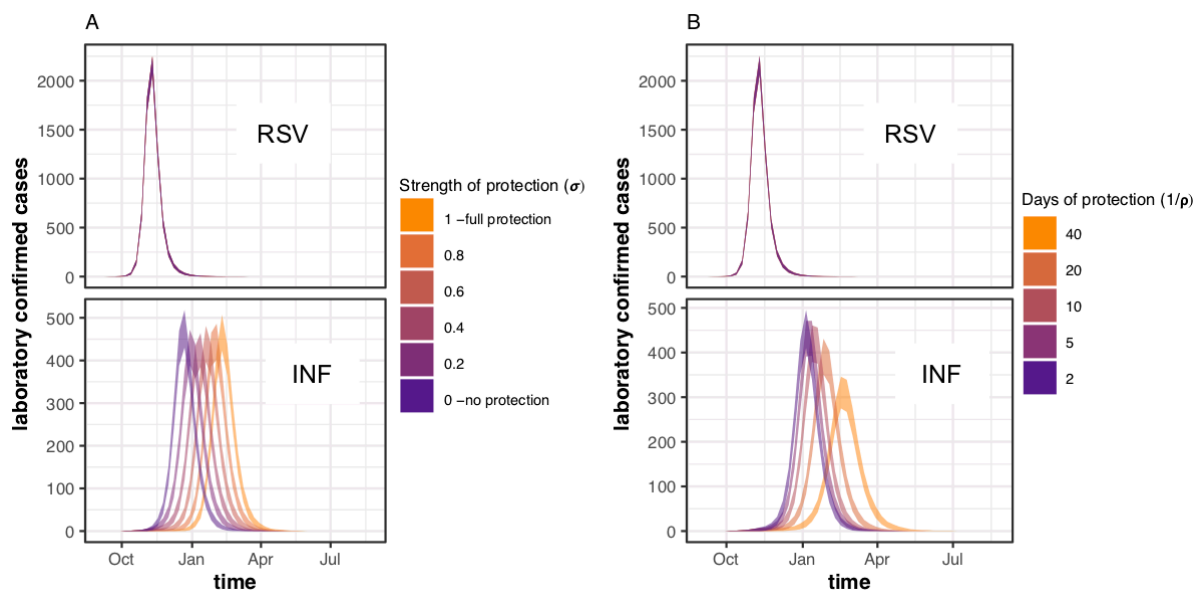


Figure 2-2: Mean weekly incidence of observed cases in under 5s (sum of age groups 0-1 and 2-4) from simulations with A) varying σ values and a fixed protection duration of 10 days ($\rho=0.1$), and B) varying ρ values,

and a fixed σ of 0.5. Simulations were run and sampled 1000 times for each parameter set and the shaded windows are the 95% quantiles for each week. In both A and B the top panel shows the observed cases for RSV, and the lower panel the cases for Influenza.

2.6.2 Correlation Analysis

The most strongly correlated parameters were consistently the transmission rate for RSV (β_{RSV}) with the RSV season start time (η_{RSV}) and the transmission rate for influenza (β_{INF}) with the detection rate for influenza (Δ_{INF}) and the start of the influenza season (η_{INF}) (Figure 2-3A). The correlation between parameters changed dependent on the values of the interaction parameters, an example of which is shown in Figure 2-3B, where the correlation coefficient between the strength of interaction (σ) and the proportion of influenza cases detected (Δ_{INF}) varies depending on the values of σ and ρ . As the strength of interaction decreases (as $\sigma \rightarrow 0$), the correlation between the strength of interaction and the proportion of influenza cases detected becomes more positive. The correlation changes across the interaction parameters for other parameter combinations are shown in the Supplement Section 10, and matrices for individual simulations are in supplement section 12.

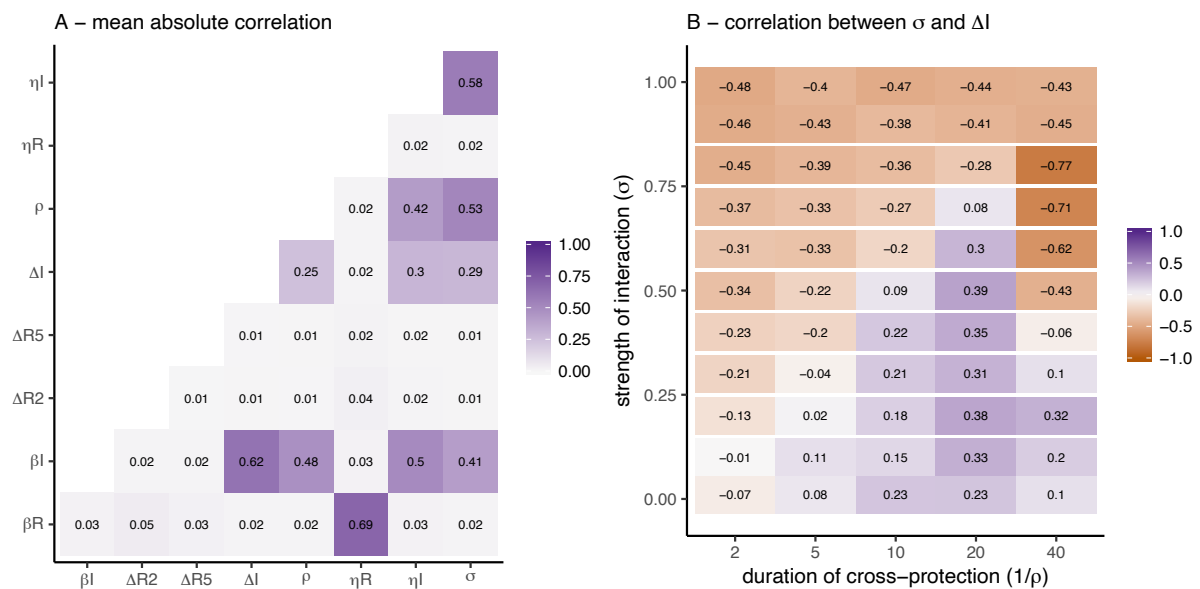


Figure 2-3. A) Mean Pearson correlation coefficient between parameters. B) Correlation coefficient between σ (strength of cross-protection) and Δ_{INF} (start day of influenza). This is shown for 1 simulation, but the patterns were similar for all (Supplementary Section 12)

2.6.3 Inferring the strength of cross-protection (σ)

Across simulations, the imprecision and inaccuracy of the estimated strength of cross-protection (σ) varied (Figure 2-4), with the imprecision ranging from 0.15 to 0.66 (where 1 is poor precision) and average imprecision decreasing as the duration of protection (ρ) increased. We did not observe a trend in the inaccuracy of the parameter estimates and they ranged from 0 to 0.24. However, the lowest value tested ($\sigma = 0.01$) was overestimated in each simulation and the highest value tested ($\sigma = 0.99$) was underestimated, showing that the extreme values are less well estimated. This may be due to the true value being very close to the parameter limit.

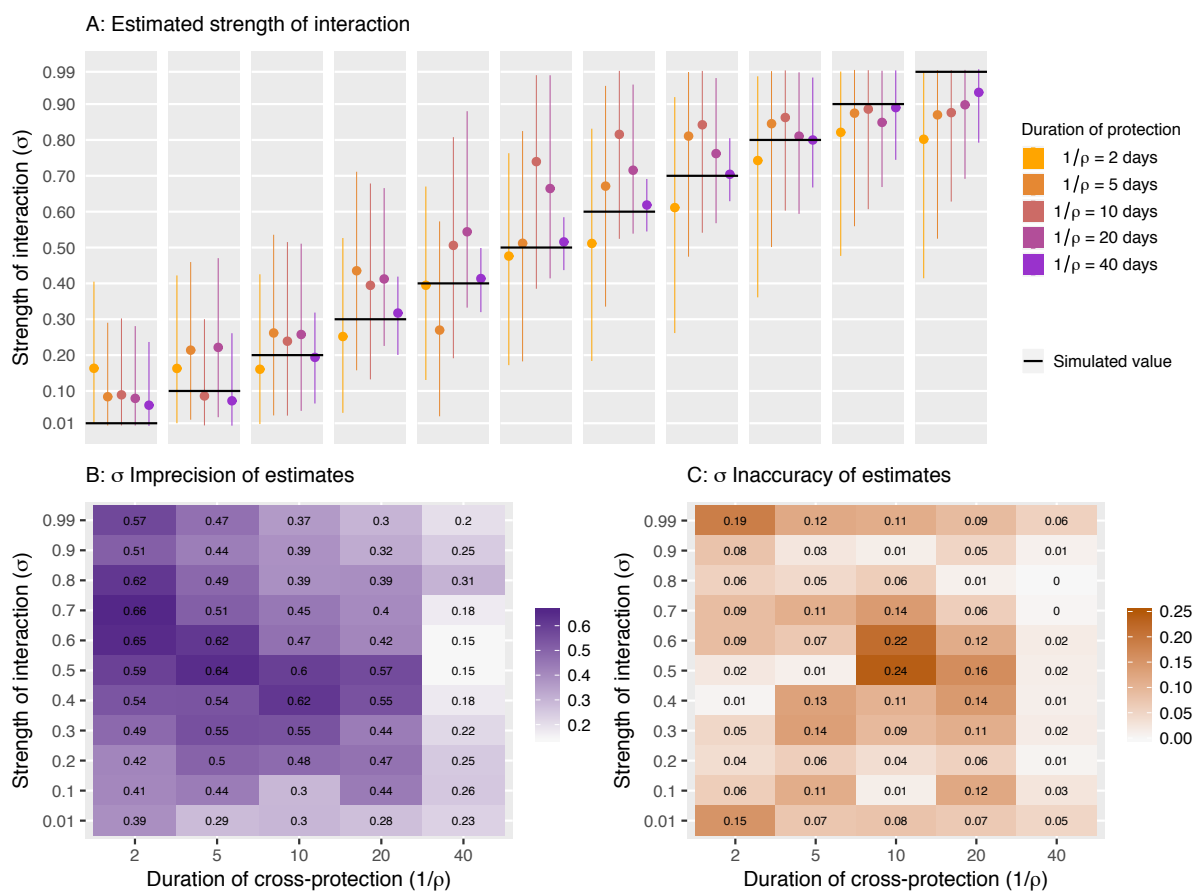


Figure 2-4. A) Estimated σ values for simulations with different σ and ρ values. Median value and 95% CI are shown. The black line is the simulated (true) value of σ in each case. B) Imprecision of σ estimates calculated as the 95% quantile range. C) Inaccuracy of the σ estimates, calculated as the difference between the posterior median and the true value.

2.6.4 Inferring the duration of cross-protection ($1/\rho$)

The imprecision of the estimated duration of cross protection ranged from 7 to 87 days (Figure 2-5). Estimates were generally less precise when the period of cross-protection is longer (Figure 2-5). In 70% of our simulations where σ interaction reduced the transmission rate by no more than 10% (i.e.

$\sigma = 0.1$ or 0.01) the duration of protection estimates exceeded an imprecision of 50 days. For scenarios assuming stronger competition estimates were much more precise. Indeed, one would expect that once the strength of competition is negligibly small the duration of such protection would be largely irrelevant. ρ estimates increased for simulations generated with longer duration of protection (smaller ρ).

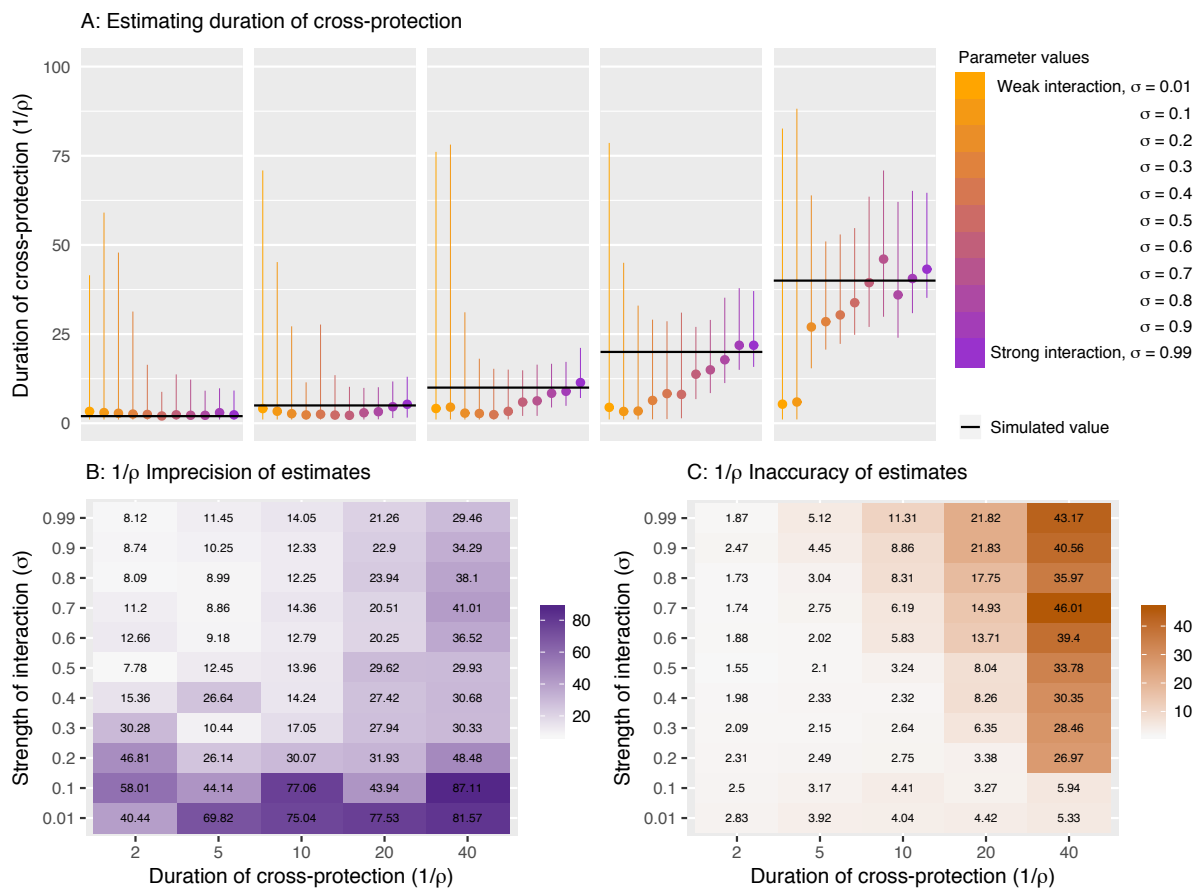


Figure 2-5. A) Estimated $1/\rho$ values for simulations with different σ and ρ . Lines represent 95% quantiles of the posterior sample and the circle represents the median value. The black line shows the true $1/\rho$ value in each case. B) Imprecision of ρ estimates calculated as the 95% quantile range. C) Inaccuracy of the ρ estimates, calculated as the difference between the posterior median and the true value.

2.6.5 Variation between replicates

Each parameter set was used to generate a further four replicate simulations of the observation process. Of these 275 simulations (5 replicates of 55 parameter combinations), 259 reached convergence at the cut-off point (see Supplement Section 11). The true parameter values were included in the 95% CI in the majority of replicates (Figure 2-6). The true value of ρ was not included in the 95% CI in 6 simulations (2%), whereas the true value of σ was not included in the 95% CI in 31

simulations (11%). These simulations were more concentrated in areas with extreme interaction strengths (0.99 and 0.01) and very short duration of protection. We conclude from this that the stochastic variation in the simulation of the observation can occasionally result in difficulty estimating the true value of the parameter.

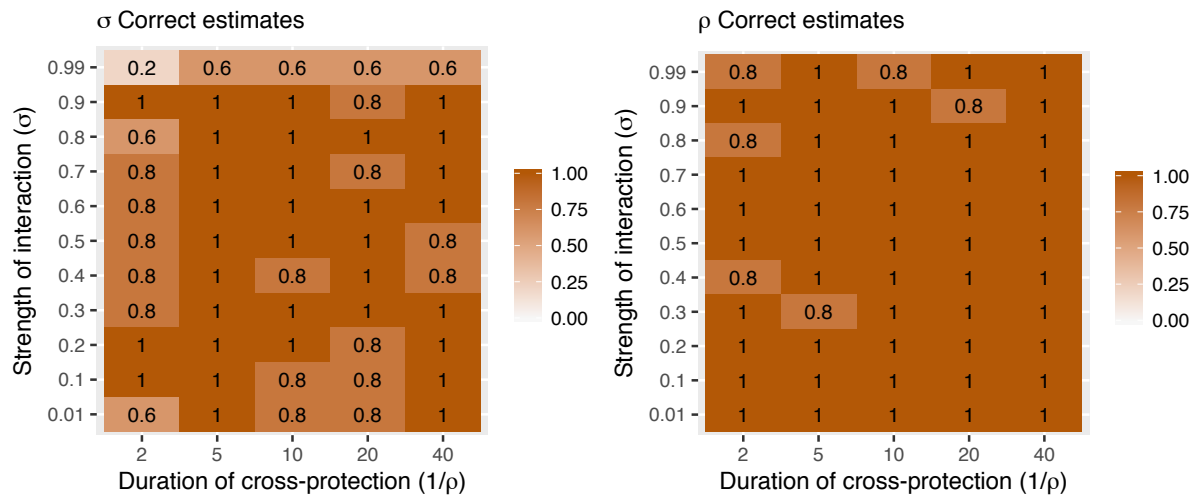


Figure 2-6: Proportion of simulations where the true value of σ (A) and ρ (B) was included in the 95% CI of the posterior estimate.

2.7 Discussion

We tested whether a transmission model including competitive interaction between RSV and influenza is identifiable from a single season of simulated high-quality surveillance data. We determined that it is possible to re-estimate strength and duration of interaction in most tested scenarios, although often imprecise due to large credible intervals, but that there are some areas of parameter space where posterior estimates are potentially misleading, particularly when the strength of interaction is assumed to be low or the duration of interaction short. However, we only estimated the parameters from information from one season at a time, and without strong priors.

Initially, we used the model to simulate the impacts different strengths and durations of interaction had on the influenza and RSV outbreaks. When altering the strength of interaction, no change was observed in the total number of cases reported, however the influenza epidemic shifted later in the season. In addition, the peak height of the influenza epidemic decreased and then increased with increasing interaction strength. This is likely due to a slowing down of the epidemic with moderate interaction, which slightly reduces the peak height counteracted by an increase in epidemic duration. The peak height then increases as the interaction reaches high values, as the strong interaction inhibits the start of the epidemic peak, therefore shifting the epidemic without altering

its shape. When increasing the duration of interaction, total influenza case numbers dropped, therefore resulting in a lower, as well as later, influenza epidemic peak.

We based our simulations on data collected through the UK surveillance system. This involved qualitatively emulating peak incidence and duration for both viruses, as well as comparative incidence and timings between viruses and age groups, based on published reports. As the simulations were generated from our model with stochastic noise, we assume that the underlying model adequately captures the transmission process in sufficient detail. In reality, surveillance data may be noisier, impacted by changes in contact patterns for example due to school holidays, varying reporting rates over the year and climatic factors. These are difficult to capture in our model without considerably increasing complexity and therefore the assumption that our model generates sufficient detail to mimic surveillance data is a limitation of this study.

While we are the first to test robustness of RSV and influenza competition inference, other identifiability studies, e.g. on Rift Valley Fever, have previously highlighted the importance of robustness testing to avoid misleading conclusions stemming largely from insufficient power of the data to inform the model parameters of interest^{49,50}. Structural and practical identifiability analysis have also been used to select appropriate models, given the data available^{51,52}, for example a study that evaluated six different Zika models, and the identifiability of parameters within each⁵¹.

Our analysis shows that there are potentially misleading results at extreme competition values, and it is almost impossible to get a “null estimate” for the strength of competition from this study. Evidence from mouse models suggest that the duration of RSV cross protection following influenza infection may last more than two weeks^{13,53} which, under the assumption that the duration of cross-protection is non-differential to the initiating virus, may suggest that the imprecision of our estimates at short durations of cross protection is unlikely to be a key risk for inference. However it may not be possible to distinguish such competition from no competition in our model, if the strength of the competition is low. We deliberately used uninformative priors for this parameter in order to be able to fully explore its identifiability, however, subsequent work may further improve precision of estimates by including prior estimates based on published evidence. This may also reduce the correlation of estimated parameters, which has challenged convergence in our simulations. Similarly, mouse models have suggested strong modulation of the RSV immune response if preceded by an influenza infection¹³, which may suggest that difficulties in our inference in scenarios that assume very small amounts of competition may not be the most relevant.

For parameter combinations where the simulated parameter value could not be re-estimated, we found that despite the relatively high assumed sample size stochastic noise from the observation model can occasionally result in incorrect estimates. This implies that inference based on a single season may be misleading purely because of the observational process associated with surveillance, however, including multiple seasons of observation should limit problems stemming from the observation process alone and further increase accuracy of estimates.

We assumed that the RSV–influenza interaction was bidirectional; particularly we assume that the strength and duration of interaction that influenza exhibits on RSV is the same as vice versa. Given that the proposed mechanisms for interaction are not virus specific this seems reasonable, and is supported by studies looking at the shift in RSV epidemics following the early 2009 influenza pandemic^{10,23,25,26}. However, the RSV epidemic in the UK typically precedes influenza and similarly we only investigate such scenario. Therefore, in this work we can only estimate the competition of RSV on influenza dynamics and do not have power to estimate the other direction. Hence our results are applicable for considerations around RSV vaccine introduction but should be treated cautiously for any studies interested in the impact of Influenza on the transmission dynamics of RSV.

This model did not include multiple strains of either RSV or influenza, which could have an impact on the interaction dynamics, as the interaction may differ between strains. Including strains would significantly increase the complexity of the model (see review on strain interaction models⁵⁴), which we think would have rendered it unidentifiable. In addition, the aim was to assess the practical identifiability of the model parameters that govern viral interaction from routine surveillance data, and in many scenarios the surveillance data does not record strain type. The biological mechanism underpinning the period of cross-immunity is that of viral infection-induced protection, which is potentially induced by many viruses so may not be specific to RSV and influenza, and may not differ between influenza subtypes/strains.

We ran the model for one season at a time in order to reduce the complexity, as in other influenza models³². We captured influenza immunity from previous seasons in the proportion of individuals susceptible for influenza at the start of the season, and RSV immunity is considered to last less than a year²⁹, so we simplified to a single season but included the major multi-season effects. A further sensitivity analysis could be to vary the susceptibility of individuals to influenza at the start of the year, in order to simulate different dominant influenza strains. We have however not included this,

as our aim here was to look at the identifiability of parameters, and these differences would be taken into account when fitting to surveillance data from different seasons. Ideally, we would fit to multiple seasons of surveillance data, in order to account for variations by year. In the model we assumed a constant, age-dependent observation rate, as in other influenza models⁵⁵. Time varying reporting rates would substantially hinder inference, in fact a previous study comparing model fit of age-dependent vs time and age-dependent reporting rates concluded it was not possible to prefer one model terms of fit alone⁵⁶, so we assume age-dependent only reporting rates for simplicity. We did not include additional seasonal effects in the model. While no or small effects have been reported for RSV and seasonal factors^{57,58}, there is stronger evidence for the impact of climatic factors on influenza transmission, particularly ambient temperature and absolute humidity⁵⁹⁻⁶¹. While this does not affect our results on identifying parameters from simulated data, it should be noted as a potential confounder when estimating these parameters using surveillance data.

Further data may help to identify parameters in the model where it currently has difficulties. Data on the frequency of co-infections would allow us to use stronger priors for the strength of interaction, as well as providing an informative data source to fit the model to. Further information on the circulation of RSV, as opposed to only clinical cases, is also important due to the current uncertainty in infection numbers. In addition, surveillance systems would ideally provide daily data on RSV and influenza cases, giving us more granularity and potentially allowing us to identify all areas of parameter space.

Behavioural changes may also impact respiratory viral circulation, after infection with a virus (staying inside while recovering), or large-scale behavioural change due to restrictions (social distancing measures in response to the SARS-CoV-2 pandemic). Whilst we do not investigate these mechanisms in this paper, such changes can have drastic impacts, such as the largely absent 2020 influenza season in Australia⁶².

Overall, this study shows that in principle interaction parameters can be estimated from high quality surveillance-like data using mathematical models, although the precision and accuracy of the estimates varies depending on the scenario and stochasticity in the surveillance data. More power to reliably infer parameters may be available if fitting multiple seasons. It also highlights the importance of validating complex models, especially in light of the rapid development of models in emergency situations, which can have large impacts on public policy⁶³.

2.8 Acknowledgments

NRW was supported by the Medical Research Council (grant number MR/N013638/1). SF is funded through a Sir Henry Dale Fellowship jointly funded by the Wellcome Trust and the Royal Society (grant number 208812/Z/17/Z). RME acknowledges funding from an HDR UK Innovation Fellowship (grant MR/S003975/1)

2.9 References

1. Waterlow, N. R., Flasche, S., Minter, A. & Eggo, R. M. Competition between RSV and influenza: limits of modelling inference from surveillance data. *Epidemics* 100460 (2021) doi:10.1016/j.epidem.2021.100460.
2. Shrestha, S., King, A. A. & Rohani, P. Statistical Inference for Multi-Pathogen Systems. *PLoS Computational Biology* **7**, e1002135–e1002135 (2011).
3. Zhao, H. *et al.* A new laboratory-based surveillance system (Respiratory Datamart System) for influenza and other respiratory viruses in England: Results and experience from 2009 to 2012. *Eurosurveillance* **19**, (2014).
4. Lafond, K. E. *et al.* Global Role and Burden of Influenza in Pediatric Respiratory Hospitalizations, 1982–2012: A Systematic Analysis. *PLOS Medicine* **13**, e1001977 (2016).
5. Shi, T. *et al.* Global, regional, and national disease burden estimates of acute lower respiratory infections due to respiratory syncytial virus in young children in 2015: a systematic review and modelling study. *Lancet (London, England)* **390**, 946–958 (2017).
6. Pneumonia Etiology Research for Child Health (PERCH) Study Group, K. L. *et al.* Causes of severe pneumonia requiring hospital admission in children without HIV infection from Africa and Asia: the PERCH multi-country case-control study. *Lancet (London, England)* **0**, (2019).
7. Bloom-Feshbach, K. *et al.* Latitudinal Variations in Seasonal Activity of Influenza and Respiratory Syncytial Virus (RSV): A Global Comparative Review. *PLoS ONE* vol. 8 e54445 (2013).
8. Opatowski, L., Baguelin, M. & Eggo, R. M. REVIEW Influenza Interaction with Cocirculating Pathogens, and Its Impact on Surveillance, Pathogenesis and Epidemic Profile: A Key Role for Mathematical Modeling. (2017) doi:10.1101/203265.
9. Velasco-Hernández, J. X., Núñez-López, M., Comas-García, A., Cherpitel, D. E. N. & Ocampo, M. C. Superinfection between Influenza and RSV alternating patterns in San Luis Potosí State, México. *PLoS ONE* **10**, (2015).
10. Mak, G. C., Wong, A. H., Ho, W. Y. Y. & Lim, W. The impact of pandemic influenza A (H1N1) 2009 on the circulation of respiratory viruses 2009-2011. *Influenza and other Respiratory Viruses* **6**, e6-10 (2012).
11. Pascalis, H. *et al.* Intense Co-Circulation of Non-Influenza Respiratory Viruses during the First Wave of Pandemic Influenza pH1N1/2009: A Cohort Study in Reunion Island. *PLoS ONE* **7**, e44755 (2012).
12. Yang, Y. *et al.* Influenza A/H1N1 2009 Pandemic and Respiratory Virus Infections, Beijing, 2009-2010. *PLoS ONE* **7**, (2012).

13. Walzl, G., Tafuro, S., Moss, P., Openshaw, P. J. & Hussell, T. Influenza virus lung infection protects from respiratory syncytial virus-induced immunopathology. *The Journal of experimental medicine* **192**, 1317–26 (2000).
14. Ascough, S., Paterson, S. & Chiu, C. Induction and Subversion of Human Protective Immunity: Contrasting Influenza and Respiratory Syncytial Virus. *Frontiers in Immunology* **9**, 323 (2018).
15. Lee, Y. J. *et al.* Non-specific Effect of Vaccines: Immediate Protection against Respiratory Syncytial Virus Infection by a Live Attenuated Influenza Vaccine. *Frontiers in Microbiology* **9**, 83 (2018).
16. Pinky, L. & Dobrovoly, H. M. Coinfections of the respiratory tract: Viral competition for resources. *PLoS ONE* **11**, (2016).
17. Shinjoh, M., Omoe, K., Saito, N., Matsuo, N. & Nerome, K. In vitro growth profiles of respiratory syncytial virus in the presence of influenza virus. *Acta virologica* **44**, 91–7 (2000).
18. Ferguson, N. M. *et al.* Strategies for containing an emerging influenza pandemic in Southeast Asia. *Nature* **437**, 209–214 (2005).
19. Laurie, K. L. *et al.* Interval Between Infections and Viral Hierarchy Are Determinants of Viral Interference Following Influenza Virus Infection in a Ferret Model. *Journal of Infectious Diseases* **212**, 1701–1710 (2015).
20. Kelly, H., Barry, S., Laurie, K. & Mercer, G. Seasonal influenza vaccination and the risk of infection with pandemic influenza: A possible illustration of nonspecific temporary immunity following infection. *Eurosurveillance* **15**, 19722 (2010).
21. Ferguson, N. M., Galvani, A. P. & Bush, R. M. Ecological and immunological determinants of influenza evolution. *Nature* **422**, 428–433 (2003).
22. Kucharski, A. J., Andreasen, V. & Gog, J. R. Capturing the dynamics of pathogens with many strains. *Journal of Mathematical Biology* (2016) doi:10.1007/s00285-015-0873-4.
23. Hirsh, S. *et al.* Epidemiological changes of Respiratory Syncytial Virus (RSV) infections in Israel. *PLoS ONE* **9**, (2014).
24. Meningher, T. *et al.* Relationships between A(H1N1)pdm09 influenza infection and infections with other respiratory viruses. *Influenza and other Respiratory Viruses* **8**, 422–430 (2014).
25. Gröndahl, B. *et al.* The 2009 pandemic influenza A(H1N1) coincides with changes in the epidemiology of other viral pathogens causing acute respiratory tract infections in children. *Infection* **42**, 303–308 (2014).
26. Casalegno, J. S. *et al.* Impact of the 2009 influenza a(H1N1) pandemic wave on the pattern of hibernal respiratory virus epidemics, France, 2009. *Eurosurveillance* **15**, 2 (2010).

27. van Asten, L. *et al.* Early occurrence of influenza A epidemics coincided with changes in occurrence of other respiratory virus infections. *Influenza and Other Respiratory Viruses* **10**, 14–26 (2016).
28. Novavax Announces Topline Results from Phase 3 Prepare™ Trial of ResVax™ for Prevention of RSV Disease in Infants via Maternal Immunization | Novavax Inc. - IR Site. <https://ir.novavax.com/news-releases/news-release-details/novavax-announces-topline-results-phase-3-preparetm-trial>.
29. Weber, A., Weber, M. & Milligan, P. Modeling epidemics caused by respiratory syncytial virus (RSV). *Mathematical Biosciences* **172**, 95–113 (2001).
30. Mossong, J. *et al.* Social contacts and mixing patterns relevant to the spread of infectious diseases. *PLoS Medicine* **5**, 0381–0391 (2008).
31. Funk, S. socialmixr: Social Mixing Matrices for Infectious Disease Modelling. (2018).
32. Baguelin, M. *et al.* Assessing Optimal Target Populations for Influenza Vaccination Programmes: An Evidence Synthesis and Modelling Study. *PLoS Medicine* **10**, (2013).
33. Henderson, F. W., Collier, A. M., Clyde, W. A. & Denny, F. W. Respiratory-Syncytial-Virus Infections, Reinfections and Immunity. *New England Journal of Medicine* **300**, 530–534 (1979).
34. Moore, H. C., Jacoby, P., Hogan, A. B., Blyth, C. C. & Mercer, G. N. Modelling the Seasonal Epidemics of Respiratory Syncytial Virus in Young Children. *PloS one* **9**, e100422 (2014).
35. R Core Team. R: A language and environment for statistical computing. R Foundation for Statistical Computing, Vienna, Austria. (2018).
36. Eddelbuettel, D. & Francois, R. Rcpp: Seamless R and C++ Integration. *Journal of Statistical Software*, **40**(8), 1-18. (2011).
37. Soetaert, K., Petzoldt, T. & Woodrow, S. Solving Differential Equations in R: Package deSolve. *Journal of Statistical Software* **33**, 1--25. (2010).
38. Reeves, R. M. *et al.* Estimating the burden of respiratory syncytial virus (RSV) on respiratory hospital admissions in children less than five years of age in England, 2007-2012. *Influenza and Other Respiratory Viruses* **11**, 122–129 (2017).
39. Weekly national flu reports: 2018 to 2019 season - GOV.UK. <https://www.gov.uk/government/statistics/weekly-national-flu-reports-2018-to-2019-season>.
40. Respiratory infections: laboratory reports 2019 - GOV.UK. <https://www.gov.uk/government/publications/respiratory-infections-laboratory-reports-2019>.

41. Ohuma, E. O. *et al.* The Natural History of Respiratory Syncytial Virus in a Birth Cohort: The Influence of Age and Previous Infection on Reinfection and Disease. *American Journal of Epidemiology* **176**, 794–802 (2012).
42. Hall, C. B., Douglas, R. G. & Geiman, J. M. Respiratory syncytial virus infections in infants: quantitation and duration of shedding. *The Journal of pediatrics* **89**, 11–5 (1976).
43. Cauchemez, S., Carrat, F., Viboud, C., Valleron, A. J. & Boëlle, P. Y. A Bayesian MCMC approach to study transmission of influenza: application to household longitudinal data. *Statistics in Medicine* **23**, 3469–3487 (2004).
44. Hayden, F. G. *et al.* Use of the Oral Neuraminidase Inhibitor Oseltamivir in Experimental Human Influenza. *JAMA* **282**, 1240 (1999).
45. Chowell, G. *et al.* Characterizing the Epidemiology of the 2009 Influenza A/H1N1 Pandemic in Mexico. *PLoS Medicine* **8**, e1000436 (2011).
46. Cori, A. *et al.* Estimating influenza latency and infectious period durations using viral excretion data. *Epidemics* **4**, 132–138 (2012).
47. Nokes, D. J. *et al.* Respiratory Syncytial Virus Epidemiology in a Birth Cohort from Kilifi District, Kenya: Infection during the First Year of Life. *The Journal of Infectious Diseases* **190**, 1828–1832 (2004).
48. Baguelin, M., Jit, M., Miller, E. & Edmunds, W. J. Health and economic impact of the seasonal influenza vaccination programme in England. *Vaccine* **30**, 3459–3462 (2012).
49. Kao, Y.-H. & Eisenberg, M. C. Practical unidentifiability of a simple vector-borne disease model: Implications for parameter estimation and intervention assessment. *Epidemics* **25**, 89–100 (2018).
50. Tuncer, N., Gulbudak, H., Cannataro, V. L. & Martcheva, M. Structural and Practical Identifiability Issues of Immuno-Epidemiological Vector–Host Models with Application to Rift Valley Fever. *Bulletin of Mathematical Biology* **78**, 1796–1827 (2016).
51. Tuncer, N., Martcheva, M., LaBarre, B. & Payoute, S. Structural and Practical Identifiability Analysis of Zika Epidemiological Models. *Bulletin of Mathematical Biology* **80**, 2209–2241 (2018).
52. Roosa, K. & Chowell, G. Assessing parameter identifiability in compartmental dynamic models using a computational approach: application to infectious disease transmission models. *Theoretical Biology and Medical Modelling* **16**, 1 (2019).
53. Hamilton, J. Club cells surviving influenza A virus infection induce temporary nonspecific antiviral immunity.

54. Kucharski, A. J. & Gog, J. R. Age profile of immunity to influenza: Effect of original antigenic sin. *Theoretical Population Biology* **81**, 102–112 (2012).
55. Magal, P. & Webb, G. The parameter identification problem for SIR epidemic models: identifying unreported cases. *Journal of Mathematical Biology* **77**, 1629–1648 (2018).
56. Dorigatti, I., Cauchemez, S., Pugliese, A. & Ferguson, N. M. A new approach to characterising infectious disease transmission dynamics from sentinel surveillance: Application to the Italian 2009-2010 A/H1N1 influenza pandemic. *Epidemics* **4**, 9–21 (2012).
57. Tian, D. D., Jiang, R., Chen, X. J. & Ye, Q. Meteorological factors on the incidence of MP and RSV pneumonia in children. *PLoS ONE* **12**, (2017).
58. Hogan, A. B. *et al.* Time series analysis of RSV and bronchiolitis seasonality in temperate and tropical Western Australia. *Epidemics* **16**, 49–55 (2016).
59. Shaman, J., Pitzer, V. E., Viboud, C., Grenfell, B. T. & Lipsitch, M. Absolute Humidity and the Seasonal Onset of Influenza in the Continental United States. *PLoS Biology* **8**, e1000316 (2010).
60. Shaman, J. & Kohn, M. Absolute humidity modulates influenza survival, transmission, and seasonality. *Proceedings of the National Academy of Sciences of the United States of America* **106**, 3243–8 (2009).
61. Lowen, A. C. & Steel, J. Roles of humidity and temperature in shaping influenza seasonality. *Journal of virology* **88**, 7692–5 (2014).
62. Sullivan, S. G. *et al.* Where has all the influenza gone? The impact of COVID-19 on the circulation of influenza and other respiratory viruses, Australia, March to September 2020. *Eurosurveillance* **25**, (2020).
63. Panovska-Griffiths, J. Can mathematical modelling solve the current Covid-19 crisis? *BMC Public Health* **20**, 551 (2020).

3 Chapter 3 - Evidence for Influenza and RSV interaction from 10 years of enhanced surveillance in Nha Trang, Vietnam, a modelling study

3.1 Research Paper Cover Sheet



London School of Hygiene & Tropical Medicine
 Keppel Street, London WC1E 7HT
 T: +44 (0)20 7299 4646
 F: +44 (0)20 7299 4656
 www.lshtm.ac.uk

RESEARCH PAPER COVER SHEET

Please note that a cover sheet must be completed for each research paper included within a thesis.

SECTION A – Student Details

Student ID Number	1402815	Title	Mrs
First Name(s)	Naomi Ruth		
Surname/Family Name	Waterlow		
Thesis Title	Mathematical Modelling of Cross-protection between Respiratory Viruses		
Primary Supervisor	Dr. Rosalind M Eggo		

If the Research Paper has previously been published please complete Section B, if not please move to Section C.

SECTION B – Paper already published

Where was the work published?	NA		
When was the work published?	NA		
If the work was published prior to registration for your research degree, give a brief rationale for its inclusion	NA		
Have you retained the copyright for the work?*	Choose an item.	Was the work subject to academic peer review?	Choose an item.

*If yes, please attach evidence of retention. If no, or if the work is being included in its published format, please attach evidence of permission from the copyright holder (publisher or other author) to include this work.

SECTION C – Prepared for publication, but not yet published


Where is the work intended to be published?	Journal of the Royal Society Interface
Please list the paper's authors in the intended authorship order:	Naomi R Waterlow, Michiko Toizumi, Edwin van Leeuwen, ..., Lay Myint-Yoshida, Rosalind M Eggo, Stefan Flasche denotes collaborators from Pasteur Institute, Khanh Hoa Hospital, National Institute of Hygiene and Epidemiology,


	and Nagasaki university.
Stage of publication	Not yet submitted

SECTION D – Multi-authored work

For multi-authored work, give full details of your role in the research included in the paper and in the preparation of the paper. (Attach a further sheet if necessary)	I worked on: Conceptualisation, Methodology, Software, Validation, Formal Analysis, Writing – Original Draft, Visualization.
--	--

SECTION E

Student Signature	
Date	10/08/2021

Supervisor Signature	
Date	24 Aug 21

3.2 Bridging Section

This paper is being prepared for journal submission. It estimates the strength and duration of cross-protection between influenza and RSV, in Nha Trang Vietnam, the impact co-infection has on the reporting rate and the impacts of vaccinating against either virus.

This chapter builds on the model developed and tested in Chapter 2, adapted to the setting of Nha Trang, Vietnam. I use a unique dataset, consisting of 11 years of enhanced surveillance of under 5-year-old children who attend hospital in Nha Trang Vietnam, with acute respiratory infection. I use parallel tempering to fit the model to the data, thereby estimating interaction parameters. I show that the population level circulation of influenza and RSV can be explained either by moderate or no cross-protection. In addition, I conclude that co-infection of the two viruses increases the chance of reporting, presumably due to an increase in severity. I also evaluate the impacts of vaccination in this setting.

While this is not the first study to look at interaction between influenza and RSV¹, it is the first that uses likelihood-based methods to fit to data, and quantitatively estimate the interaction parameters. In addition, while many papers that look at the severity of co-infections between respiratory viruses, the majority do not focus on influenza and RSV specifically²⁻⁴. This paper is therefore a valuable addition to the literature on interaction between these two respiratory viruses.

I developed the model, wrote all the code and performed the fitting analysis. I also wrote all the draft paper and made the figures. Throughout the process I received input/suggestions/edits from both my supervisors. In addition, we collaborated with the team led by Dr Lay-Myint Yoshida, who collected the data. Dr Edwin Van Leeuwen also provided advice on appropriate likelihoods to be used.

The supplementary material of the paper covers extra details on the methods and results. This is included as Appendix B in this thesis, so any references to the supplementary material can be found there.

3.3 Title page and abstract

Evidence for Influenza and RSV interaction from 10 years of enhanced surveillance in Nha Trang, Vietnam, a modelling study.

Naomi R Waterlow^{1†}, Michiko Toizumi^{2,3}, Edwin van Leeuwen^{1,4}, Hien-Anh Thi Nguyen⁵, Lay Myint-Yoshida^{2,3*}, Rosalind M Eggo^{1*}, Stefan Flasche^{1*}.

¹ *Centre for Mathematical Modeling of Infectious Disease, London School of Hygiene and Tropical Medicine, UK*

² *Department of Pediatrics, Nagasaki University Hospital, Nagasaki University, Nagasaki 852-8102, Japan*

³ *Department of Pediatric Infectious Diseases, Institute of Tropical Medicine, Nagasaki University, Nagasaki 852-8523, Japan*

⁴ *Statistics, Modelling and Economics Department, UKHSA*

⁵ *National Institute of Hygiene and Epidemiology, Hanoi, Vietnam*

† indicates corresponding author

** These authors have contributed equally*

Funding

NRW was supported by the Medical Research Council (grant number [MR/N013638/1](#)). EvL and RME declare funding from the National Institute for Health Research (NIHR) Health Protection Research Unit (HPRU) in Modelling and Health Economics, a partnership between PHE, Imperial College London, and LSHTM (grant number NIHR200908). EvL was supported by the European Union's Horizon 2020 research and innovation programme - project EpiPose (101003688). SF is funded through a Sir Henry Dale Fellowship jointly funded by the Wellcome Trust and the Royal Society (grant number [208812/Z/17/Z](#)). RME acknowledges an HDR UK Innovation Fellowship (grant: MR/S003975/1), MRC (grant: MC_PC 19065), and NIHR (grant: NIHR200908) for the Health Protection Research Unit in Modelling and Economics at LSHTM. The views expressed in this publication are those of the author(s) and not necessarily those of the funders.

Abstract

Influenza and Respiratory Syncytial Virus (RSV) interact within their host posing the concern for heterologous ecological changes following vaccination. We aimed to estimate the likely population level impact of their interaction.

We developed a two-pathogen mathematical model, and used parallel tempering to fit its parameters governing enhanced severity of co-infections and reduced acquisition following heterologous infection to 11 years of enhanced hospital-based surveillance for acute respiratory illnesses (ARI) in children under 5 years old in Nha Trang, Vietnam. We used this parameterization to explore the dependence of the case burden on the heterologous pathogen.

A total of 788 influenza, 1687 RSV and 78 dual infections were reported among children hospitalised with ARI between 5th February 2007 and 4th December 2017. The data supported either a 41% (95% Credible Interval (C): 36 - 54) reduction in heterologous acquisition during infection and for 10.0 days (95% CrI 7.1 -12.8) thereafter, or no cross protection. We estimate that co-infection increased the probability for an infection in <2y old children to be reported 7.2 fold (95% CrI 5.0 - 11.4); or 16.6 fold (95% CrI 14.5 - 18.4) in the no cross-protection and the reduced acquisition scenarios respectively. Absence of either pathogen was not to the detriment to the other.

We find stronger evidence for severity enhancing than for acquisition limiting interaction. In this setting vaccination against either pathogen is unlikely to have a major detrimental effect on the burden of disease caused by the other.

3.4 Introduction

Influenza and Respiratory Syncytial Virus (RSV) have large health and economic impacts globally, particularly in young children where they cause 870 000⁵ and 3.2 million⁶ hospitalisations in <5 year olds per year respectively. While paediatric influenza vaccines are licensed for use in some countries, global uptake is poor and efficacy depending on the match to the circulating strains. RSV vaccines are in development, with close to 20 vaccine candidates being evaluated in pre-licensure trials⁷.

The impact of vaccination may be enhanced if co-infections increase the propensity of severe disease beyond that of either pathogen⁸. However, the impact of vaccination may be lessened if vaccination reduces competitive pressure between influenza and RSV and thus leads to increased circulation of the other pathogen. Such competitive pressure has been observed in the form of cross protection in mouse studies that showed e.g. a protective effect of live attenuated influenza vaccine administration on RSV replication⁹ and influenza infection on RSV severity¹⁰, mediated by the innate immune system. Population level evidence for the effect of cross-protection on influenza and RSV epidemiology, however, is largely of observational nature: a lack of coincidence in peak timings^{11,12},

changes in RSV peak timing following unusual influenza seasons^{13–18} and alternating infection patterns¹⁹.

Cross-protection could occur through a variety of mechanisms including viral competition for resources in the host²⁰, the activation of the innate immune system such as through toll-like receptors (TLRs) 3 and 7^{21,22} or short term immune memory through surviving cells in an antiviral state (e.g. epithelial cells following influenza infection²³). Estimates of the duration of cross-protection and its biological pathway vary. Experimental infection of ferrets estimated less than 2 weeks protection between influenza A and B viruses²⁴, yet cells forming the respiratory epithelium can survive in a state of heightened antiviral activation for 3 to 12 weeks after influenza A infection, with waning of the conferred protection observable at 6 weeks²³.

In Nha Trang, Vietnam, for more than 10 years children admitted to the single public hospital with acute respiratory illness have been tested for presence of influenza and RSV infection as part of an enhanced surveillance. RSV circulation is highly seasonal, and influenza circulation varies year on year, thus giving a unique opportunity to systematically investigate evidence for their competition at population level. We use this data in combination with a dynamic transmission model to estimate the strength of influenza and RSV competition and its effects on respiratory viral circulation.

3.5 Methods

3.5.1 Study population

We used data from a hospital-based enhanced surveillance study of children with respiratory disease, as previously described^{25,26}. In brief, children younger than 5 years old who resided in 16 out of the 27 communes of Nha Trang and attended the paediatric ward in Khanh Hoa General Hospital (KHGH) in Nha Trang, central Vietnam, with Acute Respiratory Infection (ARI) were enrolled and offered a suite of additional diagnostics. ARI was defined as cough and / or difficulty breathing. Khanh Hoa hospital is a tertiary care facility and is the only public hospital for the catchment area of the study. More than 95% of all paediatric ARI admissions are typically enrolled. Upon admission, Nasopharyngeal (NP) samples were taken from patients, nucleic acid was extracted and multiplex-PCR assays were performed in order to detect infection with up to 13 respiratory viruses, including influenza A and RSV. Positive samples underwent a second, confirmatory PCR test and only individuals who tested positive in both PCRs were included. We use aggregate weekly data, from 5th February 2007 until 4th December 2017. We assumed that an ARI episode, for which Influenza or

RSV were detected from the nasopharynx on admission, was caused by the respective pathogen. The dataset excludes neonatal cases under 28 days old.

To inform transmission pathways in the population we used age specific contact-patterns, based on a contact study in the same area, conducted in 2010²⁷. In total 2002 Nha Trang residents of all ages participated in the study. A contact was defined as either skin-to-skin contact or a two-way conversation.

3.5.2 Data analysis

We calculated the correlation between all reported influenza and RSV cases each week using a Pearson's Correlation test.

Assuming no interaction (in susceptibility to or severity of dual infections), we calculated the required annual RSV infection attack rate in order to observe the reported number of dual infections (equations 1-3). We estimate the RSV attack rate rather than the influenza attack rate, as RSV is more consistent year on year (see supplement section 1 for influenza equivalent). Using a negative binomial likelihood with Brent optimization we estimated the RSV reporting rate that would correspond to the maximum likelihood of observing the reported weekly number of dual infections. We then used this estimate of the reporting rate to calculate the annual RSV population attack rate required in order to observe this many coinfecting ARI admissions. The credible intervals for the attack rate were calculated using the Hessian matrix from the optimisation. If the estimated attack rate is high, this may suggest that influenza and RSV co-infection increase severity (and hence reporting). If the estimated attack rate is low, this could suggest that co-infection is less likely than random due to competition between the viruses.

$$I_{Dual} \approx I_{Influenza} * P_{RSV} \quad (1)$$

$$P_{RSV} \approx I_{RSV} * 1/\gamma_{RSV} / \nu_{RSV} \quad (2)$$

$$AR_{RSV} \approx I_{RSV} / \nu_{RSV} \quad (3)$$

With parameters: Incidence of reported cases (I), Prevalence of Infection (P), Duration of Infection ($1/\gamma$, 9 days - Table 3-1), attack rate (AR) and estimated reporting rate (ν).

3.5.3 Model

We created an age-structured deterministic transmission model for influenza and RSV, allowing for short-term cross-protection (See Supplement for model figure). Individuals are either Susceptible (S), Infectious (I), cross-Protected (P) and Recovered (R) for influenza (INF) and (RSV).

Susceptibles become infected at force of infections λ_{INF} and λ_{RSV} , and move into the I states. They then remain infectious for $1/\gamma_{INF}$ and $1/\gamma_{RSV}$ days and during the infectious period and $1/\rho$ days thereafter they are cross-protected and thus their propensity for heterologous infection is reduced by factor σ , the strength of cross-protection. All age groups are equally susceptible to influenza, but there is reduced susceptibility to RSV in older age groups, determined by parameter τ_i .

The force of infection includes age-specific contact rates derived from a local contact survey²⁷. Modelled age-groups are: 0-1 years (infants), 2 - 4 years (pre-school), 5 - 15 years (school), 16 - 64 years (adults) and 65 + (older adults). Infection reporting rates vary by age-group and virus, and for RSV reporting rates are increased by a multiplier from 2012 onwards, due to the circulation of a new genotype that has increased the average severity of infection and thus the proportion of reported infections (ON-1)²⁸. There is also a multiplier on the RSV reporting rates for dual infections, allowing them to be reported more frequently, for example because of increased propensity for respiratory disease that would require healthcare seeking (as observed in adults⁸). Model equations are shown in supplement section 3.

We model each season individually, with an initial proportion infected with each virus (v_{INF} and v_{RSV}). For RSV we assume the only immunity at the beginning of the season is the age-specific reduction in susceptibility (leaky immunity), as immunity to reinfection typically lasts less than a year²⁹. Due to infections in previous influenza seasons and potential vaccination, susceptibility to influenza is assumed to decline exponentially at rate η with age (see supplement section 6). This is modelled as non-leaky cross-protection, due to the combination of different exposures. Due to the short-time period modelled (max 66 weeks), we do not include births, deaths or ageing, but instead hold the age-group specific population sizes constant at the levels of 2010. Parameter definitions and values are shown in Table 3-1.

Table 3-1: Parameter definitions, values and priors

Parameter	Symbol	Value	Prior	Source
Transmission rate INF	β_{INF}	Fitted	Based on $R_{0,INF}$	See supplement section 4 for calculations
Basic Reproduction Rate Influenza	$R_{0,INF}$	Fitted	Between 1 and 8	³⁰
Transmission rate RSV	β_{RSV}	Fitted	Based on $R_{0,RSV}$	See supplement section 4 for calculations
Basic Reproduction Rate RSV for strain y	$R_{0,RSV,y}$	Fitted	Between 1 and 8	³⁰
RSV age group susceptibility (0-1, 2-4, 5-15, 16-64,65+)	τ_i	Fixed	1, 0.75, 0.65, 0.65, 0.65	Based on Henderson et al (1979) ³¹ , see supplement section 5
Infectious period Influenza	$1/\gamma_{INF}$	3.8 days	-	Cauchemez et al (2004) ³² Range from published papers: 1 - 4.5 days ³²⁻³⁵
Infectious period RSV	$1/\gamma_{RSV}$	9 days	-	Weber et al (2001) ²⁹ Range from published papers 6.7-12 days ^{29,36,37}
Strength of cross-protection	σ	Fitted	0 - 1	Assuming competitive ³⁸
Duration of cross-protection	$1/\rho$	Fitted	0 - Inf days	
Proportion of each age group infected with Influenza, at the start of the season	$\delta_{INF,s}$	Fitted	0 - 1	
Proportion of each age group infected with RSV, at the start of the season	$\delta_{RSV,s}$	Fitted	0 - 1	
Proportion susceptible to influenza at the start of the season	η_s	Fitted	0 - 1	Exponential function, see supplement section 6 for details
Influenza proportion reported in ages 0-1	κ_{INF}	Fitted	0 - 0.4	
Influenza multiplier for proportion reported ages 2-5 vs 0-1	$\kappa_{INF,m}$	Fitted	0-5	
RSV proportion reported in age group i	$\kappa_{RSV,i}$	Fitted	0-0.4	No additional severity from dual infection ³⁹

RSV ON-1 reporting multiplier	$\kappa_{RSV,2012}$	Fitted	1-5	ON-1 clinically more severe ²⁸
Dual infection multiplier on RSV proportion reporting	κ_{Dual}	Fitted	1 - Inf	Based on analysis of expected RSV Attack Rate above.
Overdispersion parameter	k	Fitted	0-Inf	

To capture the annual influenza and RSV epidemics despite regular changes, particularly in the timing of influenza circulation, we defined the annual start of the season as the minimum number of combined RSV and Influenza cases (on a 4-week rolling mean) between the 1st of November and the 1st of May each season. If one or more weeks had the same rolling average, we took the first occurrence within the time window (Figure 3-1A).

3.5.4 Likelihood

We fitted the model to the age-stratified weekly number of ARI cases with nasopharyngeal carriage of either influenza or RSV using a negative binomial likelihood (see Appendix C Figure S2C for data dispersion). To fit the allocation of those cases into influenza, RSV or dual infections we added a multinomial component to the likelihood:

$$L(x|\theta) = \sum_{j=1}^{N=2} \sum_{i=1}^n (NB(\mu_{i,j}, k) + MN(p_{RSV_{i,j}}, p_{Flu_{i,j}}, p_{Dual_{i,j}})) \quad (4)$$

Where x are the reported infections, θ are the parameters, j are the two age groups 0-1 and 2-4, and i are the weeks, with n being the total number of weeks. NB is the likelihood of the observed number of cases being a random draw from a negative binomial distribution with the total number of modelled infections as the mean, μ , and the fitted overdispersion parameter, k . MN is the multinomial likelihood, with p_{RSV} , p_{Flu} and p_{Dual} being the respective probabilities of the infection with influenza, RSV or both, calculated from the ratio of model reported cases.

3.5.5 Inference

We used parallel tempering to fit the model. This method involves running multiple Markov chains simultaneously, with different ‘temperatures’ that place a weighting on the likelihood. Swaps between the chains are then proposed every x (in this case 5) iterations, and accepted with acceptance ratio:

$$R = e^{((LL(i) - LL(j)) * (\tau_j - \tau_i))}$$

Where

$$\tau_i = \frac{1}{T_i}$$

Where T_i are the temperatures. For full details of the method see Vousden *et al* (2016)⁴⁰ We ran the parallel tempering algorithm with 12 chains and 450,000 iterations. The initial 250,000 iterations were discarded as burn-in. Accepted samples from the first chain were then thinned to 1 in 10 for analysis.

3.5.6 Vaccination

To assess the maximal indirect heterologous effect vaccination could have in this environment we assumed that vaccination completely stopped the circulation of the targeted virus. We then calculated the relative change in the number of cases in the pathogen not targeted by vaccination compared to a scenario without vaccination or competition. Estimates are based on simulations from 1000 posterior samples of the estimated parameters.

3.5.7 Sensitivity analyses

We assessed the sensitivity of our estimates of the strength of interaction of influenza and RSV to the prior on the interaction parameter and to the reporting rates of dual infections. We reran the model with a prior on the interaction parameter for strong interaction, using a normal distribution with mean 0.8 and standard deviation of 0.15. In addition, we ran a version of the model where the reporting rate for dual infections and RSV was the same, as it has been reported that in this setting there is no increased severity of dual infections among hospitalised children³⁹.

3.5.8 Ethics

This study was approved by the Institutional Review Boards of the London School of Hygiene & Tropical Medicine (16166 /RR/12988) and the National Institute of Hygiene and Epidemiology in Vietnam (15IRB)

3.6 Results

3.6.1 Descriptive Analysis

A total of 788 influenza and 1687 RSV hospitalised paediatric ARI cases were reported between 5th February 2007 and 4th December 2017; 78 (9% of influenza cases and 4% of RSV cases) of these were dual infections (Figure 3-1A&B). The mean age of at admission was 22 months and 16 months for influenza and RSV cases respectively. RSV notifications showed strong consistent seasonality across years, peaking usually in the 34th week of the year, whereas influenza showed less seasonality, but typically occurs after Tết Nguyên Đán holidays and before the RSV epidemic (Figure 3-1C).

There was a small, not statistically significant, negative correlation between weekly influenza and RSV cases, with the Pearson correlation coefficient -0.074 (95% CI 0.160 to 0.009). (Figure S1)

We estimated that in order to observe the weekly reported number of dual infections when assuming independence of influenza and RSV infection, the annual RSV attack rate needed to be 720% (95% CI: 560 -1000) in ages 0-1y and 430% (95% CI: 270 - 980) in ages 2-4y. The high attack rate suggests that in fact influenza and RSV infections are not independent, but that co-infection is likely to enhance the propensity for ARI hospitalisation in this setting.

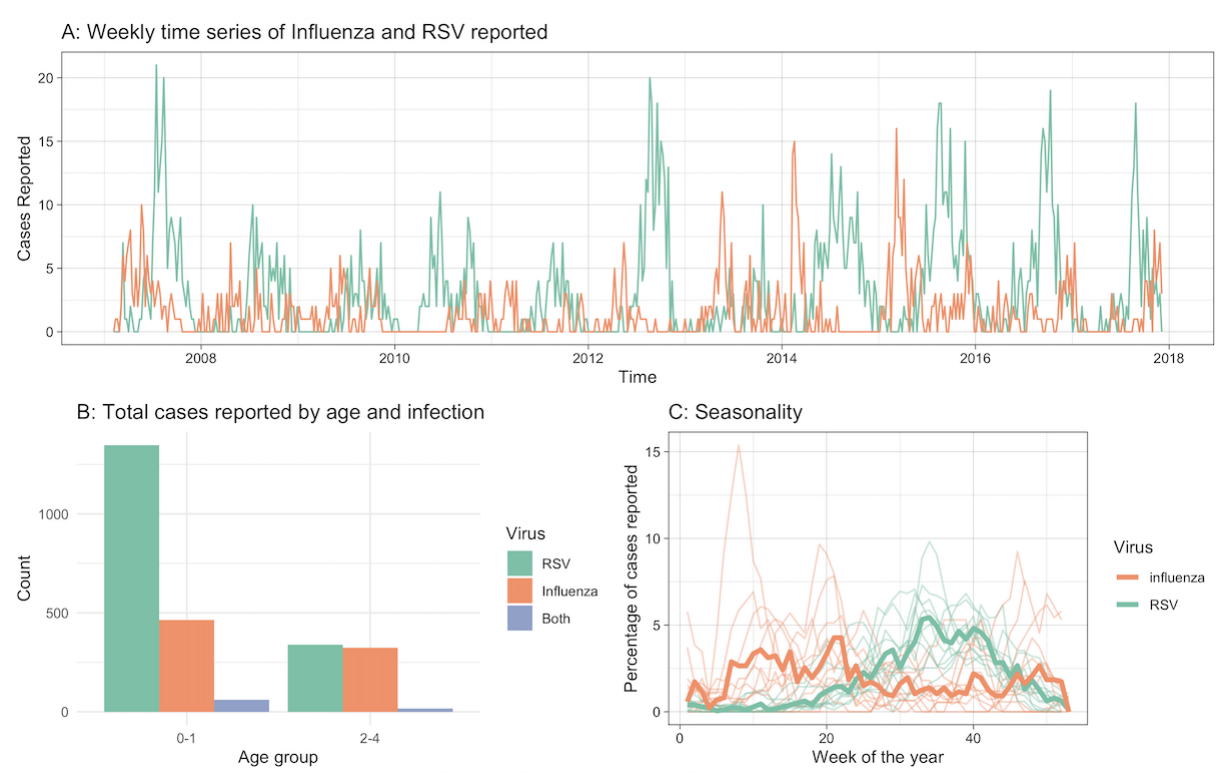


Figure 3-1: Data. A) Weekly reported infections of children under 5 years old infected with influenza and RSV over the study period. B) Total number of cases reported over the entire study period by age group and virus. C) Percentage of reported cases by week of the year for RSV and Influenza. The numerator is the weekly number

of either influenza or RSV cases reported and the denominator the total number of influenza or RSV cases reported over the relevant year. The thick lines show the combined total reported across all years, the semi-transparent lines show the 4-week moving average per year.

3.6.2 Model inference

The model was able to fit the case data for influenza and RSV well (Figure 3-2, see supplement section 7 for further fitting and convergence details). The posterior estimates for the relative reduction in heterologous acquisition rates during and following Influenza or RSV infection was bimodal, with one mode at 0.004 (95% CrI 0.000 - 0.046), indicating no interaction, and one mode at 0.41 (95% CrI 0.36 - 0.54), indicating moderate interaction, assuming a cut-off between modes at 0.2 (Figure 3-3A). The posterior for the duration of interaction also had multiple modes, with the mode corresponding to moderate interaction at 10.0 days (95% CrI 7.1 -12.8 days).

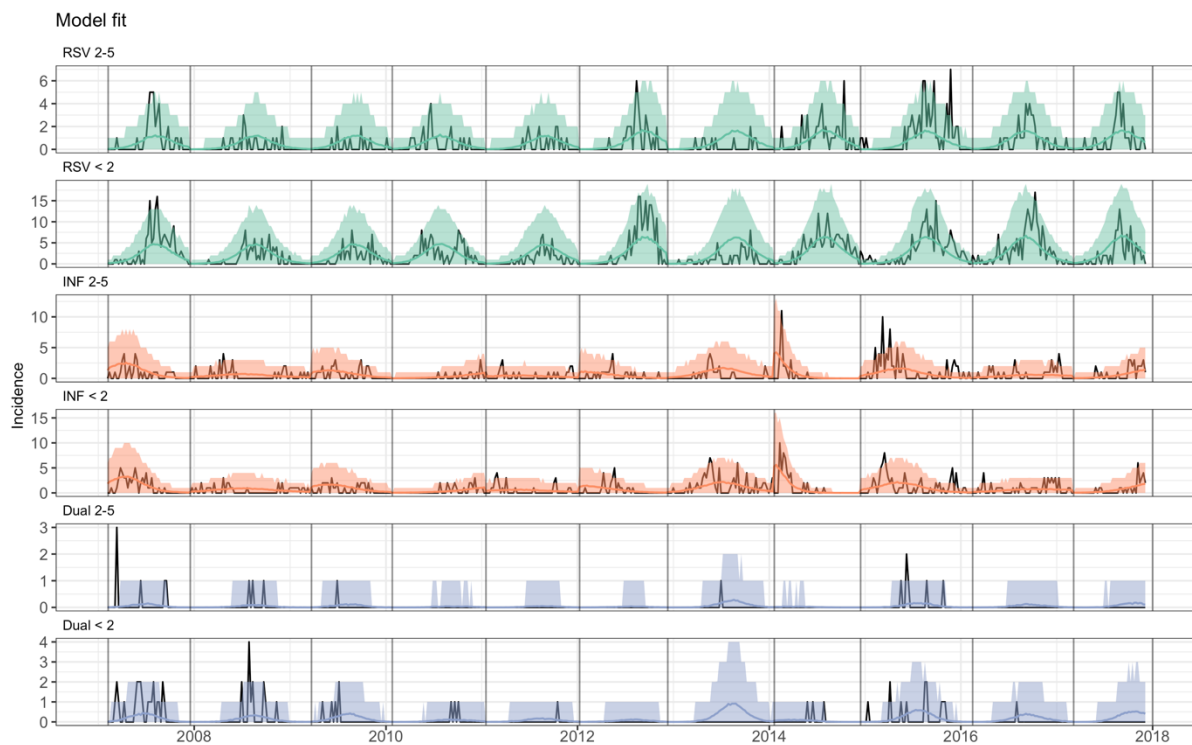


Figure 3-2: Model Fit: Black lines are the data, coloured lines are the 95% CrI posterior predictive interval. Panels show the fit by age group and Virus.

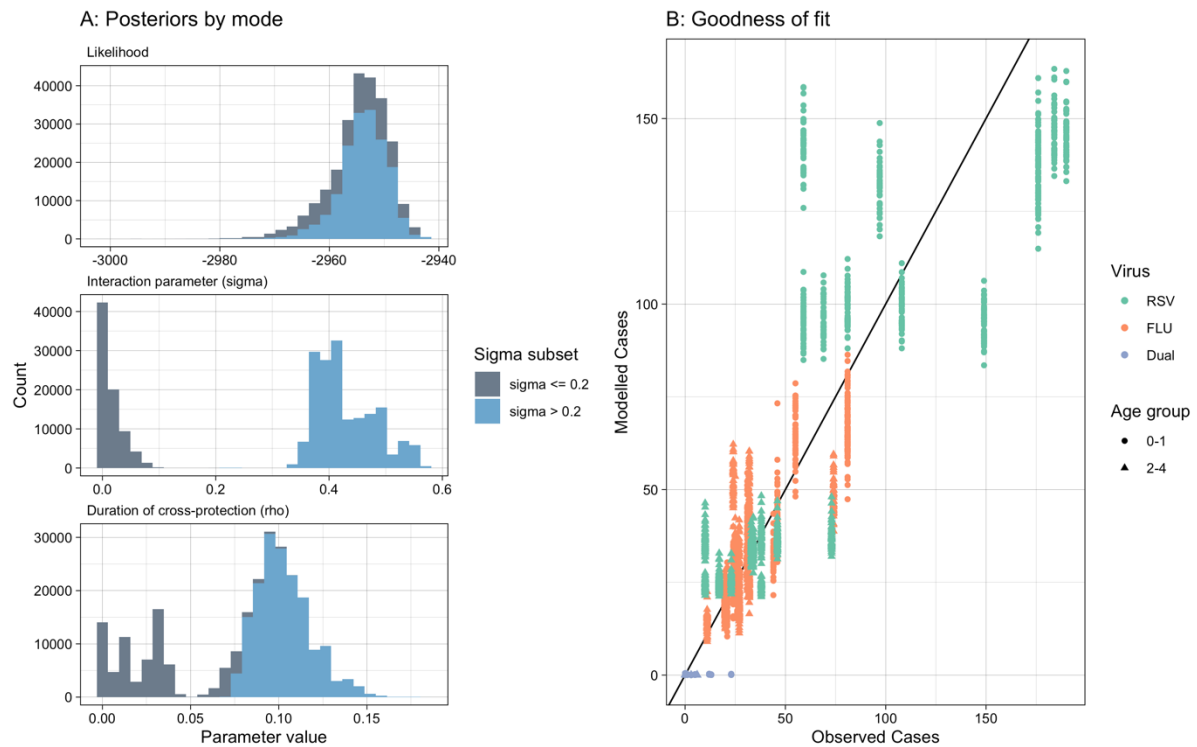


Figure 3-3 A) Posterior estimates for parameters σ and ρ , and the corresponding likelihood values. Colour is split by σ value of 0.2. B) Goodness of Fit: Observed cases by season against Modelled cases by season by virus and age group. The black line indicates the same value

The main differences between modes for other parameters were in the detection rate of influenza, which ranged from 13 to 21% of infections reported (supplement section 8) and the increased reporting for dual infections. We estimate that in the moderate interaction mode the observation of influenza and RSV coinfection among ARI cases was 8.2 (95% CrI 6.9 - 9.9) times more likely than would have been expected by chance in ages 2-4 and 16.6 (95% CrI 14.5 - 18.4) in ages 0-1. This compares to the no interaction scenario where the observation of influenza and RSV coinfection among ARI cases was 3.6 (95% CrI 2.5 - 5.8) and 7.2 (95% CrI 5.0 - 11.4) times more than would have been expected by chance in ages 2-4 and 0-1 respectively.

The posterior estimates led to R_0 's of 1.07 (95% CrI 1.06-1.1) and 1.24 (95% CrI 1.23 - 1.26) for influenza and RSV respectively. See supplement section 7 for the posteriors of other parameters.

To assess the relevance of RSV and influenza interaction on population level in this setting we simulated single pathogen versions of the parameterised model. In the case of no competition, absence of influenza (e.g. through widespread vaccination) reduced RSV hospitalisations by 4.1% (95%CrI 3.3 - 7.1%) due to a lack of co-infections with higher propensity for severe disease and absence of RSV reduced influenza hospitalisations by 7.2% (95%CrI 4.4-7.2%) in the study period. In

the moderate competition mode, absence of influenza reduced RSV hospitalisations by 5.7% (95%CrI 4.9 - 6.5%) . In the absence of RSV 1.8% (95%CrI -0.7 - 7.2%) more hospitalised cases for influenza occurred

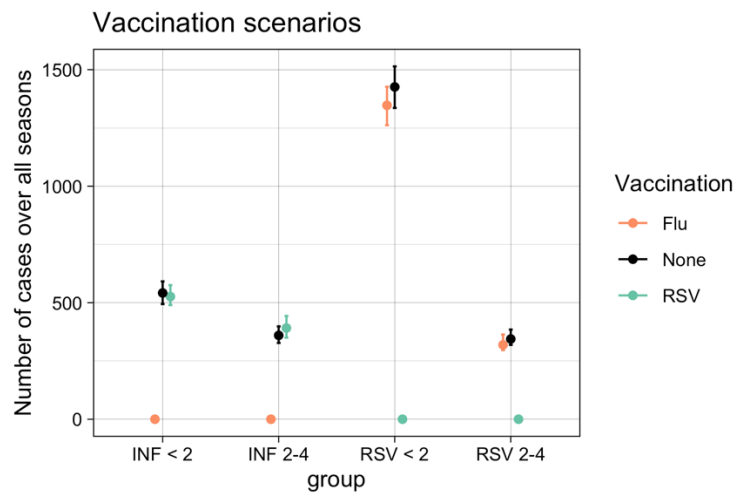


Figure 3-4: Vaccination scenarios: Number of cases modelled over all seasons, with different vaccination assumptions. Dots represent the median and lines the 95% CrI.

We estimated a seasonal attack rate ranging from 24% to 41% for RSV and 1% to 15% for Influenza (supplement section 8). For RSV, the attack rate was lowest in the oldest age group of 65+, whereas for influenza the lowest attack rates were in the youngest age group of 0-1 years old. Susceptibility to influenza at the start of the season was high, with all age groups in all years being over 87% susceptible to infection with the circulating strain (See supplement section 6).

3.6.3 Sensitivity

As a sensitivity analysis, we removed the multiplying factor for increased severity/reporting of dual infections (supplement section 9), which pushed the posterior to the no interaction mode. Further, we reran the model with a prior for strong cross-protection, which pushed the posterior to the moderate interaction mode (supplement section 10).

3.7 Discussion

We use data from more than 10 years of enhanced surveillance in Nha Trang, Vietnam to estimate the interaction of influenza and RSV epidemiology. We find that the observed data is consistent with infection reducing heterologous acquisition either by 41% (95% CrI 36% - 54%) for 10.0 days (95% CrI 7.1 -12.8 days) after infection or not at all. We estimate that influenza-RSV co-infection increases the

propensity of an infection to be reported through the ARI hospital surveillance by between 2.5 and 18.4 times. We go on to show that influenza vaccination in this setting may have little impact on the circulation of RSV but can have an added benefit in reducing hospitalisations with co-infections.

A key strength of this dataset is the inclusion of cases infected with both influenza and RSV. Surprisingly though, many dual infections are reported when the two viruses are individually at low levels of circulation which may be a result of stochastic effect owing to the low number of observed dual infections and has limited the strength of inference from them. While many papers reporting co-infections do not include timings of the co-infections⁴¹⁻⁴³, these off-peak co-infections were not observed in Texas⁴⁴. In addition, in Nha Trang influenza circulates continuously at low prevalence with small epidemics, which would result in constant low-level cross-protection, rather than a short-term more concentrated interaction after a large epidemic, such as in the UK⁴⁵. This low-level cross-protection could have been absorbed into the transmission rate of RSV, explaining the low estimate of the RSV R_0 (1.27 compared to a range of 1.2 - 9.1 in published papers³⁰). These location-specific features will need to be considered when generalising the findings. In addition, the data used only included children that attended the hospital, therefore presenting with relatively severe symptoms. The generalisability of this dataset to other settings, and therefore the model, should be considered when interpreting the results.

Much of the evidence for cross-protection is on an individual, biological level^{9,10,24}. However, this individual level cross-protection may not have an impact on population circulation, due to small numbers of infections at any point in time (in this study the seasonal attack rate for influenza varied from 0.011 - 0.15), meaning very few influenza cases at any one time, and thus a low propensity for co-infection with RSV. This sparsity may be exaggerated by clustering factors such as household transmission, reducing the opportunity for cross-infection. As an example in Kilifi, Kenya, household transmission of RSV contributes up to 52% of all RSV transmission⁴⁶. Our model assumes a well-mixed population, so does not account for any population clustering beyond the age-specific contact matrices. This assumption may impact the model more due to the relatively small population size and case reports, than a larger modelled population, due to the larger impact of stochasticity. In addition, we assume that risk of infection is age-dependent, but otherwise homogeneous. However, increased risk of influenza infection may be correlated with increased risk of RSV infection, due to demographic factors such as poor hygiene and household clustering. This may overestimate the effect of dual infections on reporting.

Evidence of cross-protection between influenza and RSV also comes from shifts in epidemic peaks, particularly after the 2009 influenza pandemic^{14–17}. However, these studies are observational, and cannot test mechanisms. As the SARS-CoV-2 pandemic has demonstrated, behavioural responses can have huge impacts on viral circulation, with many geographies seeing shifts in epidemic peaks for usually consistent viruses, such as RSV^{47,48}, due to limitations on social contacts. Fear generated from high infection rates can also drastically alter individuals behaviour⁴⁹, even without wide-spread implementations of restrictions.

Our model does not take into account different subtypes of influenza or RSV, due to the added complexity, additional parameters required and the lack of subtype specific data. We therefore assume that any cross-protection between influenza and RSV does not vary by subtype. We account for different immunity levels to circulating influenza subtypes by fitting a susceptibility parameter at the start of each season. This is necessary because we fit to each season, rather than including immunity waning and fitting over the time period combined. While the start weeks of our season are fixed manually, we account for any impacts of this by fitting the proportion infected at the start of each season for each virus. While most of the posterior estimates are reasonable, the reporting rate for influenza infections is high (between 13 and 21%). However, many milder cases (including outpatients) are included in the reports as they may seek healthcare at the hospital, thereby increasing the expected reporting rate in this context. Overall therefore, our model estimates fit the data well, as well as known aspects of influenza and RSV transmission, such as high influenza attack rates in children^{50,51}, and higher RSV severity in the youngest children⁵².

In summary, we use a novel modelling framework to interrogate a unique case time-series for single and dual infection from Nha Trang, Vietnam. We find that influenza and RSV co-infection substantially increases hospitalisation rates in children. In addition, we show that the data supports either no or moderate individual-level cross protection against infection but either way with relatively little population level impact. This alleviates some concerns of heterologous effects of RSV or influenza vaccination, however, particularly in settings with more pronounced and overlapping RSV and influenza seasons the impact of vaccination on the other pathogen's epidemiology may be more noticeable.

3.8 References

1. Velasco-Hernández, J. X., Núñez-López, M., Comas-García, A., Cherpitel, D. E. N. & Ocampo, M. C. Superinfection between Influenza and RSV alternating patterns in San Luis Potosí State, México. *PLoS ONE* **10**, (2015).
2. De Paulis, M. *et al.* Severity of viral coinfection in hospitalized infants with respiratory syncytial virus infection. *Jornal de pediatria* **87**, 307–313 (2011).
3. Arruda, E. *et al.* The burden of single virus and viral coinfections on severe lower respiratory tract infections among preterm infants: a prospective birth cohort study in Brazil. *The Pediatric infectious disease journal* **33**, 997–1003 (2014).
4. Harada, Y. *et al.* Does respiratory virus coinfection increase the clinical severity of acute respiratory infection among children infected with respiratory syncytial virus? *The Pediatric infectious disease journal* **32**, 441–445 (2013).
5. Lafond, K. E. *et al.* Global Role and Burden of Influenza in Pediatric Respiratory Hospitalizations, 1982–2012: A Systematic Analysis. *PLOS Medicine* **13**, e1001977–e1001977 (2016).
6. Shi, T. *et al.* Global, regional, and national disease burden estimates of acute lower respiratory infections due to respiratory syncytial virus in young children in 2015: a systematic review and modelling study. *Lancet (London, England)* **390**, 946–958 (2017).
7. WHO | WHO vaccine pipeline tracker. *WHO* (2016).
8. Zhang, Y. *et al.* Severity of influenza virus and respiratory syncytial virus coinfections in hospitalized adult patients. *J Clin Virol* **133**, 104685 (2020).
9. Lee, Y. J. *et al.* Non-specific Effect of Vaccines: Immediate Protection against Respiratory Syncytial Virus Infection by a Live Attenuated Influenza Vaccine. *Frontiers in Microbiology* **9**, 83–83 (2018).
10. Walzl, G., Tafuro, S., Moss, P., Openshaw, P. J. & Hussell, T. Influenza virus lung infection protects from respiratory syncytial virus-induced immunopathology. *The Journal of experimental medicine* **192**, 1317–26 (2000).
11. Glezen, W. P., Paredes, A. & Taber, L. H. Influenza in Children. *JAMA* **243**, 1345–1345 (1980).
12. Anestad, G. Interference between outbreaks of epidemic viruses. *Scandinavian Journal of Infectious Diseases* **39**, 653–654 (1982).
13. Hirsh, S. *et al.* Epidemiological changes of Respiratory Syncytial Virus (RSV) infections in Israel. *PLoS ONE* **9**, (2014).

14. Meningher, T. *et al.* Relationships between A(H1N1)pdm09 influenza infection and infections with other respiratory viruses. *Influenza and other Respiratory Viruses* **8**, 422–430 (2014).
15. Gröndahl, B. *et al.* The 2009 pandemic influenza A(H1N1) coincides with changes in the epidemiology of other viral pathogens causing acute respiratory tract infections in children. *Infection* **42**, 303–308 (2014).
16. Casalegno, J. S. *et al.* Impact of the 2009 influenza a(H1N1) pandemic wave on the pattern of hibernal respiratory virus epidemics, France, 2009. *Eurosurveillance* **15**, 2–2 (2010).
17. Mak, G. C., Wong, A. H., Ho, W. Y. Y. & Lim, W. The impact of pandemic influenza A (H1N1) 2009 on the circulation of respiratory viruses 2009-2011. *Influenza and other Respiratory Viruses* **6**, e6-10 (2012).
18. van Asten, L. *et al.* Early occurrence of influenza A epidemics coincided with changes in occurrence of other respiratory virus infections. *Influenza and Other Respiratory Viruses* **10**, 14–26 (2016).
19. Nishimura, N., Nishio, H., Lee, M. J. & Uemura, K. The clinical features of respiratory syncytial virus: Lower respiratory tract infection after upper respiratory tract infection due to influenza virus. *Pediatrics International* **47**, 412–416 (2005).
20. Pinky, L. & Dobrovoly, H. M. Coinfections of the respiratory tract: Viral competition for resources. *PLoS ONE* **11**, (2016).
21. Valkenburg, S. A. *et al.* Immunity to seasonal and pandemic influenza A viruses. *Microbes and infection* **13**, 489–501 (2011).
22. Ascough, S., Paterson, S. & Chiu, C. Induction and Subversion of Human Protective Immunity: Contrasting Influenza and Respiratory Syncytial Virus. *Frontiers in Immunology* **9**, 323–323 (2018).
23. Hamilton, J. Club cells surviving influenza A virus infection induce temporary nonspecific antiviral immunity.
24. Laurie, K. L. *et al.* Interval Between Infections and Viral Hierarchy Are Determinants of Viral Interference Following Influenza Virus Infection in a Ferret Model. *Journal of Infectious Diseases* **212**, 1701–1710 (2015).
25. Yoshida, L.-M. *et al.* Population based cohort study for pediatric infectious diseases research in Vietnam. *Tropical medicine and health* **42**, 47–58 (2014).

26. Yoshida, L. M. *et al.* VIRAL PATHOGENS ASSOCIATED WITH ACUTE RESPIRATORY INFECTIONS IN CENTRAL VIETNAMESE CHILDREN. *The Pediatric Infectious Disease Journal* **29**, 75–77 (2010).
27. Waroux, O. L. P. D. *et al.* Predicting the impact of pneumococcal conjugate vaccine programme options in Vietnam. *Human Vaccines & Immunotherapeutics* **14**, 1939–1947 (2018).
28. Yoshihara, K. *et al.* Association of RSV-A ON1 genotype with Increased Pediatric Acute Lower Respiratory Tract Infection in Vietnam. *Sci Rep* **6**, (2016).
29. Weber, A., Weber, M. & Milligan, P. Modeling epidemics caused by respiratory syncytial virus (RSV). *Mathematical Biosciences* **172**, 95–113 (2001).
30. Spencer, J. A. *et al.* Epidemiological parameter review and comparative dynamics of influenza, respiratory syncytial virus, rhinovirus, human coronavirus, and adenovirus. *medRxiv* 2020.02.04.20020404 (2020) doi:10.1101/2020.02.04.20020404.
31. Henderson, F. W., Collier, A. M., Clyde, W. A. & Denny, F. W. Respiratory-Syncytial-Virus Infections, Reinfections and Immunity. *New England Journal of Medicine* **300**, 530–534 (1979).
32. Cauchemez, S., Carrat, F., Viboud, C., Valleron, A. J. & Boëlle, P. Y. A Bayesian MCMC approach to study transmission of influenza: application to household longitudinal data. *Statistics in Medicine* **23**, 3469–3487 (2004).
33. Hayden, F. G. *et al.* Use of the Oral Neuraminidase Inhibitor Oseltamivir in Experimental Human Influenza. *JAMA* **282**, 1240–1240 (1999).
34. Chowell, G. *et al.* Characterizing the Epidemiology of the 2009 Influenza A/H1N1 Pandemic in Mexico. *PLoS Medicine* **8**, e1000436–e1000436 (2011).
35. Cori, A. *et al.* Estimating influenza latency and infectious period durations using viral excretion data. *Epidemics* **4**, 132–138 (2012).
36. Moore, H. C., Jacoby, P., Hogan, A. B., Blyth, C. C. & Mercer, G. N. Modelling the Seasonal Epidemics of Respiratory Syncytial Virus in Young Children. *PloS one* **9**, e100422–e100422 (2014).
37. Hall, C. B., Douglas, R. G. & Geiman, J. M. Respiratory syncytial virus infections in infants: quantitation and duration of shedding. *The Journal of pediatrics* **89**, 11–5 (1976).
38. Opatowski, L., Baguelin, M. & Eggo, R. M. REVIEW Influenza Interaction with Cocirculating Pathogens, and Its Impact on Surveillance, Pathogenesis and Epidemic Profile: A Key Role for Mathematical Modeling. *PLOS Pathogens* **14**, e1006770–e1006770 (2017).

39. Yoshida, L.-M. *et al.* Respiratory syncytial virus: co-infection and paediatric lower respiratory tract infections. *The European respiratory journal* **42**, 461–469 (2013).
40. Vousden, W. D., Farr, W. M. & Mandel, I. Dynamic temperature selection for parallel tempering in Markov chain Monte Carlo simulations. *Monthly Notices of the Royal Astronomical Society* **455**, 1919–1937 (2016).
41. Thongpan, I., Vongpunsawad, S. & Poovorawan, Y. Respiratory syncytial virus infection trend is associated with meteorological factors. *Sci Rep* **10**, 10931 (2020).
42. Goka, E., Vallety, P., Mutton, K. & Klapper, P. Influenza A viruses dual and multiple infections with other respiratory viruses and risk of hospitalisation and mortality. *Influenza and other Respiratory Viruses* **7**, 1079–1087 (2013).
43. Price, O. H., Sullivan, S. G., Sutterby, C., Druce, J. & Carville, K. S. Using routine testing data to understand circulation patterns of influenza A, respiratory syncytial virus and other respiratory viruses in Victoria, Australia. *Epidemiol Infect* **147**, e221 (2019).
44. Meskill, S. D., Revell, P. A., Chandramohan, L. & Cruz, A. T. Prevalence of co-infection between respiratory syncytial virus and influenza in children. *The American journal of emergency medicine* **35**, 495–498 (/03//).
45. Waterlow, N. R., Flasche, S., Minter, A. & Eggo, R. M. Competition between RSV and influenza: limits of modelling inference from surveillance data. *Epidemics* 100460 (2021) doi:10.1016/j.epidem.2021.100460.
46. Kombe, I. K., Munywoki, P. K., Baguelin, M., Nokes, D. J. & Medley, G. F. Model-based estimates of transmission of respiratory syncytial virus within households. *Epidemics* **27**, 1–11 (2019).
47. McNab, S. *et al.* Changing Epidemiology of Respiratory Syncytial Virus in Australia - delayed re-emergence in Victoria compared to WA/NSW after prolonged lock-down for COVID-19. *Clinical Infectious Diseases* (2021) doi:10.1093/cid/ciab240.
48. Gomez, G. B., Mahé, C. & Chaves, S. S. Uncertain effects of the pandemic on respiratory viruses. *Science* **372**, 1043–1044 (2021).
49. Funk, S., Salathé, M. & Jansen, V. A. A. Modelling the influence of human behaviour on the spread of infectious diseases: a review. *Journal of the Royal Society, Interface* **7**, 1247–56 (2010).
50. Minter, A. *et al.* Estimation of Seasonal Influenza Attack Rates and Antibody Dynamics in Children Using Cross-Sectional Serological Data. *The Journal of Infectious Diseases* (2020) doi:10.1093/infdis/jiaa338.

51. Jayasundara, K., Soobiah, C., Thommes, E., Tricco, A. C. & Chit, A. Natural attack rate of influenza in unvaccinated children and adults: a meta-regression analysis. *BMC Infectious Diseases* **14**, 670 (2014).
52. CDC. Learn about RSV in Infants and Young Children. *Centers for Disease Control and Prevention* <https://www.cdc.gov/rsv/high-risk/infants-young-children.html> (2020).

4 Chapter 4 - How immunity from and interaction with seasonal coronaviruses can shape SARS-CoV-2 epidemiology

4.1 Research Paper Cover Sheet



London School of Hygiene & Tropical Medicine
Keppel Street, London WC1E 7HT

T: +44 (0)20 7299 4646

F: +44 (0)20 7299 4656

www.lshtm.ac.uk

RESEARCH PAPER COVER SHEET

Please note that a cover sheet must be completed for each research paper included within a thesis.

SECTION A – Student Details

Student ID Number	1402815	Title	Mrs
First Name(s)	Naomi Ruth		
Surname/Family Name	Waterlow		
Thesis Title	Mathematical Modelling of Cross-protection between Respiratory Viruses		
Primary Supervisor	Dr. Rosalind M Eggo		

If the Research Paper has previously been published please complete Section B, if not please move to Section C.

SECTION B – Paper already published

Where was the work published?			
When was the work published?			
If the work was published prior to registration for your research degree, give a brief rationale for its inclusion			
Have you retained the copyright for the work?*	Choose an item.	Was the work subject to academic peer review?	Choose an item.

*If yes, please attach evidence of retention. If no, or if the work is being included in its published format, please attach evidence of permission from the copyright holder (publisher or other author) to include this work.


SECTION C – Prepared for publication, but not yet published

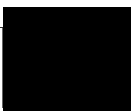
Where is the work intended to be published?	Proceedings of the National Academy of Sciences of the United States of America (PNAS)
Please list the paper's authors in the intended authorship order:	Naomi R Waterlow, Edwin van Leeuwen, Nicholas G Davies, CMMID COVID-19 working group, Stefan Flasche, Rosalind M Eggo
Stage of publication	Undergoing revision

SECTION D – Multi-authored work

For multi-authored work, give full details of your role in the research included in the paper and in the preparation of the paper. (Attach a further sheet if necessary)	I worked on: Conceptualisation, Methodology, Software, Validation, Formal Analysis, Writing – Original Draft, Visualization.
--	--

SECTION E

Student Signature	
Date	30/06/2021

Supervisor Signature	
Date	24 Aug 21

4.2 Bridging Section

This paper was made posted on *medRxiv* on the 31st of May 2021¹, and is undergoing second review (after revision following reviewer comments) at the *Proceedings of the National Academy of Sciences of the United States of America (PNAS)*. The revised paper was submitted on the 6th of September 2021. It estimates key parameters for seasonal coronavirus transmission (such as the basic reproduction number and the duration of immunity) and evaluates whether cross-protection between seasonal coronaviruses and SARS-CoV-2 could explain the relatively reduced susceptibility of children at the start of the SARS-CoV-2 pandemic. It therefore considers long-term, specific interaction and evaluates the implications of such interaction.

During the coronavirus pandemic in England and Wales, it has been observed that children are less susceptible to SARS-CoV-2²⁻⁵. It is hypothesised that this is due to interaction with seasonal human coronaviruses (HCoVs), which circulate annually. In this paper I use 5 years of coronavirus surveillance data from Public Health England to estimate key transmission parameters for seasonal HCoVs, using an age-structured dynamic model. I then simulate the introduction of SARS-CoV-2 with varying strengths of cross-protection between the seasonal HCoVs and SARS-CoV-2, to understand the impacts of cross-protection. While other models looking at interaction between coronaviruses exist⁶ – this is the first to model the assess the impact of cross-protection between seasonal HCoVs and SARS-CoV-2 focusing on the susceptibility of different age groups.

I developed the model, wrote the code, and performed the fitting analysis and simulations. I also wrote the paper and made the figures. Throughout the process I received input/suggestions/edits from both my supervisors, and an external collaborator (Dr. Edwin Van Leeuwen) who is based at PHE. I also received some advice on how to model the UK SARS-CoV-2 pandemic from Dr Nicholas G Davies and the paper went through the Centre of Mathematical Modelling of Infectious Disease's Covid-19 working group internal review.

The supplementary material of the original paper covers extra details on the methods and further projections. This is included as Appendix C in this thesis, so any references to supplementary materials can be found there.

4.3 Title page and abstract

How immunity from and interaction with seasonal coronaviruses can shape SARS-CoV-2 epidemiology

Naomi R Waterlow^{1,*}, Edwin van Leeuwen^{1,2}, Nicholas G. Davies¹, CMMID COVID-19 working group¹, Stefan Flasche¹, Rosalind M Eggo¹

¹ Centre for Mathematical Modeling of Infectious Disease, London School of Hygiene and Tropical Medicine, UK

² Statistics, Modelling and Economics Department, Public Health England, London, UK

NRW was supported by the Medical Research Council (grant number MR/N013638/1 and MR/V015737/1) and NIHR (grant COV0076). EvL was supported by the National Institute for Health Research (NIHR) Health Protection Research Unit (HPRU) in Modelling and Health Economics, a partnership between PHE, Imperial College London, and LSHTM (grant number NIHR200908). EvL was supported by the European Union's Horizon 2020 research and innovation programme - project EpiPose (101003688). SF is funded through a Sir Henry Dale Fellowship jointly funded by the Wellcome Trust and the Royal Society (grant number 208812/Z/17/Z). RME acknowledges an HDR UK Innovation Fellowship (grant: MR/S003975/1), MRC (grant: MC_PC 19065), and NIHR (grant: NIHR200908) for the Health Protection Research Unit in Modelling and Economics at LSHTM. The views expressed in this publication are those of the author(s) and not necessarily those of the NIHR or the UK Department of Health and Social Care.

CMMID Working group: The following authors were part of the Centre for Mathematical Modelling of Infectious Disease COVID-19 Working Group. Each contributed in processing, cleaning and interpretation of data, interpreted findings, contributed to the manuscript, and approved the work for publication: Rachael Pung, Paul Mee, William Waites, Damien C Tully, Katherine E. Atkins, C Julian Villabona-Arenas, Graham Medley, Frank G Sandmann, Anna M Foss, Sophie R Meakin, Carl A B Pearson, Emilie Finch, Nikos I Bosse, Christopher I Jarvis, Kiesha Prem, Alicia Rosello, Kevin van Zandvoort, Rosanna C Barnard, Jiayao Lei, Yang Liu, Adam J Kucharski, Ciara V McCarthy, Sam Abbott, Emily S Nightingale, Joel Hellewell, Thibaut Jombart, David Hodgson, Gwenan M Knight, Amy Gimma, Yung-Wai Desmond Chan, Yalda Jafari, Samuel Clifford, Timothy W Russell, Fiona Yueqian Sun, Simon R Procter, Akira Endo, Oliver Brady, Kaja Abbas, Billy J Quilty, Mark Jit, Sebastian Funk, Fabienne Krauer, Matthew Quaife, Hamish P Gibbs, W John Edmunds, Mihaly Koltai, Kathleen O'Reilly, Rachel Lowe, James D Munday.

The following funding sources are acknowledged as providing funding for the working group authors. This research was partly funded by the Bill & Melinda Gates Foundation (INV-001754: MQ; INV-003174: JYL, KP, MJ, YL; INV-016832: SRP; NTD Modelling Consortium OPP1184344: CABP, GFM; OPP1139859: BJQ; OPP1183986: ESN; OPP1191821: KO'R). BMGF (INV-016832; OPP1157270: KA). CADDE MR/S0195/1 & FAPESP 18/14389-0 (PM). EDCTP2 (RIA2020EF-2983-CSIGN: HPG). Elrha R2HC/UK FCDO/Wellcome Trust/This research was partly funded by the National Institute for Health Research (NIHR) using UK aid from the UK Government to support global health research. The views expressed in this publication are those of the author(s) and not necessarily those of the NIHR or the UK Department of Health and Social Care (KvZ). ERC Starting Grant (#757699: MQ).

Abstract

We hypothesised that cross-protection from seasonal epidemics of human coronaviruses (HCoVs) could have affected SARS-CoV-2 transmission, including generating reduced susceptibility in children. To determine what the pre-pandemic distribution of immunity to HCoVs was, we fitted a mathematical model to 6 years of seasonal coronavirus surveillance data from England and Wales. We estimated a duration of immunity to seasonal HCoVs of 7.8 years (95% CrI 6.3 - 8.1) and show that, while cross-protection between HCoV and SARS-CoV-2 may contribute to the age distribution, it is insufficient to explain the age pattern of SARS-CoV-2 infections in the first wave of the pandemic in England and Wales. Projections from our model illustrate how different strengths of cross-protection between circulating coronaviruses could determine the frequency and magnitude of SARS-CoV-2 epidemics over the coming decade, as well as the potential impact of cross-protection on future seasonal coronavirus transmission.

Significance Statement

Cross-protection from seasonal epidemics of human coronaviruses (HCoVs) has been hypothesised to contribute to the relative sparing of children during the early phase of the pandemic. Testing this relies on understanding the pre-pandemic age-distribution of recent HCoV infections, but little is known about their dynamics. Using England and Wales as a case study, we use a transmission model to estimate the duration of immunity to seasonal coronaviruses, and show how cross-protection could have affected the age distribution of susceptibility during the first wave, and alter SARS-CoV-2 transmission patterns over the coming decade.

4.4 Introduction

Due to the relatively short time since SARS-CoV-2 emerged, little is yet known about the duration of infection-induced immunity. While instances of confirmed reinfection of SARS-CoV-2 have been identified⁷, these are rare,⁸ indicating protection lasts for at least 6-8 months, which concurs with estimates from prospective studies^{9,10}. Cross-protection from seasonal human coronaviruses (HCoVs) could have impacted the transmission dynamics of SARS-CoV-2, and explain the relatively low SARS-CoV-2 infection rate in children^{3-5,11,12}. Since children likely have a higher annual attack rate of endemic HCoVs due to their higher contact rates¹³, they may be less susceptible to SARS-CoV-2 due to cross-protection.

In order to evaluate the impacts of cross-immunity, we first need to quantify the immune protection from seasonal coronaviruses. Four coronavirus strains from two different genera are endemic in humans: two are alpha-coronaviruses (HCoV-229E, HCoV-NL63) and two are beta-coronaviruses (HCoV-HKU1, HCoV-OC43); SARS-CoV-2 is a member of the latter genera as are SARS-CoV-1 and MERS-CoV. In the UK, seasonal human coronavirus (HCoV) case incidence peaks January-February each year. The first infection with seasonal HCoVs typically occurs in childhood¹⁴ and reinfection with the same strain has been observed within a year^{15,16}. However, there are also indications that immunity lasts longer, with few reinfections in a 3-year cohort study¹⁷ and sterilising immunity to homologous strains of HCoV-229E after one year in a challenge study¹⁸.

There may also be cross-protective immunity between seasonal HCoVs and SARS-family coronaviruses following infection. Human sera collected before the SARS-CoV-2 pandemic showed high IgG reactivity to seasonal HCoVs, but also low reactivity to SARS-CoV-2¹⁹, and SARS-CoV-1 infection induced antibody production against seasonal HCoVs^{20,21}. Cross-reactive T-cells to SARS-CoV-2 have been found in 20%²² to 51%²³ of unexposed individuals, with evidence that these responses stem from seasonal coronavirus infection²⁴. It has also been noted that these are more prevalent in children and adolescents²⁵.

Cross-protection from seasonal HCoVs may have, therefore, partially shaped the observed epidemiology of SARS-CoV-2. Using England and Wales as a case study, we use dynamic models to estimate: 1) the duration of infection-induced immunity to seasonal HCoVs, 2) the ability of potential cross-protection from seasonal HCoVs to explain the age patterns in the first wave of the SARS-CoV-2 pandemic, and 3) the implications of the duration of immunity and potential cross-protection on future dynamics of SARS-CoV-2.

4.5 Results

4.5.1 Seasonal HCoV and SARS-CoV-2 epidemic data

We extracted monthly, age group-stratified numbers of HCoV positive tests in England and Wales from the June 9, 2014 to February 17, 2020²⁶ and daily number of COVID-19 deaths in England and Wales during the first wave of the pandemic (March 02, 2020 to June 01, 2020)²⁷ (supplement section 1). The timeframe for the HCoV data is from the first available date until February 2020 to avoid interference from SARS-CoV-2 transmission and reporting. Annual numbers of coronavirus cases reported per year ranged from 965 to 2470, with the highest proportions of cases in ages 0 to

4 years olds (32%) and ages 65 years plus (30.0%) (Appendix C Figure S2B). The seasonal coronavirus reports showed high seasonality, with the annual peak of reporting in the first quarter of the year (Appendix C Figure S2A)

We fitted a dynamic transmission model using England and Wales as a case study (Supplement Figure S1C) using only the seasonal coronavirus model. Following infection, individuals are protected against infection with any seasonal HCoVs, with reinfection possible after a period of temporary but complete immunity. This period is determined by an artificial parameter governing the time to reinfection, due to decaying protection against homotypic viruses, and/or longer-lasting immunity against homotypic viruses but evolutionary change leading to immune escape²⁸. We do not track individual seasonal HCoV strains as available data are not sub-typed. We therefore assume that individual seasonal HCoV strains have the same parameter values, including $R_{0,HCoV}$. Transmission is seasonally forced using a cosine function.

4.5.2 Seasonal HCoVs have an R_0 of 5.9

We fitted the model to the age group-specific seasonal HCoV data from June 09, 2014 until February 17, 2020, and estimated key seasonal HCoV parameters using parallel tempering²⁹ (Figure 4-1). We fitted the artificial immunity parameter, the transmissibility, age-specific reporting proportions and two seasonal forcing parameters (Supplement Table S1). We estimated that the average duration between infection and return to susceptibility for seasonal HCoVs was 7.8 years (95% Credible Interval (CrI): 6.3 - 8.2) and that the basic reproduction number was 5.9 (95% CrI 5.5 - 6.2) (Figure 4-1B). As a sensitivity analysis, we excluded the first year of surveillance (up until July 2015), due to its different pattern, and here we estimated that the average duration between infection and return to susceptibility for seasonal HCoVs was 4.4 years (95% CrI 4.3 - 4.7) and that the basic reproduction number was 3.7 (95% CrI 3.6 - 3.8). Further details are given in the Supplement sections 2 and 3.

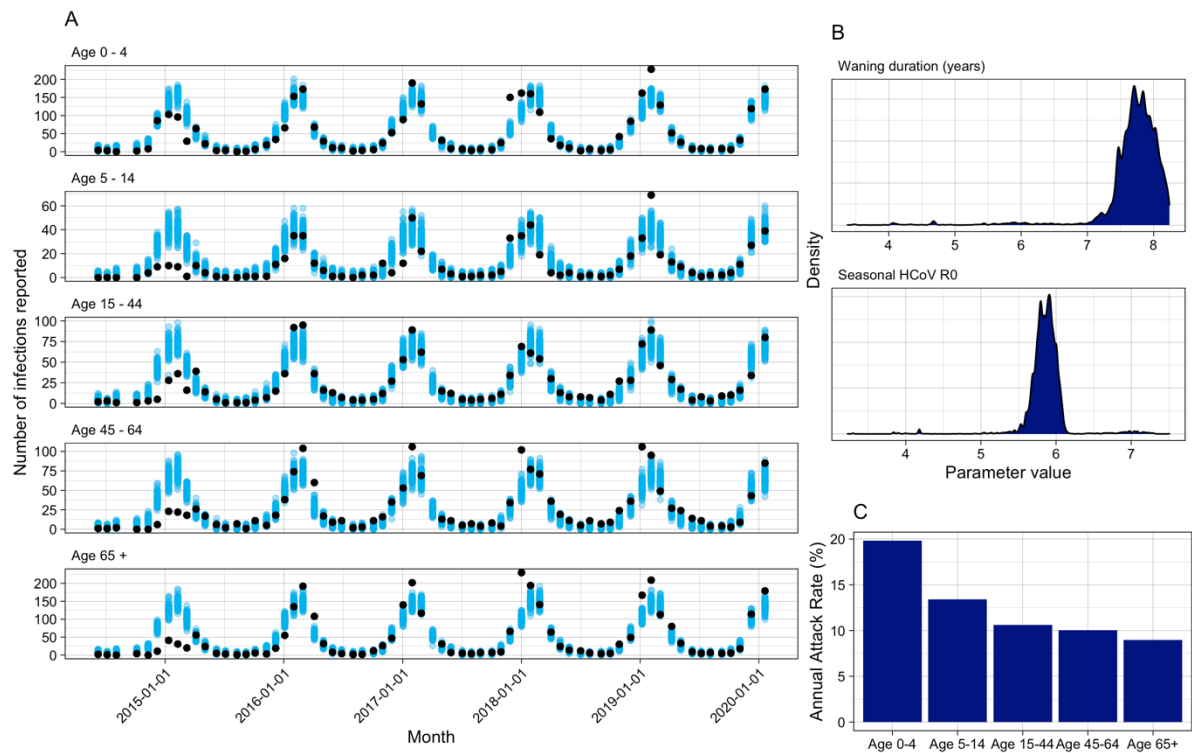


Figure 4-1: Seasonal HCoV Fit. A) Model fit for seasonal HCoV by age. Black dots show reported HCoV cases, blue are 100 random samples from the posterior. B) Posterior distributions for the duration of waning and the R_0 of seasonal HCoV. C) Mean annual attack rate for each age group from 100 samples of the posterior and the last 5 years of the fit.

4.5.3 Cross-protection from seasonal HCoVs is not sufficient to explain age-specific patterns of SARS-CoV-2 infection

We included SARS-CoV-2 into the model, where each compartment has the state for the combined seasonal HCoVs as well as the state for SARS-CoV-2 (Supplement section 2). We included cross-protection that decreases susceptibility to infection by SARS-CoV-2 by an amount, σ , for individuals in the $I_{HCoV,i}$ or $R_{HCoV,i}$ states ($\sigma = 0$ is no cross-protection and 1 is full cross-protection). We assume any interaction in the opposite direction would be negligible, due to the low proportion of the population that were infected in the first SARS-CoV-2 epidemic wave.

Using the posterior estimates of the seasonal HCoV parameters and the simulated output as initial states, we continued a simulation of epidemic seasonal HCoVs from the January 01, 2020 until June 01, 2020, including the introduction of SARS-CoV-2. Cross-protection from seasonal HCoVs and different mixing patterns (matching observed lockdown patterns, including school closures, see

Methods) were the only mechanisms we included that affected infection by SARS-CoV-2, so that we could evaluate the impact of cross-protection on the observed age distribution of cases.

For values of the cross-protection parameter between $\sigma=0$ and $\sigma=1$, we estimated $R_{0,C19}$ and the number of introductions of SARS-CoV-2 by fitting the extended model to daily reported COVID-19 deaths. We captured the national lockdown by decreasing contact rates following trends in Google mobility data³⁰. Our model fits were able to closely match the reported mortality incidence for each value of the cross-protection parameter (Supplement Figure S7). However, the resulting $R_{0,C19}$ varied widely, reaching over 25 for the strongest cross-protection (Figure 4-2A). The corresponding $R_{eff,C19}$ before the intervention on March 23 ranged between 2.25 and 3.75 (see Supplement section 3).

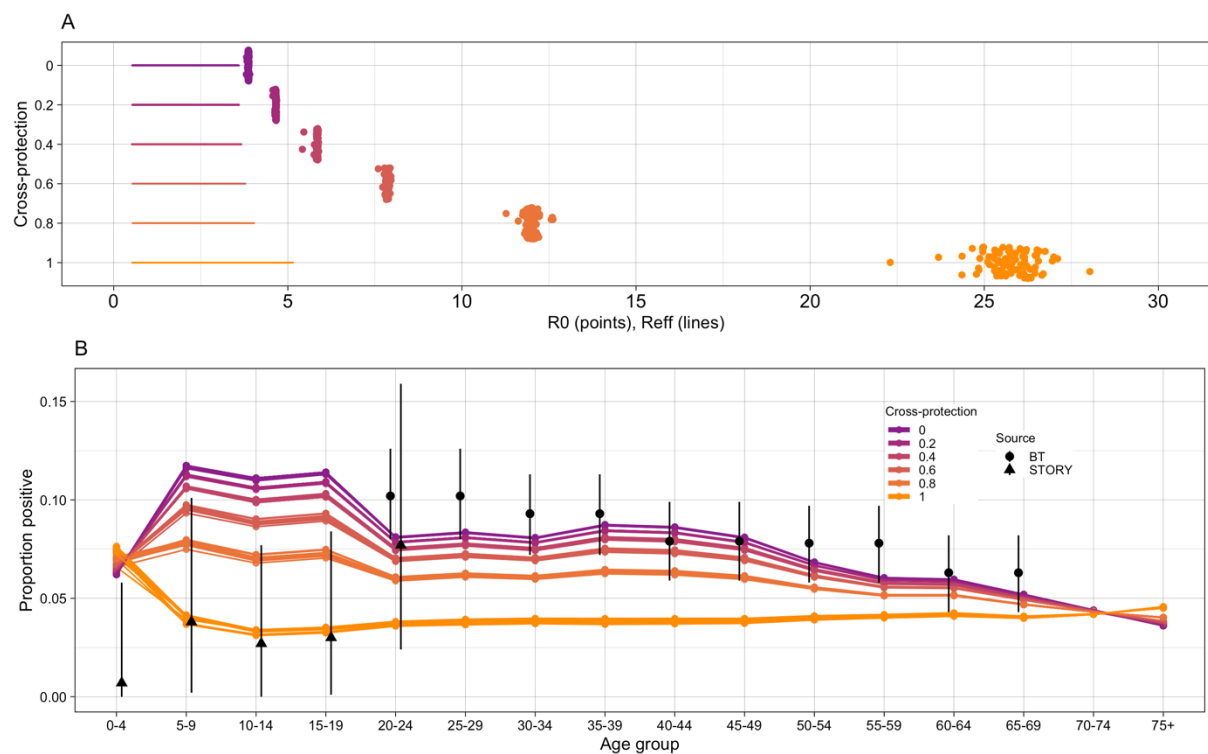


Figure 4-2: SARS-CoV-2 simulations A) Estimated R_0 values for SARS-CoV-2 with different strengths of cross-protection. Points display the $R_{0,C19}$ and lines show the range of $R_{eff,C19}$ during the simulation. B) Simulated age-specific serology rates for SARS-CoV-2 by the end of May 2020. Sources are Blood and Transplant donors (BT)³¹ and the 'What's the STORY' study (STORY)³².

We then evaluated the age distribution of infections that would be detected by serology by the end of May in our model, across the range of values of the cross-protection parameter (Figure 4-2C). In simulations with no or low cross-protection the model predicted larger proportions of children to have been infected than in older age groups, differing from observed data^{11,32}. As the strength of interaction increased, the age-distribution flattened and a smaller proportion of children became

infected. With complete protection, there was a higher rate in the youngest age groups, which has not been observed^{4,5,12,32}.

4.5.4 Future SARS-CoV2 epidemiology could be shaped by coronavirus interactions

To determine possible long-term dynamics of interacting coronaviruses, we ran 30-year projections of our model including both HCoV and SARS-CoV-2, with different assumptions on the strength of cross-protection and whether it acted from HCoV to SARS-CoV-2, or in both directions (Figure 4-3). In all scenarios we assumed no interventions, and used parameters estimated previously. For single-direction cross-protection, annual SARS-CoV-2 epidemics were projected to occur in scenarios with stronger cross-protection, whereas weaker / no cross-protection projected less frequent epidemics. However, strong cross-protection scenarios relied on very high and potentially unrealistic R_0 . In weaker cross-protection scenarios, interepidemic periods lasted multiple years following a pandemic. In scenarios with bi-directional cross-protection, SARS-CoV-2 infections also projected frequent epidemics, but led to the seasonal HCoV being disrupted. With low levels of cross-protection, SARS-CoV-2 and seasonal HCoV epidemics alternated, but as the cross-protection increased, SARS-CoV-2 epidemics became more frequent and outcompeted seasonal HCoV: while a cross-protection of 0.6 resulted in irregular dynamics of the viruses. At higher levels of cross-protection, no seasonal HCoV transmission occurred.

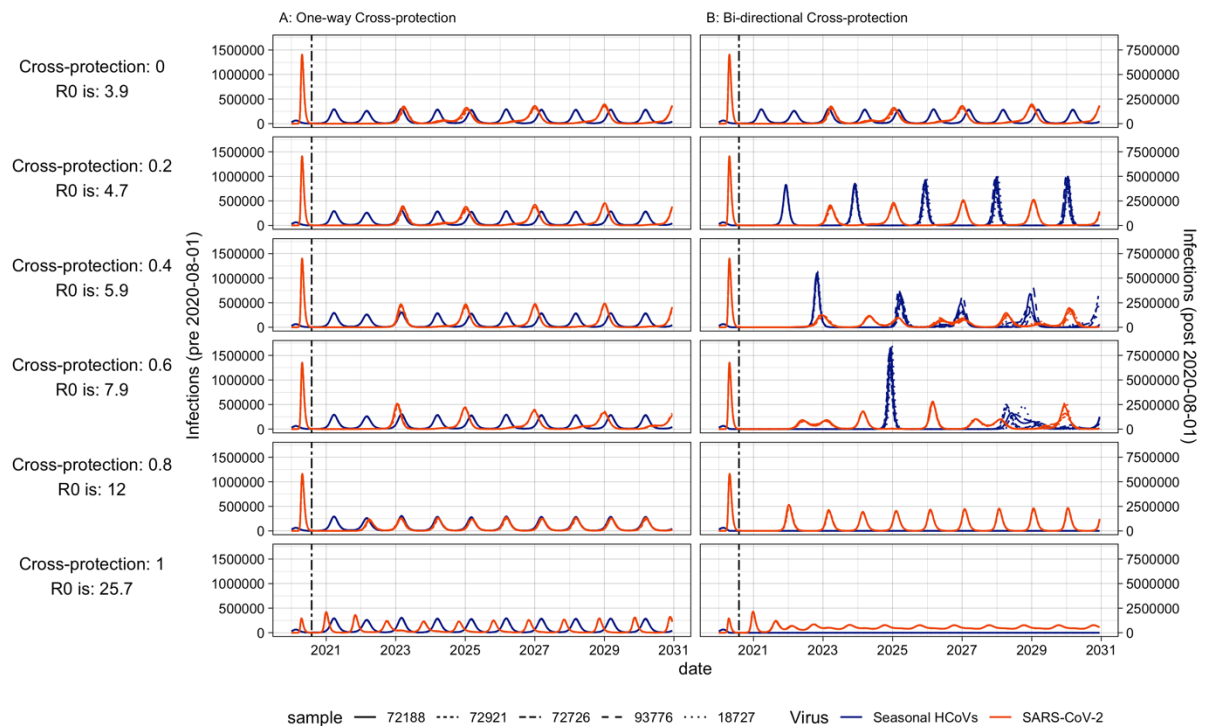


Figure 4-3: 10-year forward projections of seasonal HCoV and SARS-CoV-2 epidemics. Red indicates SARS-CoV-2, blue indicates Seasonal HCoVs. The dashed vertical line indicates a change in axis scale due to the much larger SARS-CoV-2 pandemic wave, with that to the left of the dashed line marked by the left axis and that to the right by the right axis. Cross-protection strength and estimated SARS-CoV-2 R_0 for the scenario are shown to the left of the figure. A has cross-protection from seasonal HCoV to SARS-CoV-2, and B has bidirectional cross-protection. No control measures were included. Different linetypes show different samples from the posterior of the seasonal HCoV fit.

4.6 Discussion

While it was possible to match the COVID-19 mortality data with the full range of cross-protection strengths between seasonal HCoV and SARS-CoV-2, the estimated $R_{0,C19}$ s were outside of a realistic range for very high values of cross protection. For example, a recent multi-setting study estimated the $R_{0,C19}$ to be between 3.6 and 7.3³³. Cross-protection from seasonal HCoVs to SARS-CoV-2 did not fully explain the apparent reduced susceptibility of children to SARS-CoV-2 observed during the first wave in the UK^{3,5,11,12,32}. We estimated that the R_0 for seasonal HCoVs is 5.7 (95% CrI: 5.4 - 6.0) and that time between infection and return to susceptibility 7.8 years (95% CrI 6.3 - 8.1). We found 12.8% (95% CrI: 11.9 - 13.7%) reinfection within one year for seasonal HCoVs, and the median reinfection time was 5.1 years (95% CrI: 4.7 - 5.5 years). Future projections varied in the frequency of SARS-CoV-2 epidemics, with SARS-CoV-2 epidemics every two years at low levels of cross-protection, changing to annual epidemics with increased cross-protection. In scenarios with bi-directional cross-protection, epidemics were less predictable and SARS-CoV-2 out competed

seasonal HCoVs. Further elucidating possible cross-protection and potential duration of protection is therefore critical for medium-to-long-term projections of SARS-CoV-2 epidemics.

Our estimates for the duration of homotypic protection following HCoV infection are comparable with other estimates, such as a cohort study where 8/216 (3%) confirmed infected individuals were reinfected over 5 years, and the median re-infection time in a study of 10 individuals³⁴ varied between 30 and 55 months, depending on strain. However, estimates vary, with a larger study in Michigan estimating mean strain-specific reinfection to be between 19 and 33 months³⁵, 19.9% of first infections being reinfected within 6 months in Kenya³⁶, and a historical study, of just one seasonal HCoV strain (229E), estimating the time until T cells could no longer neutralise new strains at 8-17 years²⁸. Other coronaviruses can also give indications on the duration of immunity, with T cells to SARS-CoV-1 detectable up to 11 years post-infection³⁷. Other modelling studies without age structure have estimated a substantially shorter duration of immunity, at less than a year⁶. However, these estimates imply very high annual attack rates, which are not observed in surveillance data, despite coronaviruses often being tested as part of a multiplex respiratory virus PCR panel. Despite differences in the model, such as the focus on between seasonal HCoV competition and the exclusion of alpha-coronavirus and age-structure, our model suggests that a longer period of cross-protection may be more appropriate, and should be included in the proposed range of parameters for fitting such models.

Our model estimates a longer duration of homotypic protection following HCoV infection (7.8 years) than the duration of data used to fit (~ 6 years). While this may seem counterintuitive, the estimate is based on the susceptibility of the population, which is generated by initially running the model to equilibrium. Therefore, the number of seasons used should not impact the estimate of the duration of homotypic protection, providing additional seasons does not have large differences that impact the susceptibility of the population. In our sensitivity analysis, we exclude the 1st season of data in which fewer cases are reported (roughly half the peak incidence compared to other years). Here we estimate a shorter duration of homotypic seasonal HCoV protection, yet still lasting multiple years: 4.4 years (95% CrI 4.3 - 4.7). This difference is likely due to testing differences, as it is the first year of surveillance. We would expect the estimate to not change as much when excluding other years, as these are much more conserved.

In our model, stronger cross-protection decreased the relative susceptibility to infection of children. This is in line with an American study showing that 50% of pre-pandemic donors had reactive T-cells

to SARS-CoV-2³⁸ and serological markers for a recent seasonal HCoV infection, suggesting that immune responses to seasonal HCoV could elicit cross-protection. Moreover, 48% of uninfected individuals in a cohort from Australia had cross-reactive T-cells to SARS-CoV-2 which was strongly correlated with memory T cells against seasonal coronavirus strains²⁴. Other studies among healthy individuals without SARS-CoV-2 exposure found cross-reactive T-cells targeting SARS-CoV-2 in 51%³⁹, 35%²³ 24%⁴⁰, and 20%²² of participants, suggesting a moderate amount of cross-immunity that likely stems from seasonal coronaviruses. There are indications that these cross-reactive T cells are present at higher frequency in younger vs older adults^{41,42}, correlating with our hypothesis that this could be due to increased infection from seasonal HCoVs. These cross-reactive T-cells target the conserved spike protein antigens⁴¹. Antibodies have also been shown to be cross-reactive⁴³ and back-boosting of antibodies against conserved HKU1 and OC43 spike antibodies has been observed in COVID-19 infection, with evidence for immunological imprinting⁴⁴. The persistence of antibody in the body is more varied and often shorter in duration than T-cells⁴⁵. Cross-reactive responses have also been identified in other pandemic coronaviruses^{19-21,46}, with some also showing cross-protection: SARS-CoV-1 and MERS-CoV T-cell epitopes were protective in mice against other human and bat coronaviruses⁴⁷ and a lack of HCoV-OC43 antibodies can increase SARS-CoV-2 severity in humans (adjusted odds ratio of 2.68)⁴⁸. Cross-neutralising antibodies across the clade have also been identified⁴⁹. However a longitudinal study showed that whilst cross-reactive HCoV antibodies are boosted following SARS-CoV-2 infection, this does not correlate with protection against infection or hospitalisation⁵⁰ and a lack of antibody-mediated neutralising cross-protection has been noted between sera from SARS-CoV-1 patients and SARS-CoV-2⁵¹. In addition, it has been postulated that the small variety in circulating human coronaviruses may have resulted due to competition between coronaviruses filtering out potential emergent coronaviruses⁵². Therefore, whilst there is significant amounts of corroborating evidence that some degree of cross-protection exists, the literature is not conclusive.

Our results indicate that cross-protection from seasonal coronaviruses alone cannot explain reduced susceptibility to infection of children. Other factors are needed to counteract the children's higher than average exposure probability driven by their contact behavior¹³, in order for the model to fit the serological data. One mechanism for this could be due to differences in children's immune system⁵³: children can produce broadly reactive antibodies that have not been influenced by commonly circulating pathogens and have different proportions of blood cell types, such as specific subtypes of memory B cells, and larger populations of IgM-producing cells. Genetic analysis also suggests that cross-reactivity to SARS-CoV-2 antigens cannot fully be explained by seasonal

coronaviruses, implying that other unknown viruses/factors may induce cross-immunity⁵⁴. An additional factor that could have been included in the model that would have impacts on the susceptibility of children is maternal immunity, which would have reduced the susceptibility of the youngest age group, thereby improving the model fit to the data. We also modelled cross-protection as only reducing susceptibility to infection, whereas there could also be a reduction in transmission and/or disease severity^{55–58}, which may have resulted in a further reduction of susceptibility of children, thereby explaining the observed data that we were unable to replicate. Boosting of immunity by multiple infections has also been suggested to influence cross-protection⁵⁶, where boosting by repeat infections was hypothesised to reduce the cross-protection to SARS-CoV-2. We did not include boosting in our model due to the added complexity.

The strength and implications of cross-protection between HCoVs and SARS-CoV-2 will become increasingly evident over the coming months and years. Our projections show that, depending on the extent of cross-protection, SARS-CoV-2 could eventually cause annual epidemics (strong cross-protection) or epidemics every 2 years (little cross-protection). If bi-directional cross-protection occurs, SARS-CoV-2 also has the ability to substantially disrupt seasonal HCoV transmission. This is based on our fit of the duration of immunity and the seasonal forcing parameters of seasonal HCoVs, which are likely to differ to some extent in the case of SARS-CoV-2. These scenarios are in line with others^{6,59–61}, which suggest that ongoing SARS-CoV-2 transmission is likely. Alternatively, the introduction of SARS-CoV-2 could have different impacts on seasonal HCoVs, for instance outcompeting beta-coronaviruses without affecting the circulation of alpha-coronaviruses. A similar dynamic occurred following the 2009 influenza pandemic, where the previous H1N1 strains were replaced by the 2009 H1N1 strain, but H3N2 circulation continued^{62,63}. Our modelled projections assumed that no interventions were implemented. However, HCoV circulation was disrupted in winter 2020–2021⁶⁴ likely due to social restrictions designed to curb the transmission of SARS-CoV-2. It is important to understand the longer-term dynamics of SARS-CoV-2, in order to minimise deaths and plan vaccination strategies. From an evolutionary perspective, cross-protection may be a strong driver for selection, so in the long run a less transmissible type with greater cross-protection against competing viruses may dominate.

We modelled all seasonal HCoVs as one virus, thereby assuming complete cross-protection between them. There is evidence for cross-protection between seasonal HCoVs and especially within the alpha and beta subtypes, such as the presence of cross-reactive antibodies⁶⁵ and evidence from modelling studies⁶. While in some geographies such as the US and Denmark^{6,66} differing patterns by

subtype are observed, this is not the case in the United Kingdom⁶⁷. Yet cross-protection may not be complete, or may be subtype specific (alpha- vs beta-coronaviruses), and hence our assumption could lead to an underestimation of the true duration of protection. Because the duration between homotypic infections would be longer than between infections of any subtype. We expect the single-subtype assumption used here to have a relatively small impact on the results of the cross-protection in the first wave of SARS-CoV-2, which uses the average cross-immunity profile at the end of the seasonal HCoV epidemic. However, the assumption may have a larger impact on the longer term dynamics. We also assumed that the strength of immunity to seasonal HCoVs is constant over repeated infections. An alternative mechanism would be that repeat infections strengthen immunity, as is hypothesised for some respiratory infections, such as Respiratory Syncytial Virus⁶⁸ which could have led to a different estimate of reinfection time for seasonal HCoVs. This could therefore result in higher immunity in adults and lower in children and thereby reduce the ability of cross-protection to explain the lower susceptibility to SARS-CoV-2 in children, strengthening our conclusions. Seasonal HCoV cases may have a time-varying reporting rate due to the circulation and testing of other viruses that cause respiratory illness, which could increase reporting or testing during the UK winter respiratory virus season, and reduce reporting or testing in the off season. This could affect the amplitude of the epidemics and therefore could inflate the estimate of the seasonal forcing amplitude parameter.

The emergence of SARS-CoV-2 has highlighted our lack of knowledge on coronavirus immunity and long term dynamics. In our study, we estimate that immunity against seasonal HCoVs can last years, however by necessity we made strong assumptions about the cross-immunity between seasonal HCoV strain. Further studies exploring cross-protection between strains for seasonal coronaviruses as well as routinely subtyped surveillance data would help inform future models. Nonetheless, based on the available data our study indicates that seasonal coronavirus immunity may last multiple years, which should be considered in the planning of subsequent studies. We also conclude that cross-protection from seasonal coronaviruses is not enough to explain the age susceptibility pattern of SARS-CoV-2, indicating other mechanisms must be involved. Whilst serological data could be useful to further evaluate the extent of cross-protection, the reduction in social contacts due to government interventions against SARS-CoV-2 complicates their use. Our models rely heavily on social contact matrices, and getting an accurate understanding of social contacts in the last year comes with many challenges, such as multiple changes in public health interventions with uncertain adherence. Our study highlights the importance of understanding the background environment of coronaviruses for insights into SARS-CoV-2 pandemic progression.

4.7 Materials and Methods

We created a dynamic transmission model that includes cross-protection between seasonal HCoVs and SARS-CoV-2, using England and Wales as a case study. Initially, we fit the model without SARS-CoV-2 and estimated key seasonal HCoV parameters. Next, we simulated SARS-CoV-2 introduction with varying strengths of cross-protection, to investigate the effect on age-specific susceptibility. The model was written in R⁶⁹ and the code is available at

https://github.com/cmmid/coronavirus_immunity

4.7.1 Data

We extracted the monthly, age group-stratified number of HCoV positive tests in England and Wales between June 09, 2014 and February 17, 2020, reported to Public Health England (PHE) from National Health Service (NHS) and (PHE) laboratories²¹. The sources of these cases are: Respiratory viral detections by any method (culture, direct immunofluorescence, PCR, 4-fold rise in paired sera, single high serology titre, genomic, electron microscopy, other method and method unknown". Numbers are reported in age groups: 0-4, 5-14, 15-44, 45-64 and 65+. We did not use data beyond February 2020, as we wanted to estimate seasonal HCoV parameters in the absence of SARS-CoV-2. Whilst we do not have subtype information for the PHE data collected in England and Wales, we know from studies in Scotland, where subtyping is performed, that there is reasonable consistency in circulating subtypes each year (Nickbahksh *et al.* (2020)⁶⁷).

For SARS-CoV-2, we used the daily number of deaths with a confirmed SARS-CoV-2 positive test in the preceding 28 days from March 02, 2020 until May 31, 2020 reported by the Office for National Statistics (ONS)²⁷.

To compare SARS-CoV-2 we used serology from two sources. Firstly, we used data from a study in April and May 2020 of children and young people aged up to 20-24 in England called "What's the STORY"³². This data assesses serology using the ABBOT assay, which used the Abbott assay, testing for IgG to the SARS-CoV-2 nucleocapsid protein, adjusted for sensitivity and specificity. Secondly, for adults, we used data collected through the UK NHS Blood and Transplant services³¹ between March and May 2020 which tested approximately 1000 samples per region in England using the Euroimmun assay and adjusted for the accuracy of the assay and weighted by population.

4.7.2 Cross-protection Model

We created a deterministic compartmental transmission model for coronavirus infections and their interactions. The population are either Susceptible (S), Exposed (E), Infectious (I) and Recovered (R) for both seasonal HCoVs and SARS-CoV-2. The subscripts used are “HCoV” for seasonal HCoVs and “C19” for SARS-CoV-2, with no differentiation between HCoV strains as the data are not sub-typed. Following infection, individuals enter the exposed category and become infected at rates $\lambda_{HCoV,i}$ and $\lambda_{C19,i}$ respectively, and individuals enter the infectious category at rates ν_{HCoV} and ν_{C19} . They then recover and become fully susceptible again at rate ω . The force of infection for each virus is shown in equations 1 and 2. Each compartment in the model records the state for SARS-CoV-2 and seasonal HCoVs, with one for each combination of states and all durations are exponentially distributed. At any point individuals can be infected by the other virus, although this is less likely to occur in the I and R categories, determined by the cross-protection parameter, σ . This takes into account both short term cross-protection from the activation of the immune system, and longer-term adaptive immunity. Both modelled viruses (HCoVs and SARS-CoV-2) are seasonally forced with a cosine function, which captures changes in seasonal human behaviour and climatic factors.

$$\lambda_{HCoV,i,t} = \sum_{j=1}^{j=N} \left(\left(\frac{A_{HCoV} * \beta_{HCoV}}{R_{0,HCoV}} \right) * \cos\left(\frac{2\pi}{52*7} - \phi\right) + \beta_{HCoV} \right) * \alpha_{i,j} * I_{HCoV,j} \quad (1)$$

$$\lambda_{C19,i,t} = \sum_{j=1}^{j=N} \left(\left(\frac{A_{C19} * \beta_{C19}}{R_{0,C19}} \right) * \cos\left(\frac{2\pi}{52*7} - \phi\right) + \beta_{C19} \right) * \alpha_{i,j} * I_{C19,j} \quad (2)$$

λ = Force of infection, i and j = age groups, N = total number of age groups, A = seasonal amplitude, β = transmissibility, α = contact rates, I = number Infected, ϕ = timing of seasonal forcing. R_0 is the basic reproduction number.

As the seroprevalence for SARS-CoV-2 stayed below 5% during the modelled period, we assumed that the level of cross-protection conferred by SARS-CoV-2 on HCoV is negligible during the first epidemic wave. Cross-protection was the only mechanism we included for differing susceptibility to SARS-CoV-2 infection by age group, so that we could test whether it explained the observed infection pattern.

The modelled population was stratified into 5-year bands to 75+, with constant birth rates, matching death rates and ageing in line with the population of England and Wales (Table 4-1). Age-assortative mixing was modelled proportionately to patterns of conversational and physical contacts in the POLYMOD study^{13,70}.

We ran a HCoV-only model for 15 years to reach equilibrium, and a further 5 years to generate simulations to match the data on seasonal HCoV cases from June 09, 2014 to February 17, 2020.

Table 4-1: Model Parameters

Parameter type	Parameter	Symbol	Value	Reference
Seasonal HCoV	Basic Reproduction number	$R_{0,HCoV}$	Fitted. Limits: 1-8.5	Wide range
	Transmission rate	β_{HCoV}	Fitted	Based on R_0 calculation (supplement)
	Latent period	$1/\nu_{HCoV}$	2.5 days	^{6,71}
	Duration of infectiousness	$1/\gamma_{HCoV}$	5 days	⁶
	Incubation period (time to symptoms)	$1/\delta 1_{HCoV}$	2 days	⁷²
	Reporting delay (symptom to report)	$1/\delta 2_{HCoV}$	3 days	Based on influenza model ⁷³
	Age-specific reporting proportion	$\mu_{HCoV,i}$	Fitted. Limits 0-1. Proposed on log odds scale.	
	Seasonal forcing amplitude	A	Fitted. Limits: 0 - 2	
	Seasonal forcing timing	ϕ	Fitted. Limits: - (52*7)- (52*7)	
	Immunity duration	$1/\omega$	Fitted. Limits: 100 – 3000 years	Covers range of 100 days to over 8 years
SARS-CoV-2	Basic Reproduction number	$R_{0,C19}$	Fitted	Based on R_0 calculations (see supplement).
	Transmission rate	β_{C19}	Fitted	
	Effective Reproduction Number	$R_{eff,C19}$	Fitted	R_0 * proportion susceptible (see supplement)
	Latent period	$1/\nu_{C19}$	3 days	⁶
	Duration of infectiousness	$1/\gamma_{C19}$	5 days	⁷⁴
	Time between infectiousness (entering I compartment) and death	$1/\delta_{C19}$	22 days (split over two compartments, Erlang distributed)	⁷⁵

	Age-specific infection fatality proportions (age groups 0-4, 5-14, 15-44, 45-64, 65+)	$\mu_{c19,i}$	0.00004, 0.00004, 0.00024, 0.00441, 0.06720	As in Levin ⁷⁶ , weighted by model population sizes
	Adult (15-64 years) introduction rate	$1/\eta$	Fitted	
	Duration of immunity	$1/\omega$	Fitted	Assumed equal to HCoV waning rate
Demographic	Birth rate	μ_b	640 370 per year	ONS statistical bulletin 2019 ⁷⁷
	Death rate	μ_d	640 370 per year	Equal to birth rate to maintain constant population
	Population size	N	59 439 840	ONS 2019 population estimates for England and Wales, 5-year age bands ⁷⁸

4.7.3 Inferring seasonal HCoV parameters

We used reported seasonal HCoV cases from June 09, 2014 until February 17, 2020 to avoid overlap with SARS-CoV-2, where potential cross-protection could have occurred. We defined a binomial likelihood, where modelled infection incidence maps to reported cases via an age-dependent reporting proportion, p_i . We assume equal reporting rates in age groups 5-15 and 45-65 to reduce the dimensions of the model, as initial fitting suggested these were very similar. The likelihood is therefore:

$$\log(L) \approx \sum_{i=1}^N \sum_{x=1}^X k_{x,i} \log(p_i) + (n_{x,i} - k_{x,i}) \log(1 - p_i) \quad (3)$$

where L is the likelihood, i is the age group to a total of N age groups, x are the reported monthly time points, $k_{x,i}$ are the reported HCoV cases by age group, $n_{x,i}$ are the model estimated infections per age group and p_i is the age-specific reporting rate.

We fit the model to the data using parallel tempering, adapted from Vouden *et al.*²² which is based on Monte Carlo Markov Chain (MCMC) inference. Unlike MCMC, multiple chains at different temperatures are run in parallel and swaps of parameter positions between chains are proposed. This allows more comprehensive exploration of the parameter space and allows the chains to move out of local maxima. We ran two sets of 16 chains and confirmed their convergence with the Gelman-Rubin statistic⁷⁹, which was <1.1 . We then combined the sample from both chains,

excluding the burn-in, in order to increase sample size, resulting in 93900 samples. See supplement for more details.

The percentage infected within one year and the median duration to reinfection were calculated using distribution and quantile functions from the stats R package⁶⁹.

We ran two sensitivity analyses. In the first, we excluded all data before August 2015, as the 2014/2015 year looked abnormal, and could have resulted in a different testing rate as it was the first year of data collection. In the second, we assumed that 54% of the reported data was beta-coronaviruses, as per the Nickbakshk *et al.* (2020) study from Scotland, and therefore fit to 54% of the original data (rounded to the nearest whole number).

4.7.4 Simulating SARS-CoV-2 with a range of strengths of cross-protection

We drew 100 random samples from the joint posterior distribution and simulated daily deaths reported in the first wave of the SARS-CoV-2 epidemic in England and Wales, between March 02, 2020 and May 31, 2020. We explored the full range of possible cross-protection strengths, in each case fitting the transmission and introduction rates to the death data using maximum likelihood estimation with a Poisson likelihood. We therefore created 100 simulations of HCoV and SARS-CoV-2 circulation for each strength of cross-protection.

Due to the non-pharmaceutical interventions implemented in this period (“lockdown”), we adjust the contact matrices, which are split into three categories: school contacts, household contacts and all other contacts. From February 21, 2020, when Google mobility data becomes available, we adjust our “other” contacts in line with google mobility data. From February 23, 2020, we eliminate school contacts and assume that all remaining contacts are reduced to 33% of their transmission potential, due to social distancing and behavioural changes (“micro-distancing”)⁸⁰. SARS-CoV-2 importations occur from February 15, 2020 until lockdown. See supplement for more details on the implementation of public health interventions.

To look at the proportion infected during the first wave we assumed that antibodies would take 3 weeks to rise to detectable levels after infection and not wane below the detection threshold during the study period⁸¹.

4.7.5 Projecting future dynamics of SARS-CoV-2 and Seasonal HCoVs

We ran the model for 30 years, from January 01, 2020 without any changes in contacts, in order to project the future dynamics of SARS-CoV-2. As inputs, we used the estimated parameters from the seasonal HCoV fits, as well as the estimated transmission and introduction rates fitted for each of the samples.

4.8 References

1. Waterlow, N. R. *et al.* How immunity from and interaction with seasonal coronaviruses can shape SARS-CoV-2 epidemiology. *medRxiv* 2021.05.27.21257032 (2021) doi:10.1101/2021.05.27.21257032.
2. Viner RM, Ward JL, Hudson LD, et al. Systematic review of reviews of symptoms and signs of COVID-19 in children and adolescents. *Archives of Disease in Childhood* 2021;106:802-807.
3. Davies, N. G. *et al.* Age-dependent effects in the transmission and control of COVID-19 epidemics. *Nature medicine* 1–7 (2020) doi:10.1038/s41591-020-0962-9.
4. Gaskell, K. M. *et al.* Extremely high SARS-CoV-2 seroprevalence in a strictly-Orthodox Jewish community in the UK. *medRxiv* 2021.02.01.21250839 (2021) doi:10.1101/2021.02.01.21250839.
5. Lai, C.-C., Wang, J.-H. & Hsueh, P.-R. Population-based seroprevalence surveys of anti-SARS-CoV-2 antibody: An up-to-date review. *Int J Infect Dis* **101**, 314–322 (2020).
6. Kissler, S. M. Projecting the transmission dynamics of SARS-CoV-2 through the postpandemic period | Science. <https://science.sciencemag.org/content/368/6493/860>.
7. Tillett, R. L. *et al.* Genomic evidence for reinfection with SARS-CoV-2: a case study. *The Lancet Infectious Diseases* **0**, (2020).
8. Stokel-Walker, C. What we know about covid-19 reinfection so far. *BMJ* **372**, n99 (2021).
9. Engl, P. H. Past COVID-19 infection provides some immunity but people may still carry and transmit virus. *GOV.UK* <https://www.gov.uk/government/news/past-covid-19-infection-provides-some-immunity-but-people-may-still-carry-and-transmit-virus>.
10. Dan, J. M. *et al.* Immunological memory to SARS-CoV-2 assessed for up to 8 months after infection. *Science* eabf4063–eabf4063 (2021) doi:10.1126/science.abf4063.
11. Viner, R. M. *et al.* Susceptibility to SARS-CoV-2 Infection Among Children and Adolescents Compared With Adults. *JAMA Pediatrics* (2020) doi:10.1001/jamapediatrics.2020.4573.
12. Li, X. *et al.* The role of children in transmission of SARS-CoV-2: A rapid review. *J Glob Health* **10**, 011101 (2020).
13. Mossong, J. *et al.* Social contacts and mixing patterns relevant to the spread of infectious diseases. *PLoS Medicine* **5**, 0381–0391 (2008).

14. Huang, A. T. *et al.* A systematic review of antibody mediated immunity to coronaviruses: kinetics, correlates of protection, and association with severity. *Nature Communications* **11**, 4704–4704 (2020).
15. Edridge, A. W. *et al.* Coronavirus protective immunity is short-lasting. *medRxiv* 2020.05.11.20086439-2020.05.11.20086439 (2020) doi:10.1101/2020.05.11.20086439.
16. Galanti, M. & Shaman, J. *Direct observation of repeated infections with endemic coronaviruses*. 2020.04.27.20082032 (Oxford University Press (OUP), 2020).
17. Aldridge, R. W. *et al.* Seasonality and immunity to laboratory-confirmed seasonal coronaviruses (HCoV-NL63, HCoV-OC43, and HCoV-229E): results from the Flu Watch cohort study. *Wellcome Open Res* **5**, 52 (2020).
18. Reed, S. E. The behaviour of recent isolates of human respiratory coronavirus in vitro and in volunteers: evidence of heterogeneity among 229E-related strains. *J Med Virol* **13**, 179–192 (1984).
19. Khan, S. *et al.* Analysis of Serologic Cross-Reactivity Between Common Human Coronaviruses and SARS-CoV-2 Using Coronavirus Antigen Microarray. *bioRxiv : the preprint server for biology* (2020) doi:10.1101/2020.03.24.006544.
20. Chan, K. H. *et al.* Serological responses in patients with severe acute respiratory syndrome coronavirus infection and cross-reactivity with human coronaviruses 229E, OC43, and NL63. *Clinical and Diagnostic Laboratory Immunology* **12**, 1317–1321 (2005).
21. Che, X. *et al.* Antigenic Cross-Reactivity between Severe Acute Respiratory Syndrome–Associated Coronavirus and Human Coronaviruses 229E and OC43. *The Journal of Infectious Diseases* **191**, 2033–2037 (2005).
22. Weiskopf, D. *et al.* Phenotype and kinetics of SARS-CoV-2–specific T cells in COVID-19 patients with acute respiratory distress syndrome. *Science Immunology* **5**, (2020).
23. Braun, J. *et al.* Presence of SARS-CoV-2 reactive T cells in COVID-19 patients and healthy donors. *medRxiv* 2020.04.17.20061440-2020.04.17.20061440 (2020) doi:10.1101/2020.04.17.20061440.
24. Tan, H.-X. *et al.* Adaptive immunity to human coronaviruses is widespread but low in magnitude. *medRxiv* 2021.01.24.21250074 (2021) doi:10.1101/2021.01.24.21250074.
25. Ng, K. *et al.* Pre-existing and de novo humoral immunity to SARS-CoV-2 in humans. *bioRxiv* 2020.05.14.095414-2020.05.14.095414 (2020) doi:10.1101/2020.05.14.095414.
26. Respiratory infections: laboratory reports 2019 - GOV.UK.
27. Deaths registered weekly in England and Wales, provisional - Office for National Statistics.

- <https://www.ons.gov.uk/peoplepopulationandcommunity/birthsdeathsandmarriages/deaths/bulletins/deathsregisteredweeklyinenglandandwalesprovisional/weekending7august2020>.
28. Eguia, R. *et al.* A human coronavirus evolves antigenically to escape antibody immunity. *bioRxiv* 2020.12.17.423313-2020.12.17.423313 (2020) doi:10.1101/2020.12.17.423313.
 29. Vousden, W. D., Farr, W. M. & Mandel, I. Dynamic temperature selection for parallel tempering in Markov chain Monte Carlo simulations. *Monthly Notices of the Royal Astronomical Society* **455**, 1919–1937 (2016).
 30. COVID-19 Community Mobility Report. *COVID-19 Community Mobility Report* <https://www.google.com/covid19/mobility?hl=en>.
 31. National COVID-19 surveillance reports - GOV.UK. <https://www.gov.uk/government/publications/national-covid-19-surveillance-reports>.
 32. Home | What's the STORY? <https://whatsthestory.web.ox.ac.uk/>.
 33. Ke, R., Romero-Severson, E., Sanche, S. & Hengartner, N. Estimating the reproductive number R_0 of SARS-CoV-2 in the United States and eight European countries and implications for vaccination. *Journal of Theoretical Biology* **517**, (2021).
 34. Edridge, A. W. D. *et al.* Seasonal coronavirus protective immunity is short-lasting. *Nature Medicine* **26**, 1691–1693 (2020).
 35. Petrie, J. G. *et al.* Coronavirus Occurrence in the HIVE Cohort of Michigan Households: Reinfection frequency and serologic responses to seasonal and SARS coronaviruses. *The Journal of Infectious Diseases* (2021) doi:10.1093/infdis/jiab161.
 36. Nyaguthii, D. M. *et al.* Infection patterns of endemic human coronaviruses in rural households in coastal Kenya. *Wellcome Open Res* **6**, 27 (2021).
 37. Ng, O.-W. *et al.* Memory T cell responses targeting the SARS coronavirus persist up to 11 years post-infection. *Vaccine* **34**, 2008–2014 (2016).
 38. Grifoni, A. *et al.* Targets of T Cell Responses to SARS-CoV-2 Coronavirus in Humans with COVID-19 Disease and Unexposed Individuals. *Cell*. 2020 Jun 25;181(7):1489-1501.e15.
 39. Bert, N. L. *et al.* Different pattern of pre-existing SARS-COV-2 specific T cell immunity in SARS-recovered and uninfected individuals. *bioRxiv* 2020.05.26.115832-2020.05.26.115832 (2020) doi:10.1101/2020.05.26.115832.
 40. Mateus, J. *et al.* Selective and cross-reactive SARS-CoV-2 T cell epitopes in unexposed humans. *Science* eabd3871–eabd3871 (2020) doi:10.1126/science.abd3871.
 41. Loyal, L. *et al.* Cross-reactive CD4+ T cells enhance SARS-CoV-2 immune responses upon infection and vaccination. *Science* [Internet]. 2021 Aug 31

42. Saletti, G. *et al.* Older adults lack SARS CoV-2 cross-reactive T lymphocytes directed to human **coronaviruses** OC43 and NL63. *Scientific Reports* **10**, 21447 (2020).
43. Hicks, J. *et al.* Serologic Cross-Reactivity of SARS-CoV-2 with Endemic and Seasonal Betacoronaviruses. *J Clin Immunol* (2021) doi:10.1007/s10875-021-00997-6.
44. Aydillo, T. *et al.* Immunological imprinting of the antibody response in COVID-19 patients. *Nat Commun* **12**, 3781 (2021).
45. Chia, W. N. *et al.* Dynamics of SARS-CoV-2 neutralising antibody responses and duration of immunity: a longitudinal study. *Lancet Microbe*. 2021 Jun 1;2(6):e240–9.
46. Chan, K. H. *et al.* Cross-reactive antibodies in convalescent SARS patients' sera against the emerging novel human coronavirus EMC (2012) by both immunofluorescent and neutralizing antibody tests. *Journal of Infection* **67**, 130–140 (2013).
47. Zhao, J. *et al.* Airway Memory CD4+ T Cells Mediate Protective Immunity against Emerging Respiratory Coronaviruses. *Immunity* **44**, 1379–1391 (2016).
48. Dugas, M. *et al.* Lack of antibodies against seasonal coronavirus OC43 nucleocapsid protein identifies patients at risk of critical COVID-19. *Journal of Clinical Virology* **139**, 104847 (2021).
49. Tan, C.-W. *et al.* Pan-Sarbecovirus Neutralizing Antibodies in BNT162b2-Immunized SARS-CoV-1 Survivors. *New England Journal of Medicine* (2021) doi:10.1056/NEJMoa2108453.
50. Anderson, E. M. *et al.* Seasonal human coronavirus antibodies are boosted upon SARS-CoV-2 infection but not associated with protection. *medRxiv* 2020.11.06.20227215-2020.11.06.20227215 (2020) doi:10.1101/2020.11.06.20227215.
51. Yang, R. *et al.* Lack of antibody-mediated cross-protection between SARS-CoV-2 and SARS-CoV infections. *EBioMedicine* **58**, 102890 (2020).
52. Rice, B. L., Douek, D. C., McDermott, A. B., Grenfell, B. T. & Metcalf, C. J. E. Why are there so few (or so many) circulating coronaviruses? *Trends in Immunology* **42**, 751–763 (2021).
53. Carsetti, R. *et al.* The immune system of children: the key to understanding SARS-CoV-2 susceptibility? *The Lancet Child & Adolescent Health* **4**, 414–416 (2020).
54. Tan CSS. *et al.* Pre-existing T cell-mediated cross-reactivity to SARS-CoV-2 cannot solely be explained by prior exposure to endemic human coronaviruses . *Infect Genet Evol.* 2021 Nov 1;95:105075
55. Yaqinuddin, A. Cross-immunity between respiratory coronaviruses may limit COVID-19 fatalities. *Med Hypotheses* **144**, 110049 (2020).

56. Pinotti, F. *et al.* Potential impact of individual exposure histories to endemic human coronaviruses on age-dependent severity of COVID-19. *BMC Medicine* **19**, 19 (2021).
57. Callow, K. A., Parry, H. F., Sergeant, M. & Tyrrell, D. A. J. The time course of the immune response to experimental coronavirus infection of man. *Epidemiology and Infection* **105**, 435–446 (1990).
58. Dugas, M. *et al.* Less severe course of COVID-19 is associated with elevated levels of antibodies against seasonal human coronaviruses OC43 and HKU1 (HCoV OC43, HCoV HKU1). *International Journal of Infectious Diseases* **105**, 304–306 (2021).
59. Neher, R. A., Dyrdak, R., Druelle, V., Hodcroft, E. B. & Albert, J. Potential impact of seasonal forcing on a SARS-CoV-2 pandemic. *Swiss medical weekly* **150**, w20224–w20224 (2020).
60. Oberemok, V. V., Laikova, K. V., Yurchenko, K. A., Fomochkina, I. I. & Kubyskin, A. V. SARS-CoV-2 will continue to circulate in the human population: an opinion from the point of view of the virus-host relationship. *Inflammation Research* **69**, 635–640 (2020).
61. Lavine, J. S., Bjornstad, O. N. & Antia, R. Immunological characteristics govern the transition of COVID-19 to endemicity. *Science* **371**, 741–745 (2021).
62. Summary of the 2010-2011 Influenza Season | CDC.
<https://www.cdc.gov/flu/pastseasons/1011season.htm> (2019).
63. Update: Influenza Activity --- United States, 2010--11 Season, and Composition of the 2011--12 Influenza Vaccine.
<https://www.cdc.gov/mmwr/preview/mmwrhtml/mm6021a5.htm>.
64. Public Health England, Respiratory infections: Laboratory reports 2020. GOV.UK, 26 February 2020.
<https://www.gov.uk/government/publications/respiratory-infections-laboratory-reports-2020>. Accessed 3 March 2021.
65. Meyer, B., Drosten, C. & Müller, M. A. Serological assays for emerging coronaviruses: Challenges and pitfalls. *Virus Res* **194**, 175–183 (2014).
66. Dyrdak, R., Hodcroft, E. B., Wahlund, M., Neher, R. A. & Albert, J. Interactions between seasonal human coronaviruses and implications for the SARS-CoV-2 pandemic: A retrospective study in Stockholm, Sweden, 2009–2020. *medRxiv* 2020.10.01.20205096 (2020) doi:10.1101/2020.10.01.20205096.
67. Nickbakhsh, S. *et al.* Epidemiology of Seasonal Coronaviruses: Establishing the Context for the Emergence of Coronavirus Disease 2019. *The Journal of Infectious Diseases* **222**, 17–25 (2020).

68. Henderson, F. W., Collier, A. M., Clyde, W. A. & Denny, F. W. Respiratory-Syncytial-Virus Infections, Reinfections and Immunity. *New England Journal of Medicine* **300**, 530–534 (1979).
69. R Core Team. *R: A language and environment for statistical computing*. R Foundation for Statistical Computing, Vienna, Austria. (2018).
70. S. Funk, socialmixr: Social Mixing Matrices for Infectious Disease Modelling. (2018). Version 0.1.8, published on CRAN. <https://cran.r-project.org/web/packages/socialmixr/index.html>. Accessed 30 November 2021
71. Liu, Z., Chu, R., Gong, L., Su, B. & Wu, J. The assessment of transmission efficiency and latent infection period in asymptomatic carriers of SARS-CoV-2 infection. *Int J Infect Dis* **99**, 325–327 (2020).
72. Tyrrell, D. A., Cohen, S. & Schlarb, J. E. Signs and symptoms in common colds. *Epidemiol Infect* **111**, 143–156 (1993).
73. Birrell, P. J. *et al.* Forecasting the 2017/2018 seasonal influenza epidemic in England using multiple dynamic transmission models: a case study. *BMC Public Health* **20**, (2020).
74. Davies, N. G. *et al.* Estimated transmissibility and impact of SARS-CoV-2 lineage B.1.1.7 in England. *Science* (2021) doi:10.1126/science.abg3055.
75. Byrne, A. W. *et al.* Inferred duration of infectious period of SARS-CoV-2: rapid scoping review and analysis of available evidence for asymptomatic and symptomatic COVID-19 cases. *BMJ Open* **10**, e039856 (2020).
76. Levin, A. T., Cochran, K. B. & Walsh, S. P. Assessing the Age Specificity of Infection Fatality Rates for COVID-19: Meta-Analysis & Public Policy Implications. *medRxiv* 2020.07.23.20160895-2020.07.23.20160895 (2020) doi:10.1101/2020.07.23.20160895.
77. Office for National Statistics, Deaths registered weekly in England and Wales, provisional. <https://www.ons.gov.uk/peoplepopulationandcommunity/birthsdeathsandmarriages/deaths/bulletins/deathsregisteredweeklyinenglandandwalesprovisional/weekending7august2020>. Accessed 23 February 2021
78. Estimates of the population for the UK, England and Wales, Scotland and Northern Ireland - Office for National Statistics. <https://www.ons.gov.uk/peoplepopulationandcommunity/populationandmigration/populationestimates/datasets/populationestimatesforukenglandandwalesscotlandandnorthireland>.

79. D. Vats, C. Knudson, Revisiting the Gelman-Rubin diagnostic. arXiv [Preprint] (2018). <https://arxiv.org/abs/1812.09384>. Accessed 22 February 2021
80. Health, A. G. D. of. Australian Health Protection Principal Committee (AHPPC) statement on the review of physical distancing and person density restrictions. *Australian Government Department of Health* <https://www.health.gov.au/news/australian-health-protection-principal-committee-ahppc-statement-on-the-review-of-physical-distancing-and-person-density-restrictions> (2020).
81. Centers for Disease Control and Prevention, Interim guidelines for CoVID-19 antibody testing. <https://www.cdc.gov/coronavirus/2019-ncov/lab/resources/antibody-tests-guidelines.html>. Accessed 27 February 2021

5 Discussion

5.1 Summary of Findings

Respiratory pathogens, due to both their annual circulation and their pandemic potential, have an enormous public health and economic burden around the world¹⁻⁴. They exist within an ecosystem⁵, and interactions between them could have wide-ranging implications for disease control. These interactions could occur on a non-specific, short-term basis, or through a cross-reactive immune reaction, resulting in specific, long-term interactions. Evidence for this phenomenon comes from a wide range of sources including relative timings of epidemics⁶, biological experiments in model animals⁷⁻⁹ and the detection of cross-reactive immune molecules in people¹⁰⁻¹³. However, quantifying the strength of these interactions, as well as testing their impact at a population level, requires tools to test mechanisms— for which mathematical models are ideally suited. Where models have been used, they often only model one pathogen dynamically, meaning that only one-way interaction can be investigated¹⁴, and further they do not fit to data so are unable to provide estimates of the strength and duration of cross-protection¹⁵ nor limit the parameter range of key parameters¹⁶.

In this thesis I have investigated how mathematical models can be applied to identify cross-protection between respiratory viruses, and used these models to detect cross-protection that is epidemiologically important at a population level. I have approached this from various angles, researching different types of interaction and evaluating the implications that cross-protection can have on viral dynamics. I have developed a dynamic two-pathogen mathematical model to test interaction between respiratory viruses, explored the model, and used it to examine three different epidemiological situations of importance for public health.

I will give a summary of each chapter, before discussing the strengths, limitations, and future of this work.

5.1.1 Competition between RSV and influenza: Limits of modelling inference from surveillance data

In chapter 2 I develop a model allowing for temporary cross-protection between influenza and RSV. I use the model to create simulations that qualitatively emulate a respiratory virus season in the UK, using different strengths and durations of cross-protection and including stochasticity. I then fit the

model to each simulation in order to back-infer the parameters used. I do this for each season individually, without strong priors, to assess the validity of using such an approach on UK or similar surveillance data. While the estimates were often imprecise, it was possible to quantify the strength and duration of interaction from a single season with some amount of overlap between the influenza and RSV seasons. This analysis highlighted areas of parameter space that resulted in misleading results, particularly at the extreme ends of the strength of cross-protection, and showed that stochastic noise can result in incorrect estimates. I therefore conclude that this is a valid approach, but hypothesise the need to include multiple seasons of data to reduce the impact of stochasticity. While other identifiability studies exist (such as Rift Valley fever¹⁷ and Zika¹⁸), this paper was the first to test the robustness of RSV and influenza competition inferences using dynamic models.

5.1.2 How cross-protection between Influenza and Respiratory Syncytial virus shapes paediatric hospital admissions in Nha Trang, Vietnam

In chapter 3 I extend the model developed in chapter 2 to be applicable to influenza and RSV data from a hospital-based study in Nha Trang, Vietnam. This is a unique data set containing 11 years of paediatric surveillance for influenza and RSV with PCR confirmed infections, including cases infected with both viruses. I use parallel tempering to fit the model and estimate the strength and duration of interaction between influenza and RSV in this setting. The results show two possible interaction scenarios: one where moderate cross-protection between the viruses is involved in shaping their population level dynamics; and one where the transmission dynamics of the two viruses are independent. In addition, interaction resulting in increased reporting rates plays a key role in observed case reports. However, it is also important to consider the generalisability of this study to other settings, where different epidemic patterns may result in different opportunities for competition between RSV and Influenza. In addition the data consists of small numbers, presenting challenges with the inference. The results here indicate that introduction of vaccination against either influenza or RSV has a strong effect on reducing hospitalisations due to the increased severity of dual infections, while at the same time potentially impacting transmission dynamics, resulting in increased hospitalisations due to higher levels of circulation, especially following influenza vaccination.

5.1.3 How immunity from and interaction with seasonal coronaviruses can shape SARS-CoV-2 epidemiology

Chapter 4 considers specific, longer-term interaction, rather than the temporary interaction that is investigated in Chapters 2 and 3. Using a model which includes seasonal forcing, I fit to 5 years of PHE coronavirus reports detected through any method. The inferred parameters — R_0 5.9 (95% CrI: 5.5 - 6.2) and duration between recovery and return to susceptibility of 7.8 years (95% CrI: 6.3 – 8.2) — are considerably higher than other estimates in the field¹⁶ due to differences in the limits of parameters. I highlight the importance of including a full range of estimates in the parameter range, as well as discussing why my estimates align with biological evidence. I use these estimates to answer a key question that emerged during the SARS-CoV-2 pandemic: is the reduced susceptibility of children to SARS-CoV-2 that was observed at the start of the pandemic due to cross-protection from seasonal coronavirus infection? I show that while cross-protection can help explain some reduced susceptibility, it is not sufficient to explain the observed pattern. The paper also includes a forward projection, looking at how cross-protection could influence the future dynamics of these viruses. This is a novel insight into the dynamics of coronaviruses, and cross-protection in general.

5.2 Strengths and Limitations

A specific discussion on each project is given in the relevant chapters, therefore here I will focus on the overall strengths and limitations of the thesis.

5.2.1 Strengths

Testing biological mechanisms

Existing evidence on cross-protection between respiratory viruses comes from three main sources: ecological studies looking at relative timings of epidemics⁶, biological experiments in model animals⁷⁻⁹ and the detection of cross-reactive immune molecules in humans¹⁰⁻¹³. However, such evidence alone is unable to test the causal link between these biological phenomena and the epidemic patterns at population level. Mathematical models allow testing of mechanisms and I have therefore been able to contribute evidence on three hypotheses. I first tested the hypothesis of short-term cross-protection between influenza and RSV, where I showed that there were two possible scenarios: one with no interaction and one with moderate interaction. Secondly, in the

same study, I tested the mechanism of increased reporting due to co-infections, where I showed a strong effect. The third hypothesis was that cross-protection between seasonal coronaviruses and SARS-CoV-2 caused the observed reduced susceptibility of children during the pandemic. Here I showed that cross-protection could not explain this reduced susceptibility. This linking of a biological mechanism to a population level occurrence is a key strength of this project. In terms of influenza and RSV, the only published model that has a similar aim¹⁵ has not been fit to data, and therefore may not be able to detect the subtle consequences of interaction. The model I present in this thesis, on the other hand, is the first that has rigorously tested the link between cross-protection of influenza and RSV and the population level circulation of these respiratory viruses. For coronaviruses, while there is a model evaluating cross-protection between alpha- and beta-seasonal coronaviruses¹⁶, it does not consider a full range of parameters, include any population age-distribution or compare the SARS-CoV-2 model to data, and can therefore not test the hypothesis of cross-protection between seasonal coronaviruses and SARS-CoV-2.

Data availability

The second key strength of this thesis is the quantity and quality of data that the models were fit to. In the exploration of interaction models in Chapter 2 there were indications that multiple seasons of data are required to get accurate results. In Chapter 3 I used 11 seasons of paediatric hospital cases with PCR-confirmed infections¹⁹. This is a rich data set, especially as it includes dual infections, which give extra power to detect cross-protection between influenza and RSV. In Chapter 4, while the seasonal coronavirus case data was not subtyped, I used multiple seasons from across England and Wales. I also tested the sensitivity of excluding one year of data when there were indications that there may have been differences in testing. Regarding SARS-CoV-2, deaths are highly skewed to older ages²⁰, but I therefore included serological data as the main output of interest.

However, SARS-CoV-2 antibodies responses are varied, with 5 distinct patterns being observed: negative, rapid waning (seroconversion within 180 days), slow waning (seroconversion above 180 days), persistent (relative little antibody decay) and delayed response (increase in antibodies in late convalescence)²¹. In addition, positivity of samples is dependent on the serological assay used²². Because of the variation of antibody longevity within the body, and specifically the potential rapid waning of antibodies²³, I only modelled the first wave of the UK epidemic, so as to reduce the bias on the results. In terms of 'input' data, in the UK, public health interventions were implemented at the same time, irrespective of geographic region, thereby providing an ideal setting to model the

pandemic, especially with google mobility data²⁴ available to track this. In all three of the projects, I was additionally able to include location-specific age assortative contact matrices as data inputs, which have been shown to be vital in predicting age-specific pathogen spread^{25,26}.

Inference techniques

In this thesis I used Bayesian methods to fit my models to data, specifically MCMC and parallel tempering. In chapter 2 I used MCMC, to assess the potential for detecting interaction when using standard modelling methods and surveillance data. However, in the following two chapters I developed this further, implementing parallel tempering. This method was developed in 1986 by Swendson and Wang²⁷ in the field of physics. Multiple chains are run at different temperatures, where higher temperatures accept lower likelihoods. Swaps between the temperatures are then proposed, which are accepted dependent on the temperature and likelihood differences between the two chains. Although computationally intensive compared to more standard Monte Carlo approaches, this method provides a better exploration of parameter space²⁸. This is because the higher temperature chains explore a broader range of the parameter space, while the lower temperature chains enable precision within local minima. Swapping between the chains enables the cool, precise chains to swap between areas of high likelihood that the warmer chains have identified. This would not be possible in MCMC, as to generate precision in the posterior sample you strongly reduce the chances of leaving local minimums and exploring the broader parameter space. Therefore, the trade-off between getting a well-mixed, precise result and exploring the whole parameter space, as is the case for MCMC, is relaxed. Using this method for complicated models is a key strength of this thesis and builds trust in the results. This method is also a likelihood-based inferential technique, allowing representation of the observation processes.

Transparency and Reproducibility

The philosopher Karl Popper noted that “non-reproducible single occurrences are of no significance to science”²⁹. However, the recent academic landscape is rife with non-reproducible research, with 70% of surveyed researchers unable to replicate the work of others, and a startling 50% unable to replicate their own research³⁰. I have made all my research transparent and reproducible: code for all the projects is available on GitHub, as is the data I extracted from the PHE website for Chapter 4. In addition, in Chapter 2 I specifically tested the reproducibility of the results based on the stochasticity in the system. Having shown that stochasticity could sometimes result in inaccurate

results from one season alone, I then ensured in Chapter 32 that I used multiple seasons of data. I have therefore made my research reproducible, which adds to its value in the scientific field.

5.2.2 Limitations

The often-used quote “All models are wrong, but some are useful”, attributed to George Box³¹, exemplifies many of the limitations of this thesis, and modelling in general. We cannot aim to exactly replicate, down to every strain, geographic region, and stochastic element of disease dynamics, as the complexity and detail required would be immense. Instead, we must make simplifying assumptions in our models based on our understanding of the mechanisms involved and on the questions that we want to answer, allowing us to generate believable and useful conclusions.

Simplification of the viral ecosystem

The models in this thesis all simulate two pathogens. However, this is a vast simplification of the respiratory pathogen landscape, which may therefore introduce bias. Firstly, I did not include multiple subtypes or strains for any of the modelled viruses, instead modelled them as one virus (excepting coronaviruses and SARS-CoV-2). This has different implications for each virus.

There is evidence that for influenza viruses an individual’s immunity is dependent on which previous strains they have previously been infected by, often called their “infection history”^{32–34}. In chapters 2 and 3 I accounted for potentially varied immunity levels by fitting a susceptibility parameter at the beginning of each season, however this will not have captured the full variation. For RSV, despite the presence of two subtypes (A and B) there is less evidence of differences between these subtypes in terms of severity or long-term immunity (see introduction), so the assumption here is less likely to cause a bias in the model.

The lack of strain-specific modelling may have the biggest impact on the coronavirus model in chapter 4. There are indications from other studies / settings that more complicated dynamics exist, for example alternating annual patterns¹⁶. However, this is not observed in the UK, where subtype circulation is very consistent year on year³⁵, or in Japan when over a 3 year study no subtype dynamic patterns emerged³⁶. Due to the potential different dynamics between strains the duration of immunity for seasonal coronaviruses in this study is considered as an artificial parameter. Here it measures time between recovery from the infection and return to the susceptible class rather than a strain-specific duration of cross-protection. It is this overall level of immunity that will influence the

age-specific susceptibility of SARS-CoV-2 through cross-protection. Therefore, the results regarding cross-protection are unlikely to differ if this assumption was relaxed, however differing subtype dynamics may be an explanation for the high estimate of the duration of homologous protection.

Ideally, in future work I would be able to increase the complexity of the models in this thesis, to include the multiple coronavirus and influenza strains. This would require sub-typed data, which while available for influenza in the UK³⁷, is not available for coronaviruses. Instead, a different location, such as the United States of America (USA)³⁸, would have to be used. A more complex model would also increase the difficulty of fitting.

I also do not include the impacts of other external factors that may have influenced immune dynamics. This includes interactions with other pathogens³⁹, such as influenza B, rhinovirus or pneumococcus, and external climatic factors that could have influenced the transmission dynamics. However, in both cases, the modelled viruses are the ones for which existing evidence suggested the strongest interaction is likely. Yet, it may still have confounded the results, potentially explaining the reduction in SARS-CoV-2 infections that we could not replicate in the model. When modelling coronavirus in chapter 3, where I simulated multiple consecutive seasons, I accounted for some of these external factors using a seasonal forcing mechanism. While this created realistic dynamics, it is not necessarily clear what drives this seasonality and is a limitation of this study. Using climatic data and prevalence of other infections as static inputs into the model could explain the impact of this limitation.

Unavailability of data on infection incidence

The second area of limitation across the models in this thesis is that I only had information on the disease incidence instead of infection incidence. In order to make inferences from this, I assumed a constant rate of reporting over time, and therefore also a constant rate of testing over time. This is because I did not have data on the number of tests conducted in the dataset. Respiratory viruses often cause similar symptoms, which result in individuals being tested for viruses. In high income countries this is often done using a multiplex PCR-based assay⁴⁰, resulting in infections being detected based on the circulation of other viruses that cause ILI. Therefore, it is likely that the testing rate changes seasonally, to match the incidence of ILI. I have not included time-varying testing volume in the models, as the number of negative test results were not available.

For the Nha Trang study, previous seasons did not show marked seasonality in hospitalisations¹⁹, so not including a time-dependent testing rate is likely to have negligible impacts. In the UK, where there is marked winter seasonality in ILI, the assumption on rate of testing is more likely to impact the number of reported cases.

This is especially a concern for coronaviruses as it has a higher proportion of asymptomatic/subclinical infections compared to other respiratory viruses such as influenza⁴¹, which will result in testing being strongly dependent on other, more severe, respiratory viruses. Likely, this would change the magnitude of the seasonal coronavirus report peaks. While this may bias the results, it is likely that it would mostly be absorbed into the amplitude of seasonal forcing, thereby not impacting the model's conclusions. In the ideal scenario I would have been able to use infection incidence data, collected through regular community swabbing. This would remove any bias from time-varying reporting, and reduce the number of parameters required, as reporting rates would not need to be included. Relatedly, information on infection incidence for SARS-CoV-2 was not available, and instead I used deaths and serological data. The death data will be highly skewed to at risk groups, hence the requirement for also using serology. However, due to complications of serology such as antibody waning and the impact of changing social restrictions on contact patterns, I only modelled the first wave of the epidemic in England and Wales. This limited my analysis to the initial circulation period of SARS-CoV-2, which may bias the results, as the most at risk population groups may have been infected first.

Susceptibility reduction as the mechanism of cross-protection

The third major assumption that I made across models is that cross-protection acts to reduce susceptibility rather than to reduce transmissibility. This is based on the mechanism of interaction being the innate immune system, activation of which reduces the susceptibility of individuals to a variety of pathogens⁴²⁻⁴⁴. While transmission-blocking immunity has been noted for a few pathogens, this is often observed as a result of vaccination, not natural infection^{45,46}. In addition, only in the Nha Trang setting did I allow an increased clinical severity with dual infections, by allowing a varied reporting rate.

In the case of coronaviruses, while there is some evidence that cross-protection influences clinical severity⁴⁷, the main output of the model in this thesis is the proportion of the population who would have generated specific antibodies, which is unlikely to be impacted by differences in severity.

However, it is a limitation of this thesis that it only explores cross-protection mediated through reduced susceptibility. To test this further, a model could be developed to test different mechanisms of interaction: reduced susceptibility, reduced transmissibility and altered severity. However, it is unclear whether such nuances in interaction would be identifiable during model inference. A reduction in transmissibility as well as susceptibility of SARS-CoV-2 due to cross-protection from seasonal HCoV could explain the reduced susceptibility in children that I was unable to fully describe with my coronavirus model in Chapter 4.

Generalisability

Lastly, a limitation of the work in this thesis is the generalisability of the conclusions to other settings. In all three scenarios I used location specific parameterisations, and for both influenza and RSV and the coronavirus model I fitted to data from specific regions.

The dataset used to fit the influenza/RSV model consisted of hospital patients, therefore only including relatively severe cases, which will not be representative of the community. In order to counteract this, I estimated virus and age specific reporting rates in the model. However, these may alter by geographic region and surveillance system, and therefore the model may not be generalisable beyond the currently implemented setting. In addition, many dual infections were reported at points when the two viruses were individually at low levels of circulation. It is unclear to what extent this is true in other geographic regions, but is definitely not always the case (e.g. Texas⁴⁸). Influenza circulated constantly at very low levels in Nha Trang, which is not observed in other geographies such as the UK³⁷, where there is a much more pronounced annual epidemic peak. Such seasonal differences in circulation may have a large impact on the results, as for example large shifts in peaks cannot be observed in the Nha Trang data, and there is potential for cross-protection to be absorbed into the transmission rate with year-round circulation. Therefore, the generalisability of this results to other settings is unclear, as different dynamics may be at play.

In Chapter 2 I used simulated data to test the inference tools, which is a powerful technique for determining the data needed to fit models such as those in this thesis. I intended to base the Chapter 3 on this analysis with data from England and Wales but was unable to do so due to SARS-CoV-2 related restrictions.

In the case of coronaviruses, the background level of immunity to seasonal coronaviruses will differ across geographies, due to different contact patterns and climatic features, and the extent of this will impact the extent of cross-protection and therefore the study conclusions. To further assess the generalisability of the results, fitting the same model parameterised to a different location, with local data for inference would be crucial.

5.3 Implications and future work

The research I have presented in this thesis has several implications for further study of respiratory interactions and mathematical models:

1. I have shown that my mathematical model framework can be used to investigate interaction from disease incidence as typically captured by surveillance data. Chapter 2 indicated that multiple seasons of data should be included, and models should ideally be validated, as stochasticity can affect the results.
2. Chapter 3 indicates that the introduction of RSV or influenza vaccination has the potential to affect the epidemiology of the other virus in Nha Trang, Vietnam. Further study on the wider consequences of vaccination is therefore required before such public health measures are implemented. This is a timely discussion in this setting due to the recent interest in vaccinating against influenza in Vietnam⁴⁹, and the development of in-country vaccinations⁵⁰.
3. Comparing the results of Chapter 3 to previous literature on shifts in epidemic peaks⁶ suggests that other mechanisms, such as behavioural responses, may play a greater role than currently thought in shifting epidemics. The dramatic effects of behaviour changes have recently been demonstrated on a wide scale due to the SARS-CoV-2 pandemic⁵¹. Due to this large impact, tracking contact patterns over time is of vital importance for the study of infectious disease transmission, as is being done for example in CoMix study in the UK⁵².
4. The results in Chapter 4, investigating susceptibility to coronaviruses, implies that there are more mechanisms involved in the reduction of childhood susceptibility than just interaction with seasonal coronaviruses and contact patterns. This could be due to innate differences in susceptibility between age groups⁵³.
5. In addition, Chapter 4 demonstrates the importance of collecting serological data during disease outbreaks that models can be fitted to. To understand the dynamics, serological data collection should be started as soon as possible at the start of the epidemic. This is important both to understand the early dynamics of infection, but also due to the variation

in speed of antibody waning^{21-23,54}. In addition, the representativeness of individuals enrolled in a serological study is of key importance, as many of the available studies for coronavirus are strongly biased, often by health status. This includes for example the blood donor study where individuals must be healthy to be included and the PHE SeroEpidemiological Unit (SEU) where individuals must have sought healthcare facilities.

While this thesis addresses some key questions in the field of respiratory interactions, it also identifies further gaps in knowledge.

The results from the influenza and RSV model based in Nha Trang, Vietnam, show that the data support two cross-protection scenarios: moderate or no cross-protection. In order to further narrow down and distinguish between these two modes, the model could be re-fitted with extra data. This could be for example respiratory viral samples from the community, rather than just the hospital, in order to inform the reporting rates, and hence the model fit. The findings from Vietnam may however not be generalisable to other settings, particularly those in temperate climates with more pronounced influenza epidemics. Therefore, fitting the model to a different setting such as the UK, would result in a much broader understanding of the impacts of interaction between influenza and RSV. This was the original plan for this thesis, however this project had to be postponed due to restrictions in response to the SARS-CoV-2 pandemic. In addition, it would be very interesting to fit this model framework to a dataset where a previous shift in epidemic peaks has been observed, and it was hypothesised to be due to interaction between the viruses.

In terms of coronaviruses, subtype information is not available for the PHE data, however other locations may provide the opportunity for studying these interactions. One potential data source is the National Respiratory and Enteric Virus Surveillance System (NREVSS) in the USA³⁸. This data is subtyped and covers a large geographic area, with different dynamic patterns present in the different regions. It would therefore be interesting to create a mathematical model looking at the interaction between coronavirus subtypes with a spatial element. This would be needed to capture these different dynamics across regions. Such a model may further elucidate the extent of cross-protection between coronavirus strains and demystify the importance of subtypes (alpha vs beta coronaviruses). Furthermore, this model could investigate the impacts of including an RSV-like build-up of immunity to seasonal coronaviruses, which reduces susceptibility following repeat infections.

The SARS-CoV-2 pandemic, while being completely devastating, has resulted in unique opportunities to understand respiratory viral dynamics. It is, in essence, a natural global epidemiological experiment. With different climates and different public health measures implemented in different geographical regions, there is a lot of potential to research topics that have previously been elusive. In the UK, apart from rhinovirus, the usual respiratory virus patterns were disrupted (see Figure 5-1). Of relevance to this thesis is the causes of respiratory viral epidemic timings: what is the impact of climate on respiratory viral epidemic timings as opposed to human behaviour in response to climate? What is ‘seasonal forcing’? To what extent are epidemics based on availability of susceptible individuals (potentially due to cross-protective responses) as opposed to virus or behaviour intrinsic factors? This is a key area of research where models like those used in this thesis could be effectively utilised.

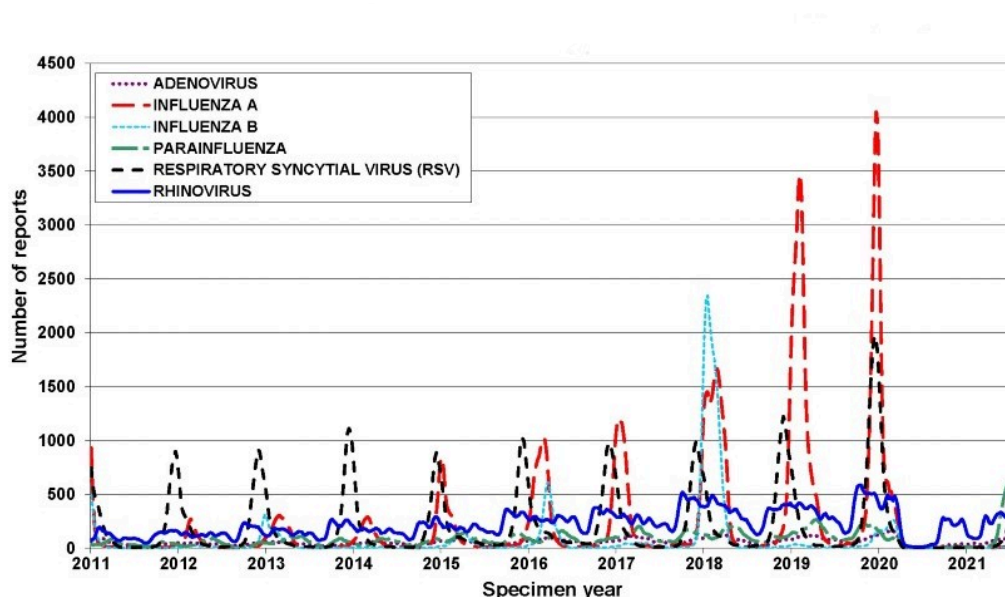


Figure 5-1: Six major respiratory viruses (positive numbers) reported from PHE and NHS laboratories (SGSS) in England and Wales between week 1, 2011 and week 29, 2021 (3-week moving average). Extracted from www.gov.uk⁵⁵

A final area of future development would be to extend the models developed in this thesis to three or more pathogens, to gain a greater understanding of the interactions within the microbiome. This would be particularly relevant to other respiratory pathogens that cause global impacts, for example pneumococcus. This is especially the case as there are already strong indications that influenza and RSV can impact the progression of pneumococcal carriage to disease⁵⁶, and vaccination against these two viruses may impact the incidence of pneumococcal disease.

5.4 Concluding Remarks

This PhD thesis aimed to improve our understanding of respiratory viral interaction that is clinically relevant on the population level. It demonstrates that surveillance data and mathematical models can be used to study these interactions, as they are able to test the underlying causal mechanisms.

5.5 References

1. WHO | Estimates for 2000–2015. *WHO* (2017).
2. Bertino, J. Cost Burden of Viral Respiratory Infections: Issues for Formulary Decision Makers. *Excerpta Medica* (2002).
3. Bont, L. *et al.* Defining the Epidemiology and Burden of Severe Respiratory Syncytial Virus Infection Among Infants and Children in Western Countries. *Infectious diseases and therapy* **5**, 271–298 (2016).
4. Karron, R. A. & Black, R. E. Determining the burden of respiratory syncytial virus disease: the known and the unknown. *www.thelancet.com* (2017) doi:10.1016/S0140-6736(17)31476-9.
5. Santacrose, L. *et al.* The Human Respiratory System and its Microbiome at a Glimpse. *Biology (Basel)* **9**, E318 (2020).
6. Li, Y. *et al.* The impact of the 2009 influenza pandemic on the seasonality of human respiratory syncytial virus: A systematic analysis. *Influenza and Other Respiratory Viruses* **n/a**.
7. Walzl, G., Tafuro, S., Moss, P., Openshaw, P. J. & Hussell, T. Influenza virus lung infection protects from respiratory syncytial virus-induced immunopathology. *The Journal of experimental medicine* **192**, 1317–26 (2000).
8. Lee, Y. J. *et al.* Non-specific Effect of Vaccines: Immediate Protection against Respiratory Syncytial Virus Infection by a Live Attenuated Influenza Vaccine. *Frontiers in Microbiology* **9**, 83–83 (2018).
9. Laurie, K. L. *et al.* Interval Between Infections and Viral Hierarchy Are Determinants of Viral Interference Following Influenza Virus Infection in a Ferret Model. *Journal of Infectious Diseases* **212**, 1701–1710 (2015).
10. Ng, K. *et al.* Pre-existing and de novo humoral immunity to SARS-CoV-2 in humans. *bioRxiv* 2020.05.14.095414-2020.05.14.095414 (2020) doi:10.1101/2020.05.14.095414.
11. Hicks, J. *et al.* Serologic Cross-Reactivity of SARS-CoV-2 with Endemic and Seasonal Betacoronaviruses. *J Clin Immunol* (2021) doi:10.1007/s10875-021-00997-6.
12. Grifoni, A. *et al.* Targets of T Cell Responses to SARS-CoV-2 Coronavirus in Humans with COVID-19 Disease and Unexposed Individuals. *Cell* (2020) doi:10.1016/j.cell.2020.05.015.

13. Bert, N. L. *et al.* Different pattern of pre-existing SARS-CoV-2 specific T cell immunity in SARS-recovered and uninfected individuals. *bioRxiv* 2020.05.26.115832-2020.05.26.115832 (2020) doi:10.1101/2020.05.26.115832.
14. Shrestha, S. *et al.* The role of influenza in the epidemiology of pneumonia. *Scientific Reports* **5**, 15314–15314 (2015).
15. Velasco-Hernández, J. X., Núñez-López, M., Comas-García, A., Cherpitel, D. E. N. & Ocampo, M. C. Superinfection between Influenza and RSV alternating patterns in San Luis Potosí State, México. *PLoS ONE* **10**, (2015).
16. Kissler, S. M. Projecting the transmission dynamics of SARS-CoV-2 through the postpandemic period | Science. <https://science.sciencemag.org/content/368/6493/860>.
17. Tuncer, N., Gulbudak, H., Cannataro, V. L. & Martcheva, M. Structural and Practical Identifiability Issues of Immuno-Epidemiological Vector–Host Models with Application to Rift Valley Fever. *Bulletin of Mathematical Biology* **78**, 1796–1827 (2016).
18. Tuncer, N., Martcheva, M., LaBarre, B. & Payoute, S. Structural and Practical Identifiability Analysis of Zika Epidemiological Models. *Bulletin of Mathematical Biology* **80**, 2209–2241 (2018).
19. Althouse, B. M. *et al.* Seasonality of respiratory viruses causing hospitalizations for acute respiratory infections in children in Nha Trang, Vietnam. *International Journal of Infectious Diseases* **75**, 18–25 (2018).
20. Levin, A. T., Cochran, K. B. & Walsh, S. P. Assessing the Age Specificity of Infection Fatality Rates for COVID-19: Meta-Analysis & Public Policy Implications. *medRxiv* 2020.07.23.20160895-2020.07.23.20160895 (2020) doi:10.1101/2020.07.23.20160895.
21. Chia, W. N. *et al.* Dynamics of SARS-CoV-2 neutralising antibody responses and duration of immunity: a longitudinal study. *The Lancet Microbe* **0**, (2021).
22. Meyer, B. Waning antibodies to SARS-CoV-2 – Don’t panic. *The Lancet Regional Health – Europe* **4**, (2021).
23. Ibarondo, F. J. *et al.* Rapid Decay of Anti–SARS-CoV-2 Antibodies in Persons with Mild Covid-19. *New England Journal of Medicine* **383**, 1085–1087 (2020).
24. COVID-19 Community Mobility Report. *COVID-19 Community Mobility Report* <https://www.google.com/covid19/mobility?hl=en>.
25. Mossong, J. *et al.* Social contacts and mixing patterns relevant to the spread of infectious diseases. *PLoS Medicine* **5**, 0381–0391 (2008).
26. Carrat, F. *et al.* Time lines of infection and disease in human influenza: a review of volunteer challenge studies. *Am J Epidemiol* **167**, 775–785 (2008).

27. Swendsen, R. H. & Wang, J.-S. Replica Monte Carlo Simulation of Spin-Glasses. *Phys. Rev. Lett.* **57**, 2607–2609 (1986).
28. Vousden, W. D., Farr, W. M. & Mandel, I. Dynamic temperature selection for parallel tempering in Markov chain Monte Carlo simulations. *Monthly Notices of the Royal Astronomical Society* **455**, 1919–1937 (2016).
29. Reproducibility. *Wikipedia* (2021).
30. Baker, M. 1,500 scientists lift the lid on reproducibility. *Nature* **533**, 452–454 (2016).
31. All models are wrong. *Wikipedia* (2021).
32. Zhang, A., Stacey, H. D., Mullarkey, C. E. & Miller, M. S. Original Antigenic Sin: How First Exposure Shapes Lifelong Anti-Influenza Virus Immune Responses. *The Journal of Immunology* **202**, 335–340 (2019).
33. Knight, M., Changrob, S., Li, L. & Wilson, P. C. Imprinting, immunodominance, and other impediments to generating broad influenza immunity. *Immunol Rev* **296**, 191–204 (2020).
34. Combadière, B., Sibénil, S. & Duffy, D. Keeping the memory of influenza viruses. *Pathol Biol (Paris)* **58**, e79-86 (2010).
35. Nickbakhsh, S. *et al.* Epidemiology of Seasonal Coronaviruses: Establishing the Context for the Emergence of Coronavirus Disease 2019. *The Journal of Infectious Diseases* **222**, 17–25 (2020).
36. Matoba, Y. *et al.* Detection of the Human Coronavirus 229E, HKU1, NL63, and OC43 between 2010 and 2013 in Yamagata, Japan. *Japanese Journal of Infectious Diseases* **68**, 138–141 (2015).
37. National flu and COVID-19 surveillance reports. *GOV.UK*
<https://www.gov.uk/government/statistics/national-flu-and-covid-19-surveillance-reports>.
38. Coronavirus Surveillance Data - NREVSS | CDC.
<https://www.cdc.gov/surveillance/nrevss/coronavirus/index.html> (2021).
39. Opatowski, L. *et al.* Assessing pneumococcal meningitis association with viral respiratory infections and antibiotics: insights from statistical and mathematical models. *Proceedings of the Royal Society B: Biological Sciences* **280**, (2013).
40. Nickbakhsh, S. *et al.* Extensive multiplex PCR diagnostics reveal new insights into the epidemiology of viral respiratory infections. *Epidemiol Infect* **144**, 2064–2076 (2016).
41. Galanti, M. *et al.* Rates of asymptomatic respiratory virus infection across age groups. *Epidemiol Infect* **147**, e176 (2019).

42. Cheemarla, N. R. *et al.* Dynamic innate immune response determines susceptibility to SARS-CoV-2 infection and early replication kinetics. *Journal of Experimental Medicine* **218**, (2021).
43. Earl, P. L., Americo, J. L. & Moss, B. Insufficient Innate Immunity Contributes to the Susceptibility of the Castaneous Mouse to Orthopoxvirus Infection. *J Virol* **91**, e01042-17 (2017).
44. Moens, L. & Meyts, I. Recent human genetic errors of innate immunity leading to increased susceptibility to infection. *Current Opinion in Immunology* **62**, 79–90 (2020).
45. Lowen, A. C. *et al.* Blocking Interhost Transmission of Influenza Virus by Vaccination in the Guinea Pig Model. *Journal of Virology* **83**, 2803–2818 (2009).
46. Carter, R. Transmission blocking malaria vaccines. *Vaccine* **19**, 2309–2314 (2001).
47. Pinotti, F. *et al.* Potential impact of individual exposure histories to endemic human coronaviruses on age-dependent severity of COVID-19. *BMC Medicine* **19**, 19 (2021).
48. Meskill, S. D., Revell, P. A., Chandramohan, L. & Cruz, A. T. Prevalence of co-infection between respiratory syncytial virus and influenza in children. *The American journal of emergency medicine* **35**, 495–498 (/03//).
49. Le, X. T. T. *et al.* Rural–urban differences in preferences for influenza vaccination among women of childbearing age: implications for local vaccination service implementation in Vietnam. *Tropical Medicine & International Health* **26**, 228–236 (2021).
50. Made-in-Vietnam seasonal influenza vaccines are available. *vietnamnews.vn*
<http://vietnamnews.vn/society/483927/made-in-vietnam-seasonal-influenza-vaccines-are-available.html>.
51. Williams, T. C., Sinha, I., Barr, I. G. & Zambon, M. Transmission of paediatric respiratory syncytial virus and influenza in the wake of the COVID-19 pandemic. *Eurosurveillance* **26**, 2100186 (2021).
52. CoMix study - Social contact survey in the UK. *CMMID Repository*
<https://cmmid.github.io/topics/covid19/comix-reports.html> (2020).
53. Carsetti, R. *et al.* The immune system of children: the key to understanding SARS-CoV-2 susceptibility? *The Lancet Child & Adolescent Health* **4**, 414–416 (2020).
54. Long, Q.-X. *et al.* Clinical and immunological assessment of asymptomatic SARS-CoV-2 infections. *Nat Med* **26**, 1200–1204 (2020).
55. Six major respiratory viruses reported from PHE and NHS laboratories (SGSS) in England and Wales between week 1, 2011 and week 29, 2021. *GOV.UK*
<https://www.gov.uk/government/publications/respiratory-virus-circulation-england->

and-wales/six-major-respiratory-viruses-reported-from-phe-and-nhs-laboratories-sgss-in-england-and-wales-between-week-1-2009-and-week-23-2019.

56. Li, Y., Peterson, M. E., Campbell, H. & Nair, H. Association of seasonal viral acute respiratory infection with pneumococcal disease: a systematic review of population-based studies. *BMJ Open* **8**, e019743 (2018).

6 Appendices

Appendix A Supplementary material for Chapter 2

Supplementary information for
**“Interactions between RSV and influenza: limits of modelling
inference from surveillance data “**

Naomi R Waterlow¹, Stefan Flasche¹, Amanda Minter¹, Rosalind M Eggo¹

*¹Department of Infectious Disease Epidemiology, London School of Hygiene and Tropical Medicine,
UK*

Appendix A Supplementary material for Chapter 2	149
A.1 Model equations	150
A.2 Full model Diagram	152
A.3 R ₀ calculation.....	152
A.4 Susceptibility to RSV.....	153
A.5 Generating simulations	153
A.6 Sensitivity of introductions	155
A.7 Priors and parameter limits	157
A.8 Simulated data total case numbers	158
A.9 Individuals within infectious compartments.....	159
A.10 Parameter correlations	162
A.11 Convergence	170
A.12 Individual Simulation Analysis.....	171
A.13 Varying the R ₀	199

$$\lambda_{RSV_{ij}} = \sum \beta_{RSV} \alpha_{ij} I_{RSV_j} \quad (1)$$

$$\lambda_{INF_{ij}} = \sum \beta_{INF} \alpha_{ij} I_{INF_j} \quad (2)$$

$$\frac{dSS_i}{dt} = -\tau_i \lambda_{RSV_i} SS_i - \lambda_{INF_i} SS_i$$

$$\frac{dIS_i}{dt} = \tau_i \lambda_{RSV_i} SS_i - (1 - \sigma) \lambda_{INF_i} IS_i - \gamma_{RSV} IS_i$$

$$\frac{dPS_i}{dt} = \gamma_{RSV} IS_i - \rho PS_i - (1 - \sigma) \lambda_{INF_i} PS_i$$

$$\frac{dRS_i}{dt} = \rho PS_i - \lambda_{INF_i} RS_i$$

$$\frac{dSI_i}{dt} = \lambda_{INF_i} SS_i - (1 - \sigma) \tau_i \lambda_{RSV_i} SI_i - \gamma_{INF} SI_i$$

$$\frac{dII_i}{dt} = (1 - \sigma) \lambda_{INF_i} IS_i + (1 - \sigma) \tau_i \lambda_{RSV_i} SI_i - \gamma_{INF} II_i - \gamma_{RSV} II_i$$

$$\frac{dPI_i}{dt} = \lambda PS_i - \gamma_{INF} PI_i + \gamma_{RSV} II_i + \lambda_{INF_i} RS_i$$

$$\frac{dSP_i}{dt} = \gamma_{INF} SI_i - \rho SP_i - (1 - \sigma) \tau_i \lambda_{RSV_i} SP_i$$

$$\frac{dIP_i}{dt} = (1 - \sigma) \tau_i \lambda_{RSV} SP_i - \gamma_{RSV} IP_i + \gamma_{INF} II_i + \tau_i \lambda_{RSV_i} SR_i$$

$$\frac{dSR_i}{dt} = \rho SP_i - \tau_i \lambda_{RSV_i} SR_i$$

$$\frac{dRR_i}{dt} = \gamma_{RSV}IP_i + \gamma_{INF}PI_i$$

States

The first letter of the state indicates the state for RSV, the second letter indicates the state for Influenza.

E.g. SS_i is shorthand for $S_{RSV,i}S_{INF,i}$

S - Susceptible

I - Infected

P – Partially cross protected

R – Recovered

Subscripts

INF - Influenza

RSV – Respiratory Syncytial Virus

Parameters

$\lambda_{i,j}$ – transmission rate between age groups I and J

β – transmission rate

α_{ij} – contact rate between group I and j

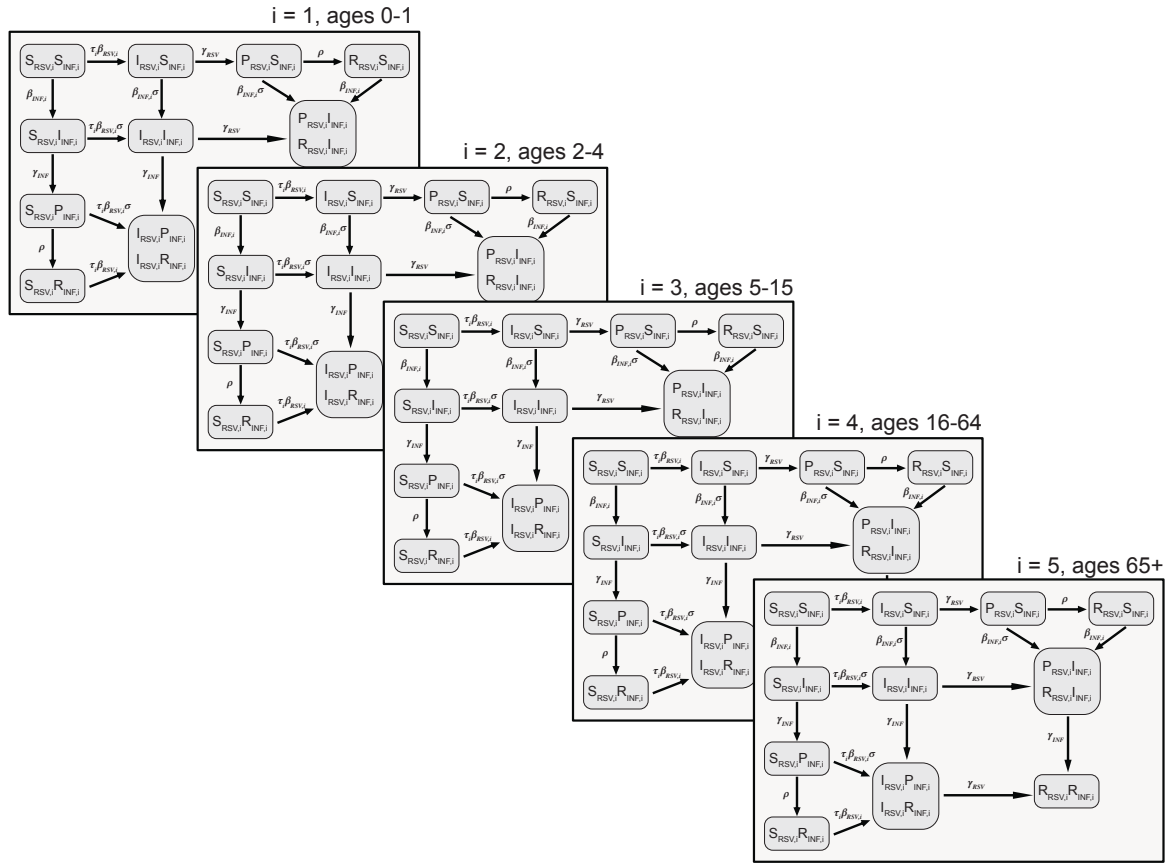
τ_i - age group susceptibility to RSV

σ – level of cross-protection

γ – rate of recovery

ρ – rate of loss of cross-protection

A.2 Full model Diagram



Appendix A Figure S1: Model diagram for RSV and Influenza (INF) demonstrating all age groups. Population can be Susceptible (S), Infected (I), Protected (P) or Recovered (R) to each virus. For each virus, following infection, infectiousness wanes at a constant rate, and the population enters the P state. Here they are immune to the virus they were infected by and protected to a varying extent against infection from the second virus. This protection wanes at a rate which we change, and the population enters the R compartment. In the R compartment the population is immune to the virus it was infected by, but not the other virus. Parameters are: recovery rate for RSV and Influenza (γ_{RSV} and γ_{INF}), age susceptibility to infection (τ_i), the transmission parameters for RSV and Influenza ($\beta_{RSV,i}$ and $\beta_{INF,i}$), strength of cross-protection (σ) and rate of protection loss (ρ). Values are given in Table 1. The age is denoted by the subscript (i).

A.3 R_0 calculation

The R_0 for each virus was calculated using the method described in Diekmann *et al* (2009)¹, assuming no interaction between the viruses. The R_0 is the dominant eigenvalue of the matrix

$$-T\Sigma^{-1}$$

where T is the transmission part of the Jacobean matrix, describing the production of new infections, and Σ is the transition part, describing changes in state¹. See reference for further details.

$$T_{INF} = \begin{bmatrix} \beta_{INF} * \alpha_{i,j} & \cdots & \beta_{INF} * \alpha_{i,j} \\ \vdots & \ddots & \vdots \\ \beta_{INF} * \alpha_{i,j} & \cdots & \beta_{INF} * \alpha_{i,j} \end{bmatrix} \quad T_{RSV} = \begin{bmatrix} \tau_j * \beta_{RSV} * \alpha_{i,j} & \cdots & \tau_i * \beta_{RSV} * \alpha_{i,j} \\ \vdots & \ddots & \vdots \\ \tau_j * \beta_{RSV} * \alpha_{i,j} & \cdots & \tau_j * \beta_{RSV} * \alpha_{i,j} \end{bmatrix}$$

$$\Sigma_{INF} = \begin{bmatrix} \gamma_{INF} & 0 & 0 & 0 & 0 \\ 0 & \gamma_{INF} & 0 & 0 & 0 \\ 0 & 0 & \gamma_{INF} & 0 & 0 \\ 0 & 0 & 0 & \gamma_{INF} & 0 \\ 0 & 0 & 0 & 0 & \gamma_{INF} \end{bmatrix} \quad \Sigma_{RSV} = \begin{bmatrix} \gamma_{RSV} & 0 & 0 & 0 & 0 \\ 0 & \gamma_{RSV} & 0 & 0 & 0 \\ 0 & 0 & \gamma_{RSV} & 0 & 0 \\ 0 & 0 & 0 & \gamma_{RSV} & 0 \\ 0 & 0 & 0 & 0 & \gamma_{RSV} \end{bmatrix}$$

Subscripts

INF - Influenza

RSV – Respiratory Syncytial Virus

Parameters

β – transmission rate

α_{ij} – contact rate between group *i* and *j*

τ_i - age group susceptibility to RSV

γ – rate of recovery

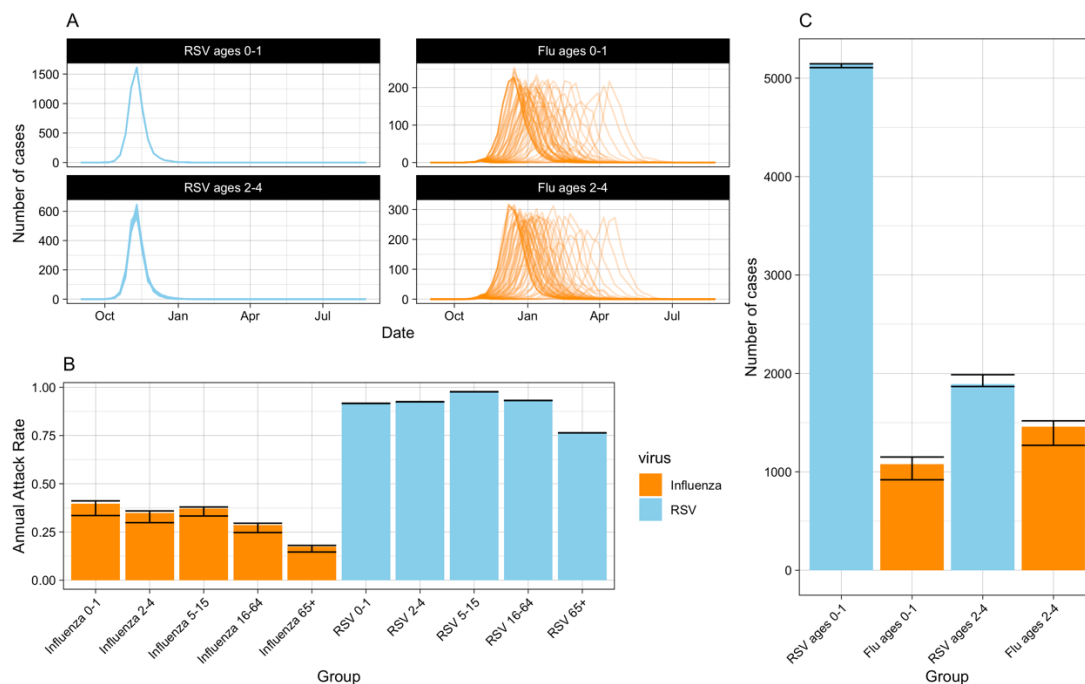
A.4 Susceptibility to RSV

RSV susceptibility differs with age, as indicated by a longitudinal study by Henderson et al. (1979) in which they determined that at 1st exposure 98.4% of children became infected, at second exposure 74.5% of children became infected and at 3rd exposure 65.4% of children became infected². As it is estimated that almost all children are infected by 24 months of age³, we used these figures as the reduced susceptibility of age groups (ages 0-1 = 100% susceptible, ages 2-4 = 75% susceptible, ages 5 and over = 65% susceptible).

A.5 Generating simulations

We generated simulations using our model with different parameter combinations, using a binomial sampling process to model observed cases (see main methods section for more details). We calibrated the detection and transmission rates for the viruses in the under-five population to observed values in the UK, by visually matching simulation output to epidemic peak incidence and duration⁴. In addition, we set the rates for RSV to different values in each age group, as younger

infants have been shown to be more likely to present with severe symptoms⁵. Overall, our simulations emulated UK data, with higher RSV incidence in infants compared to young children, fewer influenza as compared to RSV cases. RSV incidence peaked in the same week each simulation, whereas the influenza incidence peak varied over a time span of 6 months, with the majority of simulations over a 4-month time span (Appendix A Figure S2). Across simulations, the median number of RSV cases observed was 5143 (95% quantiles (95%Q) 5107 – 5146) in 0-1 year olds and 1891 (95%Q 1867 – 1986) in 2-4 year olds. This compares to 1077 (95%Q 919 – 1150) and 1457 (95%Q 1269 – 1518) for influenza in the respective age groups. The mean annual attack rates across all age groups were 31% (95%Q 27-34%) for influenza and 90% (95%Q 90-90%) for RSV.



Appendix A Figure S2: A) Simulations from one replicate of the parameter combinations, showing the spread of timings of the epidemics. B) Annual Attack rates for the different viruses and age groups. Bars show the median value and the error bars the 95% quantiles. C) Median number of cases reported across simulations for each age group and virus combination. Error bars show the 95% quantiles.

Appendix A Table S1: parameters used in the model for the proportion of infections detected by age group and virus.

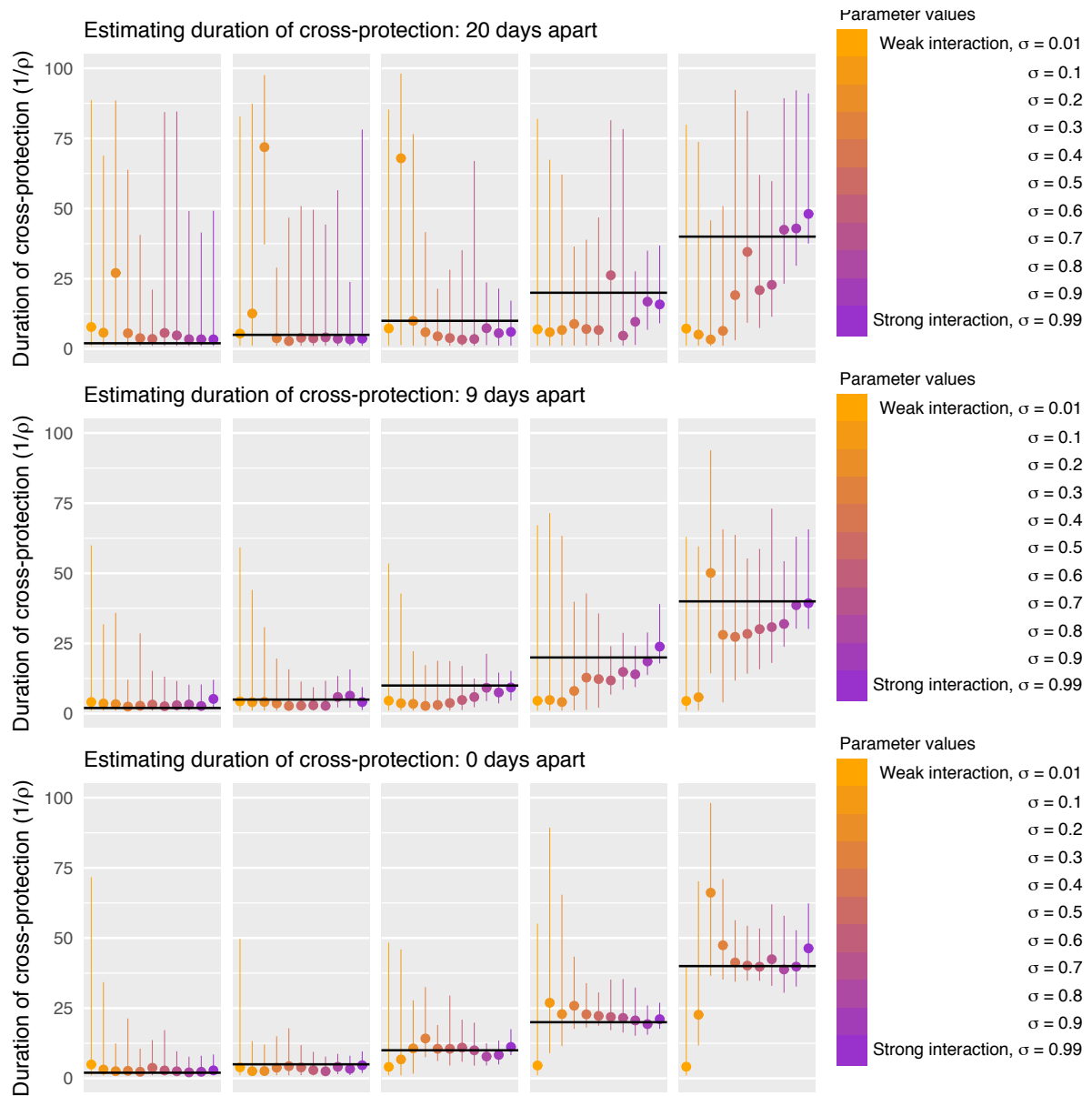
Parameter	Symbol	Value
Proportion of RSV infections in ages 0-1 hospitalised	Δ_{R1}	0.004
Proportion of RSV infections in ages 2-4 hospitalised	Δ_{R2}	0.001
Proportion of Influenza infections in ages 0-4 hospitalised	Δ_I	0.002

A.6 Sensitivity of introductions

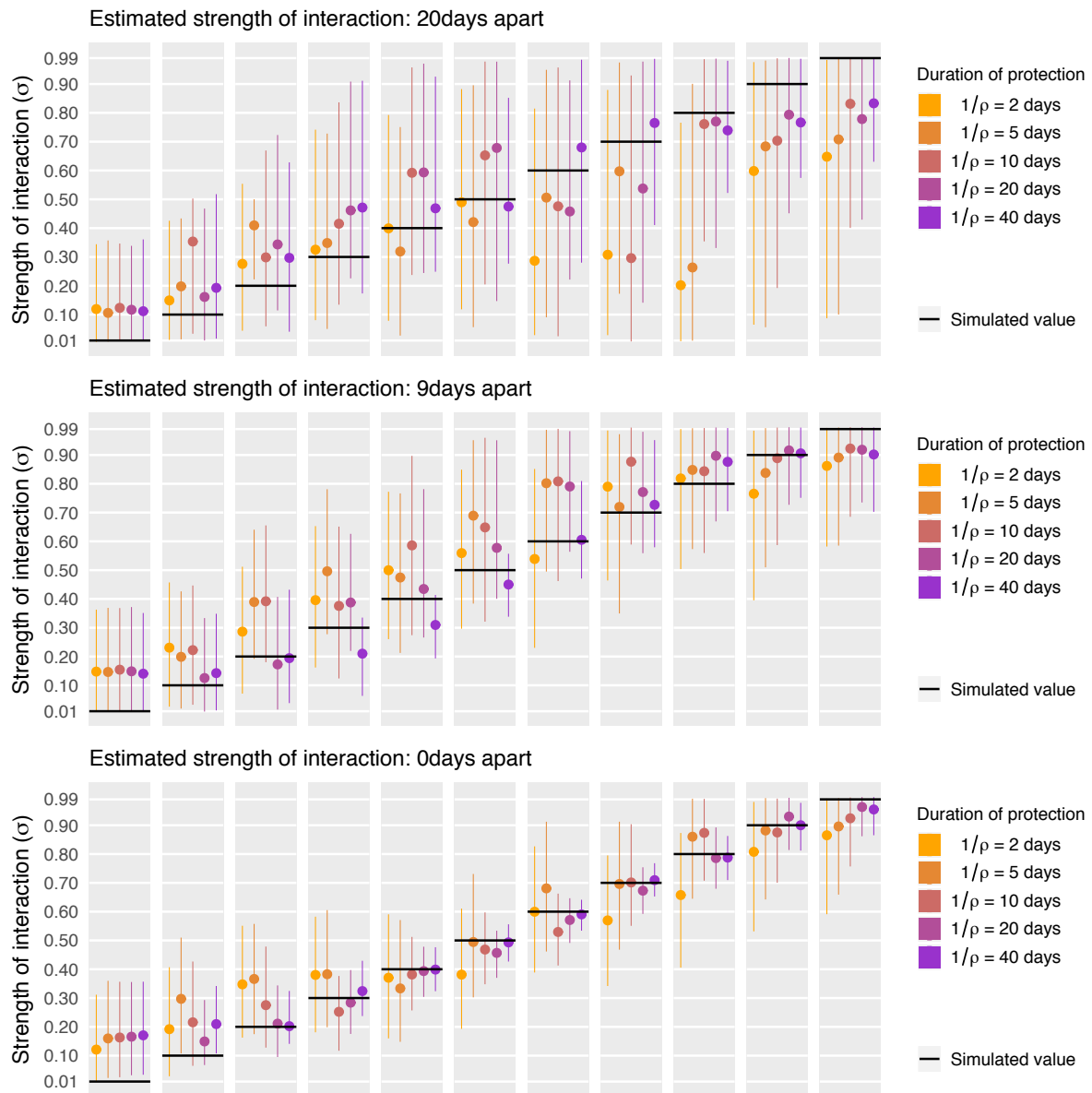
Introduction of influenza as a one-off infection at season start time (η_I) was also tested to look at the sensitivity of the assumption. With a single introduction the influenza epidemic was suppressed for the whole season at certain parameter values. This occurred when there was strong interaction between the two viruses and the introduction of influenza occurred during the peak of the RSV epidemic. As such behaviour is not seen in England, we judged the assumption of low-level constant introduction to be more valid.

Parameter limits were kept constant, except for the limit on σ , which either ranged from 0 to 1 (competitive interaction only) or from 1 to -1 (allowing for synergistic as well as competitive interaction). Although we do not think a synergistic relationship between influenza and RSV is likely, we thought including it may allow the chain to more effectively explore the parameter space. However, for values between 0.2 and 0 no MCMC chains converged when allowing for synergistic interaction, so in all subsequent runs σ was limited between 0 and 1.

We ran a sensitivity analysis on the start times of the viruses, running / fitting extra simulations with influenza and RSV starting on the same day and 20 days apart. These simulations were run as in the main paper, however limited to 250000 iterations after burn in. When the viruses were seeded on the same day (and there was greater overlap of epidemics), the estimates for both interaction parameters were more precise (Figure S2) than the standard simulations. Conversely, when influenza was seeded later than standard, the estimates were less precise.



Appendix A Figure S3: Estimated p values from MCMC inference for simulations with different σ and p values. Median value and 95% CrI are shown. The black line is the simulated (true) value of p in each case. The different plots show simulations with different intervals between influenza and RSV start times.



Appendix A Figure S4: Estimated σ values from MCMC inference for simulations with different σ and ρ values. Median value and 95% CrI are shown. The black line is the simulated (true) value of σ in each case. The different plots show simulations with different intervals between influenza and RSV start times.

A.7 Priors and parameter limits

Appendix A Table S2: Prior distributions and limits for the parameters used in the model during the Markov Chain Monte Carlo (MCMC) fitting process. *sd* = standard deviation.

Parameter	Symbol	Prior distribution	Lower Limit	Upper Limit
R_0 for RSV used to calculate basic transmission rate	$\beta_{0,RSV}$	Normal distribution, mean=3, sd=0.6	0	Infinity

R_0 for Influenza used to calculate basic transmission rate	$\beta_{0,INF}$	Lognormal distribution, mean=0.3, sd=0.6, shifted by 1	0	Infinity
Time of first RSV infection	η_{RSV}	Uniform between day 0 and day 60	0	60
Time of first influenza infection	η_{INF}	Uniform between day 0 and day 60	0	60
Proportion of RSV infections in ages 0-1 hospitalised	$\Delta_{RSV,1}$	Uniform	0	Infinity
Proportion of RSV infections in ages 2-4 hospitalised	$\Delta_{RSV,2}$	Uniform	0	Infinity
Proportion of Influenza infections in ages 0-4 hospitalised	Δ_{INF}	Uniform	0	Infinity
Strength of interaction	σ	Uniform between 0 and 1	0	1 (or -1 for sensitivity check – see supplementary section 6)
Rate of loss of cross-protection	ρ	Uniform between 0.01 and 1	0	1

A.8 Simulated data total case numbers

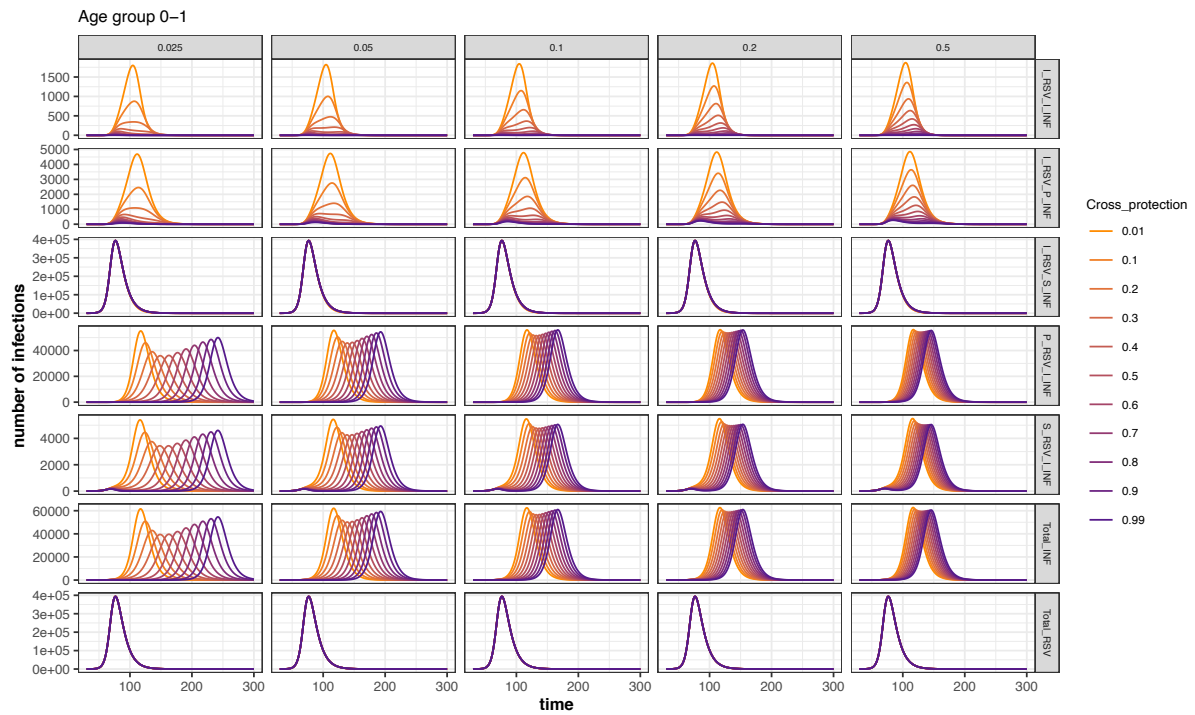
Appendix A Table S3: shows the total number of infections with different duration of cross-protection. The level of cross-protection is fixed at $\sigma = 0.5$.

1/duration of cross-protection (ρ)	Number of RSV cases	Number of Influenza cases
2	3182023	1294980
5	3181955	1292596
10	3182035	1283034
20	3182200	1245207
40	3182284	1152700

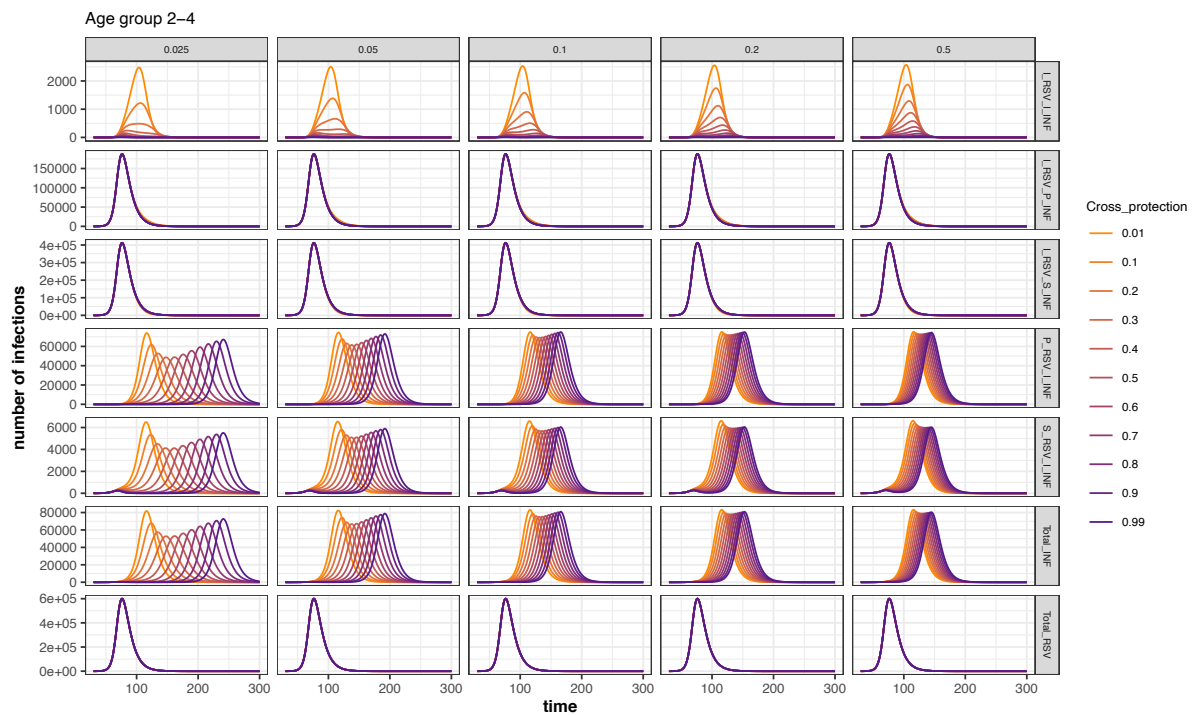
Appendix A Table S4: shows the total number of infections with different duration of cross-protection. The duration of cross-protection is fixed at $1/\rho = 10$.

Strength of cross-protection (σ)	Number of RSV cases	Number of Influenza cases
1	3182422	1303752
0.8	3182341	1297009
0.6	3182152	1287792
0.4	3181936	1279325
0.2	3182025	1281968
0	3183181	1314065

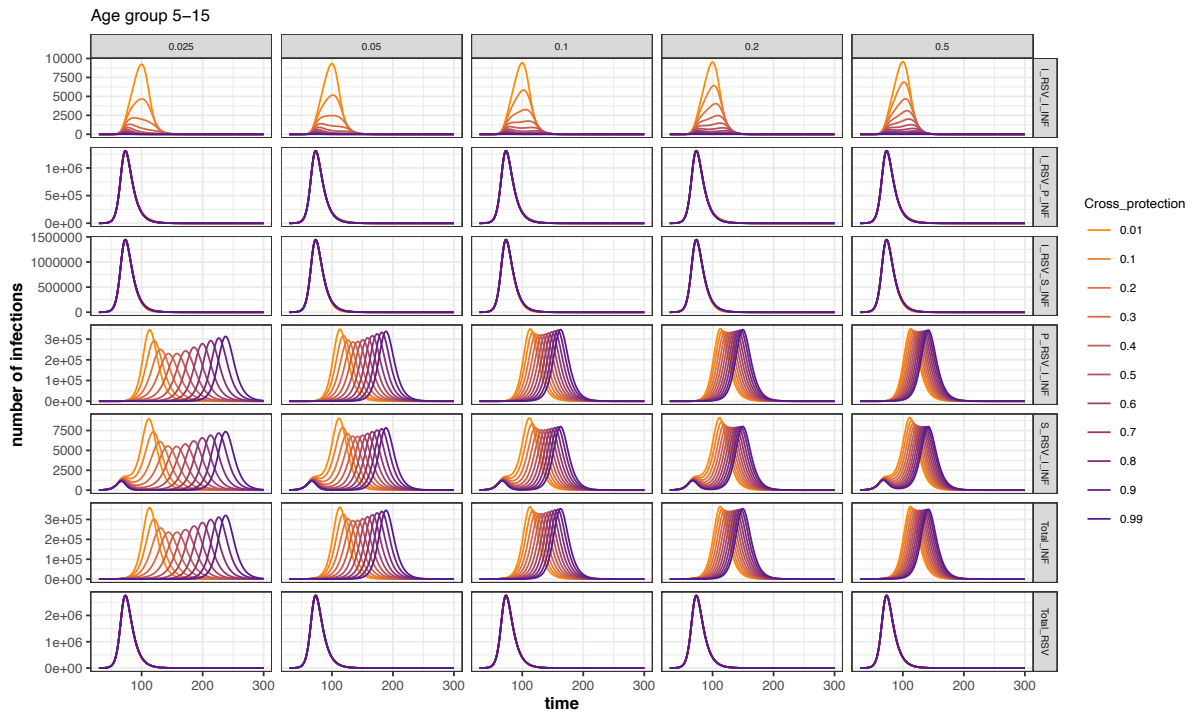
A.9 Individuals within infectious compartments



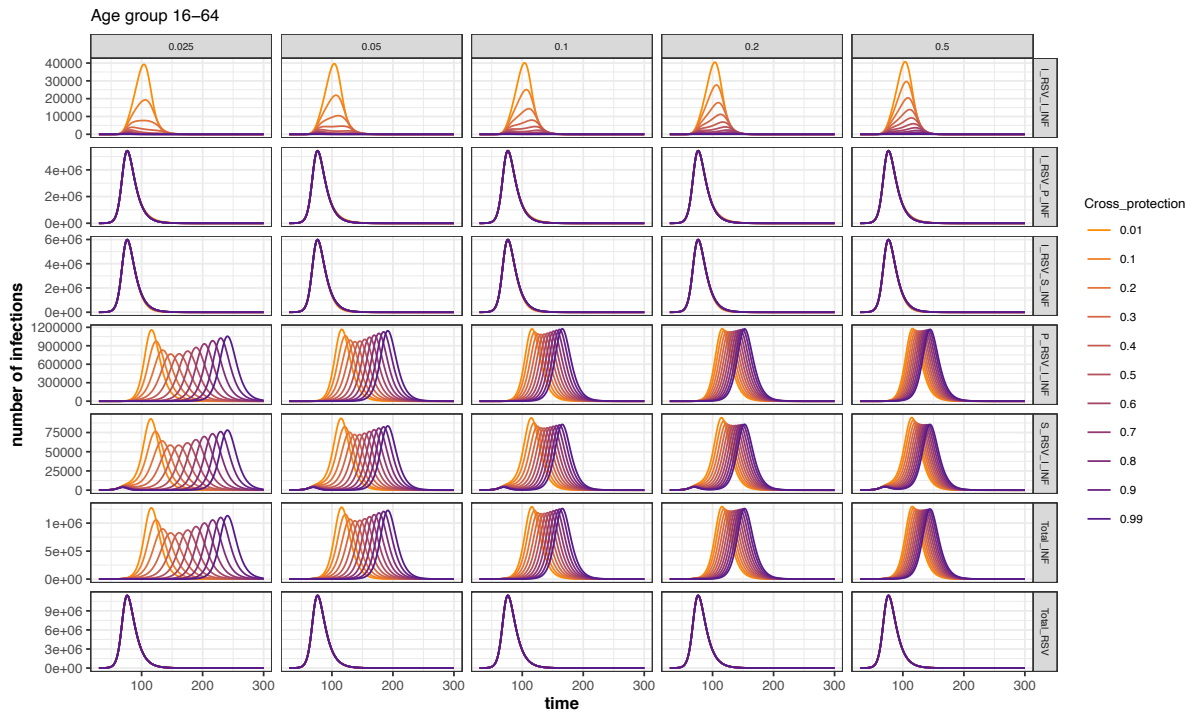
Appendix A Figure S5: Individuals within each infectious compartment for the age group 0-1. Horizontal facets show the ρ value, colours the σ value. Vertical facets show the different infectious compartments



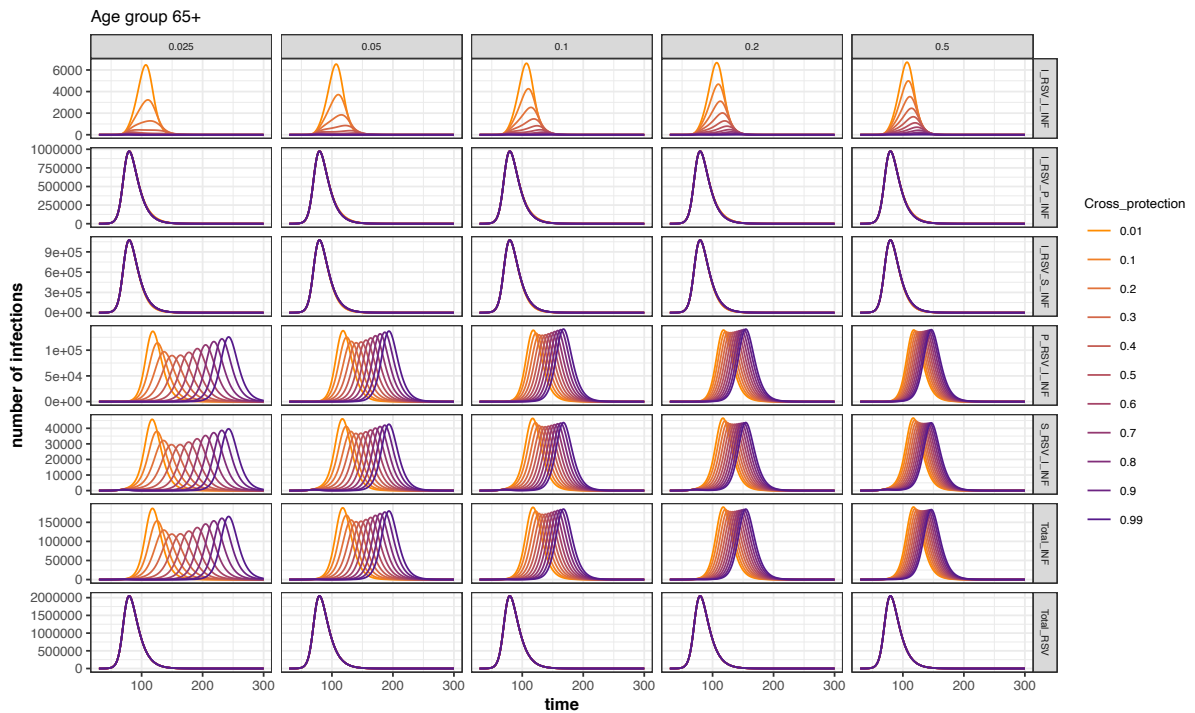
Appendix A Figure S6: Individuals within each infectious compartment for the age group 2-4. See Figure S2 legend for more details.



Appendix A Figure S7: Individuals within each infectious compartment for the age group 5-15. See Figure S2 legend for more details.



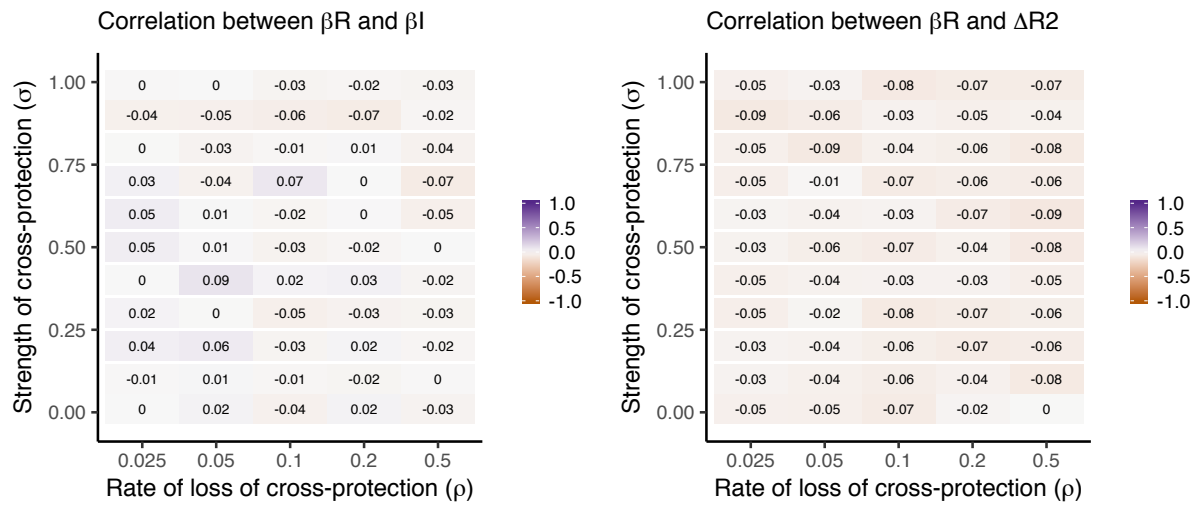
Appendix A Figure S8: Individuals within each infectious compartment for the age group 16-64. See Figure S2 legend for more details.



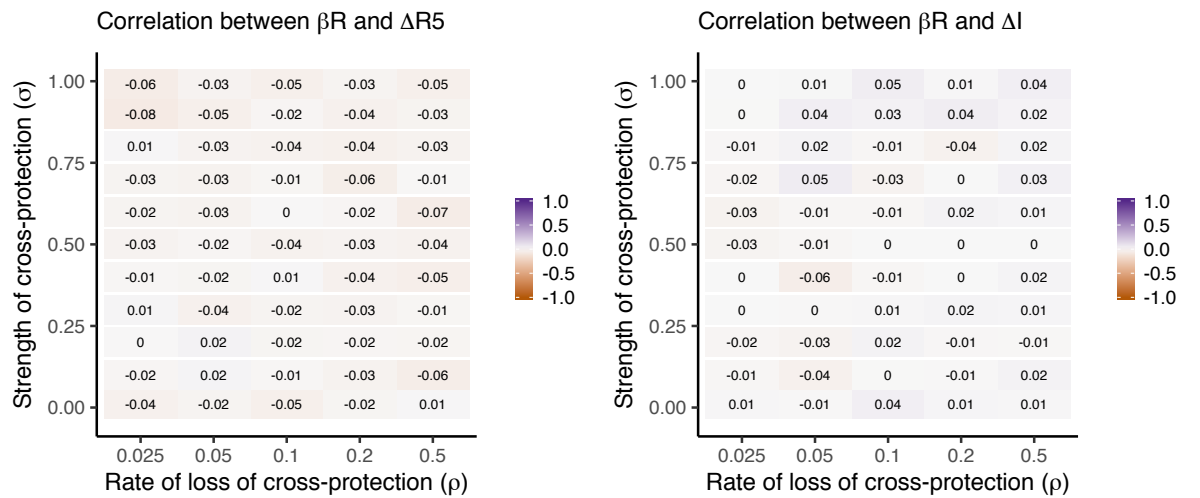
Appendix A Figure S9: Individuals within each infectious compartment for the age group 65+. See Figure S2 legend for more details.

A.10

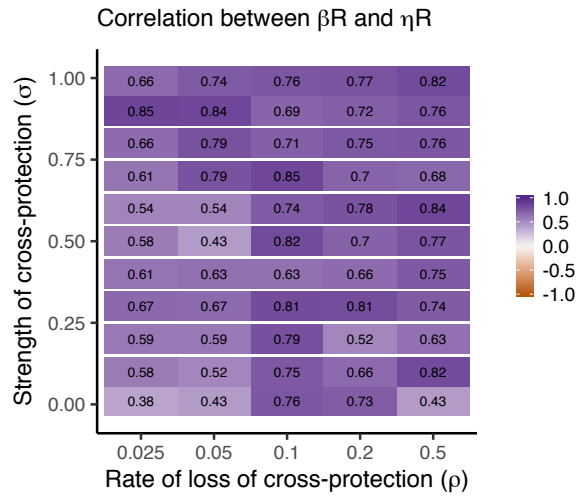
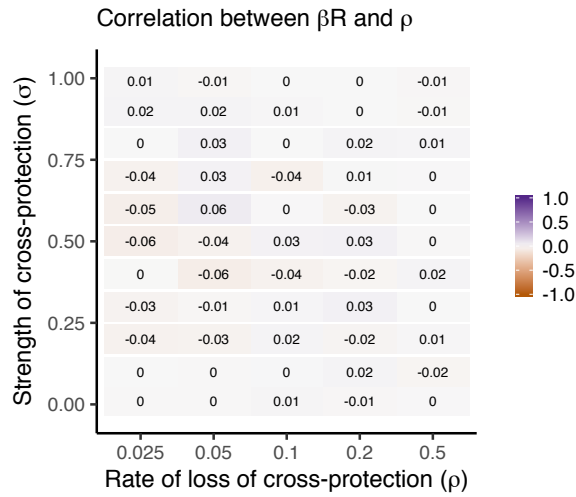
Parameter correlations



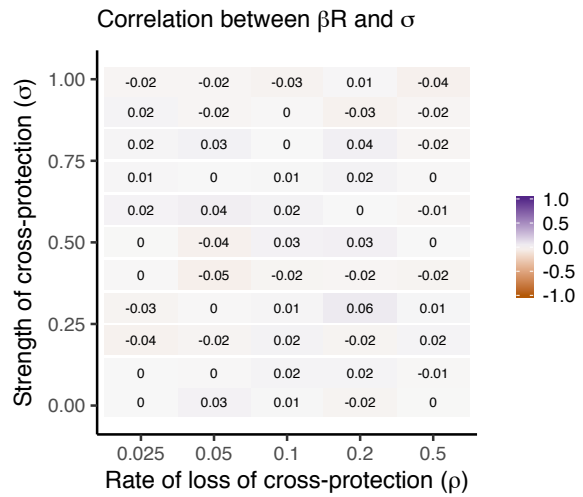
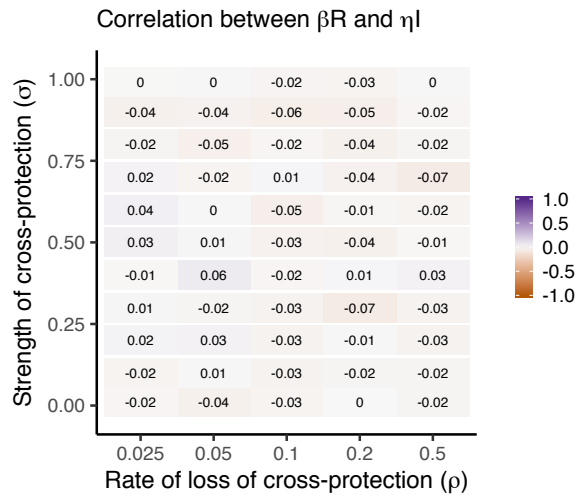
Appendix A Figure S10: Pearson correlation coefficients for parameter combinations specified in the title, with changing interaction parameters (ρ and σ).



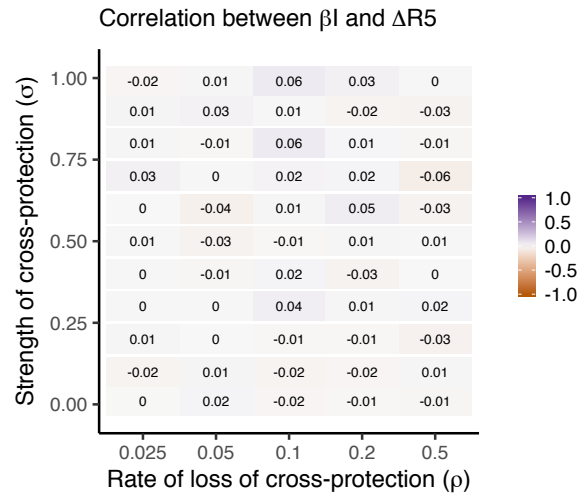
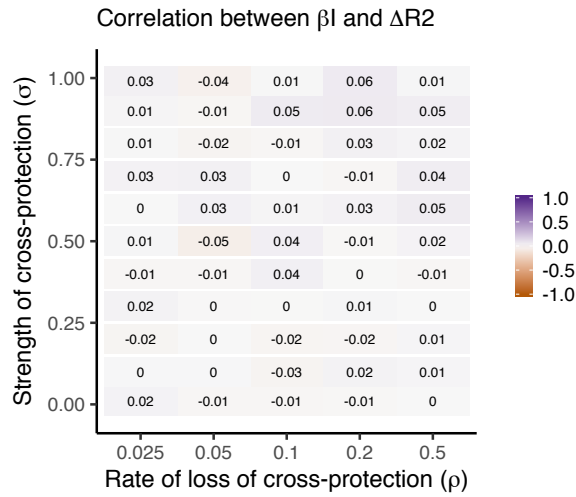
Appendix A Figure S11: Pearson correlation coefficients for parameter combinations specified in the title, with changing interaction parameters (ρ and σ).



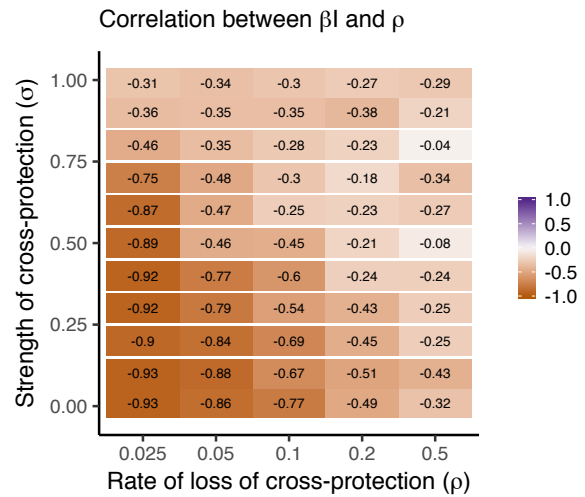
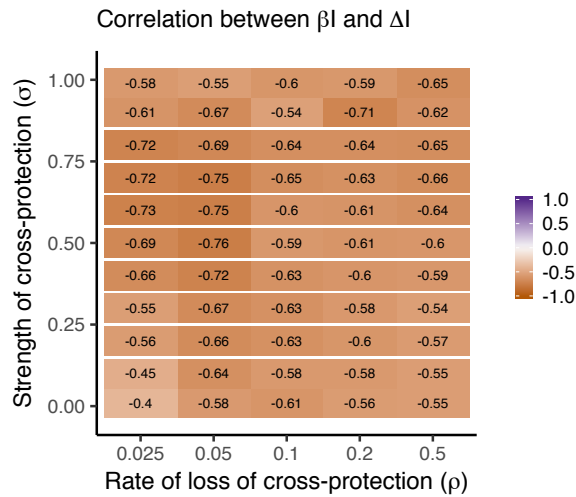
Appendix A Figure S12: Pearson correlation coefficients for parameter combinations specified in the title, with changing interaction parameters (ρ and σ).



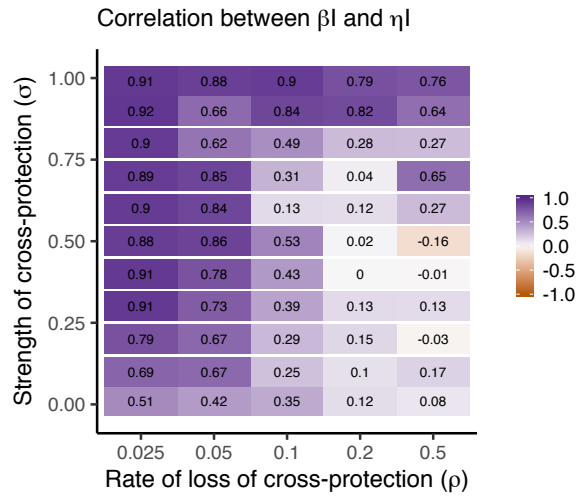
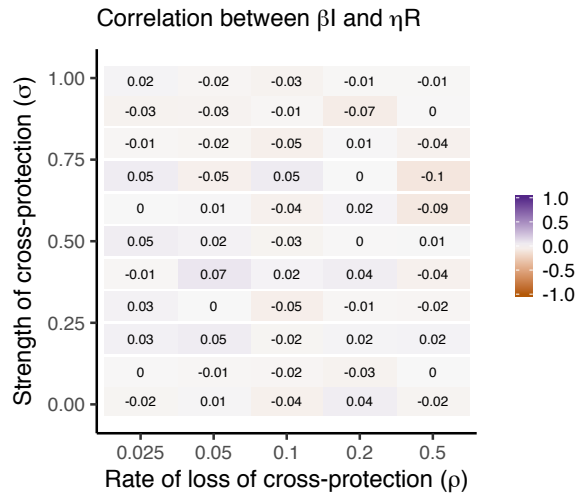
Appendix A Figure S13: Pearson correlation coefficients for parameter combinations specified in the title, with changing interaction parameters (ρ and σ).



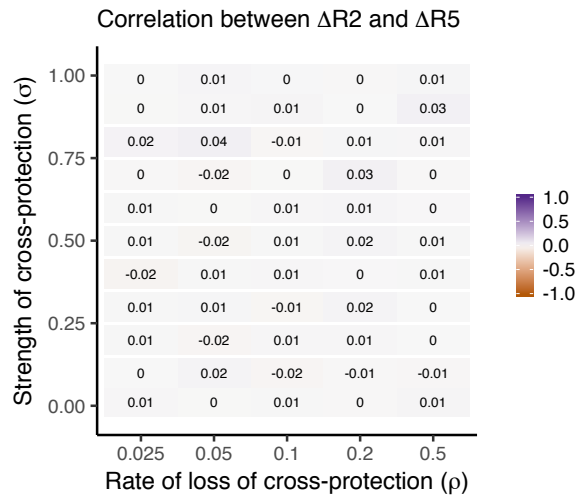
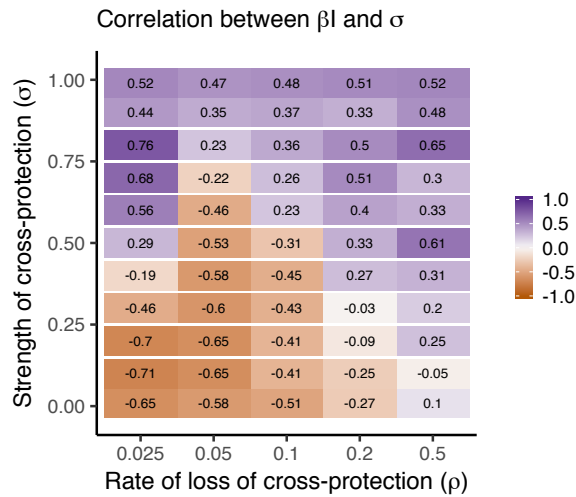
Appendix A Figure S14: Pearson correlation coefficients for parameter combinations specified in the title, with changing interaction parameters (ρ and σ).



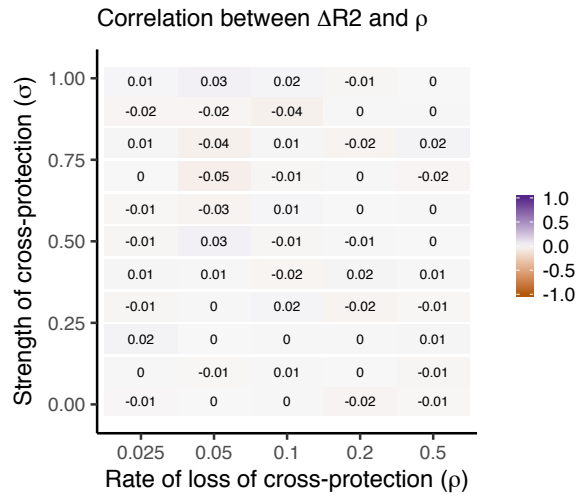
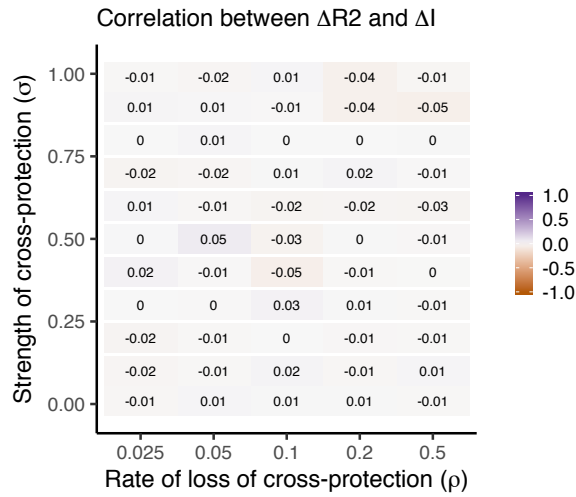
Appendix A Figure S15: Pearson correlation coefficients for parameter combinations specified in the title, with changing interaction parameters (ρ and σ).



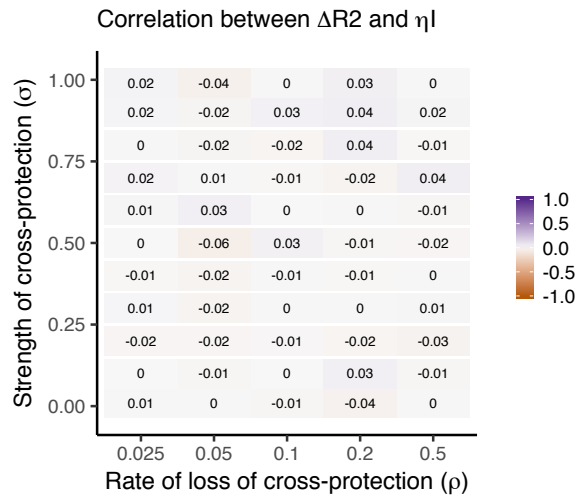
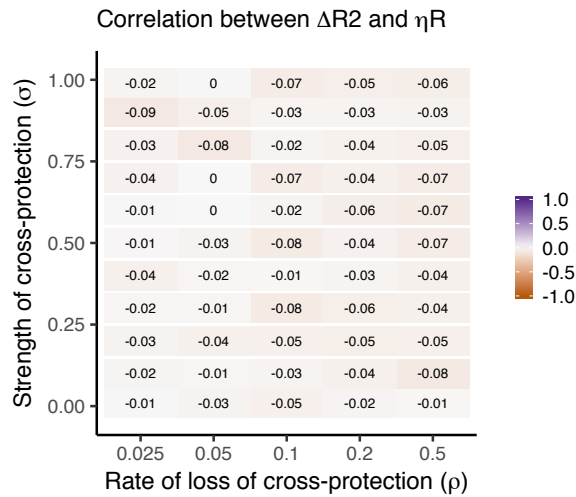
Appendix A Figure S16: Pearson correlation coefficients for parameter combinations specified in the title, with changing interaction parameters (ρ and σ).



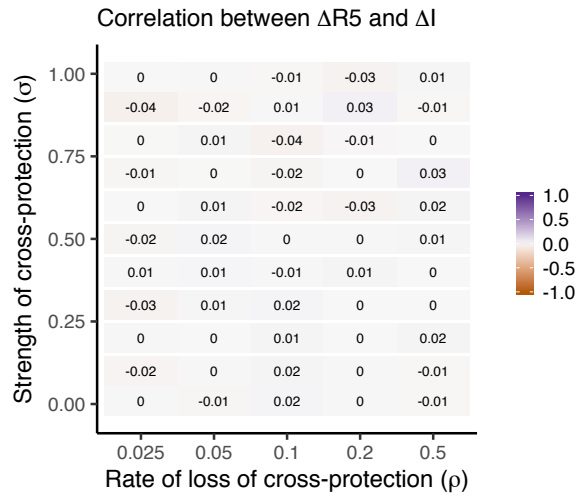
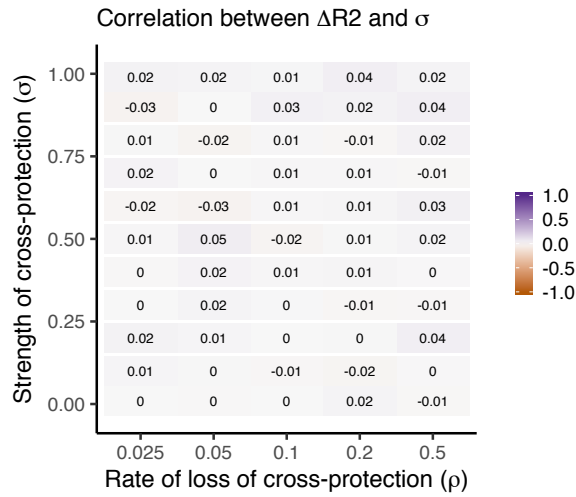
Appendix A Figure S17: Pearson correlation coefficients for parameter combinations specified in the title, with changing interaction parameters (ρ and σ).



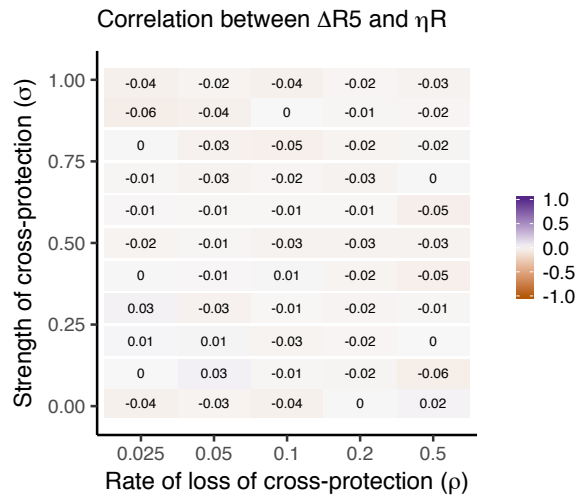
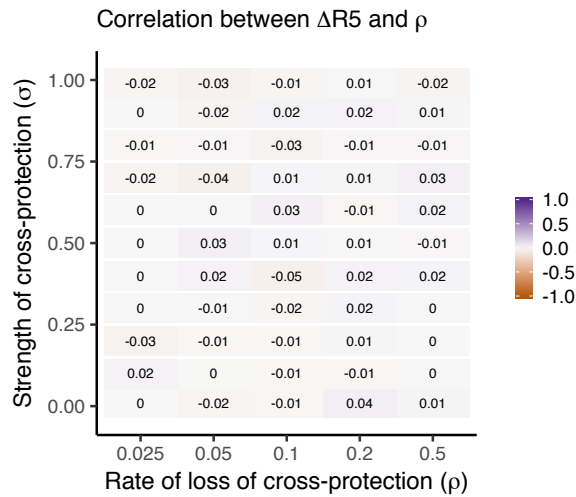
Appendix A Figure S18: Pearson correlation coefficients for parameter combinations specified in the title, with changing interaction parameters (ρ and σ).



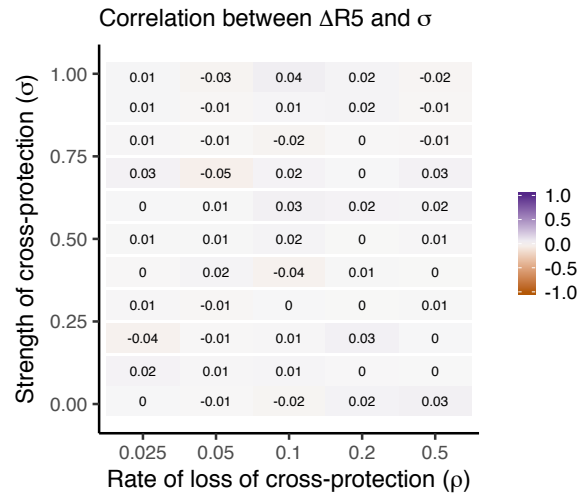
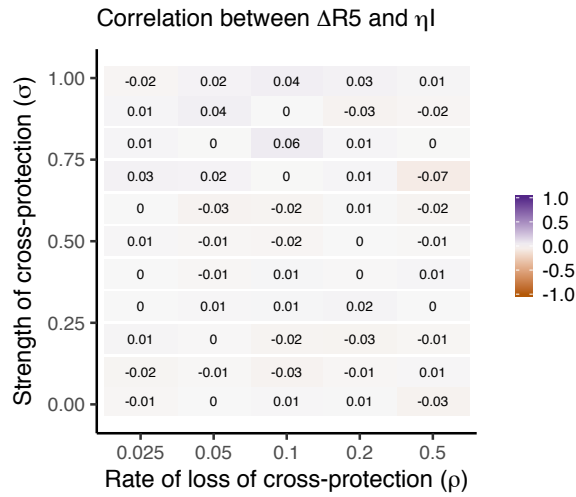
Appendix A Figure S19: Pearson correlation coefficients for parameter combinations specified in the title, with changing interaction parameters (ρ and σ).



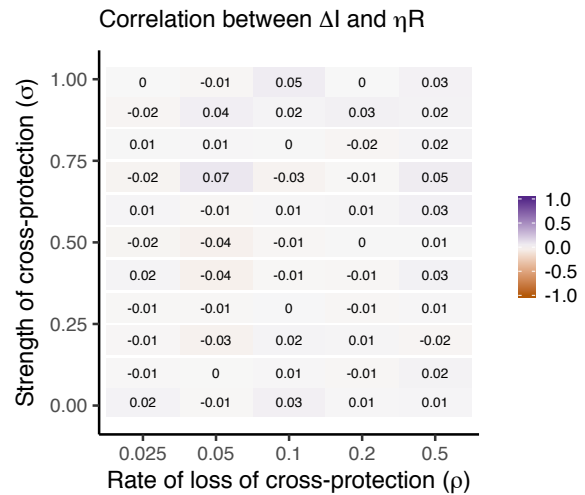
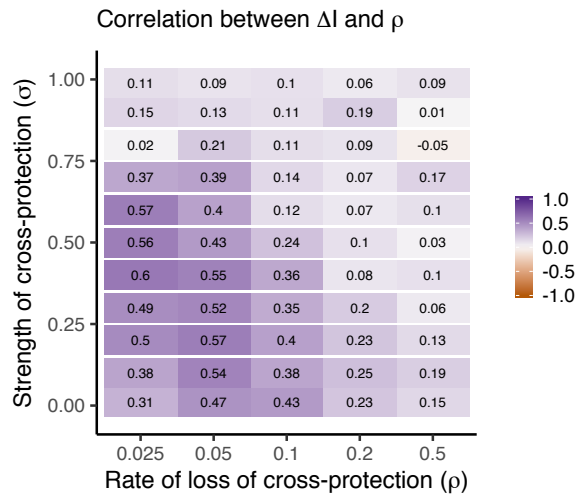
Appendix A Figure S20: Pearson correlation coefficients for parameter combinations specified in the title, with changing interaction parameters (ρ and σ).



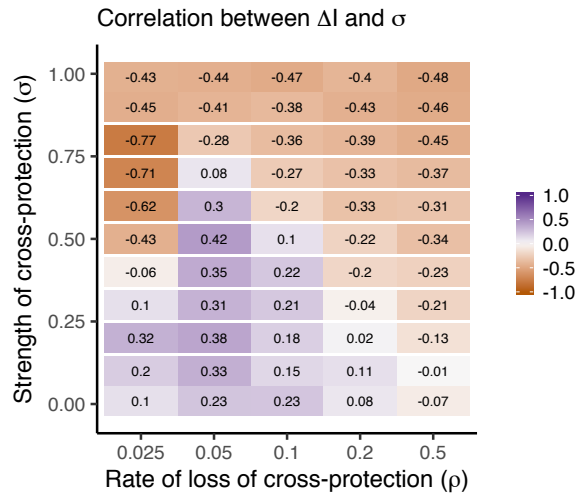
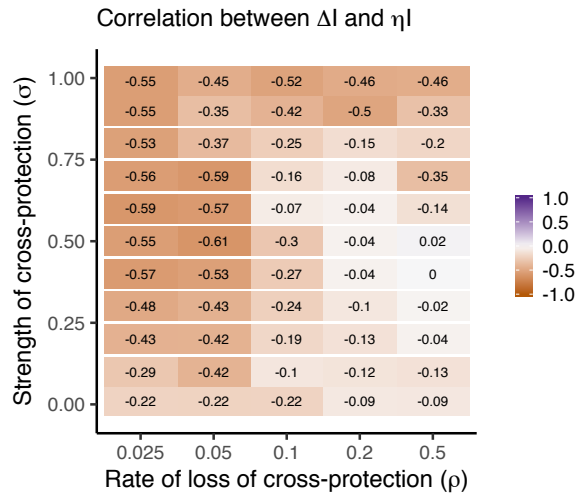
Appendix A Figure S21: Pearson correlation coefficients for parameter combinations specified in the title, with changing interaction parameters (ρ and σ).



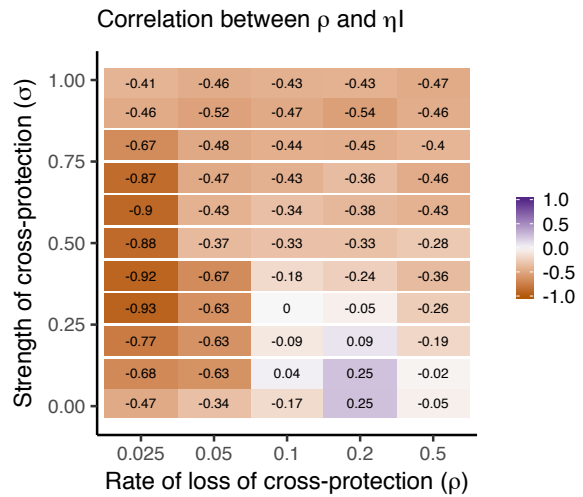
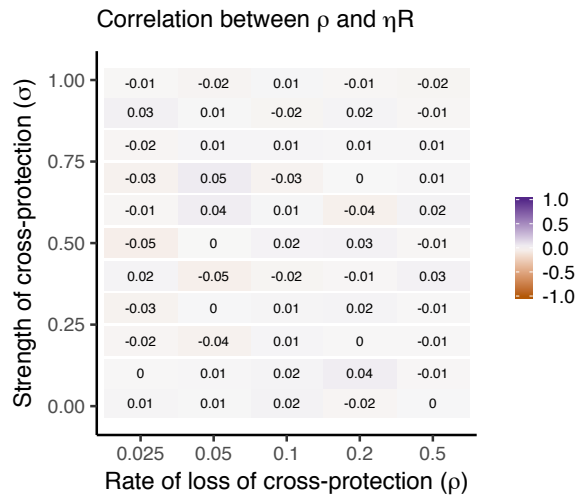
Appendix A Figure S22: Pearson correlation coefficients for parameter combinations specified in the title, with changing interaction parameters (ρ and σ).



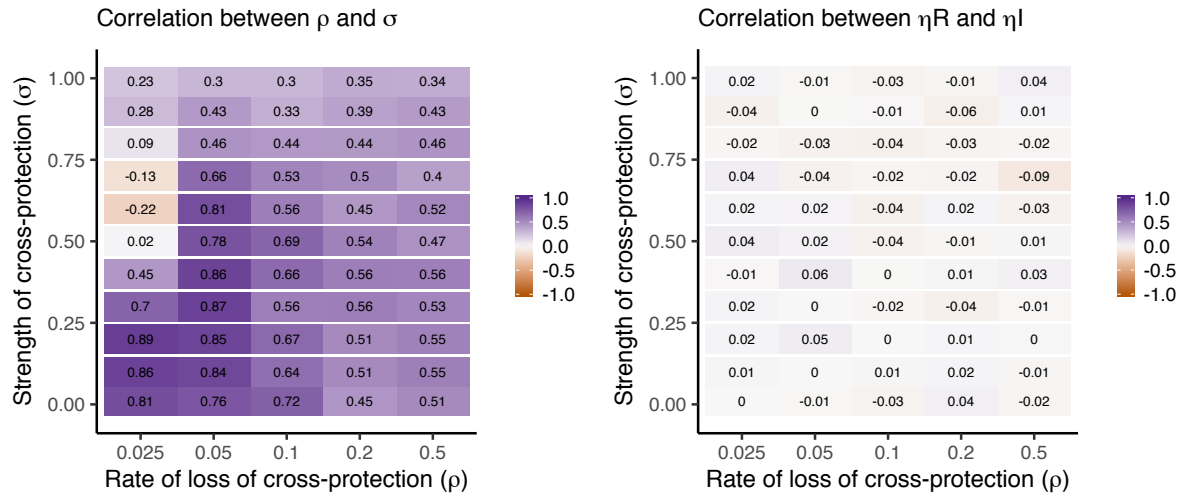
Appendix A Figure S23: Pearson correlation coefficients for parameter combinations specified in the title, with changing interaction parameters (ρ and σ).



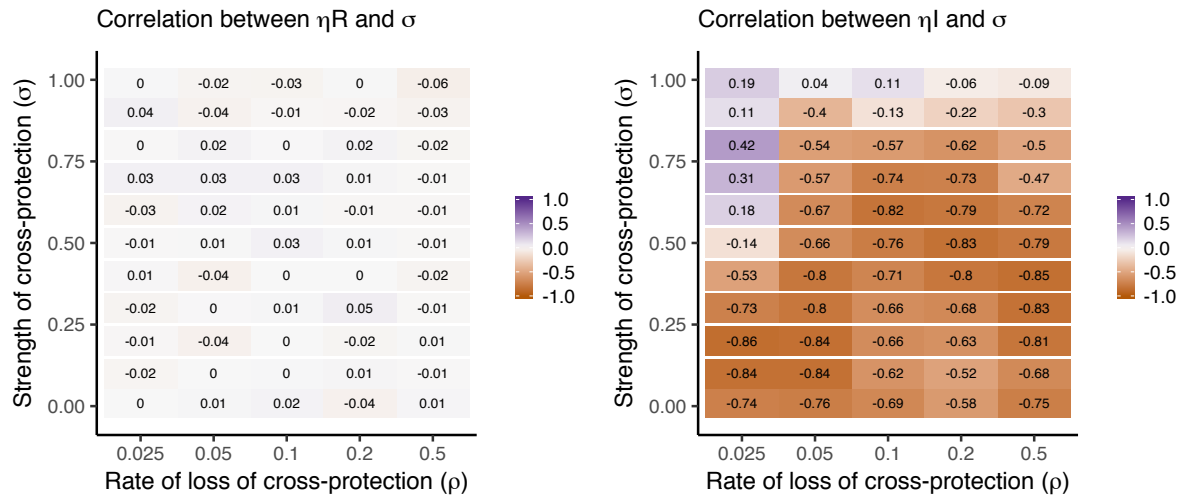
Appendix A Figure S24: Pearson correlation coefficients for parameter combinations specified in the title, with changing interaction parameters (ρ and σ).



Appendix A Figure S25: Pearson correlation coefficients for parameter combinations specified in the title, with changing interaction parameters (ρ and σ).



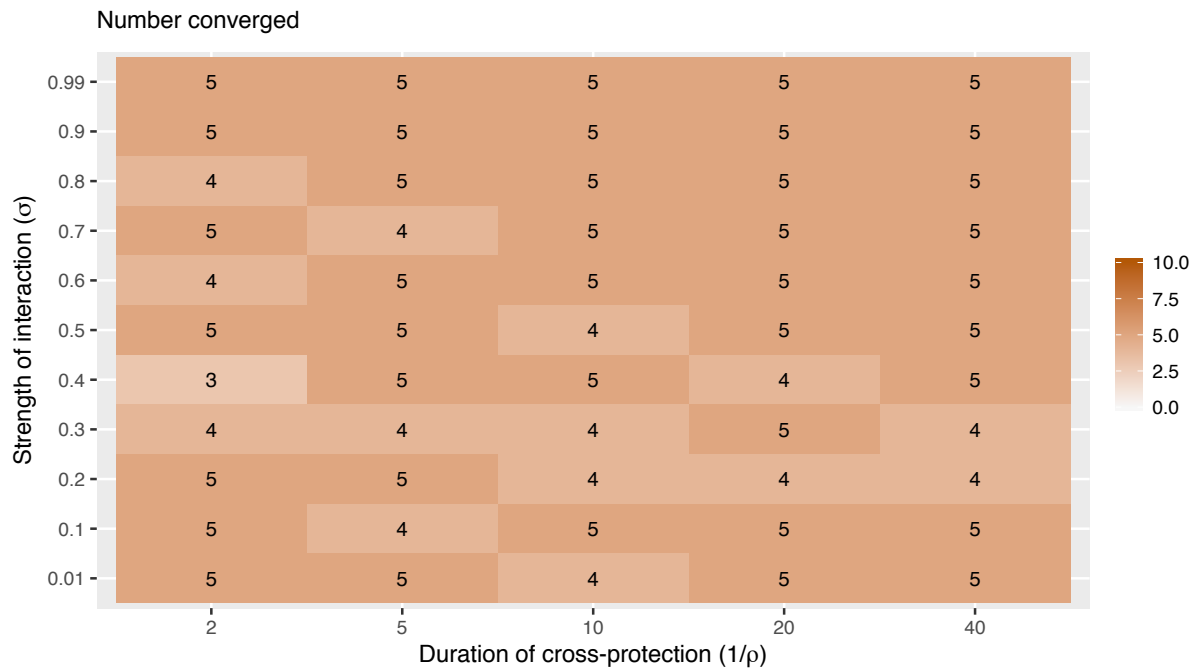
Appendix A Figure S26: Pearson correlation coefficients for parameter combinations specified in the title, with changing interaction parameters (ρ and σ).



Appendix A Figure S27: Pearson correlation coefficients for parameter combinations specified in the title, with changing interaction parameters (ρ and σ).

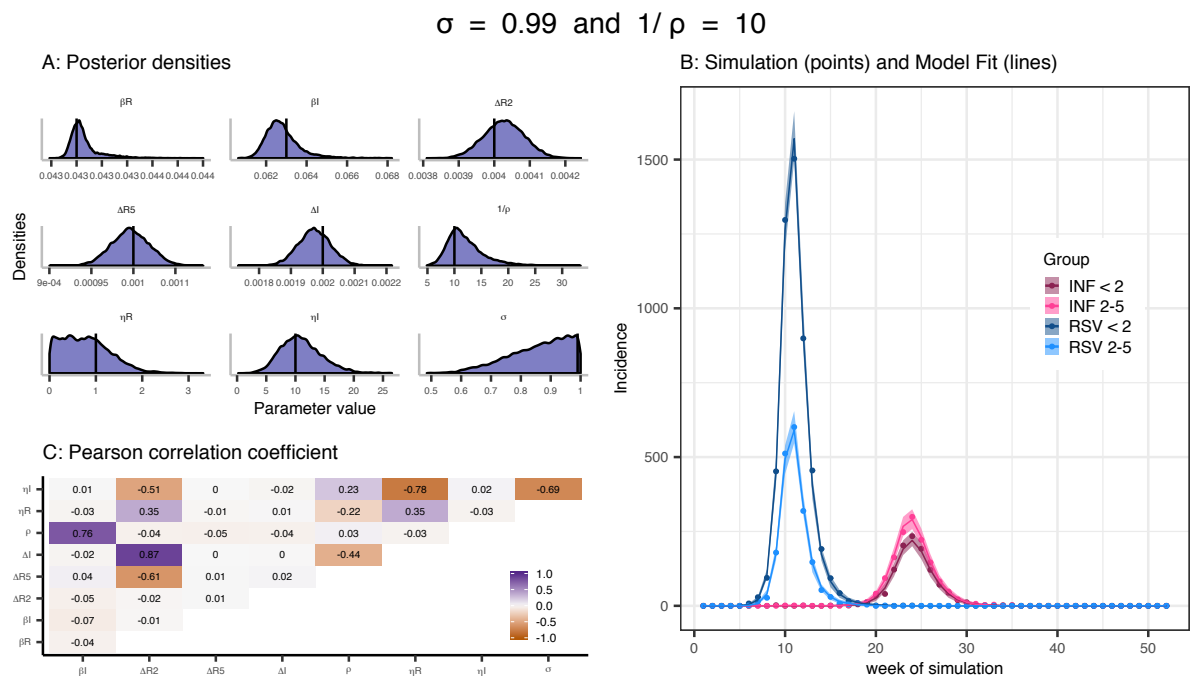
A.11 Convergence

For each simulation, we generated 5 replicates, for which we ran two chains with 450 000 iterations as burn in followed by a further 250 000 iterations. For chains that did not converge, we extended the chains for a further 250 000 iterations iteratively until convergence was reached or a total of 1 200 000 iterations were run. Figure S27 shows the number of runs that reached convergence for each parameter combination. We expect that all runs will converge with sufficient iterations, however we were faced with computational limits.



Appendix A Figure S28: Number of Simulations for which the MCMC chains converged.

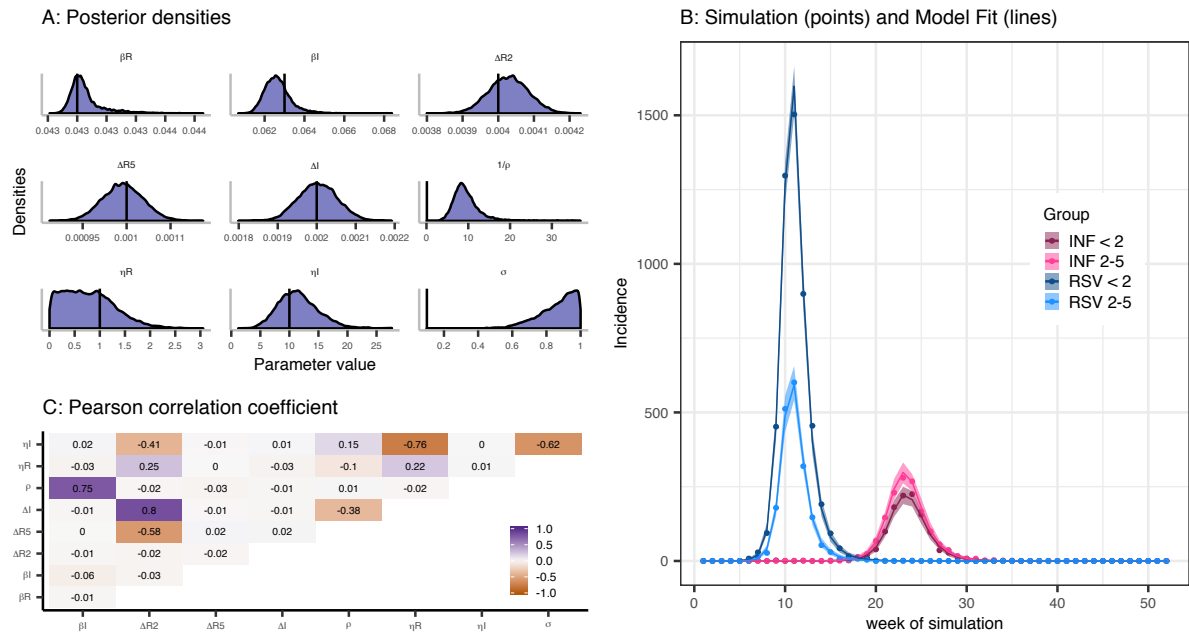
A.12 Individual Simulation Analysis



Appendix A Figure S29: Inference results for simulation with $\sigma = 0.99$ and $\rho = 0.1$. A: Posterior densities for all estimate parameters. The black vertical line represents the simulated (true) value. B: Points – simulated weekly incidence from the simulation, by virus and age group. Lines represent the model fit using the median value from the posterior distribution for each parameter. Ribbons represent 95% quantiles of the model fit (CIs) C:

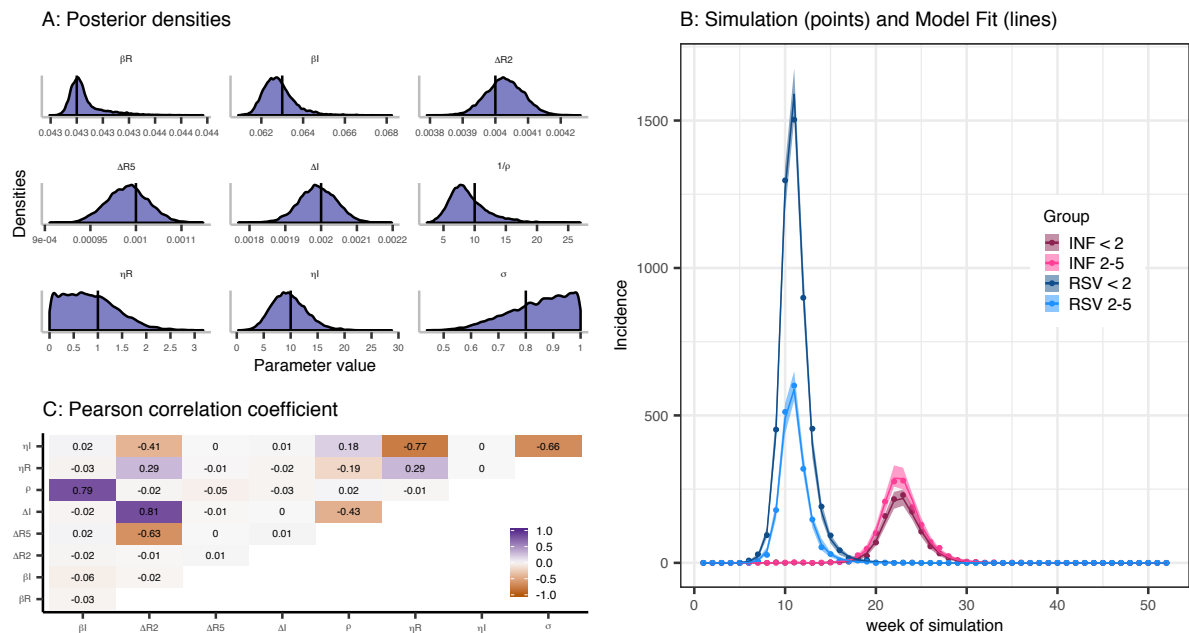
Pearson correlation coefficient between each parameter combination in the model.

$$\sigma = 0.1 \text{ and } 1/\rho = 0.1$$



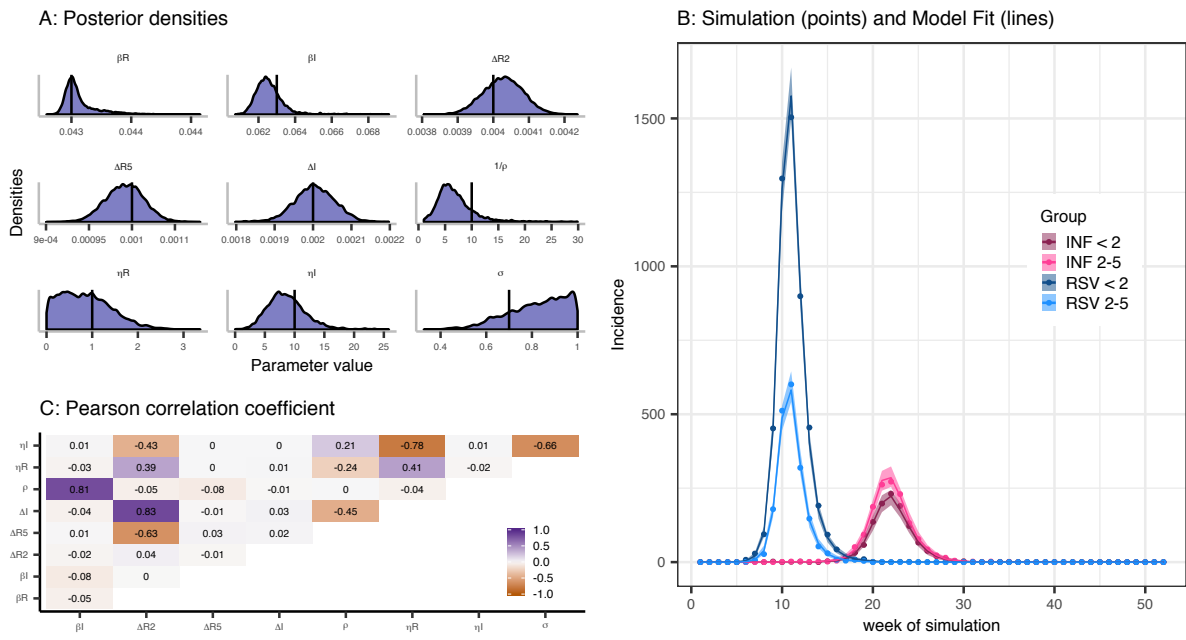
Appendix A Figure S30: Inference results for simulation with $\sigma = 0.1$ and $\rho = 0.1$. See the legend of Figure S28 for more details.

$$\sigma = 0.8 \text{ and } 1/\rho = 10$$



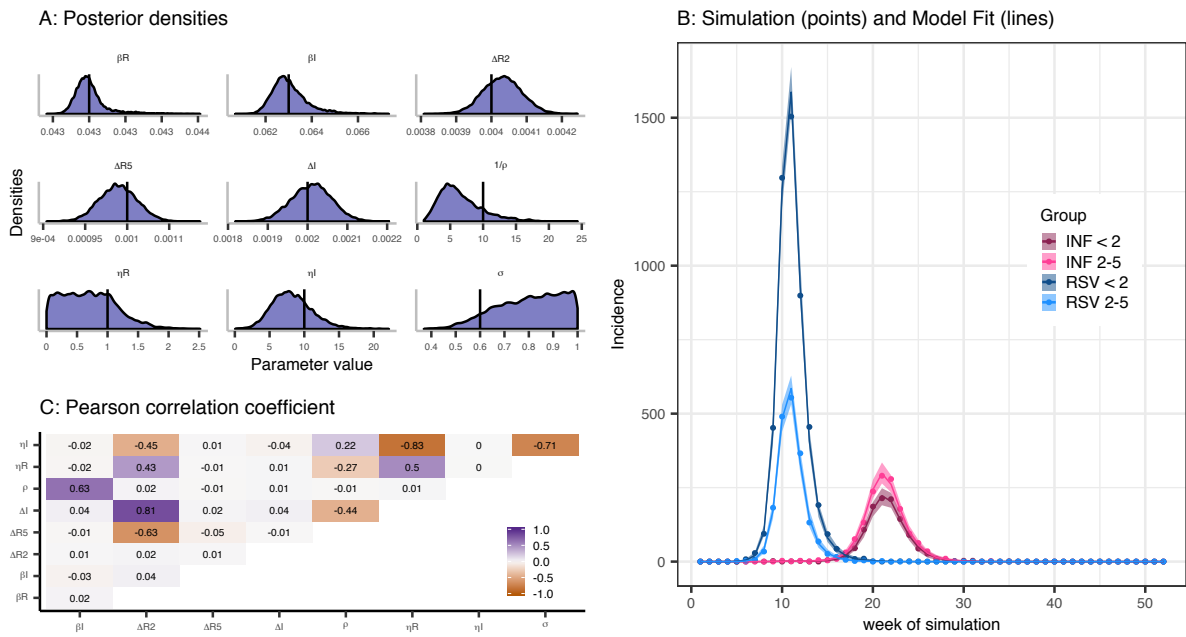
Appendix A Figure S31: Inference results for simulation with $\sigma = 0.8$ and $\rho = 0.1$. See the legend of Figure S28 for more details.

$\sigma = 0.7$ and $1/\rho = 10$



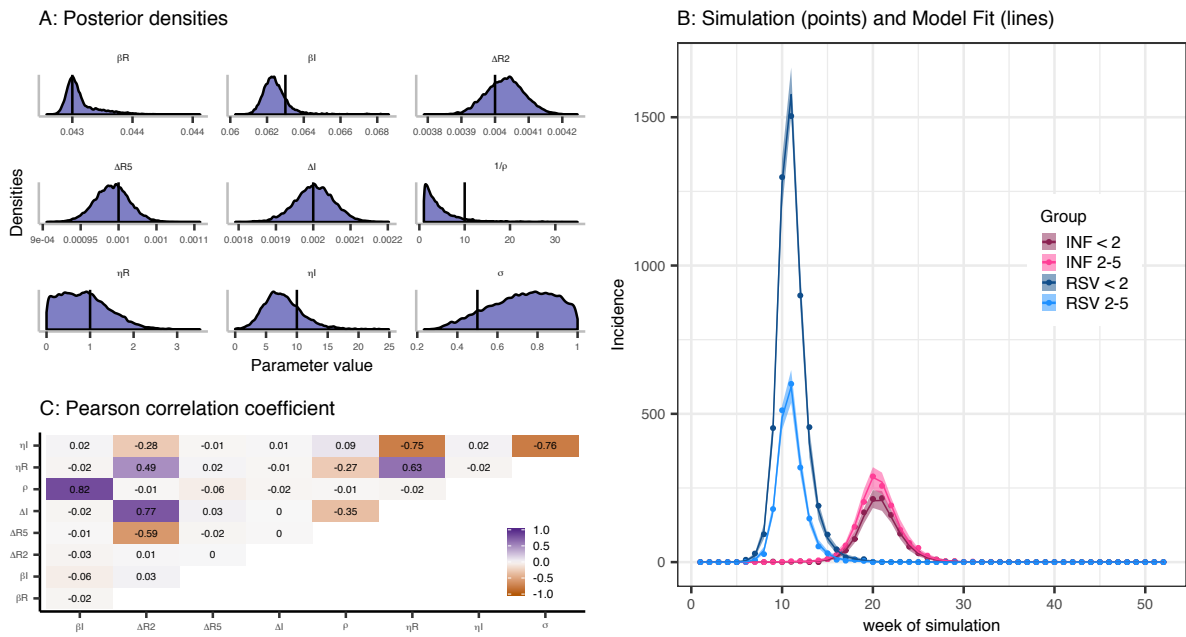
Appendix A Figure S32: Inference results for simulation with $\sigma = 0.7$ and $\rho = 0.1$. See the legend of Figure S28 for more details

$\sigma = 0.6$ and $1/\rho = 10$



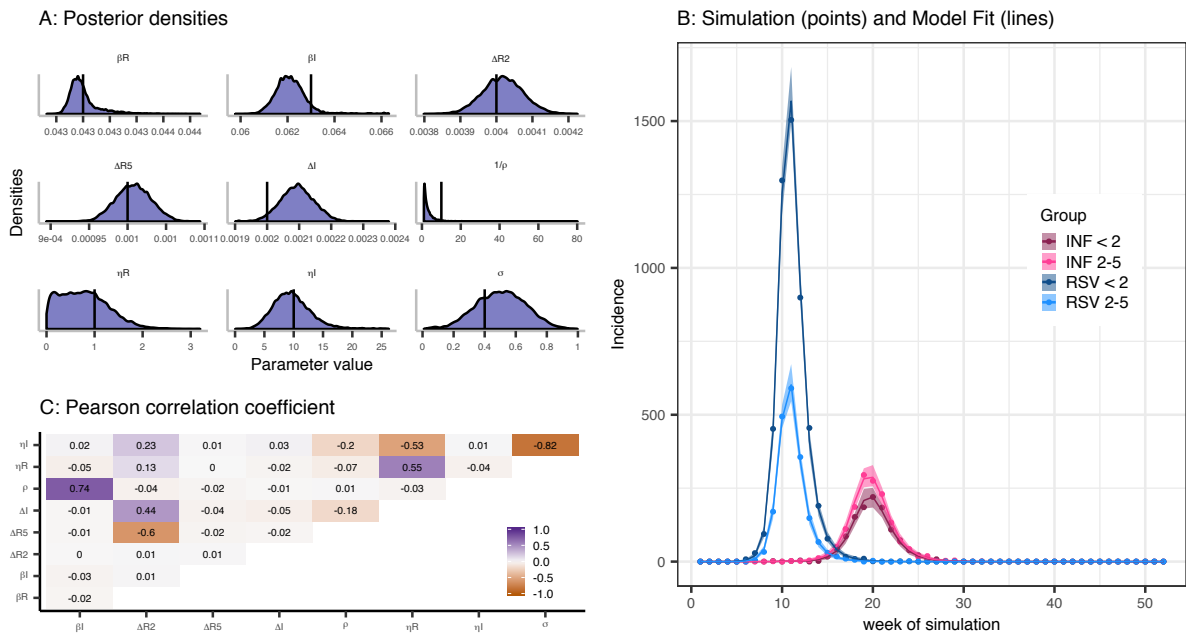
Appendix A Figure S33: Inference results for simulation with $\sigma = 0.6$ and $\rho = 0.1$. See the legend of Figure S28 for more details.

$\sigma = 0.5$ and $1/\rho = 10$



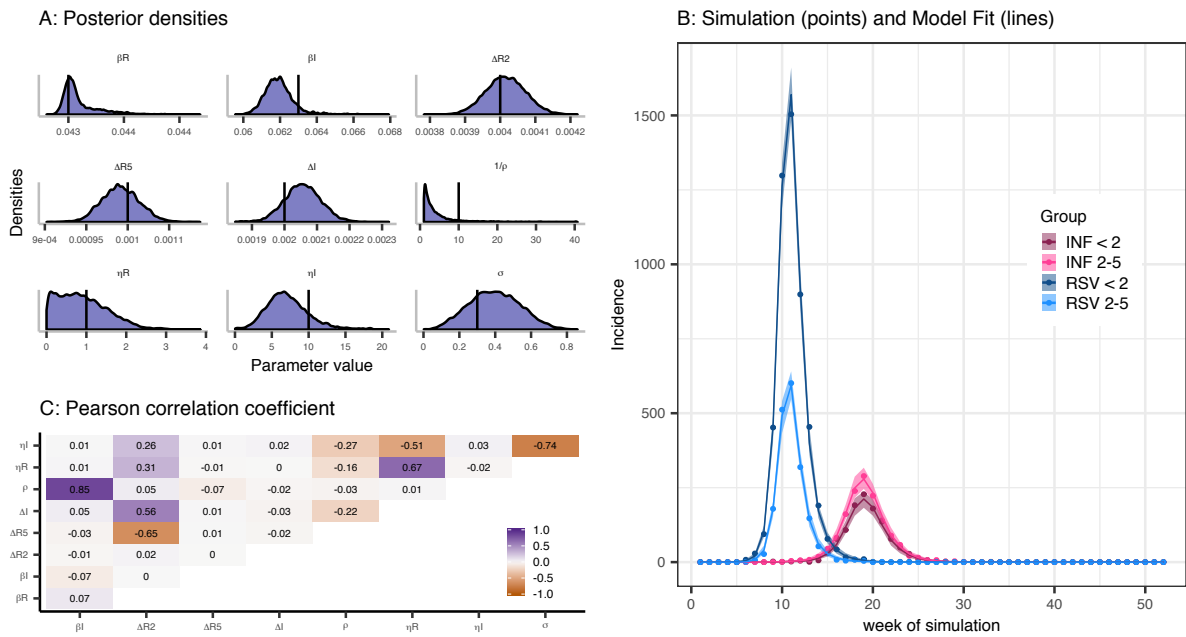
Appendix A Figure S34: Inference results for simulation with $\sigma = 0.5$ and $\rho = 0.1$. See the legend of Figure S28 for more details.

$\sigma = 0.4$ and $1/\rho = 10$



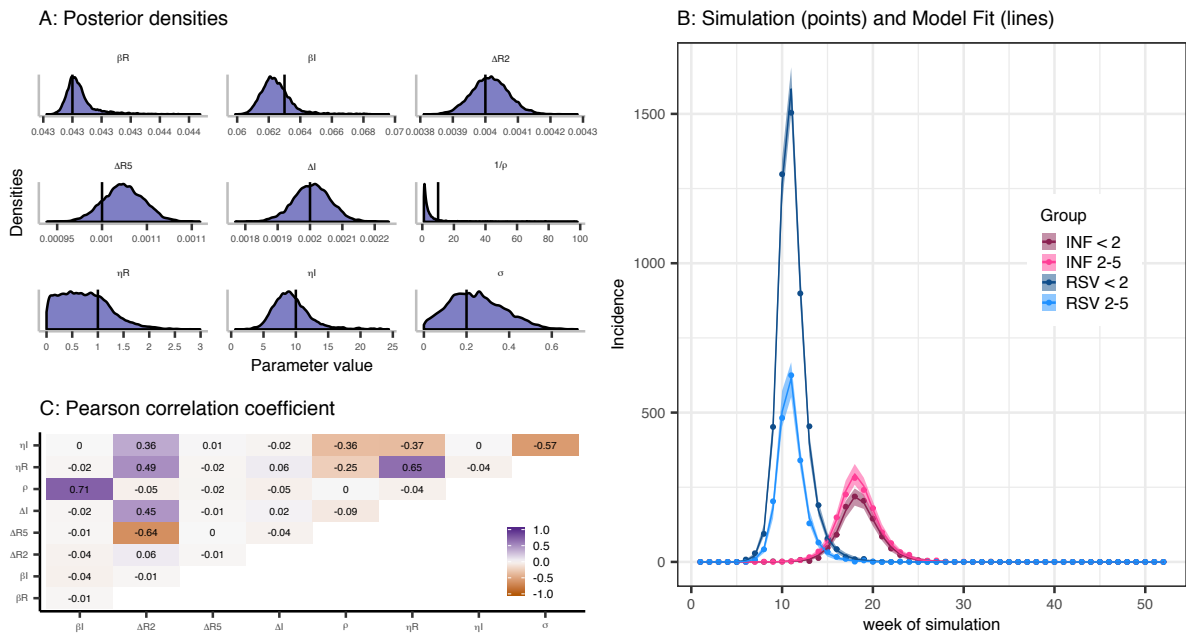
Appendix A Figure S35: Inference results for simulation with $\sigma = 0.4$ and $\rho = 0.1$. See the legend of Figure S28 for more details.

$\sigma = 0.3$ and $1/\rho = 10$

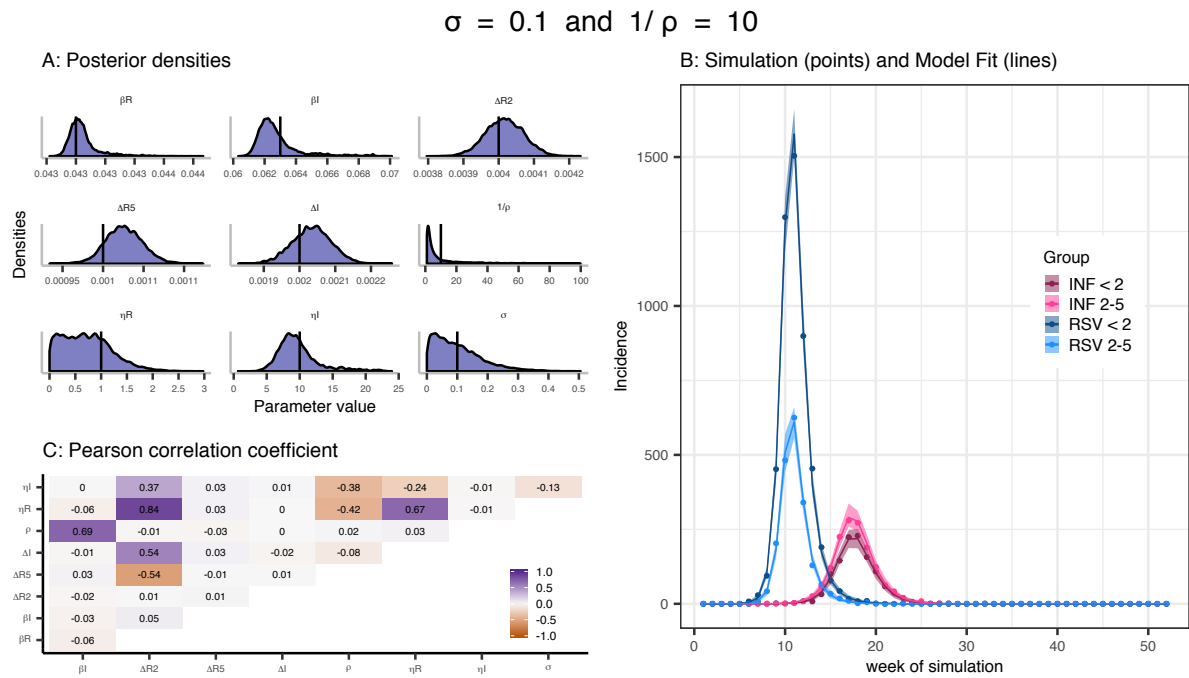


Appendix A Figure S36: Inference results for simulation with $\sigma = 0.3$ and $\rho = 0.1$. See the legend of Figure S28 for more details.

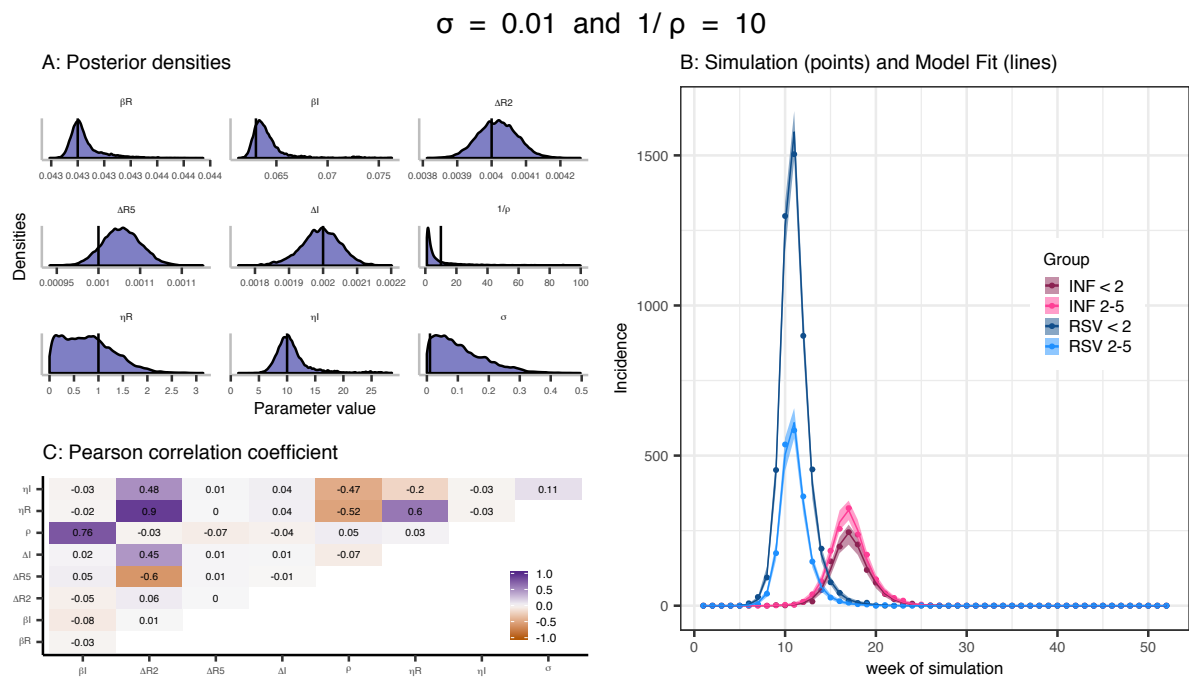
$\sigma = 0.2$ and $1/\rho = 10$



Appendix A Figure S37: Inference results for simulation with $\sigma = 0.2$ and $\rho = 0.1$. See the legend of Figure S28 for more details.

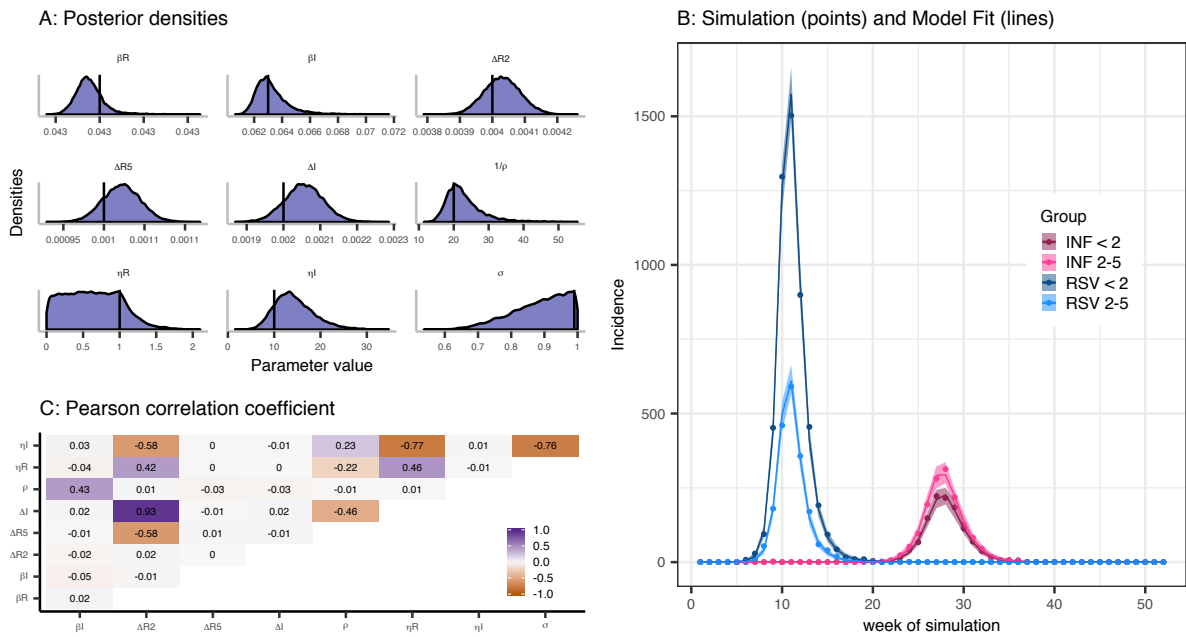


Appendix A Figure S38: Inference results for simulation with $\sigma = 0.1$ and $\rho = 0.1$. See the legend of Figure S28 for more details.



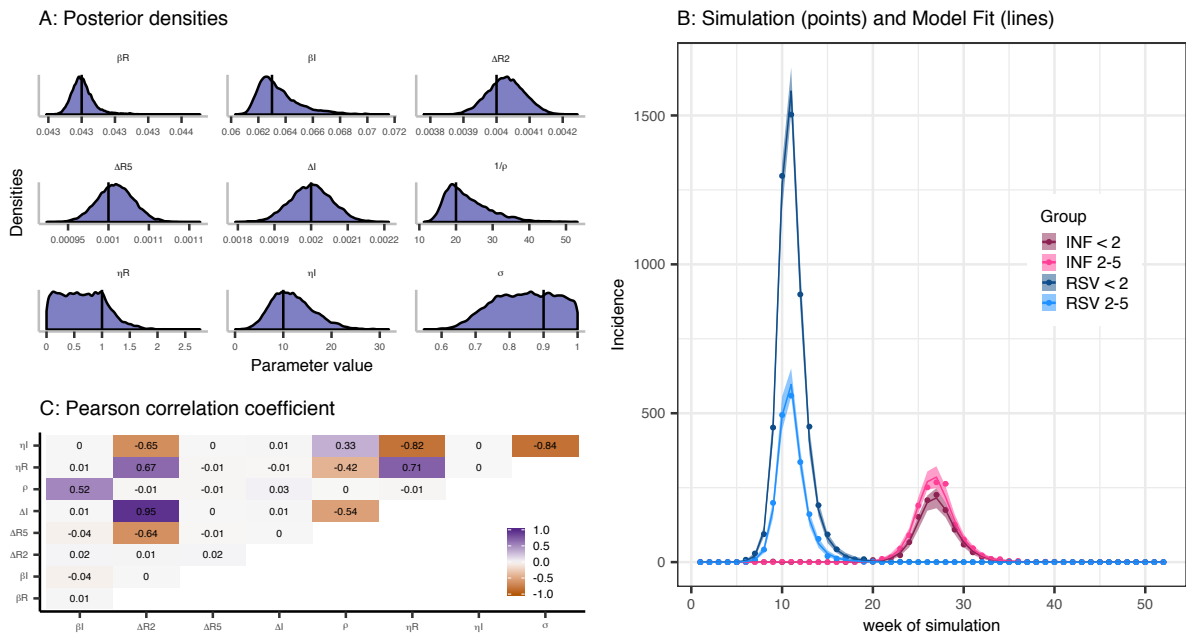
Appendix A Figure S39: Inference results for simulation with $\sigma = 0.01$ and $\rho = 0.1$. See the legend of Figure S28 for more details.

$\sigma = 0.99$ and $1/\rho = 20$



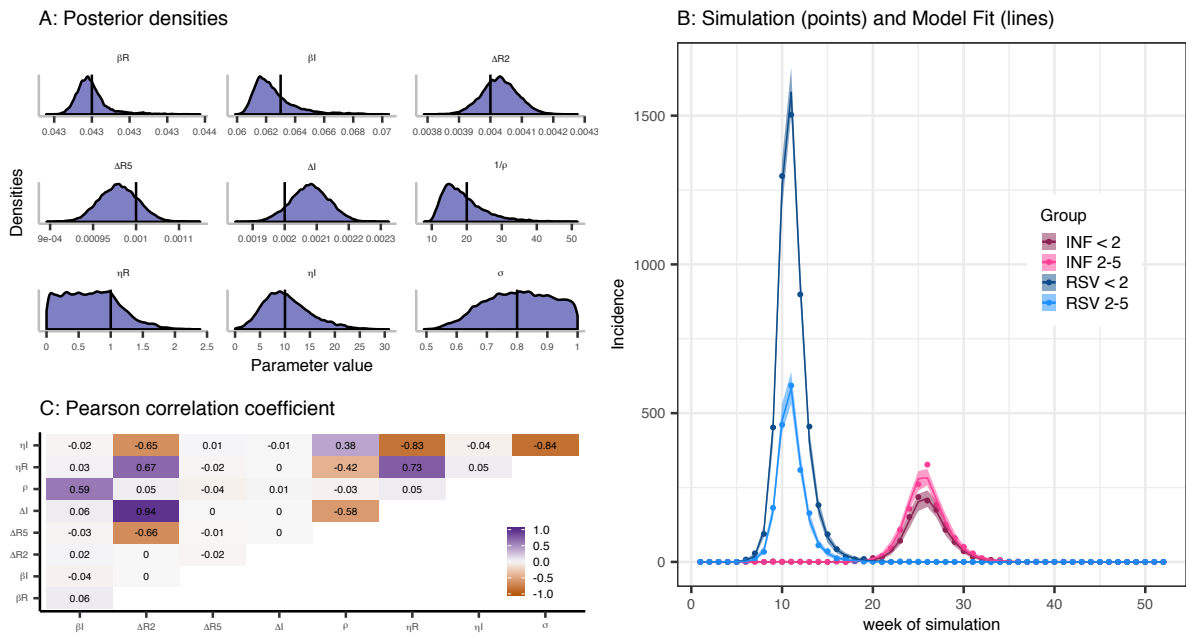
Appendix A Figure S40: Inference results for simulation with $\sigma = 0.99$ and $\rho = 0.05$. See the legend of Figure S28 for more details.

$\sigma = 0.9$ and $1/\rho = 20$



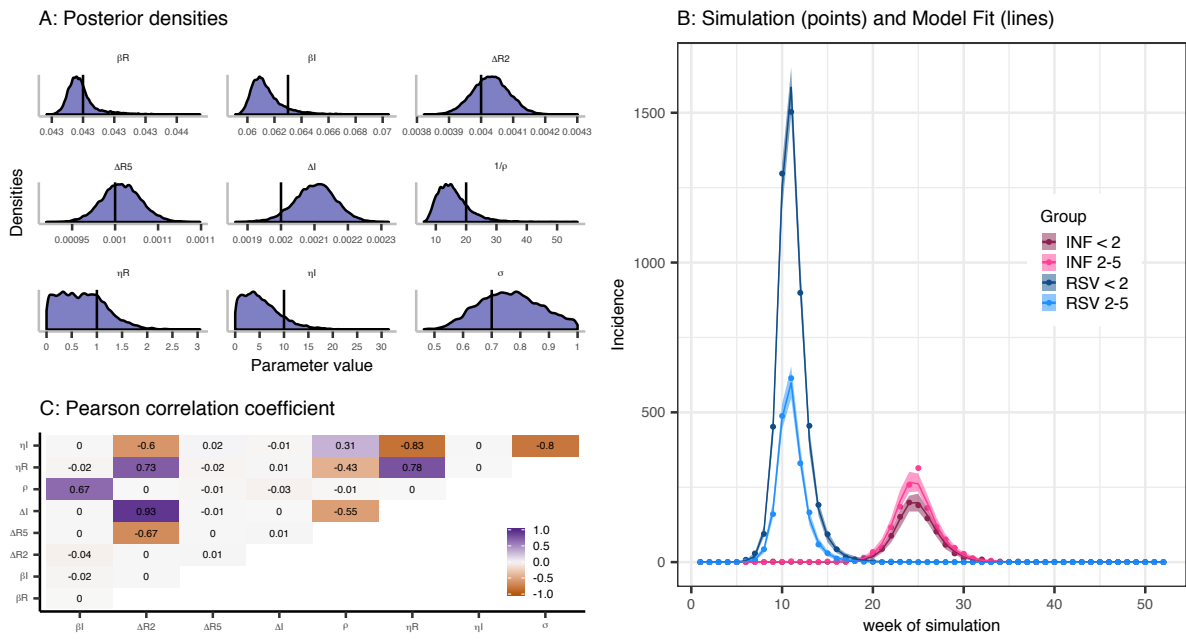
Appendix A Figure S41: Inference results for simulation with $\sigma = 0.9$ and $\rho = 0.05$. See the legend of Figure S28 for more details

$\sigma = 0.8$ and $1/\rho = 20$



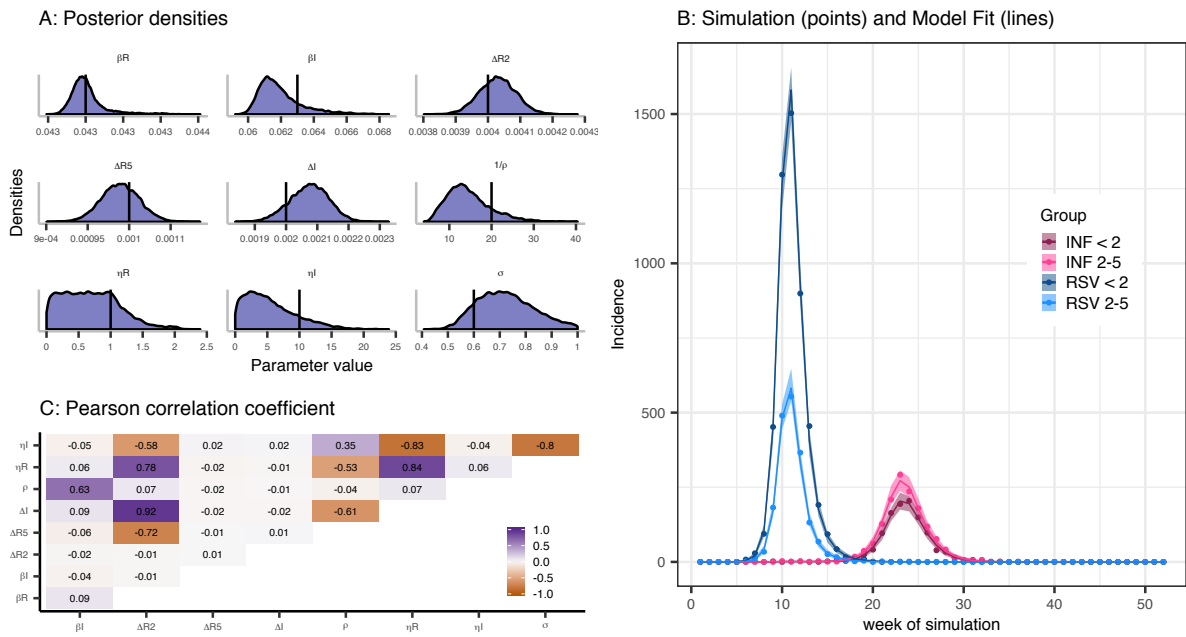
Appendix A Figure S42: Inference results for simulation with $\sigma = 0.8$ and $\rho = 0.05$. See the legend of Figure S28 for more details

$\sigma = 0.7$ and $1/\rho = 20$



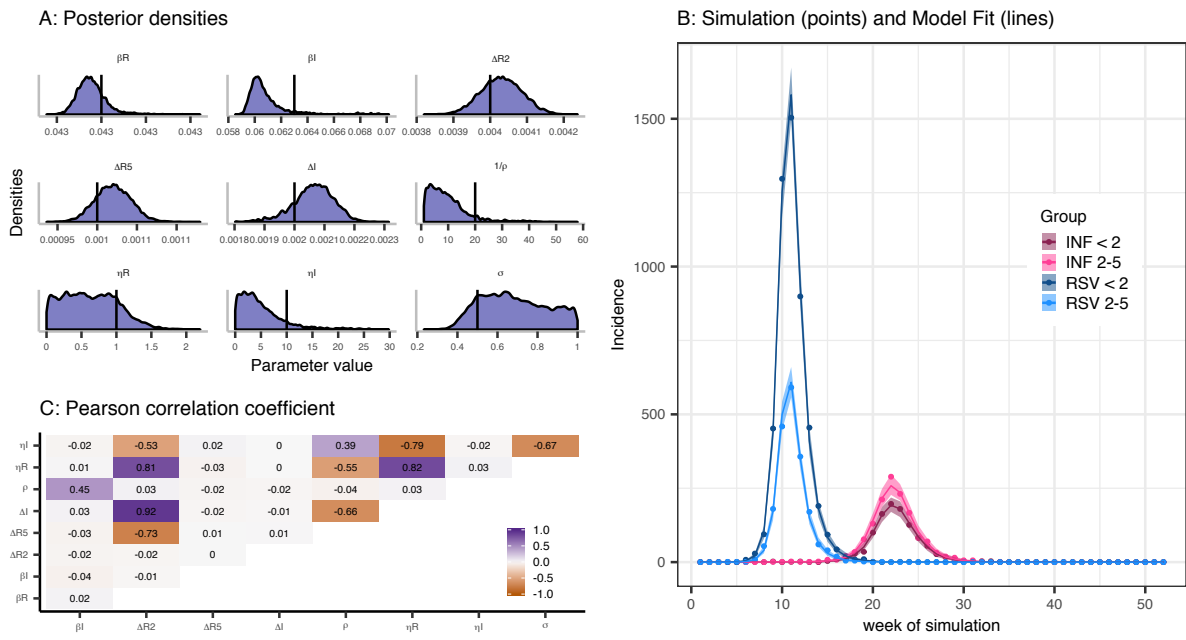
Appendix A Figure S43: Inference results for simulation with $\sigma = 0.7$ and $\rho = 0.05$. See the legend of Figure S28 for more details.

$\sigma = 0.6$ and $1/\rho = 20$



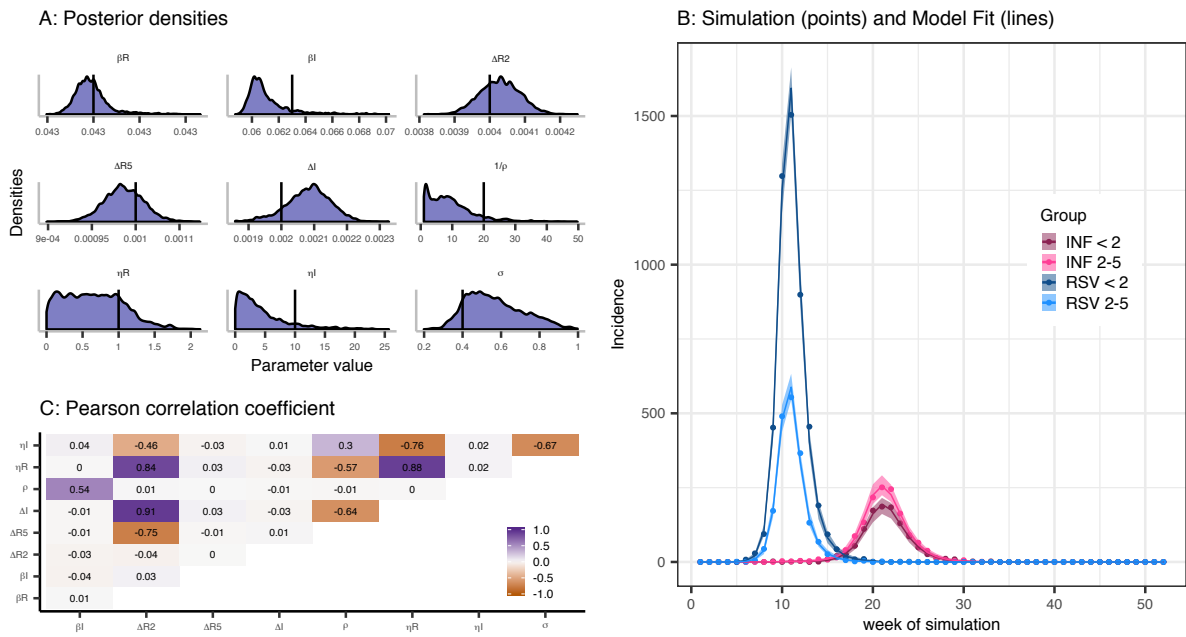
Appendix A Figure S44: Inference results for simulation with $\sigma = 0.6$ and $\rho = 0.05$. See the legend of Figure S28 for more details.

$\sigma = 0.5$ and $1/\rho = 20$



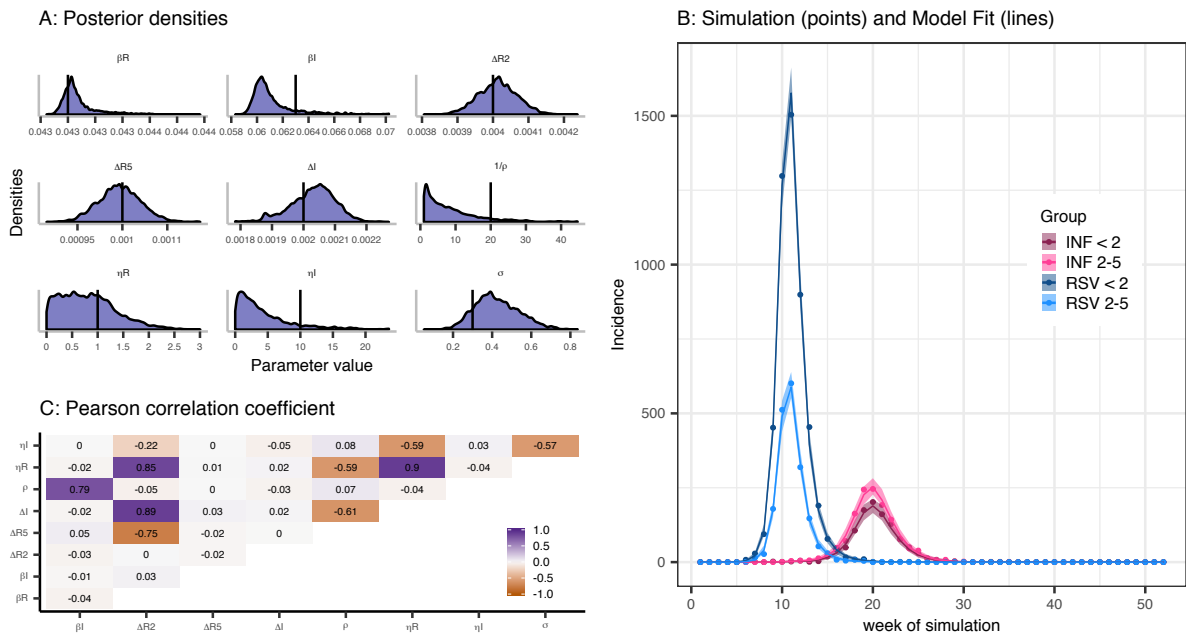
Appendix A Figure S45: Inference results for simulation with $\sigma = 0.5$ and $\rho = 0.05$. See the legend of Figure S28 for more details.

$\sigma = 0.4$ and $1/\rho = 20$



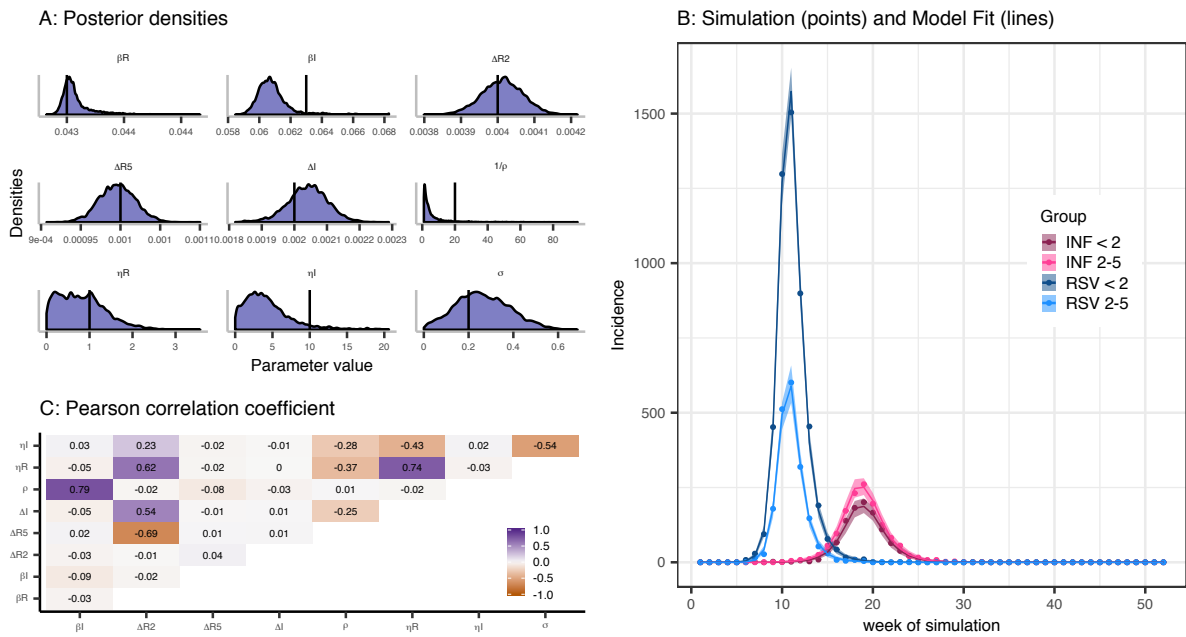
Appendix A Figure S46: Inference results for simulation with $\sigma = 0.4$ and $\rho = 0.05$. See the legend of Figure S28 for more details.

$\sigma = 0.3$ and $1/\rho = 20$



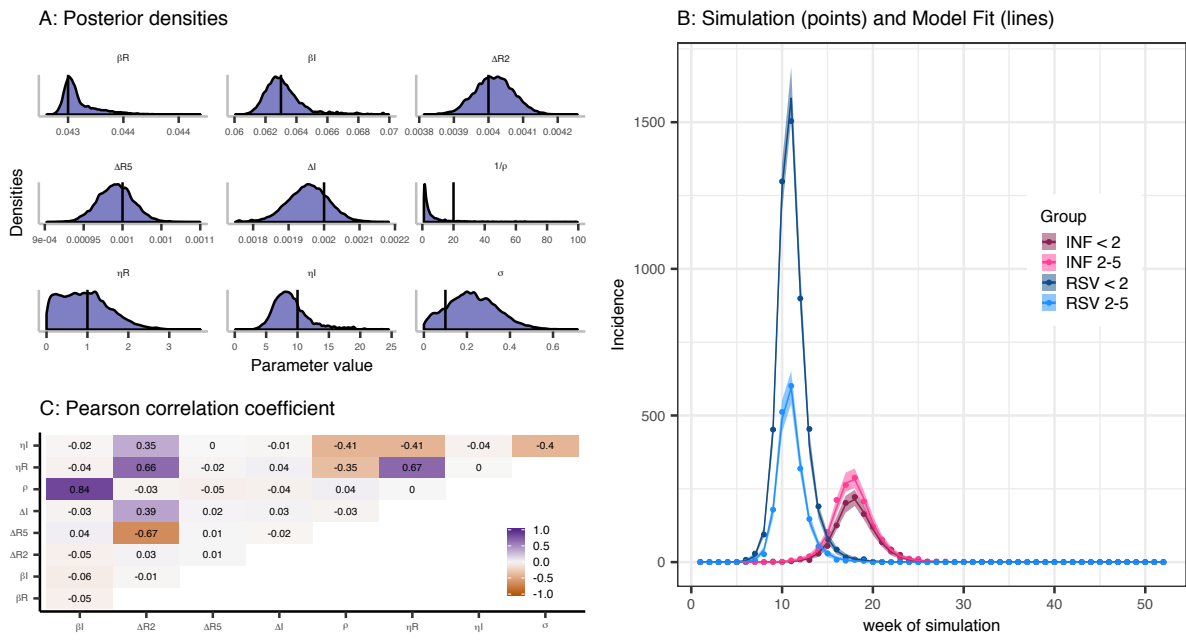
Appendix A Figure S47: Inference results for simulation with $\sigma = 0.3$ and $\rho = 0.05$. See the legend of Figure S28 for more details.

$\sigma = 0.2$ and $1/\rho = 20$



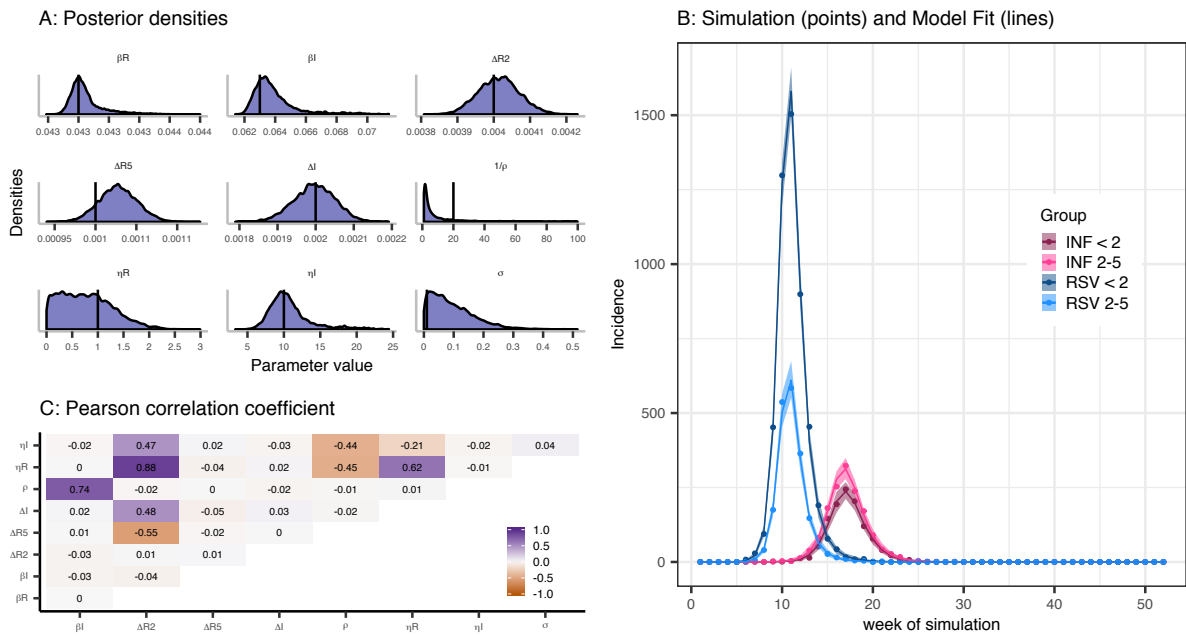
Appendix A Figure S48: Inference results for simulation with $\sigma = 0.2$ and $\rho = 0.05$. See the legend of Figure S28 for more details.

$\sigma = 0.1$ and $1/\rho = 20$



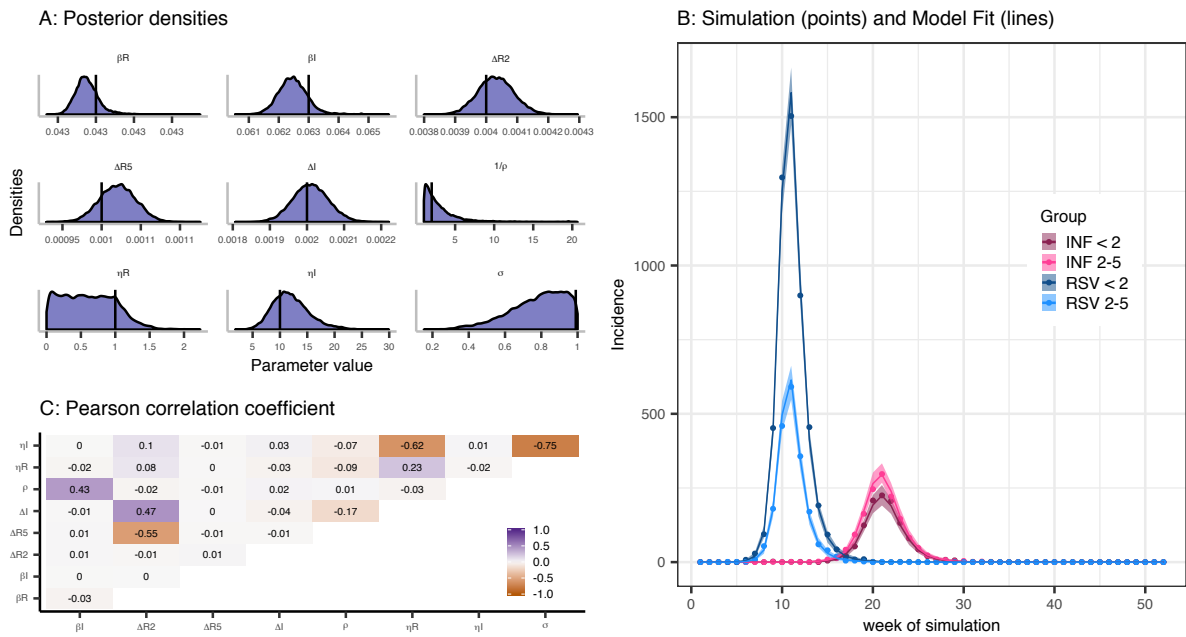
Appendix A Figure S49: Inference results for simulation with $\sigma = 0.1$ and $\rho = 0.05$. See the legend of Figure S28 for more details.

$\sigma = 0.01$ and $1/\rho = 20$



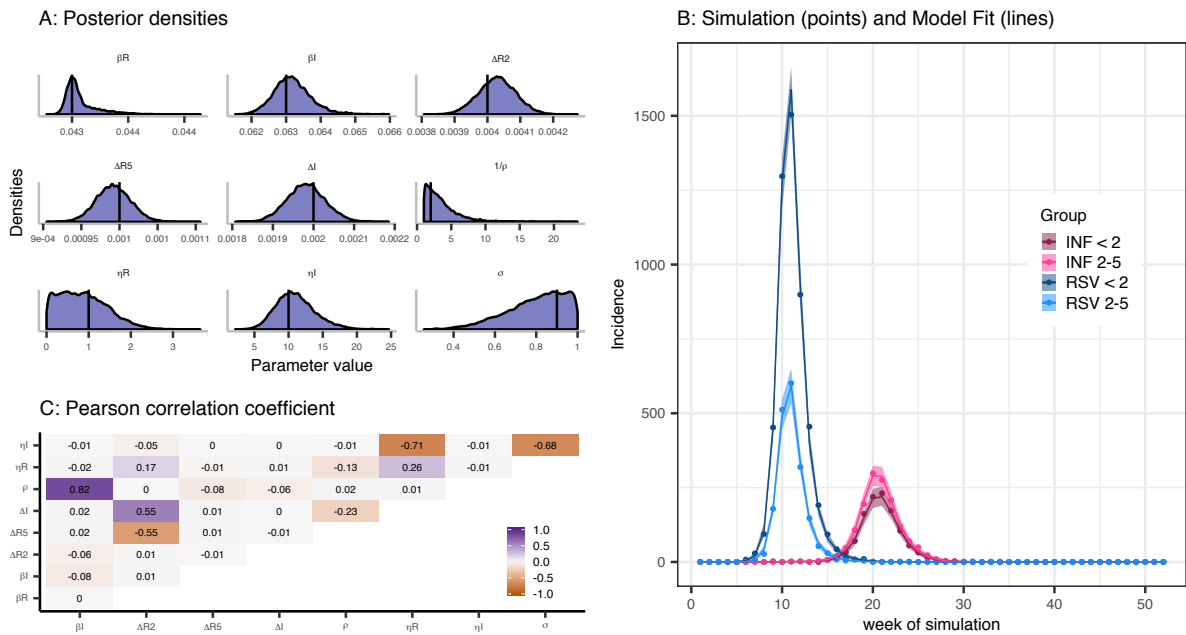
Appendix A Figure S50: Inference results for simulation with $\sigma = 0.01$ and $\rho = 0.05$. See the legend of Figure S28 for more details.

$\sigma = 0.99$ and $1/\rho = 2$



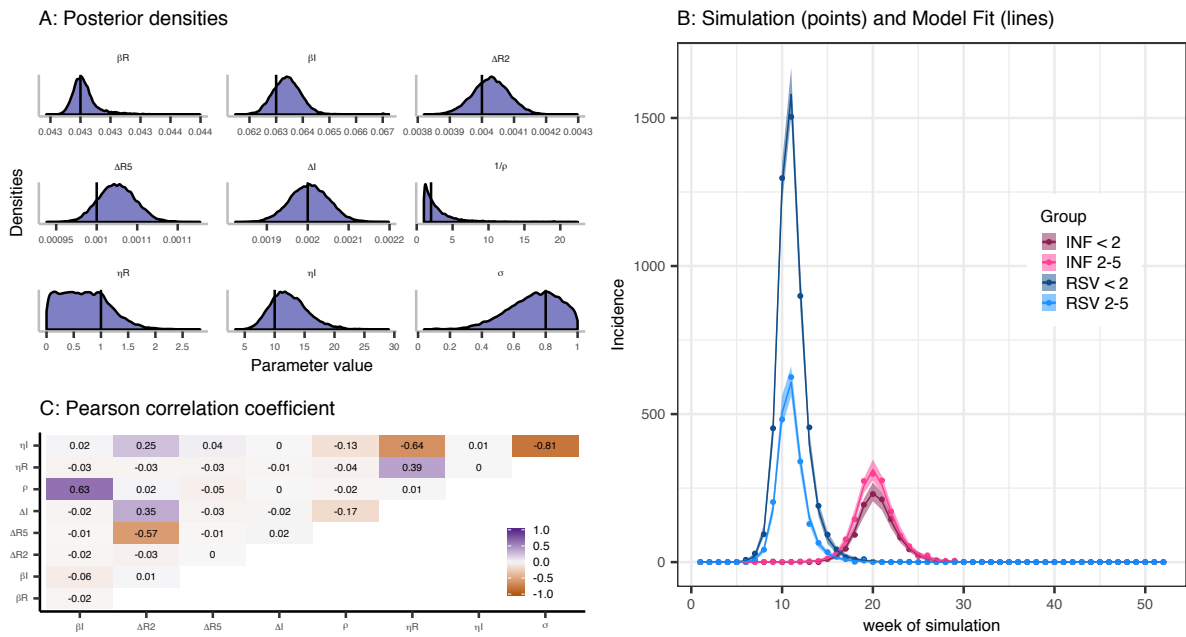
Appendix A Figure S51: Inference results for simulation with $\sigma = 0.99$ and $\rho = 0.5$. See the legend of Figure S28 for more details.

$\sigma = 0.9$ and $1/\rho = 2$



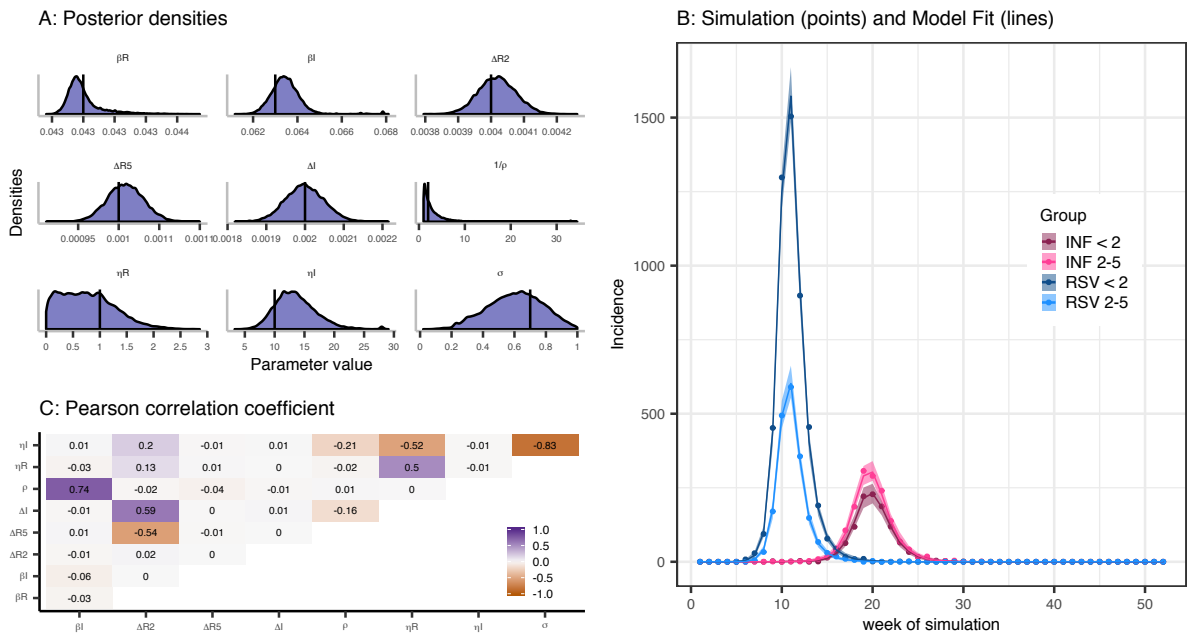
Appendix A Figure S52: Inference results for simulation with $\sigma = 0.9$ and $\rho = 0.5$. See the legend of Figure S28 for more details.

$\sigma = 0.8$ and $1/\rho = 2$



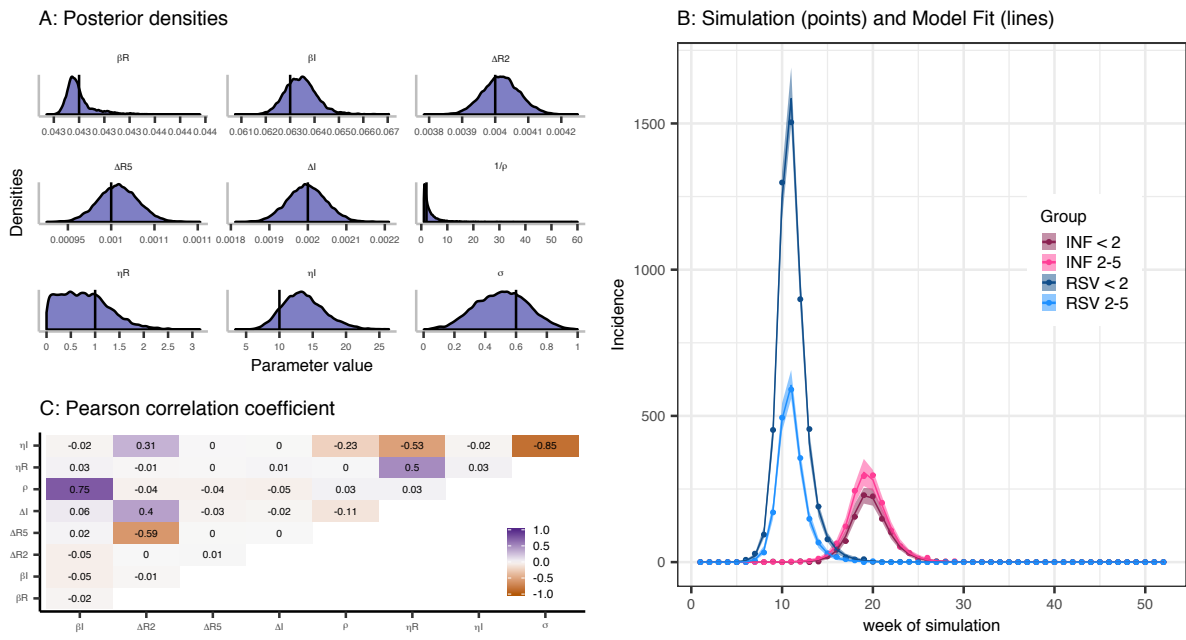
Appendix A Figure S53: Inference results for simulation with $\sigma = 0.8$ and $\rho = 0.5$. See the legend of Figure S28 for more details.

$\sigma = 0.7$ and $1/\rho = 2$



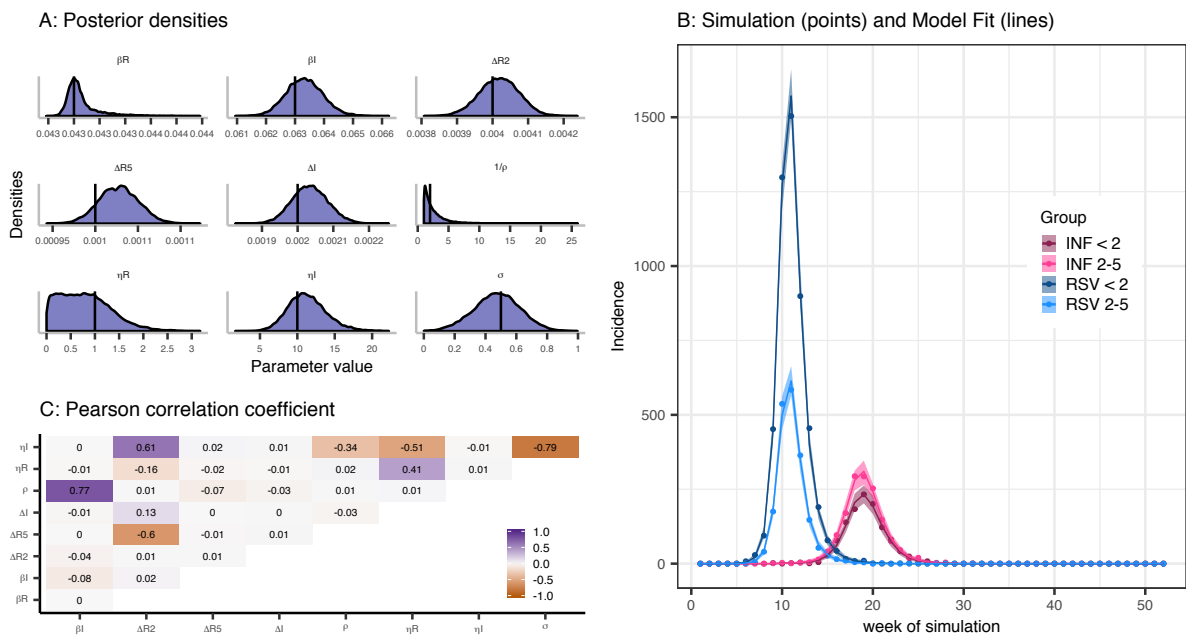
Appendix A Figure S54: Inference results for simulation with $\sigma = 0.7$ and $\rho = 0.5$. See the legend of Figure S28 for more details.

$\sigma = 0.6$ and $1/\rho = 2$



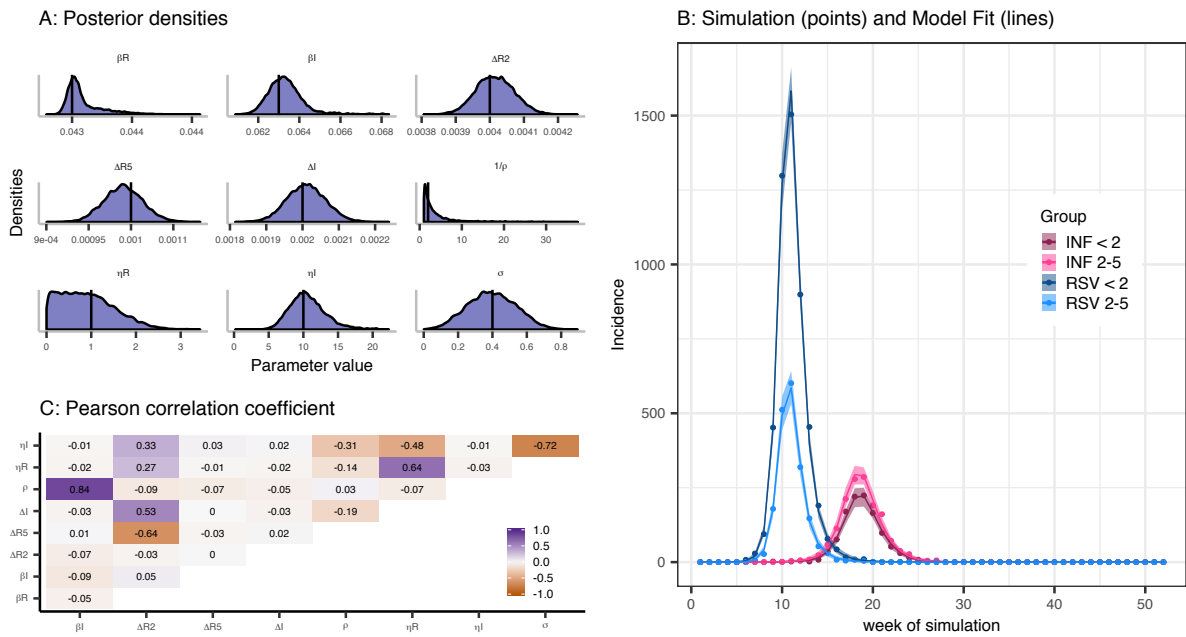
Appendix A Figure S55: Inference results for simulation with $\sigma = 0.6$ and $\rho = 0.5$. See the legend of Figure S28 for more details.

$\sigma = 0.5$ and $1/\rho = 2$



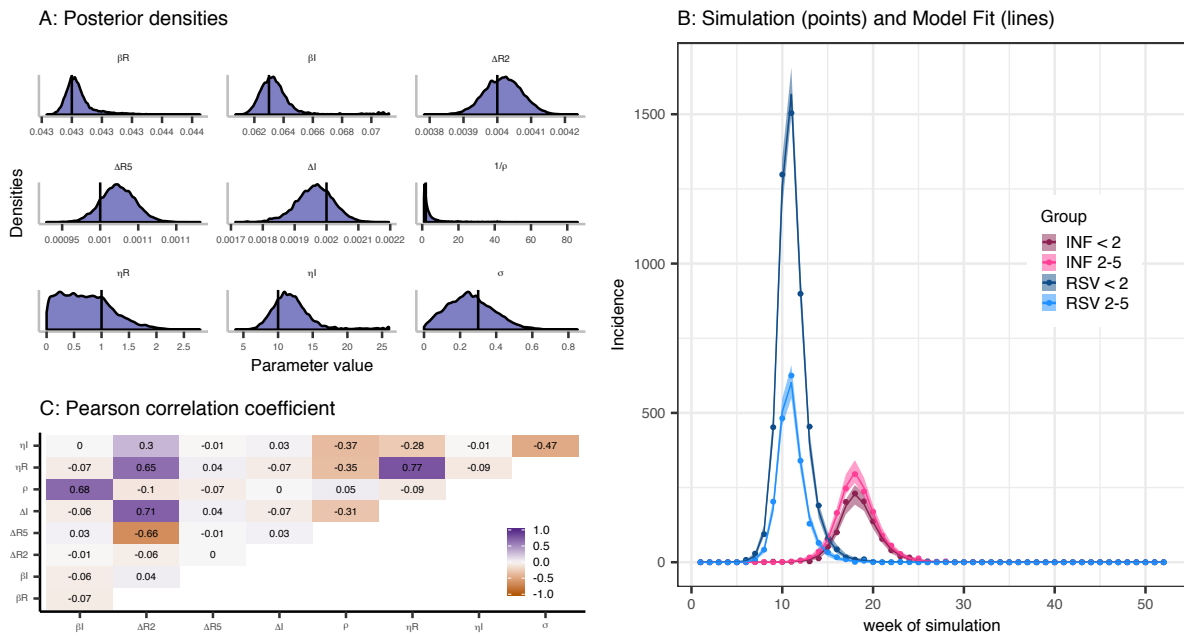
Appendix A Figure S56: Inference results for simulation with $\sigma = 0.5$ and $\rho = 0.5$. See the legend of Figure S28 for more details.

$\sigma = 0.4$ and $1/\rho = 2$



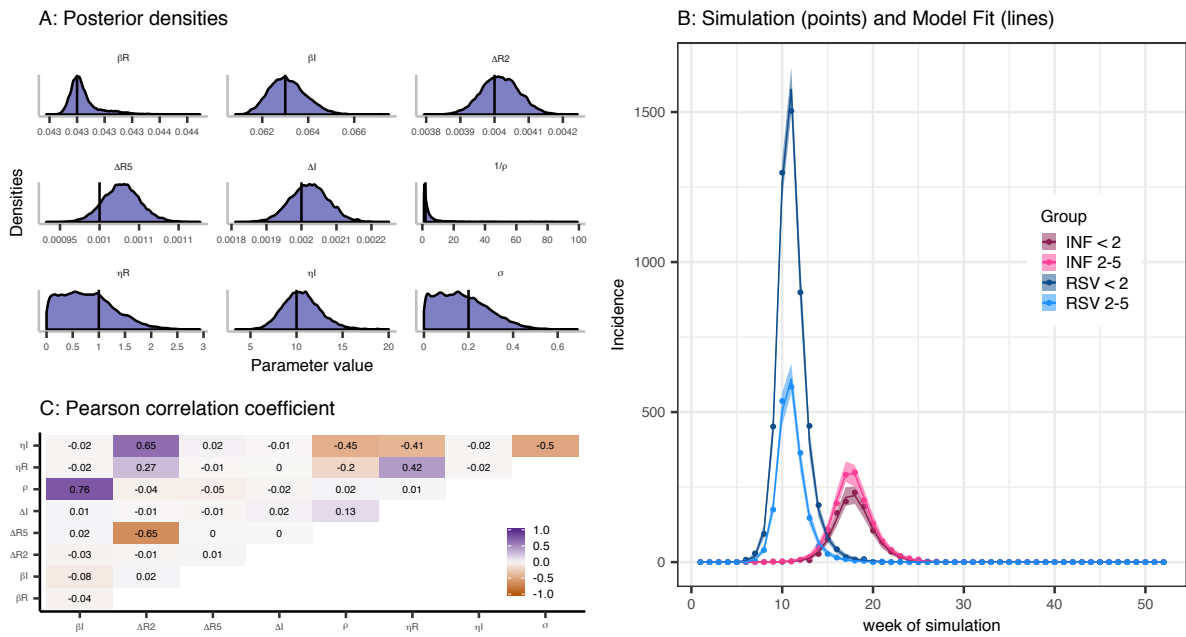
Appendix A Figure S57: Inference results for simulation with $\sigma = 0.4$ and $\rho = 0.5$. See the legend of Figure S28 for more details.

$\sigma = 0.3$ and $1/\rho = 2$



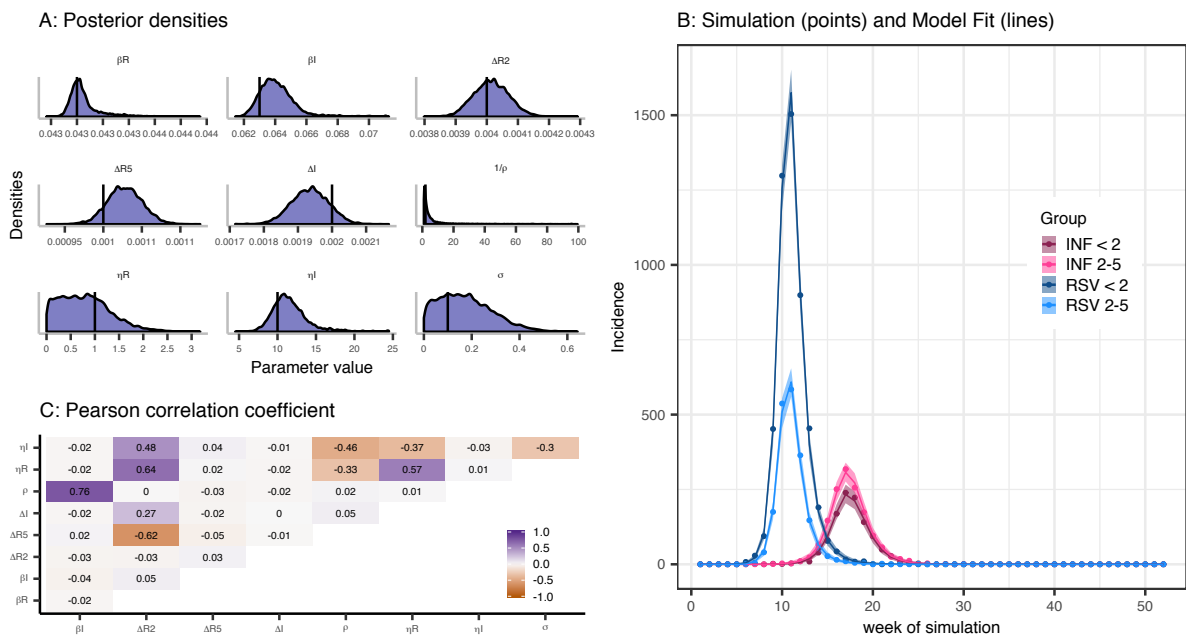
Appendix A Figure S58: Inference results for simulation with $\sigma = 0.3$ and $\rho = 0.5$. See the legend of Figure S28 for more details.

$\sigma = 0.2$ and $1/\rho = 2$



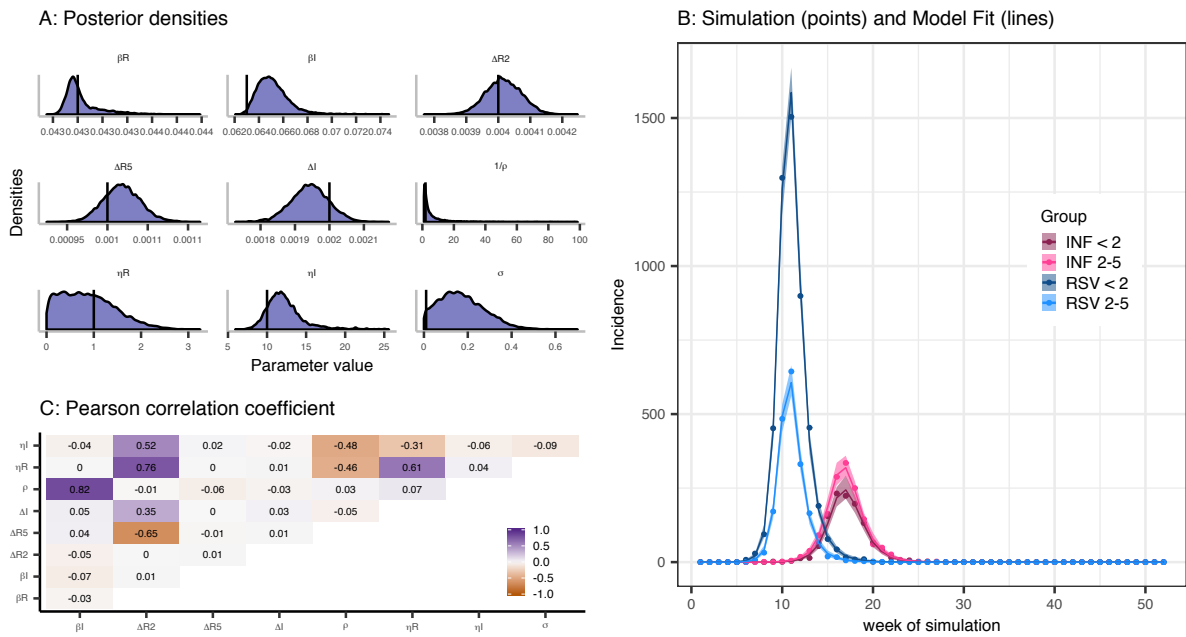
Appendix A Figure S59: Inference results for simulation with $\sigma = 0.2$ and $\rho = 0.5$. See the legend of Figure S28 for more details.

$\sigma = 0.1$ and $1/\rho = 2$



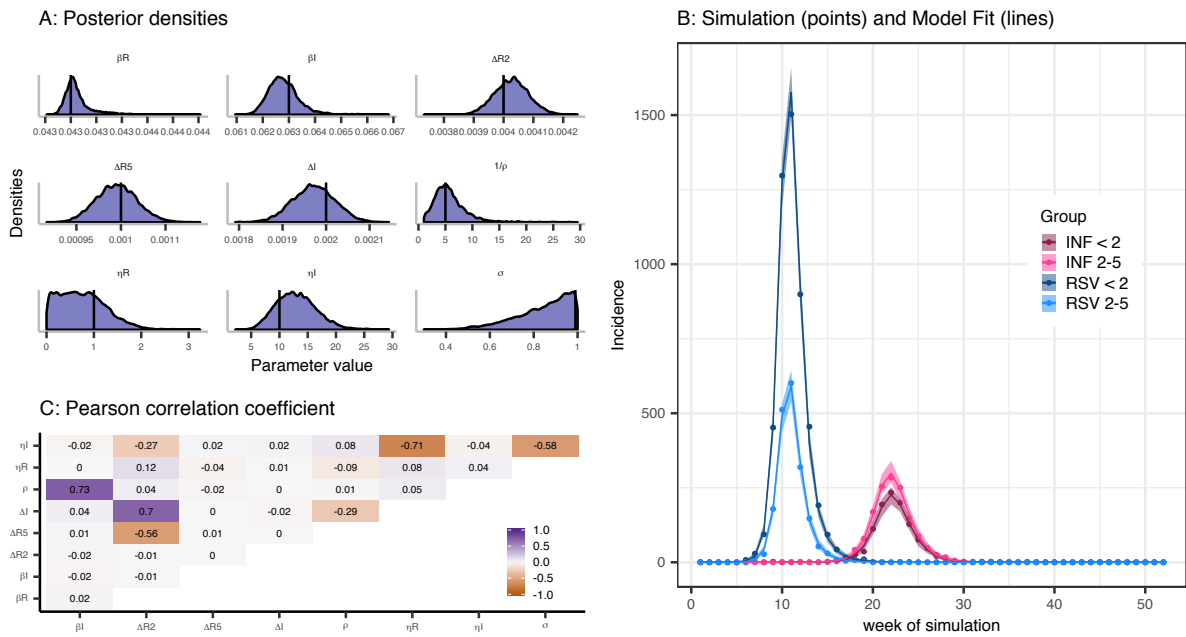
Appendix A Figure S60: Inference results for simulation with $\sigma = 0.1$ and $\rho = 0.5$. See the legend of Figure S28 for more details.

$\sigma = 0.01$ and $1/\rho = 2$



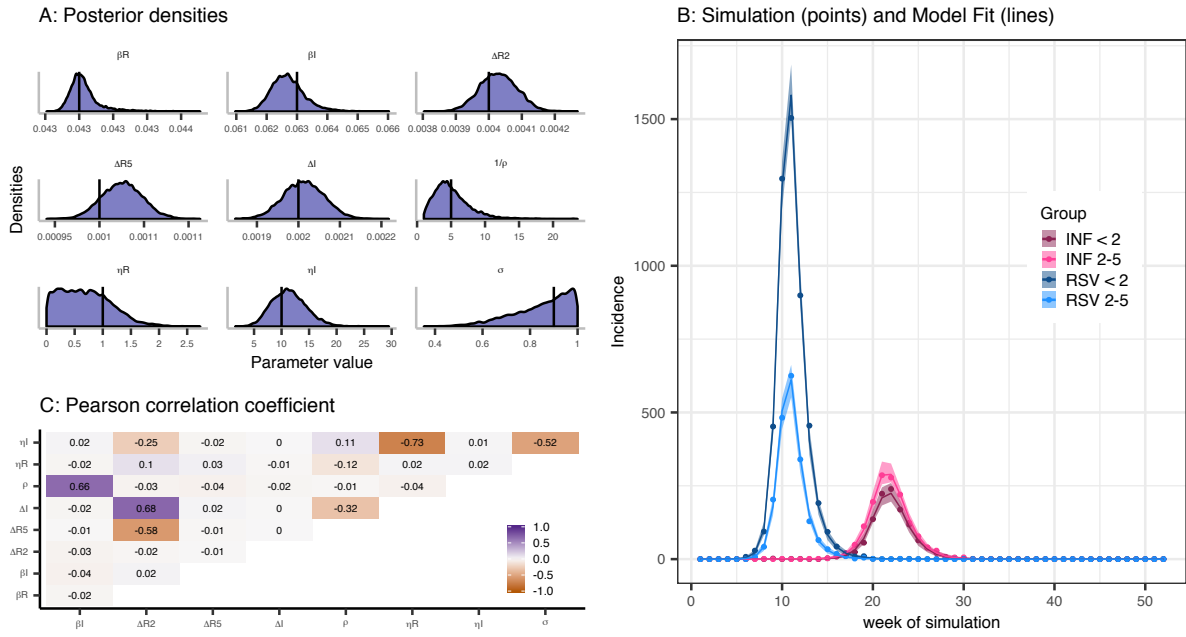
Appendix A Figure S61: Inference results for simulation with $\sigma = 0.01$ and $\rho = 0.5$. See the legend of Figure S28 for more details

$\sigma = 0.99$ and $1/\rho = 5$



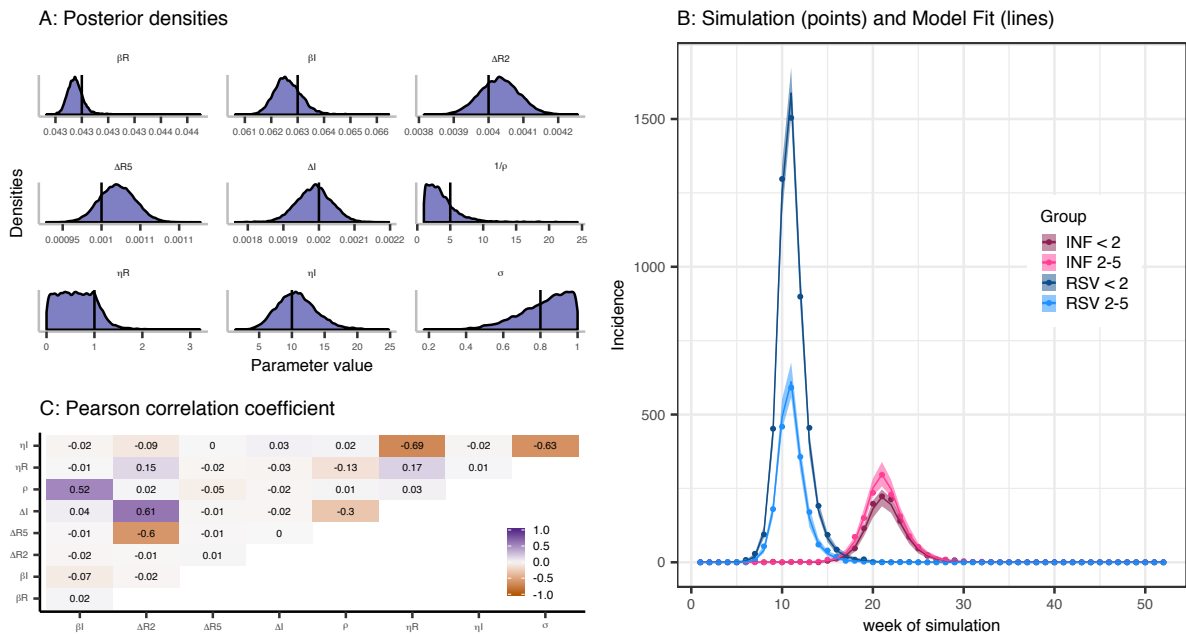
Appendix A Figure S62: Inference results for simulation with $\sigma = 0.99$ and $\rho = 0.2$. See the legend of Figure S28 for more details.

$\sigma = 0.9$ and $1/\rho = 5$



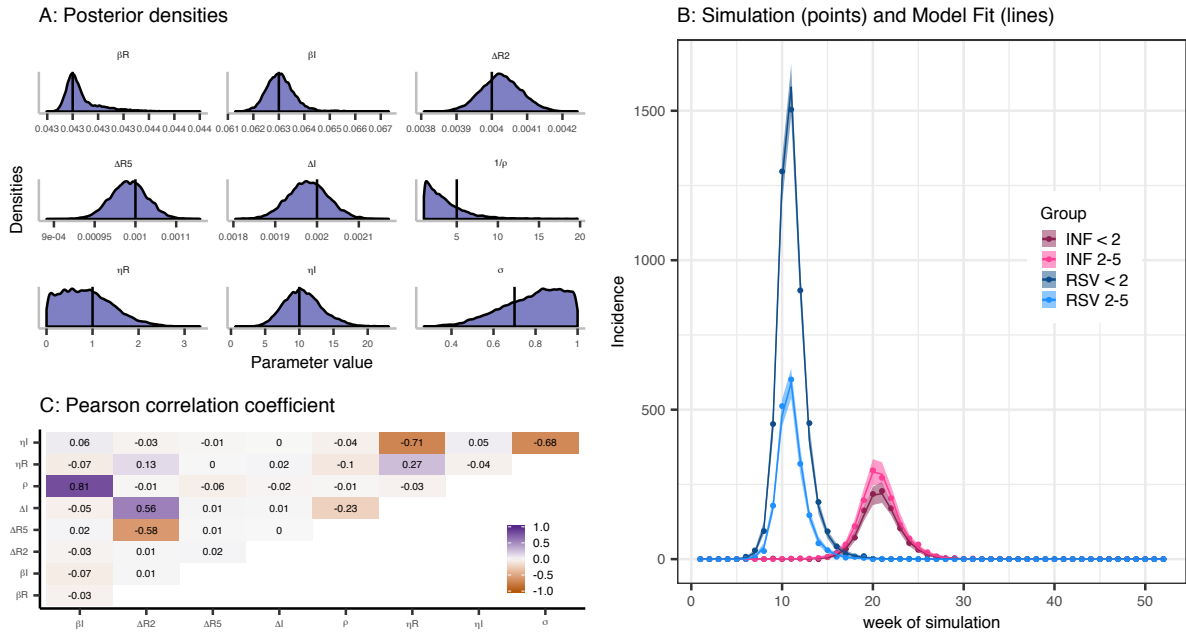
Appendix A Figure S63: Inference results for simulation with $\sigma = 0.9$ and $\rho = 0.2$. See the legend of Figure S28 for more details.

$\sigma = 0.8$ and $1/\rho = 5$



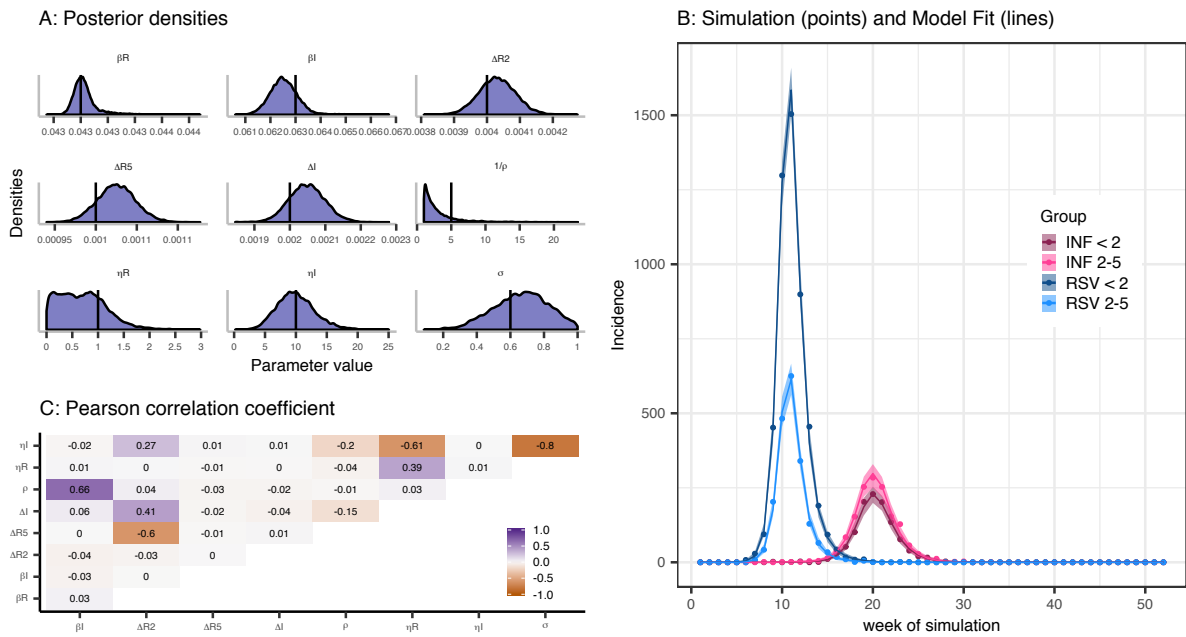
Appendix A Figure S64: Inference results for simulation with $\sigma = 0.8$ and $\rho = 0.2$. See the legend of Figure S28 for more details.

$\sigma = 0.7$ and $1/\rho = 5$



Appendix A Figure S65: Inference results for simulation with $\sigma = 0.7$ and $\rho = 0.2$. See the legend of Figure S28 for more details.

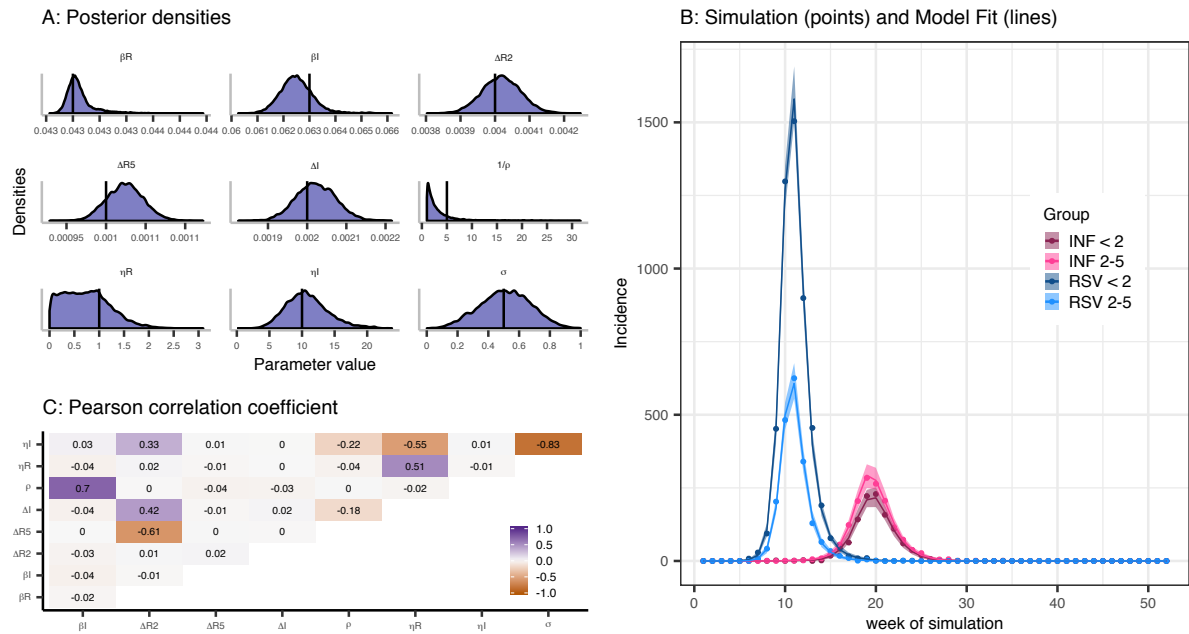
$\sigma = 0.6$ and $1/\rho = 5$



Appendix A Figure S66: Inference results for simulation with $\sigma = 0.6$ and $\rho = 0.2$. See the legend of Figure S28 for more details.

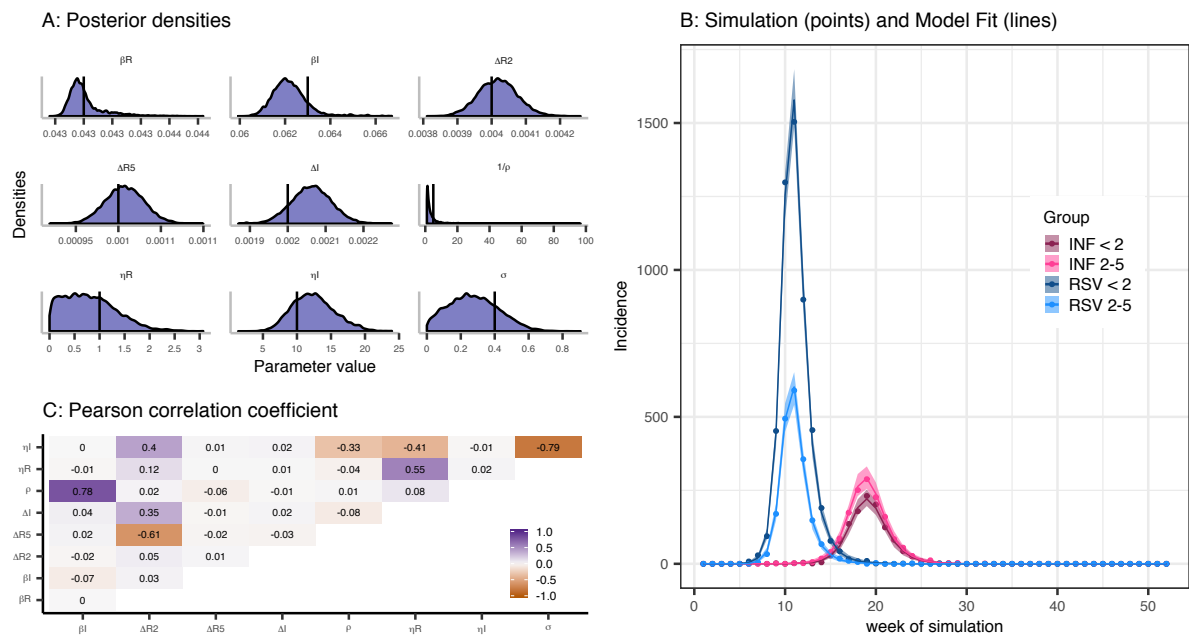
more details.

$\sigma = 0.5$ and $1/\rho = 5$



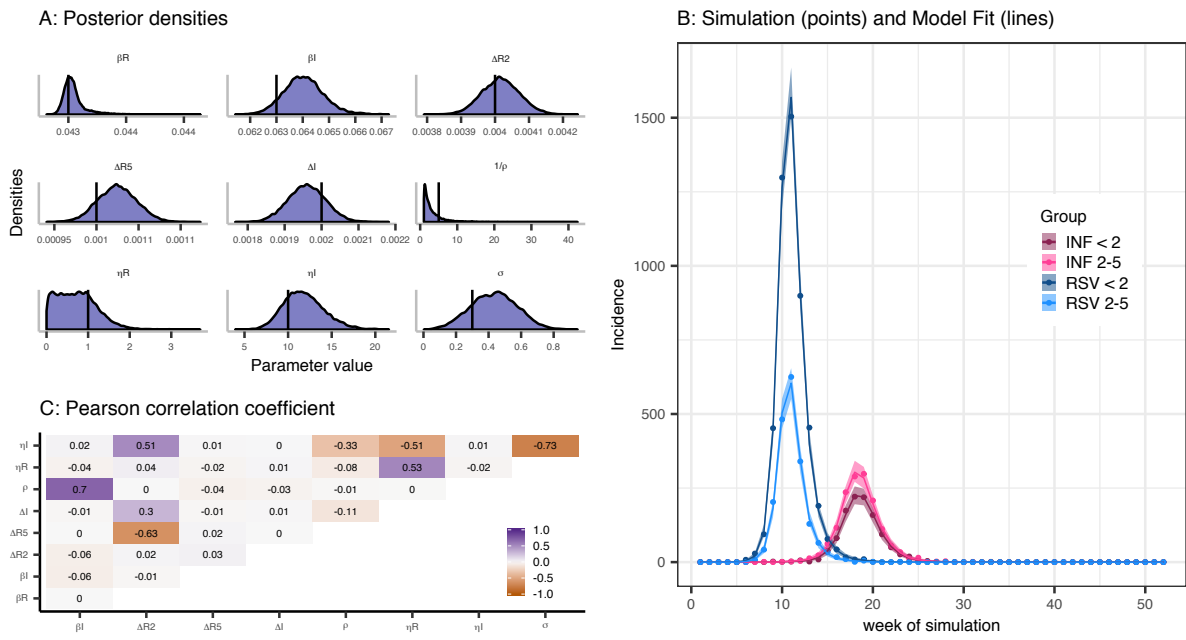
Appendix A Figure S67: Inference results for simulation with $\sigma = 0.5$ and $\rho = 0.2$. See the legend of Figure S28 for more details.

$\sigma = 0.4$ and $1/\rho = 5$



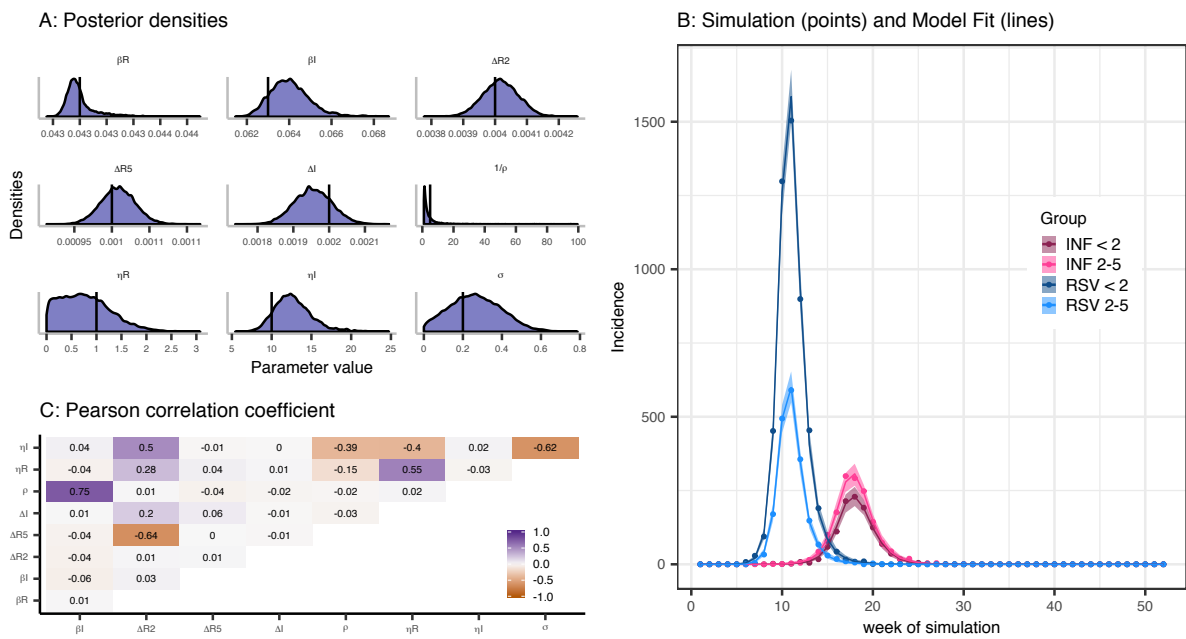
Appendix A Figure S68: Inference results for simulation with $\sigma = 0.4$ and $\rho = 0.2$. See the legend of Figure S28 for more details.

$\sigma = 0.3$ and $1/\rho = 5$



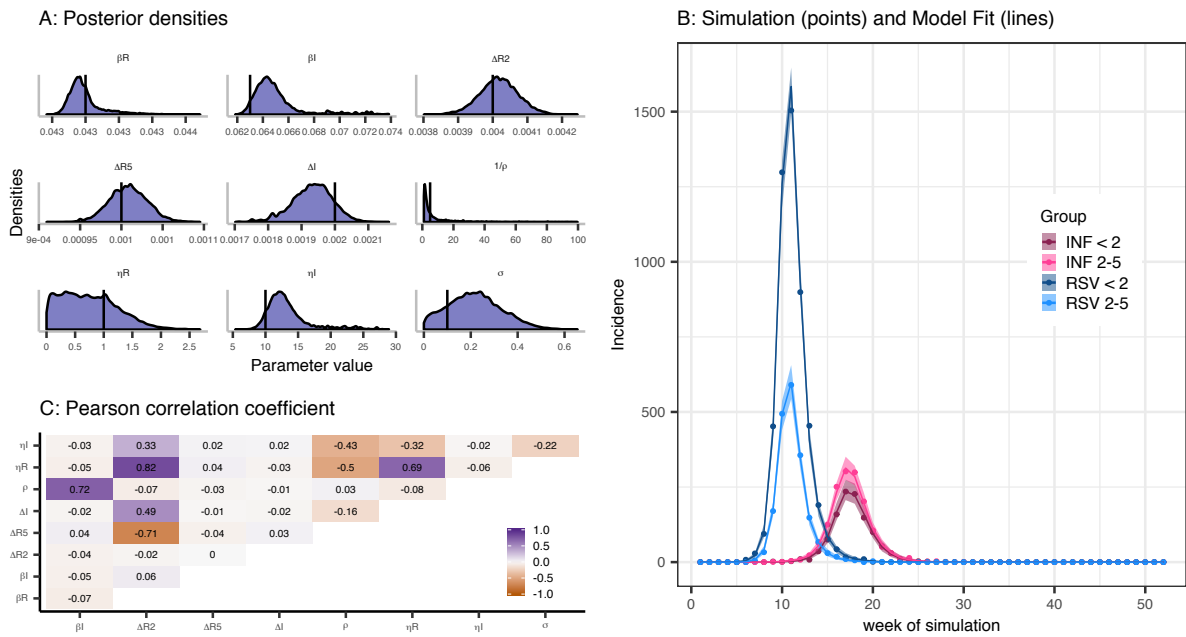
Appendix A Figure S69: Inference results for simulation with $\sigma = 0.3$ and $\rho = 0.2$. See the legend of Figure S28 for more details.

$\sigma = 0.2$ and $1/\rho = 5$



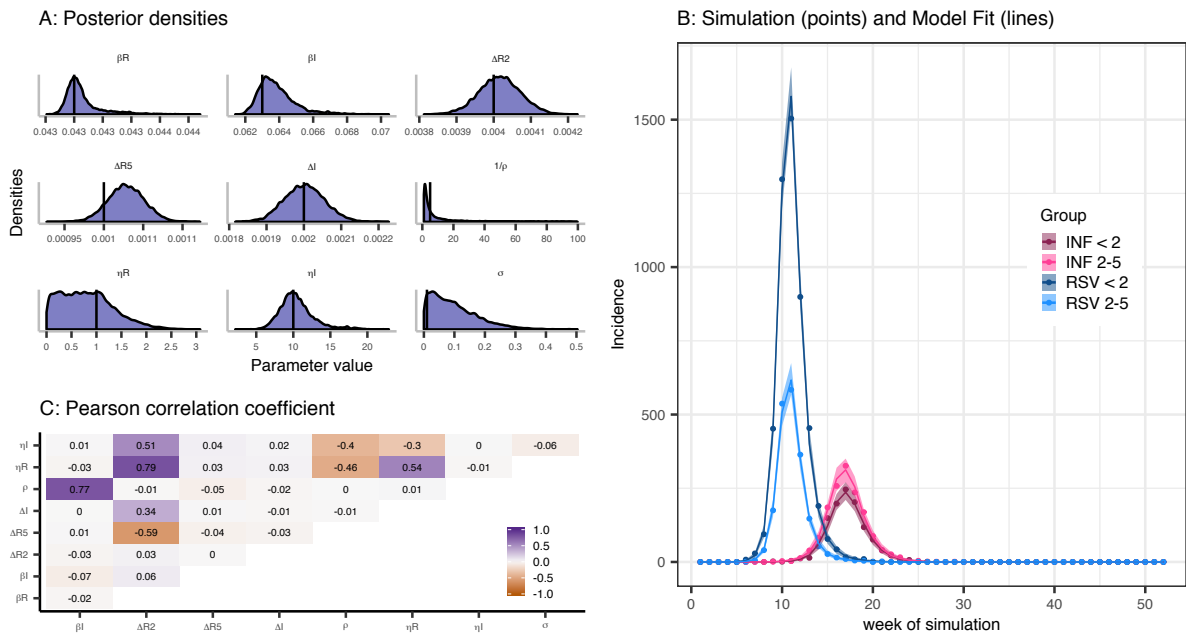
Appendix A Figure S70: Inference results for simulation with $\sigma = 0.2$ and $\rho = 0.2$. See the legend of Figure S28 for more details.

$\sigma = 0.1$ and $1/\rho = 5$



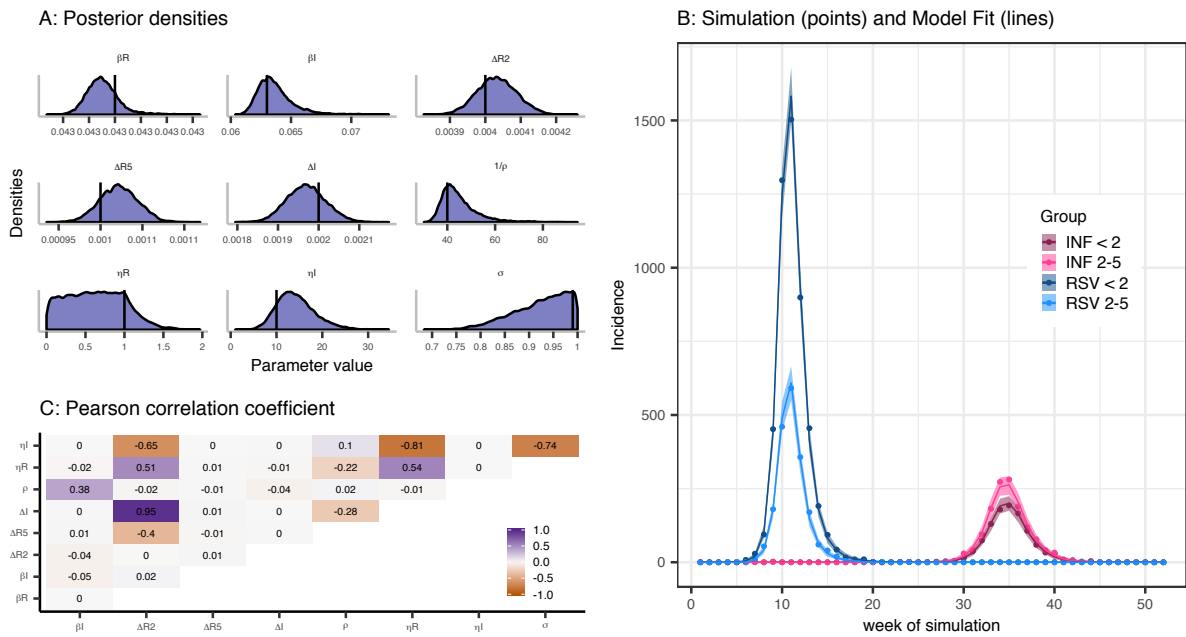
Appendix A Figure S71: Inference results for simulation with $\sigma = 0.1$ and $\rho = 0.2$. See the legend of Figure S28 for more details.

$\sigma = 0.01$ and $1/\rho = 5$



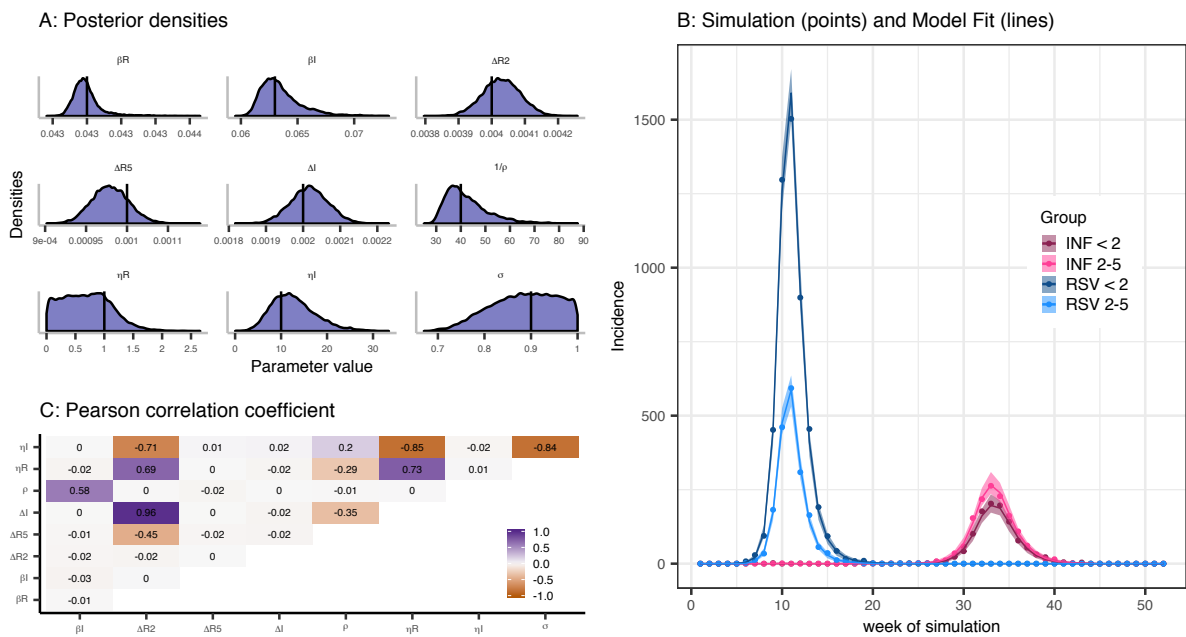
Appendix A Figure S72: Inference results for simulation with $\sigma = 0.01$ and $\rho = 0.2$. See the legend of Figure S28 for more details.

$\sigma = 0.99$ and $1/\rho = 40$



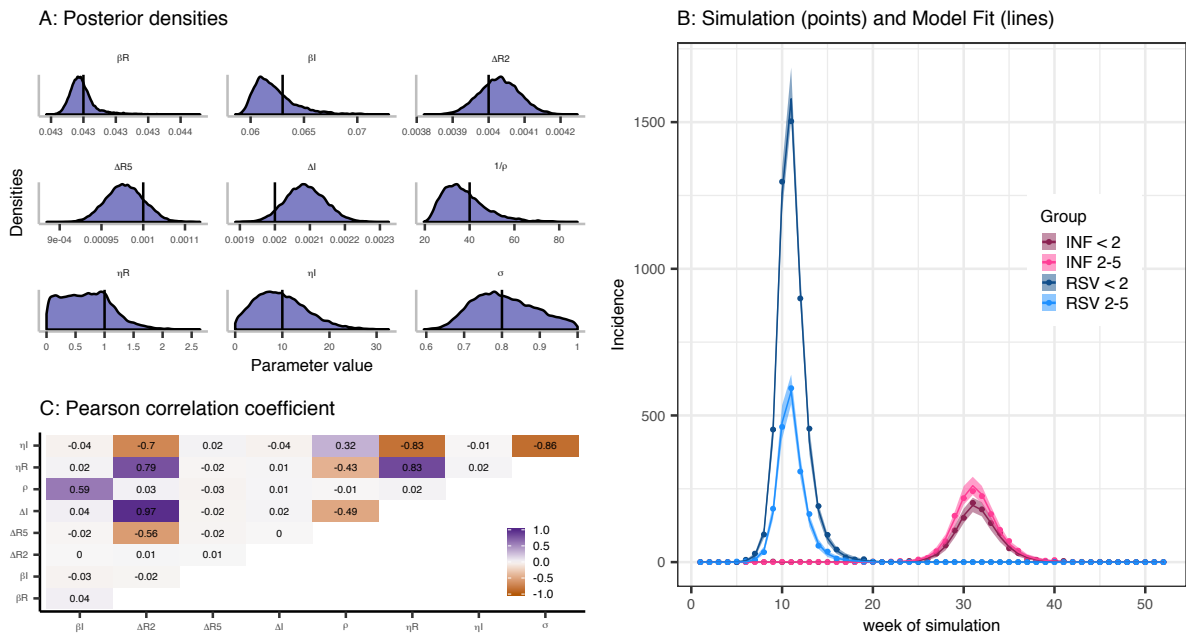
Appendix A Figure S73: Inference results for simulation with $\sigma = 0.99$ and $\rho = 0.025$. See the legend of Figure S28 for more details.

$\sigma = 0.9$ and $1/\rho = 40$



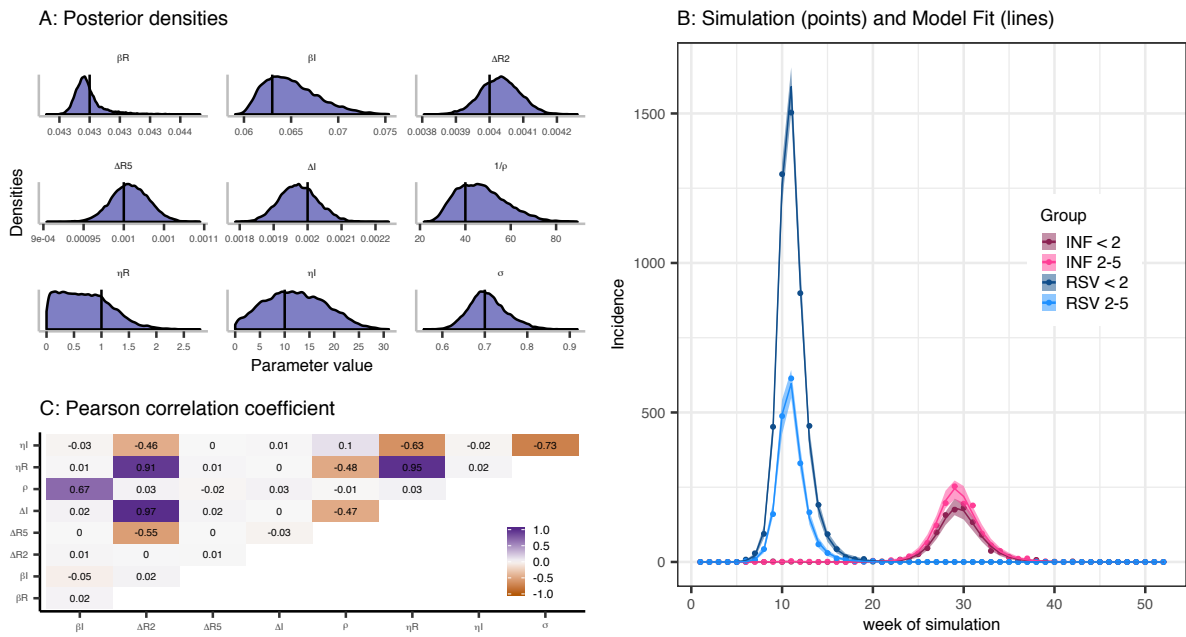
Appendix A Figure S74: Inference results for simulation with $\sigma = 0.9$ and $\rho = 0.025$. See the legend of Figure S28 for more details.

$\sigma = 0.8$ and $1/\rho = 40$



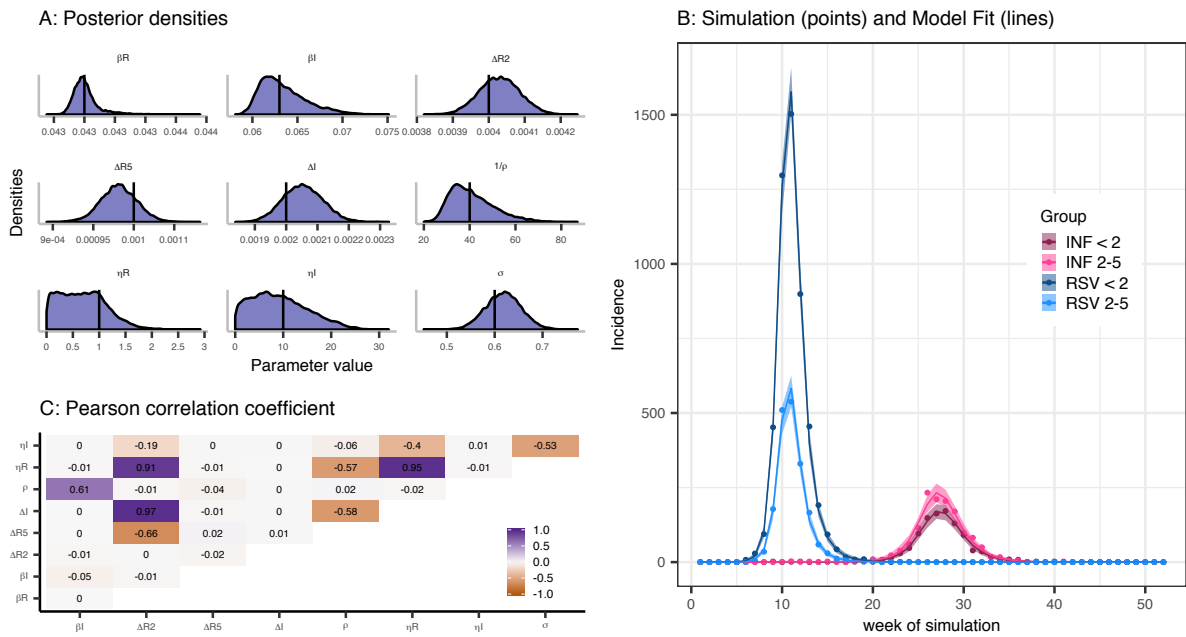
Appendix A Figure S75: Inference results for simulation with $\sigma = 0.8$ and $\rho = 0.025$. See the legend of Figure S28 for more details.

$\sigma = 0.7$ and $1/\rho = 40$



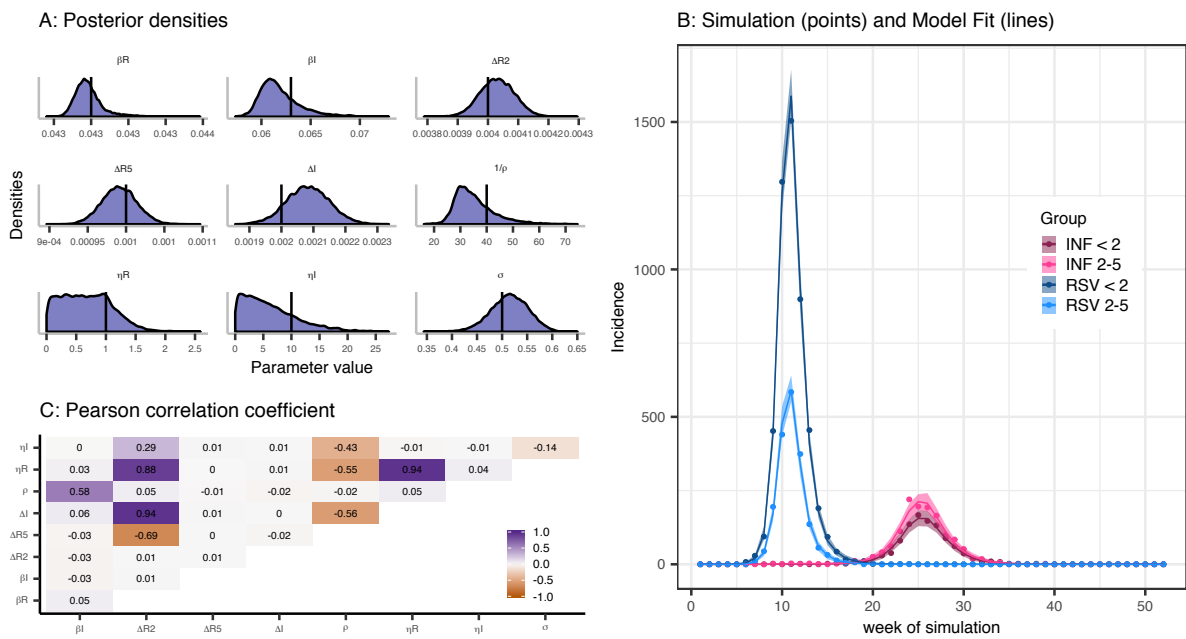
Appendix A Figure S76: Inference results for simulation with $\sigma = 0.7$ and $\rho = 0.025$. See the legend of Figure S28 for more details.

$\sigma = 0.6$ and $1/\rho = 40$



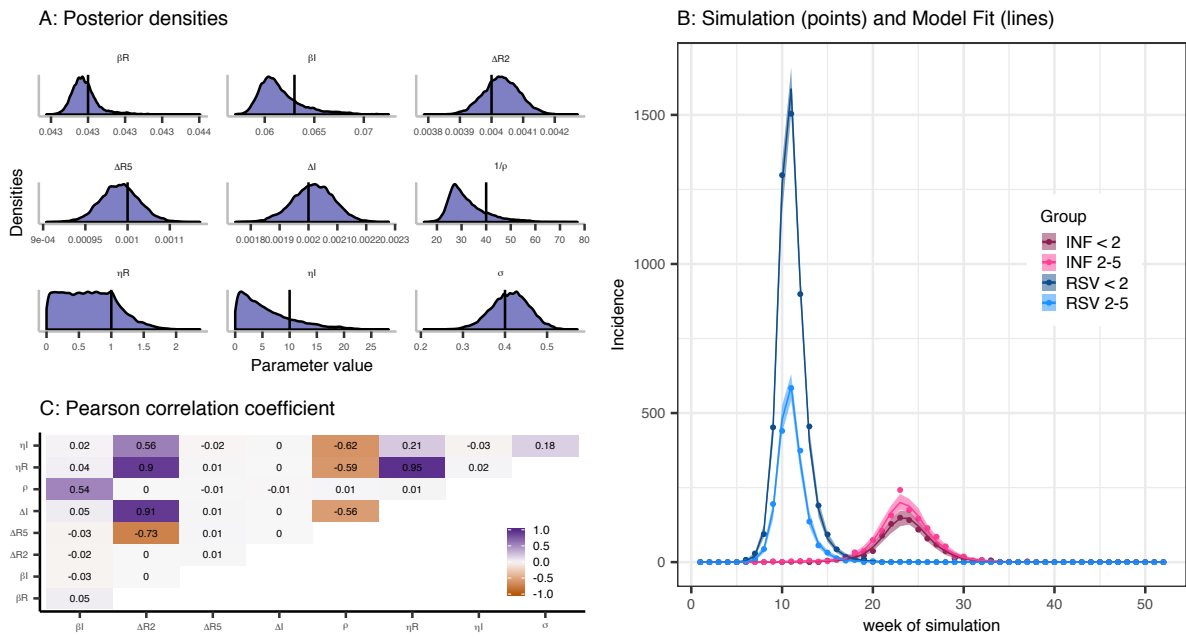
Appendix A Figure S77: Inference results for simulation with $\sigma = 0.6$ and $\rho = 0.025$. See the legend of Figure S28 for more details.

$\sigma = 0.5$ and $1/\rho = 40$



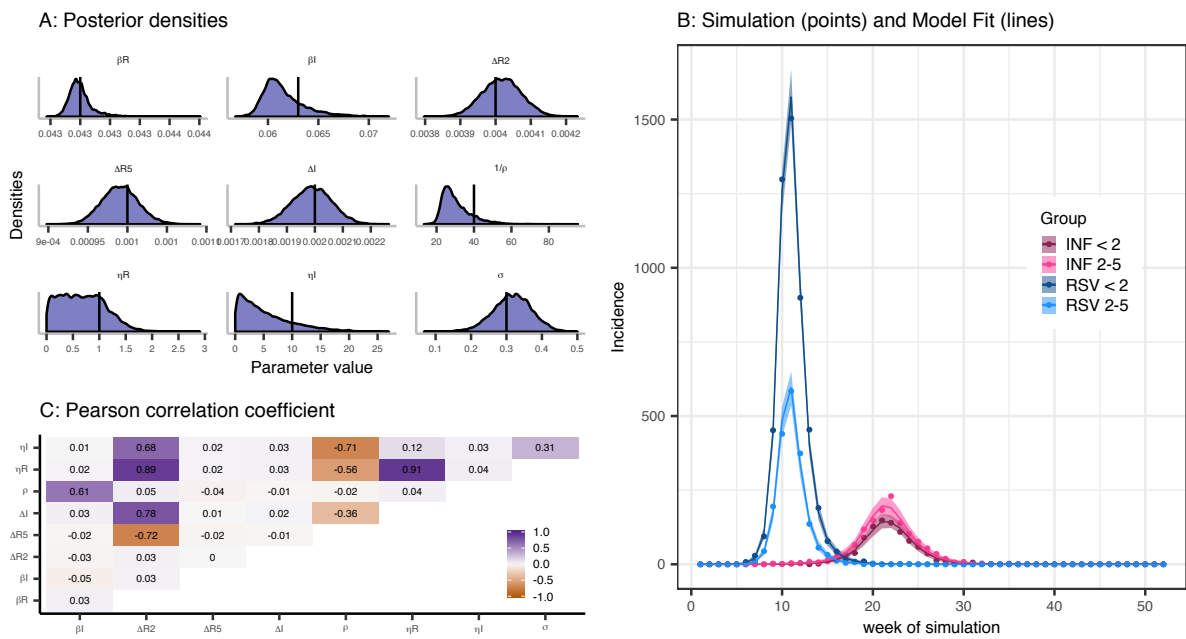
Appendix A Figure S78: Inference results for simulation with $\sigma = 0.5$ and $\rho = 0.025$. See the legend of Figure S28 for more details.

$\sigma = 0.4$ and $1/\rho = 40$



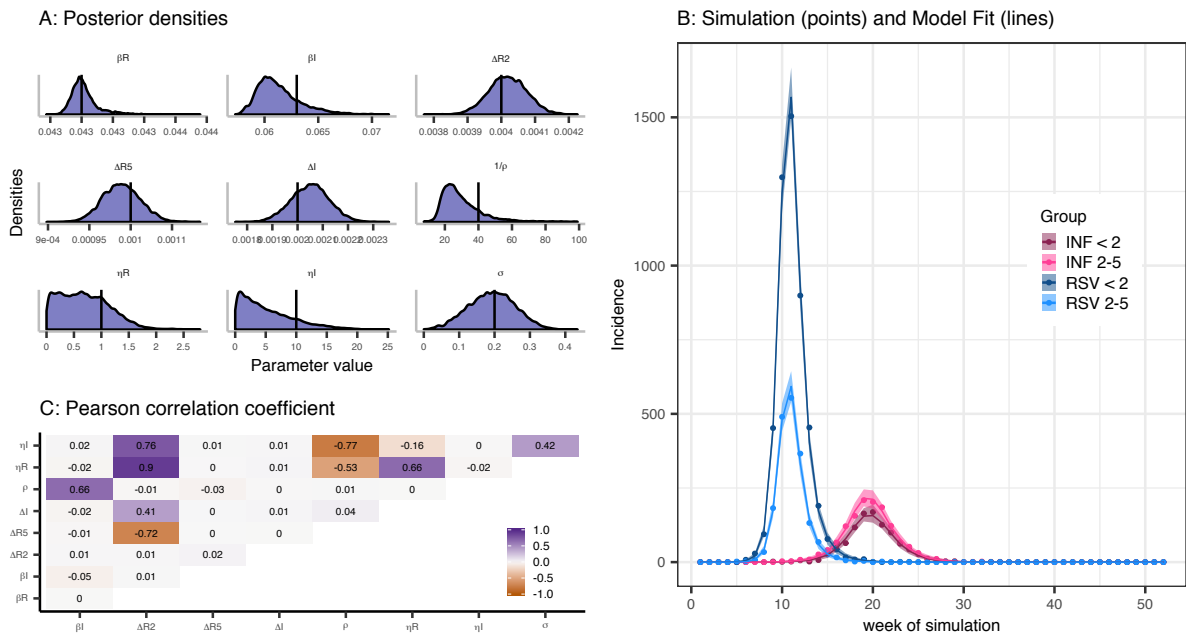
Appendix A Figure S79: Inference results for simulation with $\sigma = 0.4$ and $\rho = 0.025$. See the legend of Figure S28 for more details.

$\sigma = 0.3$ and $1/\rho = 40$



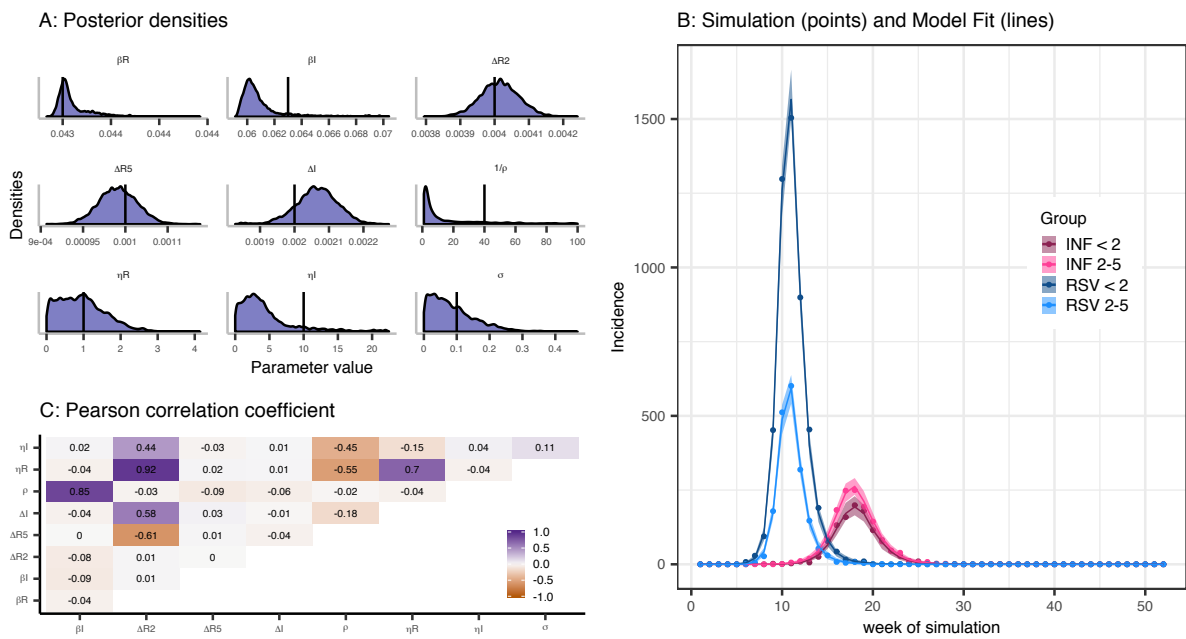
Appendix A Figure S80: Inference results for simulation with $\sigma = 0.3$ and $\rho = 0.025$. See the legend of Figure S28 for more details.

$\sigma = 0.2$ and $1/\rho = 40$



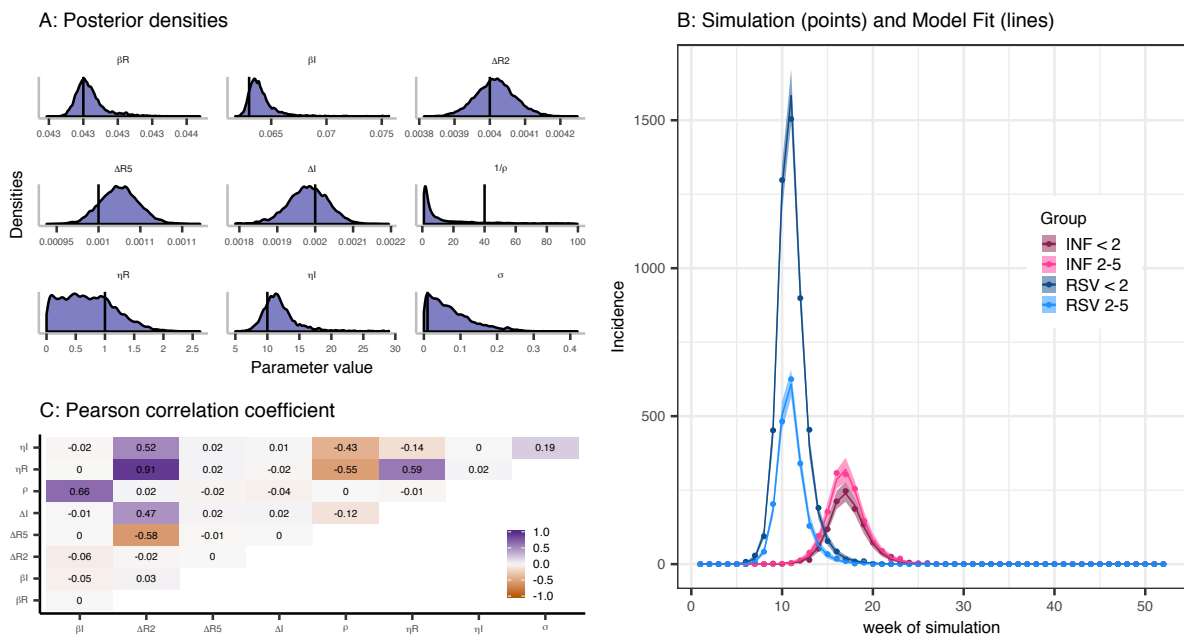
Appendix A Figure S81: Inference results for simulation with $\sigma = 0.2$ and $\rho = 0.025$. See the legend of Figure S28 for more details.

$\sigma = 0.1$ and $1/\rho = 40$



Appendix A Figure S82: Inference results for simulation with $\sigma = 0.1$ and $\rho = 0.025$. See the legend of Figure S28 for more details.

$\sigma = 0.01$ and $1/\rho = 40$



Appendix A Figure S83: Inference results for simulation with $\sigma = 0.01$ and $\rho = 0.025$. See the legend of Figure S28 for more details.

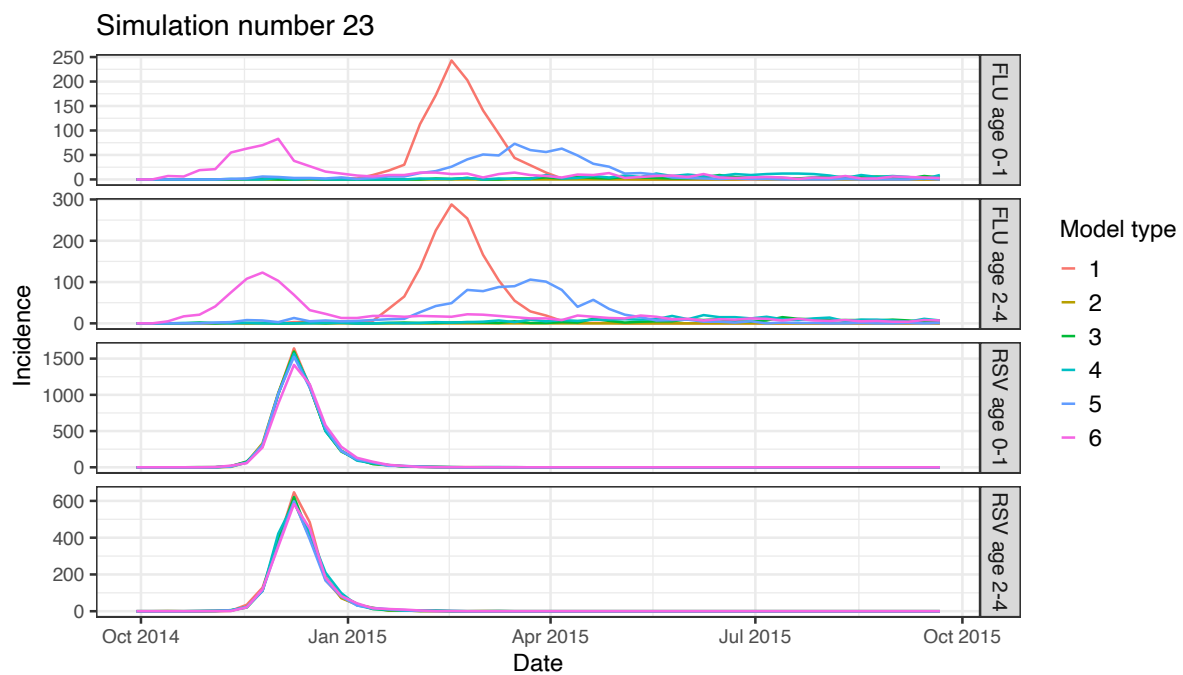
A.13 Varying the R_0

The R_0 value we used for influenza was 2.91. This led to reasonable epidemics and an $R_{\text{effective}}$ at the start of the simulated season of 1.55. Some previous estimates have placed R_0 for influenza below 2. We therefore modelled 5 additional scenarios, all with an R_0 of 1.98.

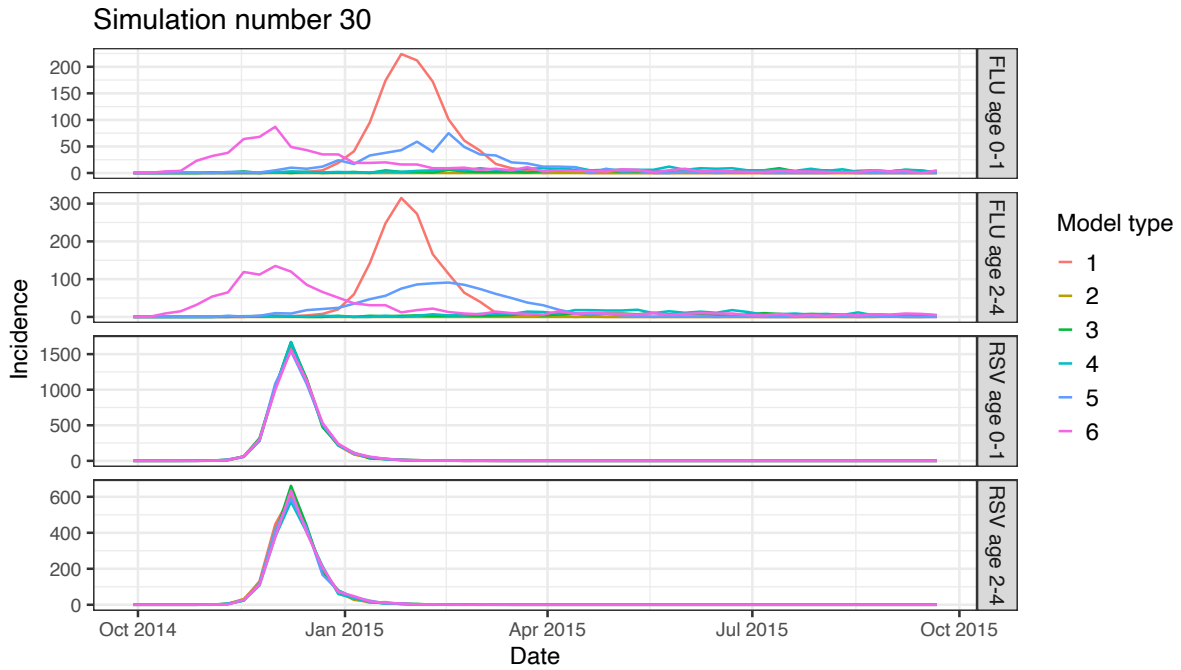
- 1) Original parameters (R_0 2.91, $R_{\text{effective}}$ 1.55)
- 2) Reduced R_0 (1.98, $R_{\text{effective}}$ 1.06)
- 3) Reduced R_0 (1.98), increased importation (125 cases per day, $R_{\text{effective}}$ 1.06)
- 4) Reduced R_0 (1.98, $R_{\text{effective}}$ 1.09), increased importation (125 cases per day), increased influenza susceptibility (3% increased, upper bound of the confidence intervals for susceptibility that we used from Baguelin et al. 2013)
- 5) Reduced R_0 (1.98, $R_{\text{effective}}$ 1.26), increased importation (125 cases per day), increased influenza susceptibility (20% increased)
- 6) Reduced R_0 (1.98, $R_{\text{effective}}$ 1.26), increased importation (5000 cases per day), increased influenza susceptibility (20% increased)

These simulations, along with the simulations for the original parameter values ($R_0 = 2.91$), are shown Figures S83 – S87 for five combinations of parameter sets.

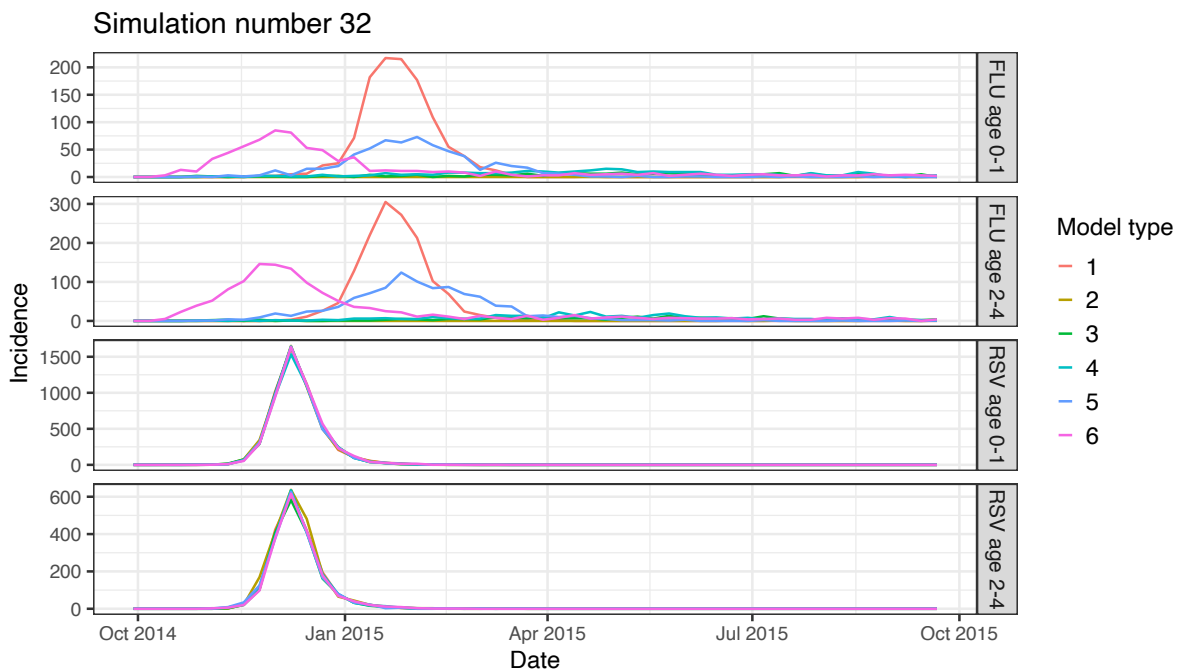
In none of the scenarios other than the original were we able to replicate the influenza epidemic. In all additional scenarios, influenza peak incidence was lower and the duration of the epidemics was longer than a typical influenza season in the UK. While an increased amount of importations allowed the peak to shift forward the width and peak height in the additional scenarios indicated an R_0 that in combination with the observed susceptibility was not compatible in the model with the shape of a typical influenza season in the UK. The typical influenza season in the UK lasts less than 2.5 months/10 weeks^{6,7} and occurs after/during the RSV epidemic⁸, so these simulations were not deemed appropriate.



Appendix A Figure S84: Simulations with different model parameters, for Simulation 23 ($\sigma = 0.99$, $1/\rho = 2$ days). Model types are 1 – original parameter values with and R_0 of 2.91. 2 – R_0 of 1.98. 3 – R_0 of 1.98 and increased importation (125 imports per day) , 4 – R_0 of 1.98, increased importation (125 imports per day) and 3% increased susceptibility. 5 – R_0 of 1.98, increased importation (125 imports per day) and 20% increased susceptibility. 6 – R_0 of 1.98, increased importation (5000 imports per day) and 20% increased susceptibility.

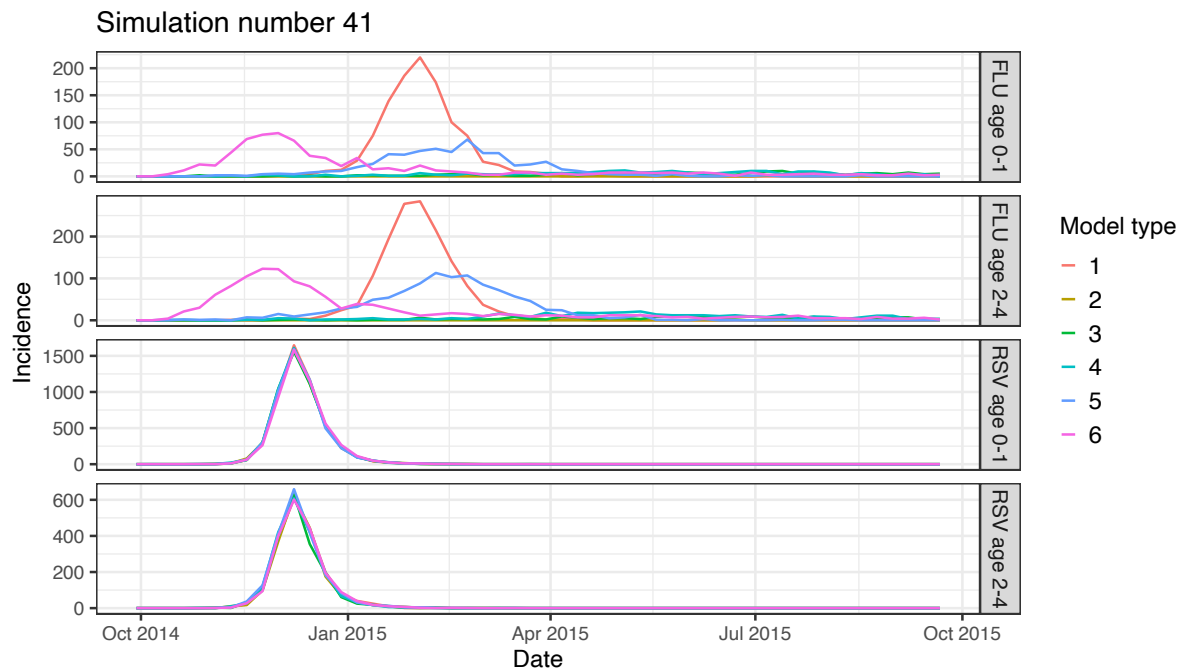


Appendix A Figure S 85: Simulations with different model parameters, for Simulation 30 ($\sigma = 0.7$, $1/\rho = 2$ days). Model types are 1 – original parameter values with and R_0 of 2.91. 2 – R_0 of 1.98. 3 – R_0 of 1.98 and increased importation (125 imports per day) , 4 – R_0 of 1.98, increased importation (125 imports per day) and 3% increased susceptibility. 5 – R_0 of 1.98, increased importation (125 imports per day) and 20% increased susceptibility. 6 – R_0 of 1.98, increased importation (5000 imports per day) and 20% increased susceptibility.

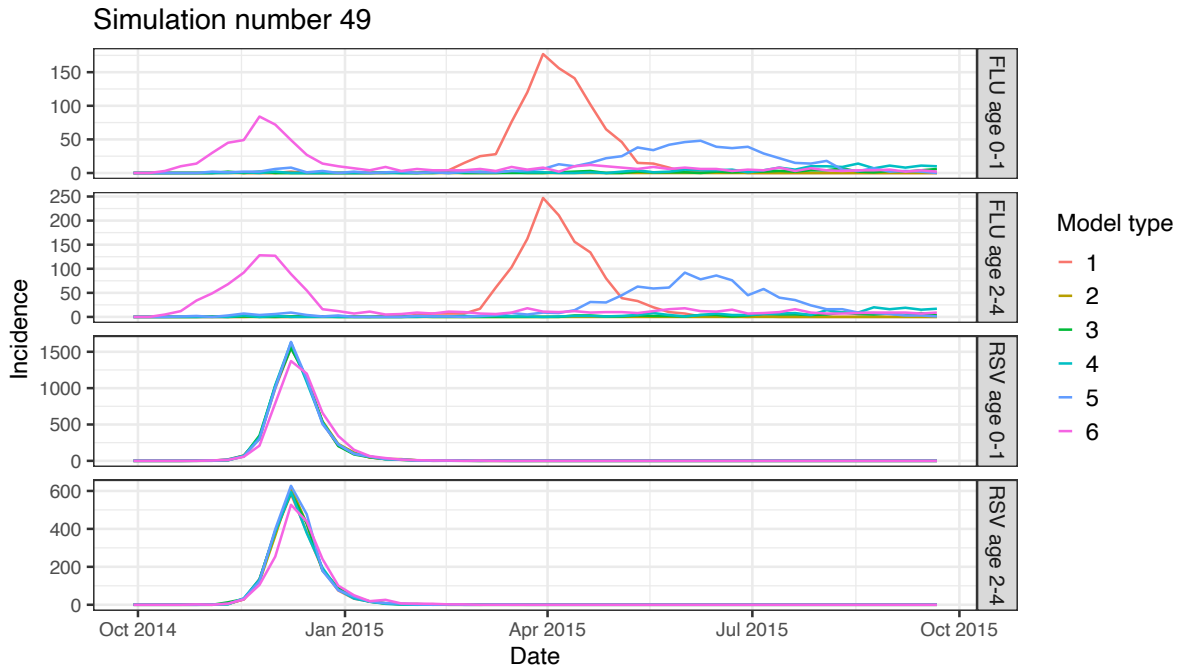


Appendix A Figure S 86: Simulations with different model parameters, for Simulation 32 ($\sigma = 0.1$, $1/\rho = 2$ days). Model types are 1 – original parameter values with and R_0 of 2.91. 2 – R_0 of 1.98. 3 – R_0 of 1.98 and increased importation (125 imports per day) , 4 – R_0 of 1.98, increased importation (125 imports per day) and 3%

increased susceptibility. 5 – R_0 of 1.98, increased importation (125 imports per day) and 20% increased susceptibility. 6 – R_0 of 1.98, increased importation (5000 imports per day) and 20% increased susceptibility.



Appendix A Figure S 87: Simulations with different model parameters, for Simulation 41 ($\sigma = 0.3$, $1/\rho = 10$ days). Model types are 1 – original parameter values with and R_0 of 2.91. 2 – R_0 of 1.98. 3 – R_0 of 1.98 and increased importation (125 imports per day) , 4 – R_0 of 1.98, increased importation (125 imports per day) and 3% increased susceptibility. 5 – R_0 of 1.98, increased importation (125 imports per day) and 20% increased susceptibility. 6 – R_0 of 1.98, increased importation (5000 imports per day) and 20% increased susceptibility.



Appendix A Figure S88: Simulations with different model parameters, for Simulation 49 ($\sigma = 0.6$, $1/p = 40$ days). Model types are 1 – original parameter values with and R_0 of 2.91. 2 – R_0 of 1.98. 3 – R_0 of 1.98 and increased importation (125 imports per day) , 4 – R_0 of 1.98, increased importation (125 imports per day) and 3% increased susceptibility. 5 – R_0 of 1.98, increased importation (125 imports per day) and 20% increased susceptibility. 6 – R_0 of 1.98, increased importation (5000 imports per day) and 20% increased susceptibility.

1. Diekmann, O., Heesterbeek, J. A. P. & Roberts, M. G. The construction of next-generation matrices for compartmental epidemic models. *J. R. Soc. Interface* **7**, 873–85 (2010).
2. Henderson, F. W., Collier, A. M., Clyde, W. A. & Denny, F. W. Respiratory-Syncytial-Virus Infections, Reinfections and Immunity. *N. Engl. J. Med.* **300**, 530–534 (1979).
3. Glezen, W. P., Taber, L. H., Frank, A. L. & Kasel, J. A. Risk of primary infection and reinfection with respiratory syncytial virus. *Am. J. Dis. Child.* **140**, 543–6 (1986).
4. Reeves, R. M. *et al.* Estimating the burden of respiratory syncytial virus (RSV) on respiratory hospital admissions in children less than five years of age in England, 2007-2012. *Influenza Other Respi. Viruses* **11**, 122–129 (2017).
5. Ohuma, E. O. *et al.* The natural history of respiratory syncytial virus in a birth cohort: the influence of age and previous infection on reinfection and disease. *Am. J. Epidemiol.* **176**, 794–802 (2012).
6. Fleming, D. M. & Elliot, A. J. Lessons from 40 years' surveillance of influenza in England and Wales. *Epidemiology and Infection* **136**, 866–875 (2008).
7. Jick, H. & Hagberg, K. W. Effectiveness of influenza vaccination in the United Kingdom, 1996-2007. *Pharmacotherapy* **30**, 1199–1206 (2010).
8. Gov.uk. Six major respiratory viruses reported from PHE and NHS laboratories (SGSS) in England and Wales between weeks 01/2007 and 44/201. Available at: https://www.gov.uk/government/uploads/system/uploads/attachment_data/file/639687/six_pathogens_-_Jan2007-Aug2017.pdf. (Accessed: 6th October 2017)

Supplementary Information for

“How cross-protection between Influenza and Respiratory Syncytial virus shapes pediatric hospital admissions in Nha Trang, Vietnam”

Naomi R Waterlow¹, Michiko Toizumi, Edwin van Leeuwen^{1,4}, ... , Lay Myint-Yoshida^{2,3*}, Rosalind M Eggo^{1*}, Stefan Flasche^{1*}.

¹ Centre for Mathematical Modeling of Infectious Disease, London School of Hygiene and Tropical Medicine, UK

² Department of Pediatrics, Nagasaki University Hospital, Nagasaki University, Nagasaki 852-8102, Japan

³ Department of Pediatric Infectious Diseases, Institute of Tropical Medicine, Nagasaki University, Nagasaki 852-8523, Japan

⁴ Statistics, Modelling and Economics Department, Public Health England, London, UK

* These authors have contributed equally

... denotes collaborators from Pasteur Institute, Khanh Hoa Hospital, National Institute of Hygiene and Epidemiology, and Nagasaki university.

Appendix B	Supplementary material for Chapter 3	205
B.1	Estimated influenza attack rate	206
B.2	Data.....	206
B.3	Model equations.....	207
B.4	R_0 equations.....	209
B.5	Susceptibility to RSV.....	210
B.6	Susceptibility to Influenza.....	210
B.7	Parallel tempering.....	211
B.8	Attack Rates	213
B.9	Sensitivity to severity of dual infected cases	213
B.10	Prior Sensitivity	214
B.11	Modelled correlation	215
B.12	References	217

B.1 Estimated influenza attack rate

Assuming no interaction (in susceptibility to or severity of dual infections), we calculated the required annual influenza infection attack rate in order to achieve the observed number of dual infections (equations 1-3). Using a negative binomial likelihood with Brent optimization we estimated the RSV reporting rate that would correspond to the maximum likelihood of observing the reported weekly number of dual infections. We then used this estimate of the reporting rate to calculate the annual RSV population attack rate required in order to observe this many dual cases. The confidence intervals for the attack rate were calculated using the Hessian matrix from the optimisation.

$$I_{Dual} \simeq I_{RSV} * P_{Influenza} \quad (1)$$

$$P_{Influenza} \simeq I_{Influenza} * 1/\gamma_{Influenza} / \nu_{Influenza} \quad (2)$$

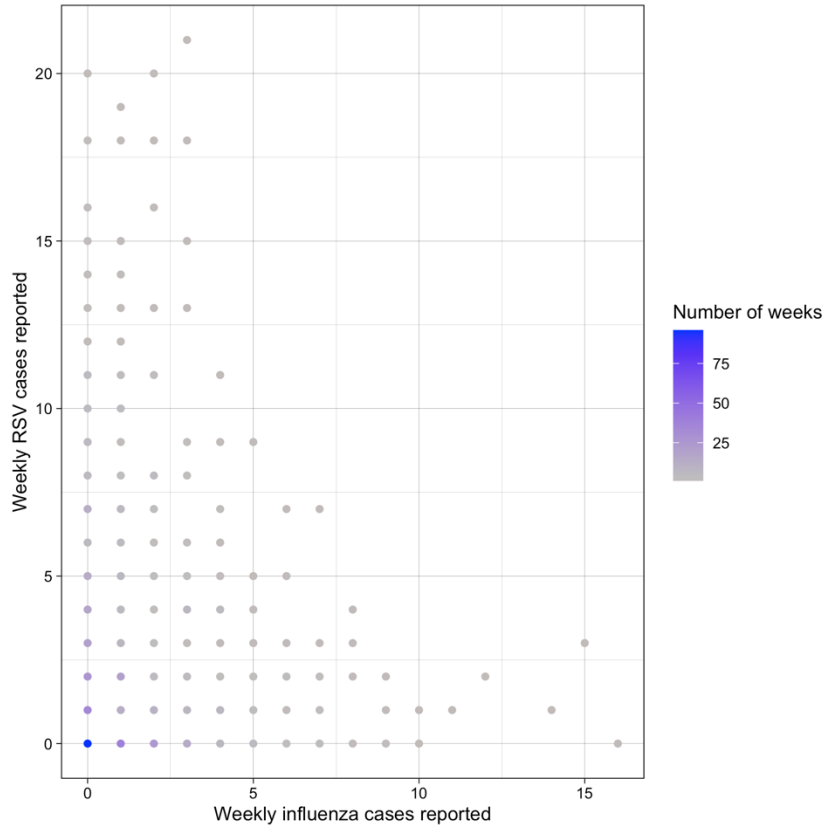
$$AR_{Influenza} \simeq I_{Influenza} / \nu_{Influenza} \quad (3)$$

With parameters: Incidence of reported cases (I), Prevalence of Infection (P), Duration of Infection ($1/\gamma_{INF}$), 3.8 days - see main text Table 1) and estimated reporting rate (ν).

We estimated that in order to achieve the weekly reported number of dual infections given no interaction, we would require an annual influenza attack rate of 4.4 (3.4 -6.5) in ages 0-1 and 1.3 (0.9 - 3.0) in ages 2-4.

B.2 Data

The annual mean number of ARI admissions under the age of 15 was 1030, ranging from 595 to 1299, with 94% being enrolled in the study. Of enrolled patients, the median age was 15.9 months, with an interquartile range of 8.5 to 25.3 months. This compares to 19.9 months (IQR: 11.6 – 30.4) for RSV positive patients and 13.7 months (IQR: 6.7 – 22.2) for the RSV positive patients. Figure S1 shows a scatter plot between the weekly Influenza and RSV cases.



Appendix B Figure S1: Reported cases. Scatter plot of weekly influenza and RSV cases reported through the enhanced surveillance study in less than 5-year-olds over the whole time period.

B.3 Model equations

Full model equations are shown below. Each compartment includes the state for both RSV and influenza, with the first letter indicating the state for RSV, and the second for influenza. E.g. SS_i is shorthand for $S_{RSV,i}S_{INF,i}$. Subscripts used are “INF” for influenza and “RSV”

$$\lambda_{INF,i} = \sum_{j=1}^5 \beta_{INF} \alpha_{ij} I_{INF,j} \quad (4)$$

$$\lambda_{RSV,i} = \sum_{j=1}^5 \beta_{RSV} \alpha_{ij} I_{RSV,j} \quad (5)$$

$$\frac{dSS_i}{dt} = -\tau_i \lambda_{RSV,i} SS_i - \lambda_{INF,i} SS_i - \epsilon_{INF} - \epsilon_{RSV}$$

$$\frac{dIS_i}{dt} = \tau_i \lambda_{RSV,i} SS_i - (1 - \sigma) \lambda_{INF,i} IS_i - \gamma_{RSV} IS_i + \epsilon_{RSV}$$

$$\frac{dPS_i}{dt} = \gamma_{RSV}IS_i - \rho PS_i - (1 - \sigma)\lambda_{INF_i}PS_i$$

$$\frac{dRS_i}{dt} = \rho PS_i - \lambda_{INF_i}RS_i$$

$$\frac{dSI_i}{dt} = \lambda_{INF_i}SS_i - (1 - \sigma)\tau_i\lambda_{RSV_i}SI_i - \gamma_{INF}SI_i + \epsilon_{INF}$$

$$\frac{dII_i}{dt} = (1 - \sigma)\lambda_{INF_i}IS_i + (1 - \sigma)\tau_i\lambda_{RSV_i}SI_i - \gamma_{INF}II_i - \gamma_{RSV}II_i$$

$$\frac{dPI_i}{dt} = \lambda PS_i - \gamma_{INF}PI_i + \gamma_{RSV}II_i + \lambda_{INF_i}RS_i$$

$$\frac{dSP_i}{dt} = \gamma_{INF}SI_i - \rho SP_i - (1 - \sigma)\tau_i\lambda_{RSV_i}SP_i$$

$$\frac{dIP_i}{dt} = (1 - \sigma)\tau_i\lambda_{RSV}SP_i - \gamma_{RSV}IP_i + \gamma_{INF}II_i + \tau_i\lambda_{RSV_i}SR_i$$

$$\frac{dSR_i}{dt} = \rho SP_i - \tau_i\lambda_{RSV_i}SR_i$$

$$\frac{dRR_i}{dt} = \gamma_{RSV}IP_i + \gamma_{INF}PI_i$$

Where:

$\lambda_{i,j}$ - force of infection between age groups I and J

β - transmission rate

α_{ij} - contact rate between group I and j

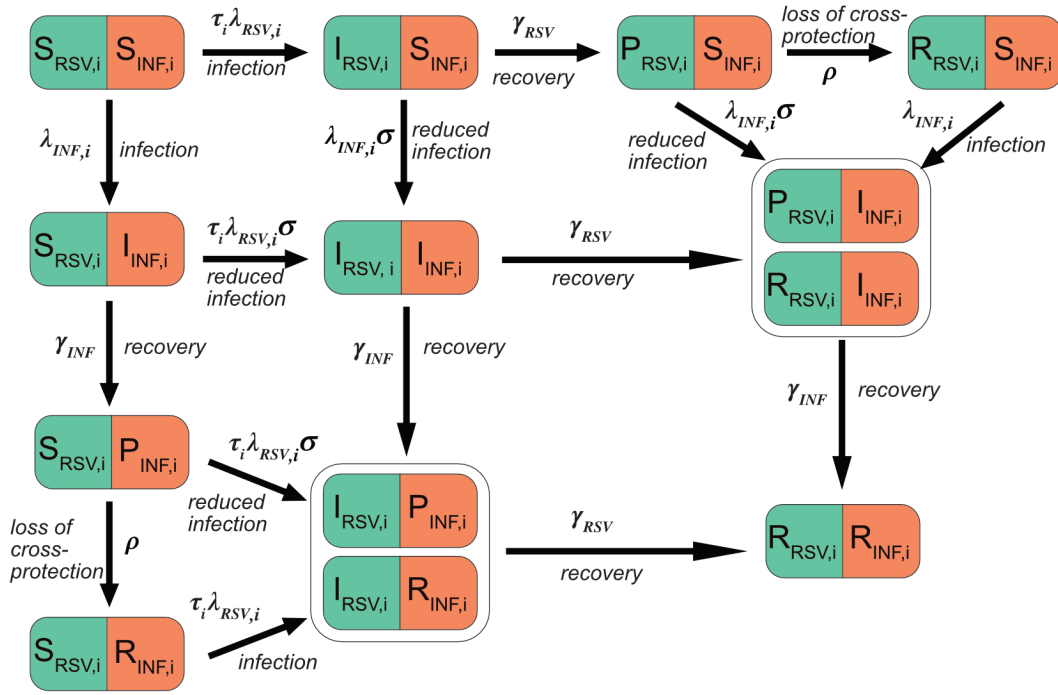
τ_i - age group susceptibility to RSV

σ - level of cross-protection

γ - rate of recovery

ρ - rate of loss of cross-protection

ϵ - introduction rate from external sources



B.4 R_0 equations

The R_0 's were calculated as the dominant eigenvalue of the matrix

$$-T\Sigma^{-1}$$

Where T is the transmission matrix, describing new infections, and Σ is the transition matrix, describing other changes in state. This method is described in full in Diekmann *et al* (2009)¹

$$T_{INF} = \begin{bmatrix} \beta_{INF} * \alpha_{i,j} & \cdots & \beta_{INF} * \alpha_{i,j} \\ \vdots & \ddots & \vdots \\ \beta_{INF} * \alpha_{i,j} & \cdots & \beta_{INF} * \alpha_{i,j} \end{bmatrix} \quad T_{RSV} = \begin{bmatrix} \tau_j * \beta_{RSV} * \alpha_{i,j} & \cdots & \tau_i * \beta_{RSV} * \alpha_{i,j} \\ \vdots & \ddots & \vdots \\ \tau_j * \beta_{RSV} * \alpha_{i,j} & \cdots & \tau_j * \beta_{RSV} * \alpha_{i,j} \end{bmatrix}$$

$$\Sigma_{INF} = \begin{bmatrix} \gamma_{INF} & 0 & 0 & 0 & 0 \\ 0 & \gamma_{INF} & 0 & 0 & 0 \\ 0 & 0 & \gamma_{INF} & 0 & 0 \\ 0 & 0 & 0 & \gamma_{INF} & 0 \\ 0 & 0 & 0 & 0 & \gamma_{INF} \end{bmatrix} \quad \Sigma_{RSV} = \begin{bmatrix} \gamma_{RSV} & 0 & 0 & 0 & 0 \\ 0 & \gamma_{RSV} & 0 & 0 & 0 \\ 0 & 0 & \gamma_{RSV} & 0 & 0 \\ 0 & 0 & 0 & \gamma_{RSV} & 0 \\ 0 & 0 & 0 & 0 & \gamma_{RSV} \end{bmatrix}$$

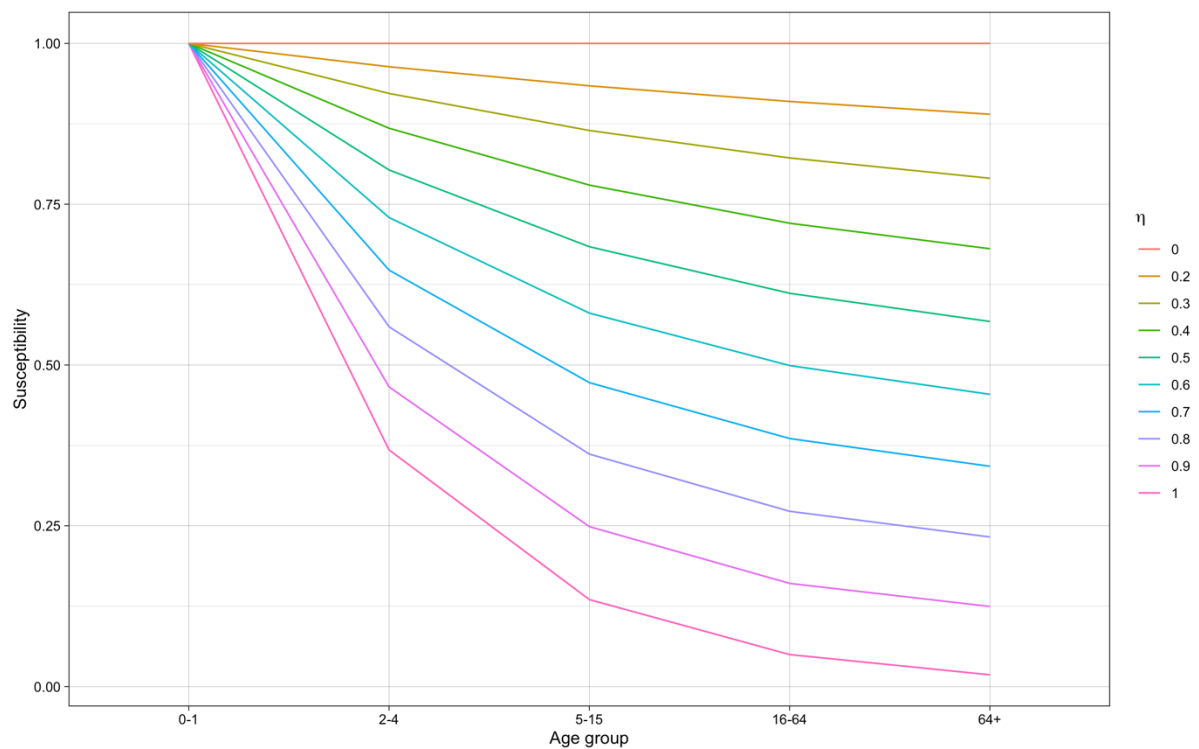
B.5 Susceptibility to RSV

We used a longitudinal study by Hendersen et a. (1979) to determine age-susceptibility to RSV infection. They estimated that at 1st exposure 98.4% of children became infected, at second exposure 74.5% of children became infected and at 3rd exposure 65.4% of children became infected². As most children are infected by 24 months of age, we used the susceptibility estimates for the age groups: ages 0-1 = 100% susceptible, ages 2-4 = 75% susceptible, ages 5 and over = 65% susceptible³.

B.6 Susceptibility to Influenza

Influenza susceptibility each season (s) is determined by the parameter η_s using the inverse density of an exponential distribution at each age group (i, where ages 0-1 is age group zero, up to ages 65+ at age group four). Equation 6 shows the calculations and example susceptibility profiles are shown in Figure S2.

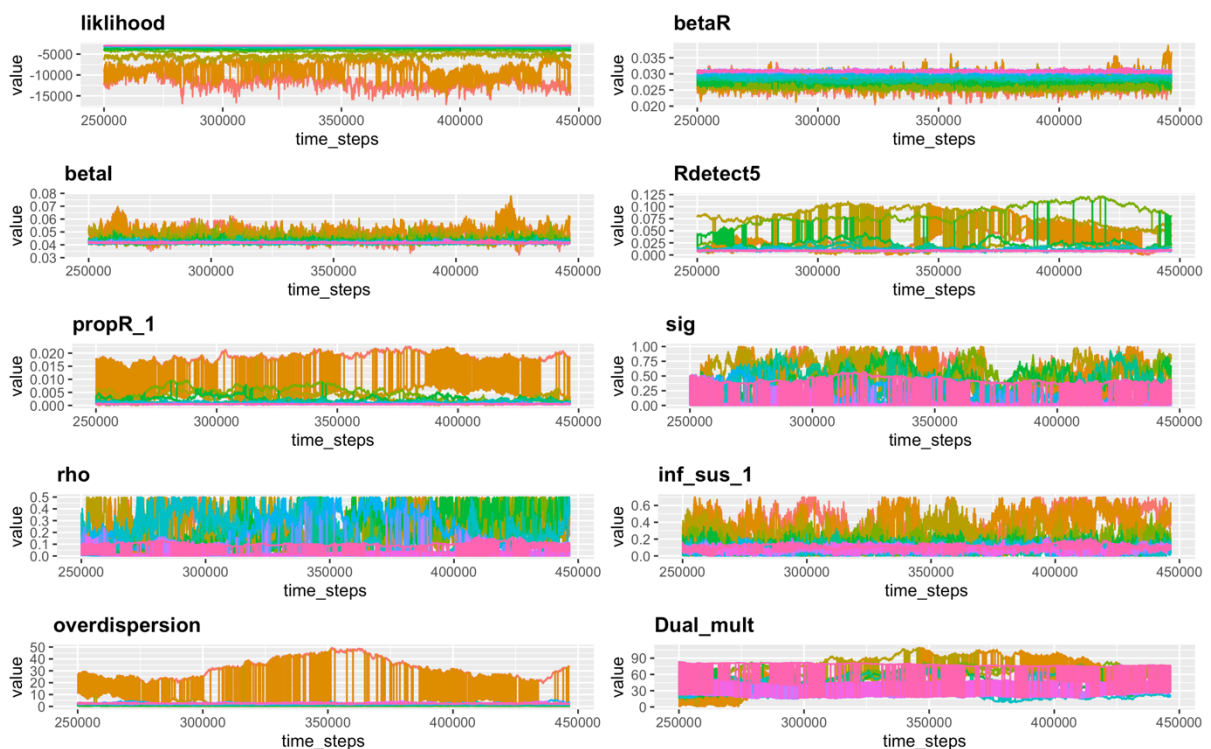
$$\text{Susceptibility}_{i,s} = \eta_s e^{(-\eta_s i)} + 1 - \eta_s \quad (6)$$



Appendix B Figure S2: Susceptibility. Susceptibility to influenza by age group for different values of η .

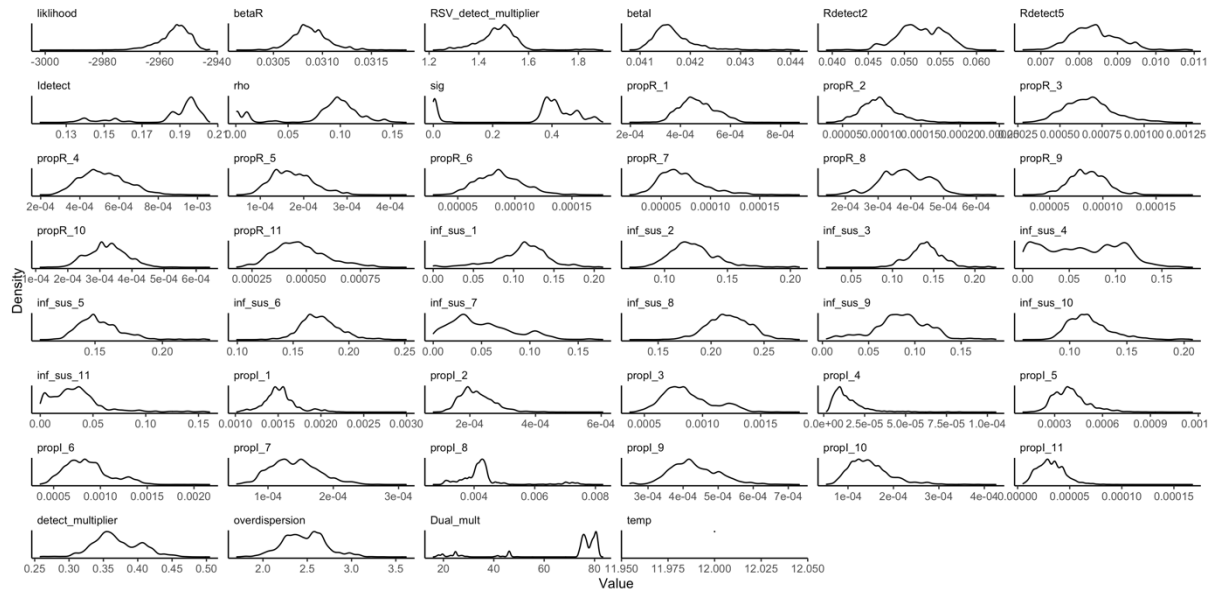
B.7 Parallel tempering

Our parallel tempering algorithm was implemented in R and we used Amazon Web Services (AWS) to run it. We proposed swaps with the next temperature chains every 5 iterations. We ran the parallel tempering algorithm using a covariance matrix to propose parameters. We removed 250000 iterations as burn in, followed by 200000 more samples, and assessed convergence using the Geweke statistic in the null chain (Chain with temperature 1). This calculates the difference between the two sample means of the first 10 and last 50% of the chain, divided by its estimated standard error, resulting in a Z score. Note however that due to the large number of parameters (44), the multiple modes and the swapping between chains as a result of the parallel tempering the Geweke statistic is not an ideal measure of convergence in this situation. Despite this, all key parameters (transmission rates, interaction parameters, dual detection rate) had a Z score within the 95% confidence interval and overall over 80% of parameters fell within a 99% confidence interval. Figure S3 shows one of the traces for a sample of parameters, thinned to 1 in 10. Figure S4 shows the final posterior densities of each parameter, and table S1 describes the distribution.

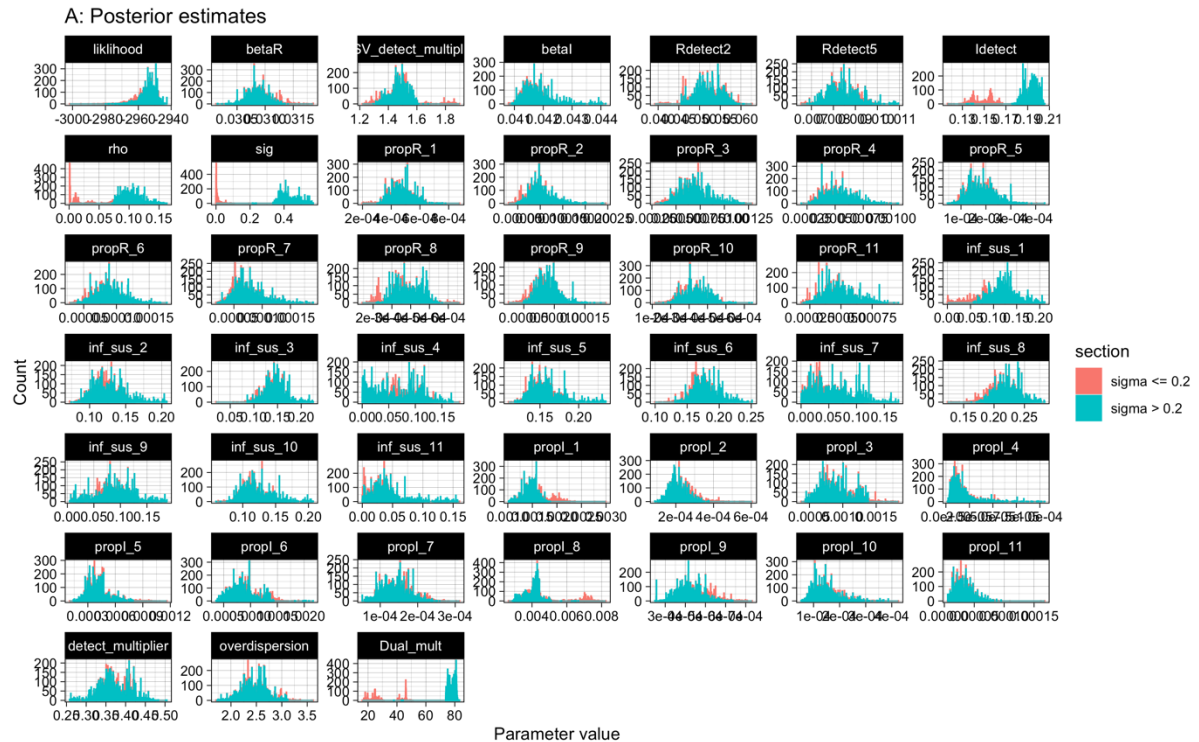


Appendix B Figure S3: Parallel Tempering Trace. Sample trace from parallel tempering, showing a subsection of parameters. Each colour is a chain at a different temperature, where the main chain is pink and the chain at

the highest temperatures is red. The chains are thinned to 1:10. Parameters are: β_{RSV} - RSV transmission rate, β_{INF} - Influenza transmission rate, $R_{detect5}$ - RSV proportion detected in ages 2 to 4, propR_1 - $\delta_{RSV,1}$ - proportion infected with RSV at the start of season 1, sig - σ - strength of interaction, ρ - $\rho - 1/\text{duration}$ of interaction, inf_sus_1 - η_1 - susceptibility parameter defining susceptibility to influenza at the start of season 1 (see supplement section 6), overdispersion - k - overdispersion parameter for negative binomial, Dual_mult - K_{Dual} - multiplier for the proportion reported if dual infected as opposed to RSV infected.



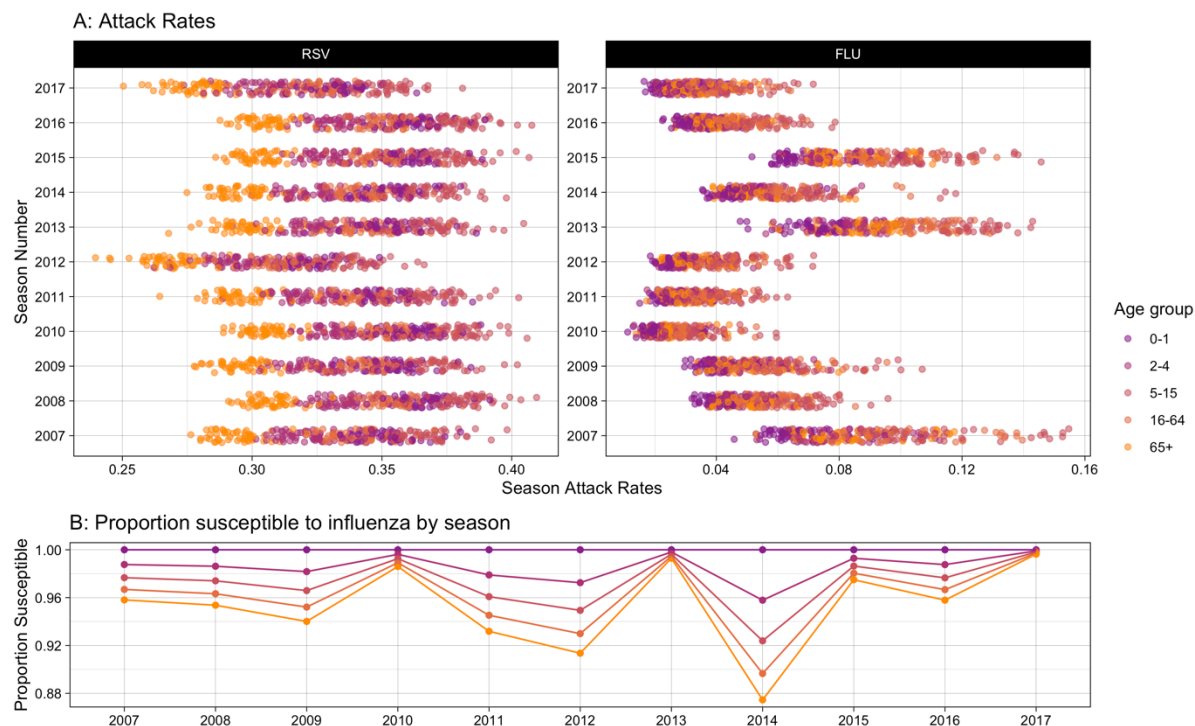
Appendix B Figure S4: Posterior Density. Density of fitted parameters from the final sample.



Appendix B Figure S5: Posterior parameter estimates, split by the value of sigma (interaction parameter)

B.8 Attack Rates

Figure S5 shows the Attack Rates for each virus, season and age group, as well as the susceptibility to influenza at the start of the season by age group, calculated from 50 posterior samples.

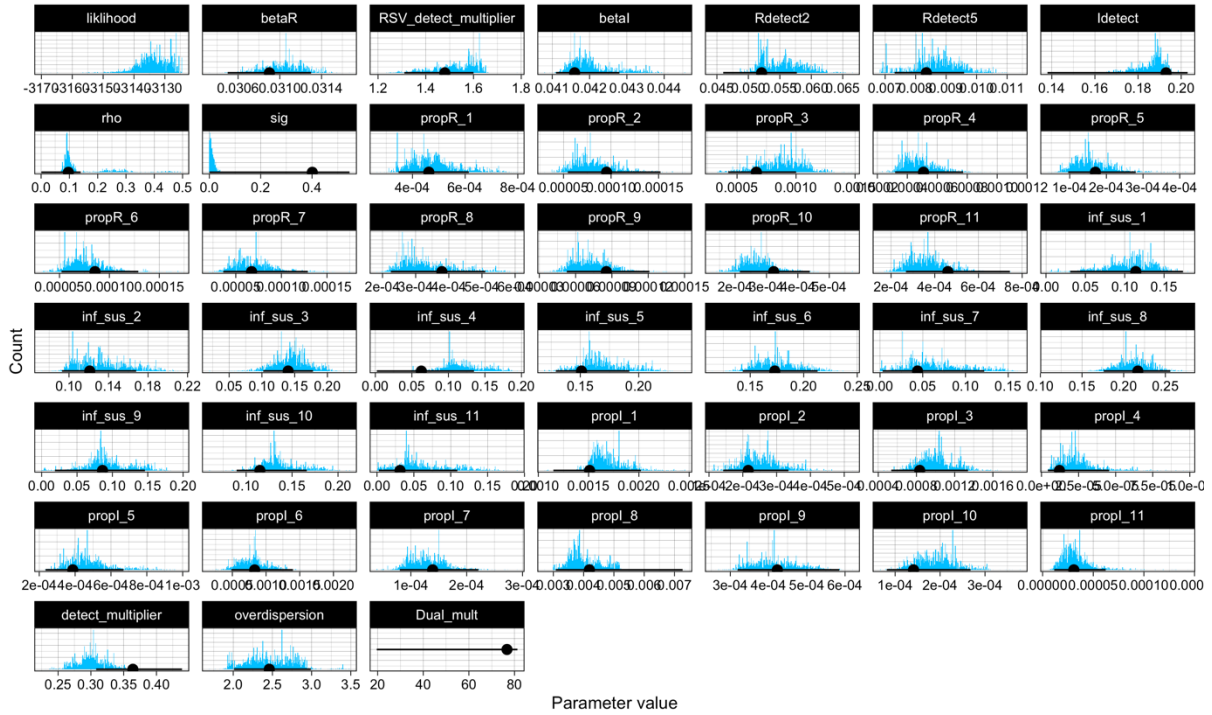


Appendix B Figure S6: Modelled Output. A) Season attack rates for influenza and RSV by age group. B) Proportion susceptible to influenza at the beginning of the season for each year by age group, using the median value of the posterior samples. Each year the susceptibility of each age group is defined by one parameter in an exponential function, see supplement for details.

B.9 Sensitivity to severity of dual infected cases

We tested the assumption of the severity of dual infected cases, by rerunning the fit without the parameter that multiplied the proportion of RSV detected to give a new dual infection detection rate. Instead the dual infections had the same reporting rate as for RSV. This set of chains were run for 100000 iterations and 50000 was discarded as burnin, and then the remaining samples were thinned to 1 in 10. Cross-protection estimates overlapped with estimates of the 'no interaction' mode in the main model, with the posterior for interaction at 0.008 (95% CrI 0.00 - 0.04) compared to 0.004 (95% CrI 0.000 - 0.046).

A: Posterior estimates

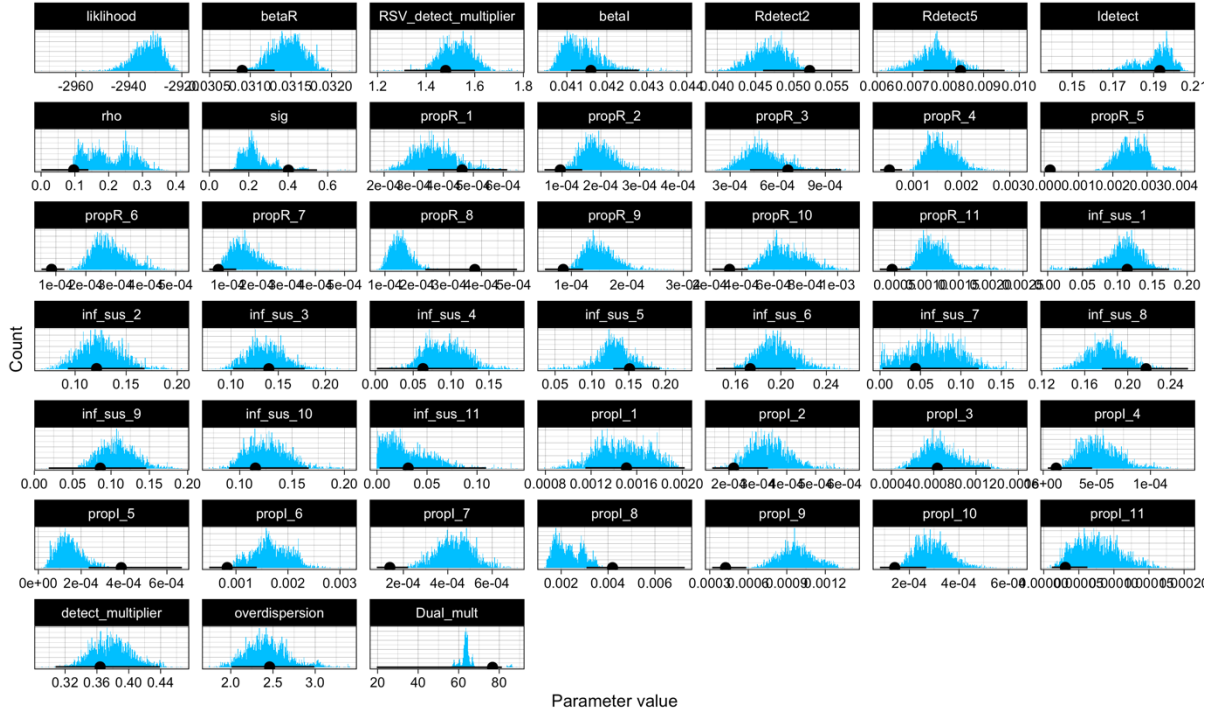


Appendix B Figure S7:Parameter Density. Density of fitted parameters from the final sample. Black lines show the median and 95% CrI for the main model run.

B.10 Prior Sensitivity

As a sensitivity analysis, we reran the model fit with a prior for a high strength of interaction (normal distribution, mean = 0.8, standard deviation = 0.15). This is due to the existing evidence of cross-protection. Figure S6 shows the posterior estimates for the parameters. This set of chains were run for 100000 iterations and 25000 was discarded as burnin, and then the remaining samples were thinned to 1 in 10. Cross-protection estimates overlapped with estimates of the ‘moderate interaction’ mode in the main model, with the posterior for interaction at 0.22 (95% CrI 0.13 - 0.47) compared to 0.41 (95% 0.36 - 0.54) and the duration of cross-protection at 5.2 days (95% CrI 3.1 - 10) compared to 10.0 days (95% CrI 7.1 -12.8 days).

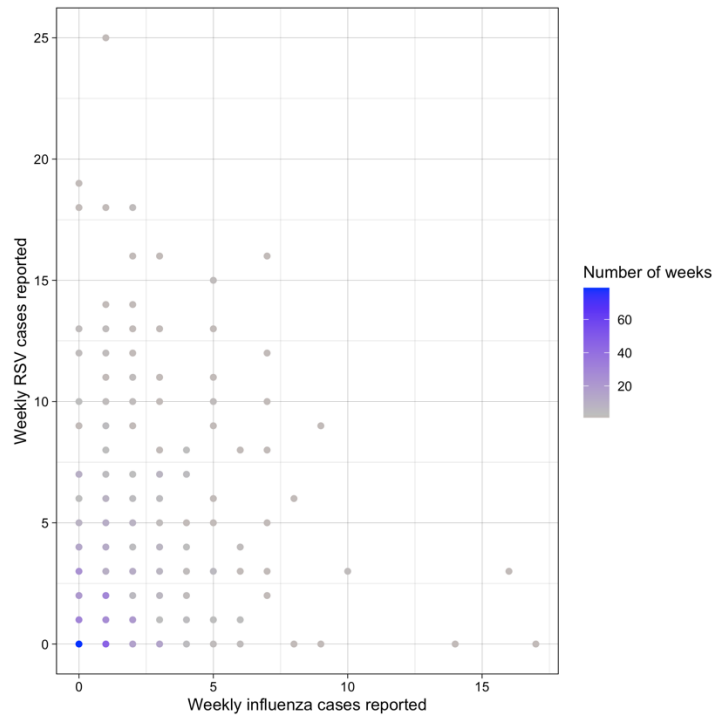
A: Posterior estimates



Appendix B Figure S8: Parameter Density with interaction prior. Density of fitted parameters from the model with a prior for strong cross-protection.

B.11 Modelled correlation

Figure S8 shows the correlation between weekly cases of influenza and RSV reported from one sample of the model output. (cf. input data Figure S1, which shows the same overall trend).



Appendix B Figure S8: Model version of Figure S1. Scatter plot of weekly influenza and RSV cases reported in the model over the whole time period.

1. Diekmann, O., Heesterbeek, J. A. P. & Roberts, M. G. The construction of next-generation matrices for compartmental epidemic models. *J. R. Soc. Interface* **7**, 873–85 (2010).
2. Henderson, F. W., Collier, A. M., Clyde, W. A. & Denny, F. W. Respiratory-Syncytial-Virus Infections, Reinfections and Immunity. *N. Engl. J. Med.* **300**, 530–534 (1979).
3. Glezen, W. P., Paredes, A. & Taber, L. H. Influenza in Children. *JAMA* **243**, 1345–1345 (1980).

Supplementary Information for
**“How immunity from and interaction with seasonal coronaviruses
 can shape SARS-CoV-2 epidemiology”**

Naomi R Waterlow^{1,}, Edwin van Leeuwen^{1,2}, Nicholas G. Davies¹, CMMID COVID-19 working group¹,
 Stefan Flasche¹, Rosalind M Eggo¹.*

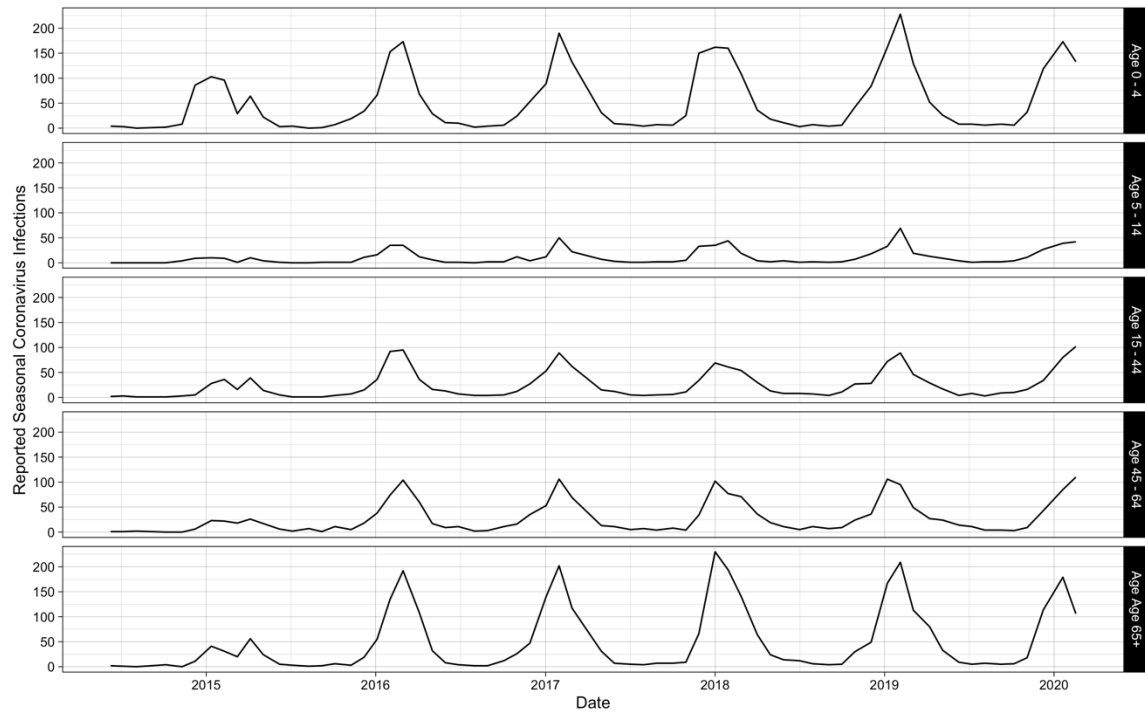
¹ *Centre for Mathematical Modeling of Infectious Disease, London School of Hygiene and Tropical
 Medicine*

² *Statistics, Modelling and Economics Department, Public Health England, London, UK*

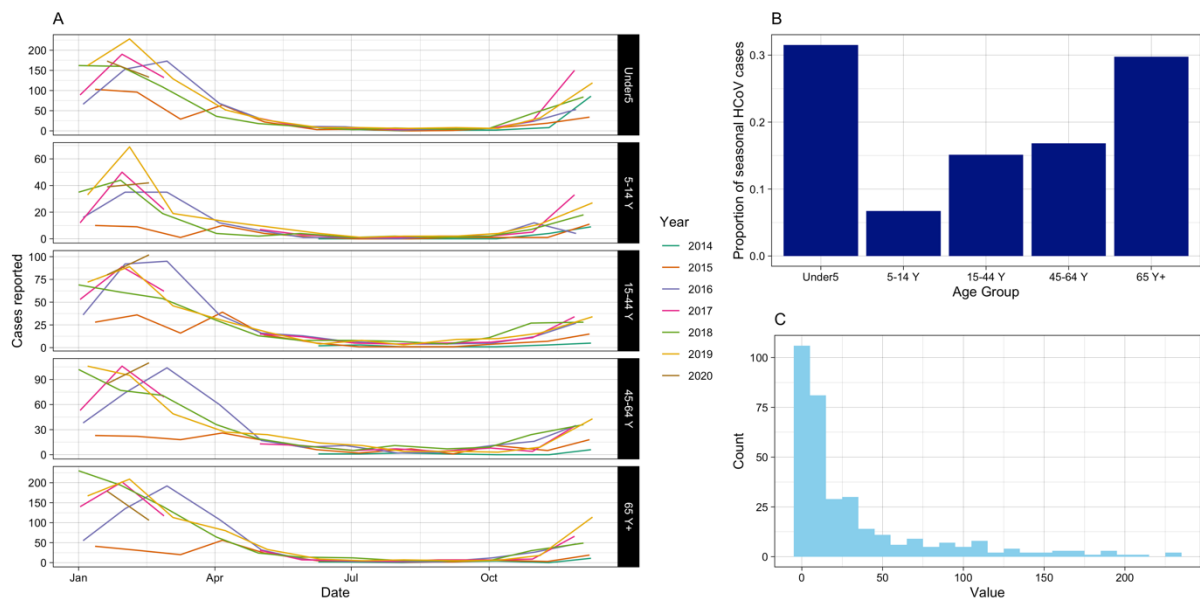
Appendix C	Supplementary material for Chapter 4	218
C.1	Data.....	219
C.2	Model equations.....	220
C.3	R ₀ calculations.....	223
C.4	Parallel Tempering.....	226
C.5	Attack Rates.....	229
C.6	Simulating lockdown.....	230
C.7	SARS-CoV-2 death simulations.....	231
C.8	Sensitivity - Duration of immunity.....	231
C.9	Sensitivity - Excluding 2014 season.....	232
C.10	Sensitivity - Only beta-coronaviruses.....	234
C.11	Comparison with existing estimates.....	236
C.12	References.....	238

C.1 Data

We excluded one data point (April 03, 2017) as it was a duplicate of January 30, 2017, and due to the trend in the epidemic we assumed that January 30, 2017 was the correct one.

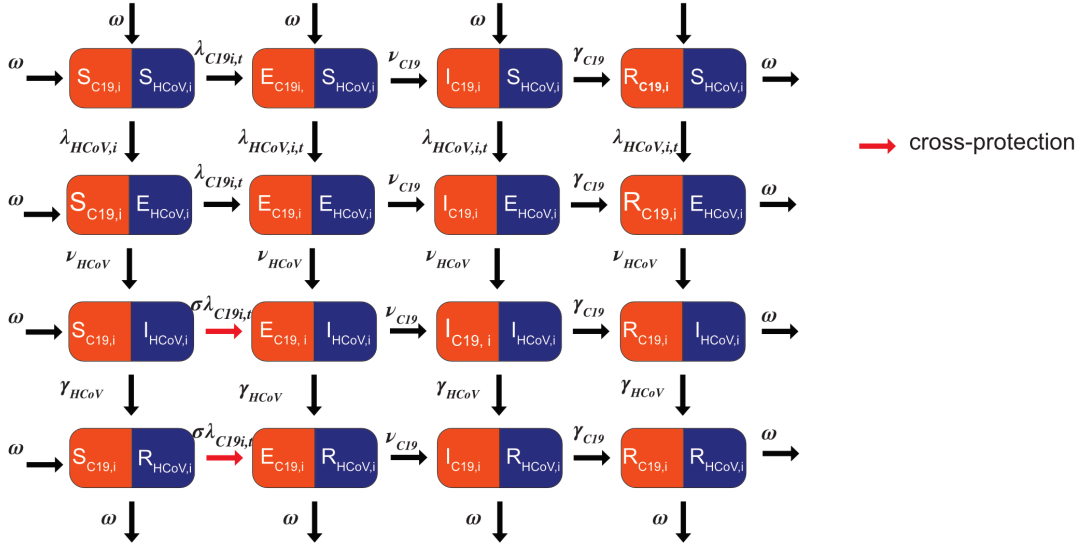


Appendix C Figure S1: Seasonal Coronavirus reported cases



Appendix C Figure S2: A) Seasonality of seasonal coronavirus reports by age and year. B) Proportion of all seasonal coronavirus cases reported by age group. C) Histogram of the monthly number of seasonal coronavirus cases reported

C.2 Model equations



Appendix C Figure S3: Model Figure

$$\lambda_{HCov,i,t} = \sum_{j=1}^{j=N} \left(\left(\frac{A_{HCov} * \beta_{HCov}}{R_{0,HCov}} \right) * \cos\left(\frac{2\pi}{52*7} - \phi\right) + \beta_{HCov} \right) * \alpha_{i,j} * I_{HCov,j} \quad (1)$$

$$\lambda_{C19,i,t} = \sum_{j=1}^{j=N} \left(\left(\frac{A_{C19} * \beta_{C19}}{R_{0,C19}} \right) * \cos\left(\frac{2\pi}{52*7} - \phi\right) + \beta_{C19} \right) * \alpha_{i,j} * I_{C19,j} \quad (2)$$

$$\begin{aligned} \frac{dSS_i}{dt} = & -\lambda_{C19,i} SS_i - \lambda_{HCov,i,t} SS_i + \omega_{C19} RS_i + \omega_{HCov} SR_i + \mu_{a,i} SS_{i-1} - \mu_{a,i+1} SS_i + \mu_{b,i} \\ & - \mu_{d,i} SS_i \end{aligned}$$

$$\begin{aligned} \frac{dES_i}{dt} = & -\nu_{C19} ES_i - \lambda_{HCov,i,t} ES_i + \lambda_{C19,i} SS_i + \omega_{HCov} ER_i + \mu_{a,i} ES_{i-1} - \mu_{a,i+1} ES_i \\ & - \mu_{d,i} ES_i \end{aligned}$$

$$\frac{dIS_i}{dt} = -\gamma_{C19} IS_i - \lambda_{HCov,i,t} IS_i + \nu_{C19} ES_i + \omega_{HCov} IR_i + \mu_{a,i} IS_{i-1} - \mu_{a,i+1} IS_i - \mu_{d,i} IS_i$$

$$\frac{dRS_i}{dt} = -\omega_{C19} RS_i - \lambda_{HCov,i,t} RS_i + \gamma_{C19} IS_i + \omega_{HCov} RR_i + \mu_{a,i} RS_{i-1} - \mu_{a,i+1} RS_i - \mu_{d,i} RS_i$$

$$\begin{aligned}\frac{dSE_i}{dt} = & -\lambda_{C19,i}SE_i - \nu_{HCov}SE_i + \omega_{C19}RE_i + \lambda_{HCov,i,t}SS_i + \mu_{a,i}SE_{i-1} - \mu_{a,i+1}SE_i \\ & - \mu_{d,i}SE_i\end{aligned}$$

$$\begin{aligned}\frac{dEE_i}{dt} = & -\nu_{C19}EE_i - \nu_{HCov}EE_i + \lambda_{C19,i}SE_i + \lambda_{HCov,i,t}ES_i + \mu_{a,i}EE_{i-1} - \mu_{a,i+1}EE_i \\ & - \mu_{d,i}EE_i\end{aligned}$$

$$\frac{dIE_i}{dt} = -\gamma_{C19}IE_i - \nu_{HCov}IE_i + \nu_{C19}EE_i + \lambda_{HCov,i,t}RS_i + \mu_{a,i}IE_{i-1} - \mu_{a,i+1}IE_i - \mu_{d,i}IE_i$$

$$\begin{aligned}\frac{dRE_i}{dt} = & -\omega_{C19}RE_i - \nu_{HCov}RE_i + \gamma_{C19}IE_i + \lambda_{HCov,i,t}RS_i + \mu_{a,i}RE_{i-1} - \mu_{a,i+1}RE_i \\ & - \mu_{d,i}RS_i\end{aligned}$$

$$\frac{dSI_i}{dt} = -\sigma\lambda_{C19,i}SI_i - \gamma_{HCov}SI_i + \omega_{C19}RI_i + \nu_{HCov}SE_i + \mu_{a,i}SI_{i-1} - \mu_{a,i+1}SI_i - \mu_{d,i}SI_i$$

$$\frac{dEI_i}{dt} = -\nu_{C19}EI_i - \gamma_{HCov}EI_i + \sigma\lambda_{C19,i}SI_i + \nu_{HCov}EE_i + \mu_{a,i}EI_{i-1} - \mu_{a,i+1}EI_i - \mu_{d,i}EI_i$$

$$\frac{dII_i}{dt} = -\gamma_{C19}II_i - \gamma_{HCov}II_i + \nu_{C19}EI_i + \nu_{HCov}IE_i + \mu_{a,i}II_{i-1} - \mu_{a,i+1}II_i - \mu_{d,i}II_i$$

$$\frac{dRI_i}{dt} = -\omega_{C19}RI_i - \gamma_{HCov}RI_i + \gamma_{C19}II_i + \nu_{HCov}RE_i + \mu_{a,i}RI_{i-1} - \mu_{a,i+1}RI_i - \mu_{d,i}RI_i$$

$$\begin{aligned}\frac{dSR_i}{dt} = & -\sigma\lambda_{C19,i}SR_i - \omega_{HCov}SR_i + \omega_{C19}RR_i + \gamma_{HCov}SI_i + \mu_{a,i}SR_{i-1} - \mu_{a,i+1}SR_i \\ & - \mu_{d,i}SR_i\end{aligned}$$

$$\begin{aligned}\frac{dER_i}{dt} = & -\nu_{C19}ER_i - \omega_{HCov}ER_i + \sigma\lambda_{C19,i}SR_i + \gamma_{HCov}EI_i + \mu_{a,i}ER_{i-1} - \mu_{a,i+1}ER_i \\ & - \mu_{d,i}ER_i\end{aligned}$$

$$\frac{dIR_i}{dt} = -\gamma_{C19}IR_i - \omega_{HCov}IR_i + \nu_{HCov}ER_i + \gamma_{HCov}II_i + \mu_{a,i}IR_{i-1} - \mu_{a,i+1}IR_i - \mu_{d,i}IR_i$$

$$\frac{dRR_i}{dt} = -\omega_{C19}RR_i - \omega_{HCov}RR_i + \gamma_{C19}IR_i + \gamma_{HCov}RI_i + \mu_{a,i}RR_{i-1} - \mu_{a,i+1}RR_i - \mu_{d,i}RR_i$$

States

The first letter of the state indicates the state for SARS-CoV-2, the second letter indicates the state for HCoVs.

S: Susceptible

E: Exposed

I: Infected

R: Recovered

Subscripts

C19: SARS-CoV-2

HCoV: Seasonal HCoVs

i, j: age groups

t: time

Appendix C Table S1: Model Parameters

Parameter type	Parameter	Symbol	Value	Reference
Seasonal HCoV	Basic Reproduction number	$R_{0,HCoV}$	Fitted. Limits: 1-8.5	Wide range
	Transmission rate	β_{HCoV}	Fitted	Based on R_0 calculation (supplement)
	Latent period	$1/\nu_{HCoV}$	2.5 days	1,2
	Duration of infectiousness	$1/\gamma_{HCoV}$	5 days	1
	Incubation period (time to symptoms)	$1/\delta 1_{HCoV}$	2 days	3
	Reporting delay (symptom to report)	$1/\delta 2_{HCoV}$	3 days	Based on influenza model ⁴
	Age-specific reporting proportion	$\mu_{HCoV,i}$	Fitted. Limits 0-1. Proposed on log odds scale.	
	Seasonal forcing amplitude	A	Fitted. Limits: 0 - 2	
	Seasonal forcing timing	ϕ	Fitted. Limits: - (52*7)- (52*7)	

	Immunity duration	$1/\omega$	Fitted. Limits: 100 - 3000	Covers range of 100 days to over 8 years
SARS-CoV-2	Basic Reproduction number	$R_{0,C19}$	Fitted	Based on R_0 calculations (see supplement).
	Transmission rate	β_{C19}	Fitted	
	Effective Reproduction Number	$R_{eff,C19}$	Fitted	R_0 * proportion susceptible (see supplement)
	Latent period	$1/\nu_{C19}$	3 days	¹
	Duration of infectiousness	$1/\gamma_{C19}$	5 days	⁵
	Time between infectiousness (entering I compartment) and death	$1/\delta_{C19}$	22 days (split over two compartments, Erlang distributed)	⁶
	Age-specific infection fatality proportions (age groups 0-4, 5-14, 15-44, 45-64, 65+)	$\mu_{C19,i}$	0.00004, 0.00004, 0.00024, 0.00441, 0.06720	As in Levin ⁷ , weighted by model population sizes
	Adult (15-64 years) introduction rate	$1/\eta$	Fitted	
	Duration of immunity	$1/\omega$	Fitted	Assumed equal to HCoV waning rate
Demographic	Birth rate	μ_b	640 370 per year	ONS statistical bulletin 2019 ⁸
	Death rate	μ_d	640 370 per year	Equal to birth rate to maintain constant population
	Population size	N	59 439 840	ONS 2019 population estimates for England and Wales, 5-year age bands ⁹

C.3 R_0 calculations

We used the method described by Diekmann *et al.* (2009)¹¹ to calculate the R_0 for each virus. The dominant eigenvalue of the matrix is the R_0 of the matrix $-T\Sigma^{-1}$, where T is the transmission part of the Jacobian matrix, describing new infections and Σ is the transition part, describing changes in the infectious state. See reference for further details. For seasonal HCoVs we used the base transmission rate.

For each age group, compartments in the matrix are SE and SI, and ES and IS, as we calculate the R_0 assuming no cross-protection. The first row/column represents the E compartments, and the second row represents the I compartment for the first age group. Only the transmissions for the first age group are shown. Three dots (...) represent the pattern continuing, one dot (.) represents equations not shown because they do not refer to the first age group.

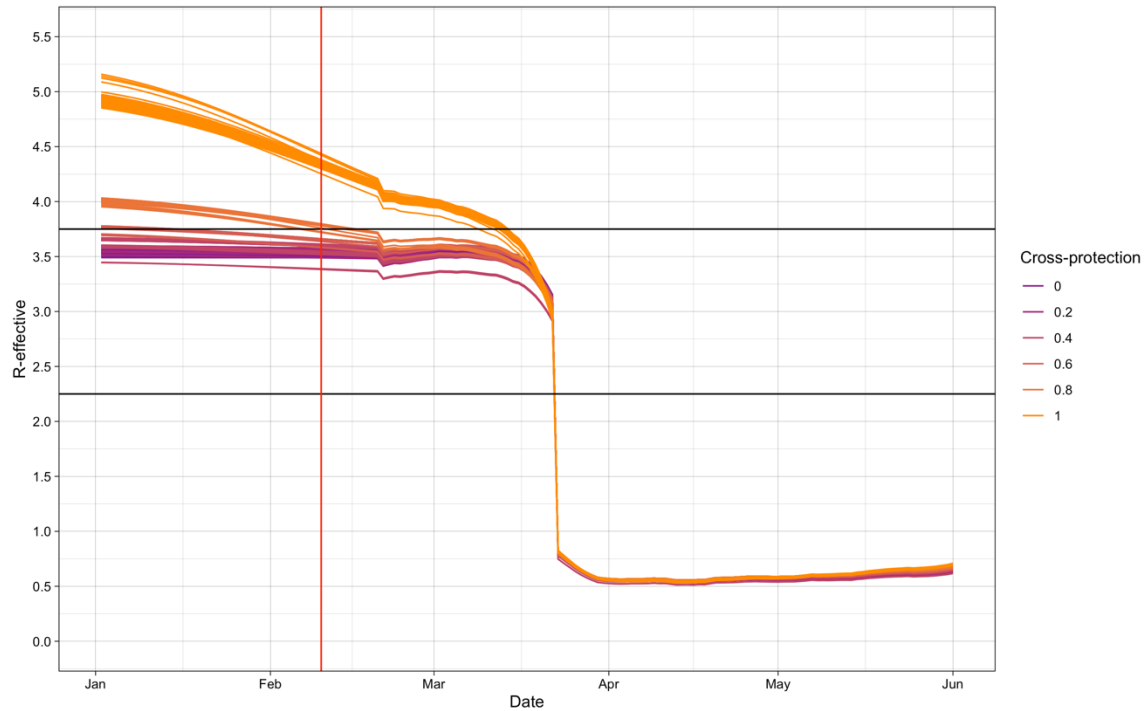
$$T_{C19} = \begin{pmatrix} 0 & \beta_{C19} \alpha_{i,j} & 0 & \beta_{C19} \alpha_{i,j} & \dots & \beta_{C19} \alpha_{i,j} \\ 0 & 0 & 0 & 0 & \dots & 0 \\ 0 & \beta_{C19} \alpha_{i,j} & . & . & . & . \\ 0 & 0 & . & . & . & . \\ 0 & \beta_{C19} \alpha_{i,j} & . & . & . & . \\ \dots & \dots & . & . & . & . \\ 0 & \beta_{C19} \alpha_{i,j} & . & . & . & . \end{pmatrix}$$

$$T_{HCov} = \begin{pmatrix} 0 & \beta_{HCov} \alpha_{i,j} & 0 & \beta_{HCov} \alpha_{i,j} & \dots & \beta_{HCov} \alpha_{i,j} \\ 0 & 0 & 0 & 0 & \dots & 0 \\ 0 & \beta_{HCov} \alpha_{i,j} & . & . & . & . \\ 0 & 0 & . & . & . & . \\ 0 & \beta_{HCov} \alpha_{i,j} & . & . & . & . \\ \dots & \dots & . & . & . & . \\ 0 & \beta_{HCov} \alpha_{i,j} & . & . & . & . \end{pmatrix}$$

$$\Sigma_{C19} = \begin{pmatrix} -\nu_{C19} - \mu\alpha_i & 0 & 0 & \dots & 0 \\ -\nu_{C19} & -\gamma_{C19} - \mu\alpha_i & 0 & \dots & 0 \\ \mu\alpha_{i+1} & 0 & . & . & . \\ 0 & \mu\alpha_{i+1} & . & . & . \\ 0 & 0 & . & . & . \\ \dots & \dots & . & . & . \\ 0 & 0 & . & . & . \end{pmatrix}$$

$$\Sigma_{HCoV} = \begin{pmatrix} -\nu_{HCoV} - \mu\alpha_i & 0 & 0 & \dots & 0 \\ -\nu_{HCoV} & -\gamma_{HCoV} - \mu\alpha_i & 0 & \dots & 0 \\ \mu\alpha_{i+1} & 0 & \cdot & \cdot & \cdot \\ 0 & \mu\alpha_{i+1} & \cdot & \cdot & \cdot \\ 0 & 0 & \cdot & \cdot & \cdot \\ \dots & \dots & \cdot & \cdot & \cdot \\ 0 & 0 & \cdot & \cdot & \cdot \end{pmatrix}$$

For the SARS-CoV-2 simulations we calculated the R_{eff} through time (Figure S1), which is influenced by the R_0 , the level of cross-protection and the seasonal HCoV circulation. The $R_{effective}$ is the largest eigenvalue of the NGM where each row is multiplied by the proportion susceptible in that age group. Estimates for the $R_{effective}$ in the UK of SARS-CoV-2 before lockdown were between 2.25 and 3.75, so we used these as boundaries. During this period it was only the highest level of cross-protection that did not have an appropriate R_0 .



Appendix C Figure S4: $R_{\text{effective}}$ values over time for SARS-CoV-2. Blue lines indicate $R_{\text{effective}}$ for simulations at different levels of cross-protection. Black lines show the $R_{\text{effective}}$ limits of 2.25 and 3.75 and the red line shows the date of SARS-CoV-2 introduction.

C.4 Parallel Tempering

We proposed chains to swap with the chain of the next lowest temperature every 5 iterations of the MCMC. The highest and lowest temperatures were fixed at 1000 and 1 (the null chain). The number of chains was then adjusted to achieve an acceptance rate of swaps of between 0.15 and 0.25 . Swaps were accepted based on our swapping equation, adapted from Vousden *et al*¹² following the equation:

$$R = e^{\left(\frac{LL(i) - LL(j)}{\tau_j - \tau_i}\right)}$$

Where

$$\tau_i = \frac{1}{T_i}$$

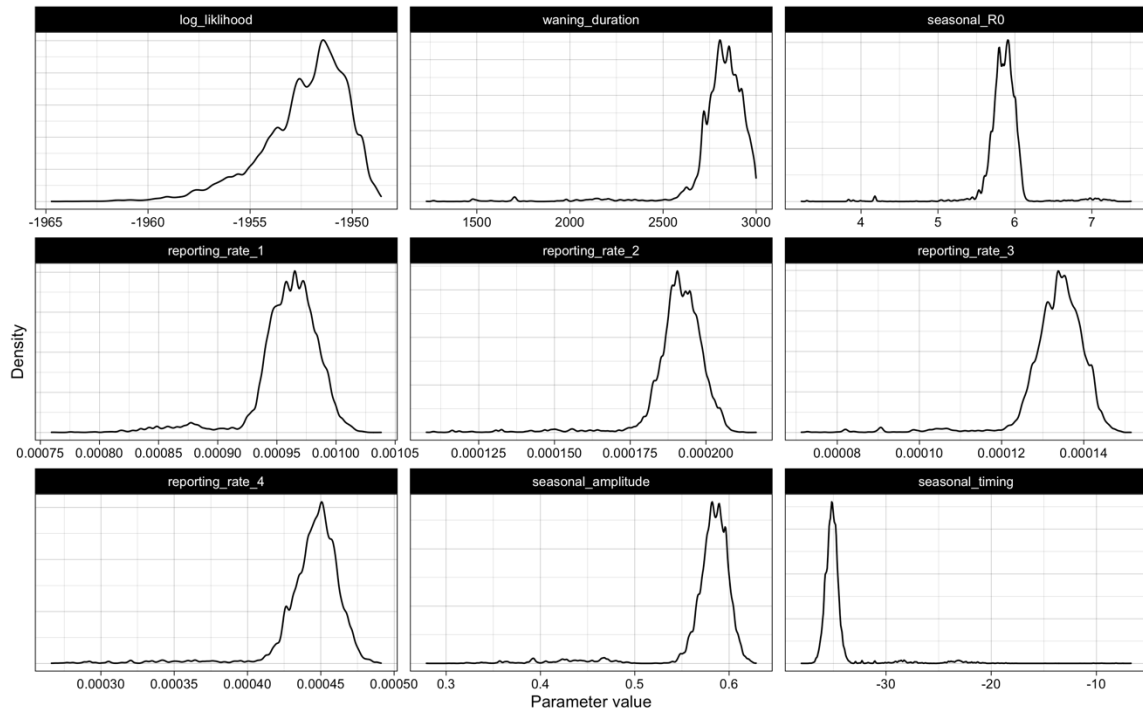
And T_i is the temperature of chain i , and $LL(i)$ is the log likelihood of chain i .

We then ran the parallel tempering algorithm from multiple different start values, each with 16 chains. Within each chain parameters were proposed using a covariance matrix. This resulted in two

converged chains, which we confirmed by checking that the Gelman-Rubin statistic¹³ was <1.1 . We discarded 12000 iterations of each as burn in and then combined the samples from the two converged regions to increase the sample size. A set of chains is shown in Figure S2. Figure S3 shows the posterior distribution for all parameters and they are summarised in Table S1.



Appendix C Figure S5: Trace plots of one replicate showing all 16 chains. Each colour is one chain, with bright pink being the coolest (null) chain.

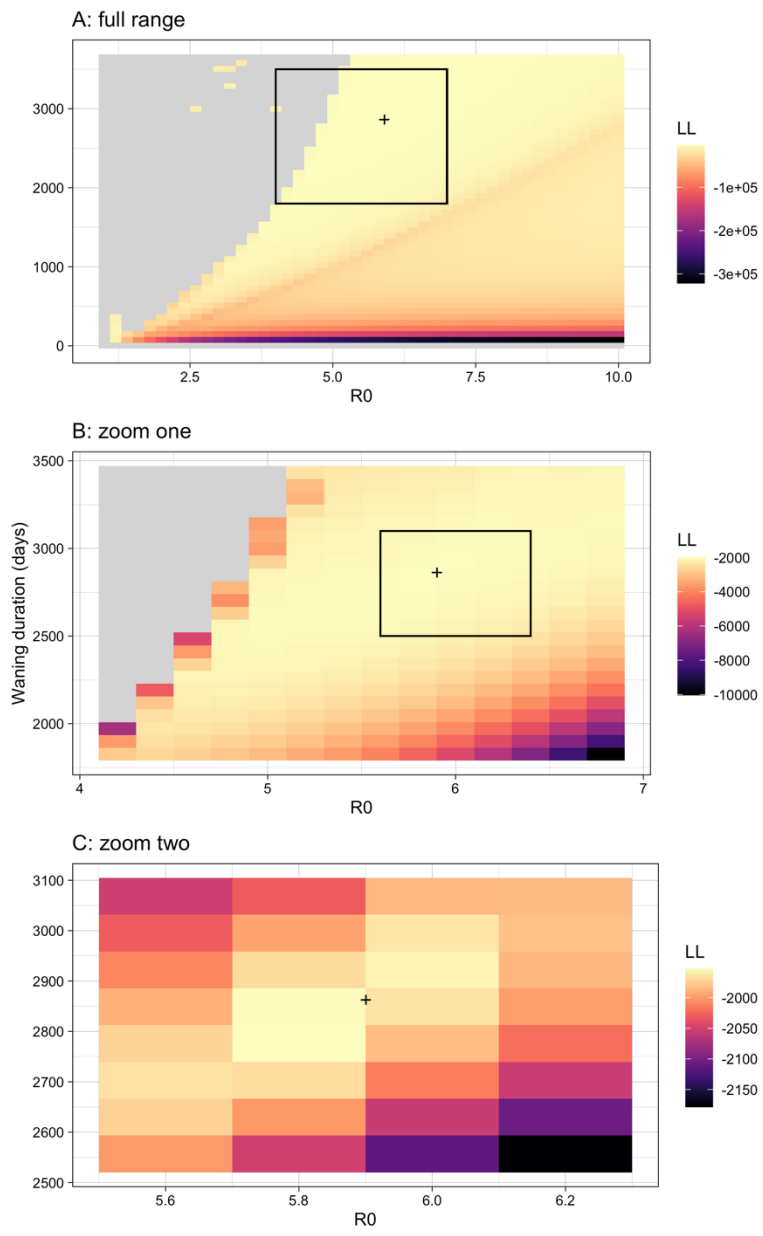


Appendix C Figure S6: Posterior distributions of fitted parameters for the HCoV fit.

Appendix C Table S2: Median and 95% quantiles of the posterior distributions of fitted HCoV parameters.

Parameter	Symbol	Median (95% CrI)
Basic Reproduction number	$R_{0,HCoV}$	5.9 (5.5 - 6.2)
Immunity duration	ω	7.8 (6.3 - 8.2)
Age-specific reporting proportion 0-4	$\mu_{HCoV,i}$	0.00096 (0.00087 - 0.00100)
Age-specific reporting proportion 5 - 14, 45-64	$\mu_{HCoV,i}$	0.00019 (0.00016 - 0.00020)
Age-specific reporting proportion 15-44	$\mu_{HCoV,i}$	0.00013 (0.00011 - 0.00014)
Age-specific reporting proportion 65+	$\mu_{HCoV,i}$	0.00058 (0.00043 - 0.00061)
Seasonal forcing amplitude	A	0.58 (0.42 - 0.61)
Seasonal forcing timing	φ	-35.1 (-36.2 - -24.1)

Figure S6 shows a heatmap of the likelihood of the model at different value of R_0 and durations of immunity waning. One sample from the posterior of the fit was taken, and all parameter values apart from the R_0 and the duration of waning were kept constant. The log likelihood was then calculated for each combination of R_0 and waning durations. The fitted value is shown with a +.



Appendix C Figure S7: Likelihood plane with varying R_0 and duration of waning. A) shows the full range B) and C) show zoomed in areas. Colour indicates the likelihood value. The black rectangles show the area zoomed in on and the '+' symbol shows the estimated values from the parallel tempering fits.

C.5 Attack Rates

Average annual attack rates for the seasonal HCoV are shown in Table S2. This is the mean attack rate for each age group, averaged over 100 samples from the joint posterior and the last 5 years in our seasonal HCoV fit.

Appendix C Table S 3: Mean attack rates by age group. Values given are mean across 100 random samples from the posterior and the last 5 years of the seasonal HCoV fit.

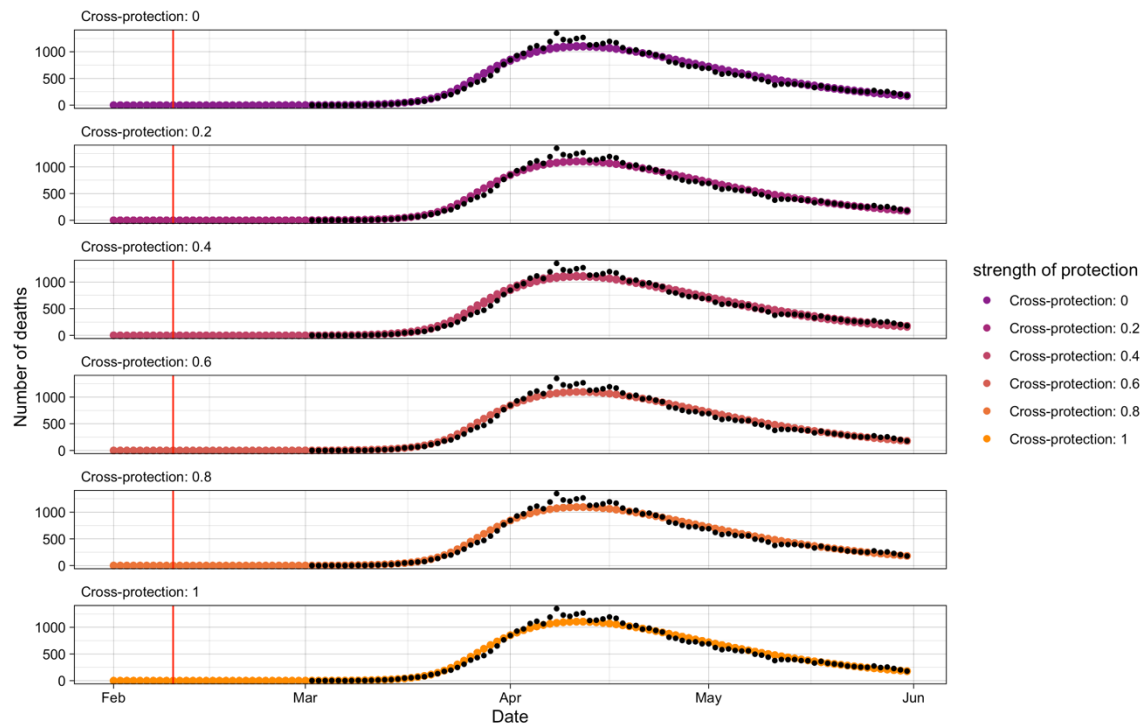
Age group	Attack rate (%)
< 5	19.9
5 - 14	13.9
15 - 44	11.0
45 - 64	10.4
65+	9.3

C.6 Simulating lockdown

Due to the non-pharmaceutical interventions implemented in this period (“lockdown”), we adjust the contact matrices, which are split into three categories: school contacts, household contacts and other contacts. Other contacts included all other categories reported in the POLYMOD dataset. We then adjusted the contacts as follows.

- From February 21, 2020 (when google mobility data first becomes available), we adjust our ‘other’ contacts group by the average change in retail/recreation, workplace, grocery/pharmacy and transit stations, according to the Google Mobility UK records
- From March 23, 2020 (lockdown including school closures), school contacts are reduced to 0 with no re-attribution of those contacts.
- From March 23, 2020 (lockdown), Other and household contacts are multiplied by a ‘social distancing factor’ which we set at 0.33. This simulates other interventions such as social distancing, increased hand washing and mask wearing, and we chose the value based on being within a plausible range and appropriate looking simulations. We adapt households as the original contact matrix includes all household interactions, including visitors.
- Importations occur from the date of SARS-CoV-2 introduction (February 15, 2020) in the UK until the March 23, 2020 (lockdown). The date of SARS-CoV-2 introduction was chosen as a plausible value that allowed the simulated deaths to peak at the right time of year.

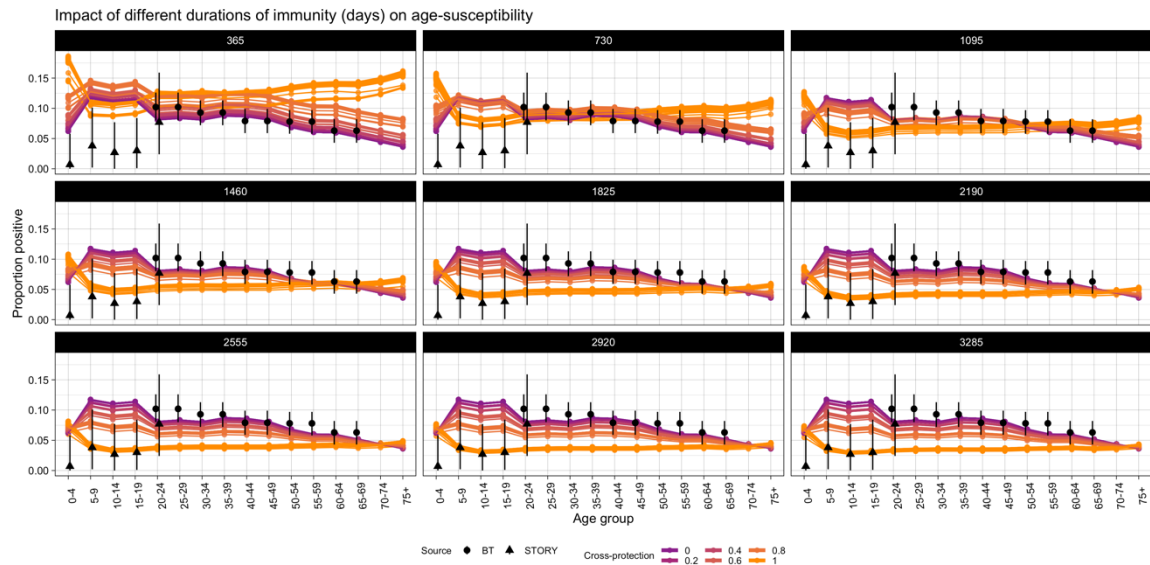
C.7 SARS-CoV-2 death simulations



Appendix C Figure S8: Fit to deaths. SARS-CoV-2 death simulations compared to the death data, with varying strength of cross-protection. The red line indicates the date of SARS-COV-2 introduction.

C.8 Sensitivity - Duration of immunity

To assess the sensitivity of our duration of immunity on the age-susceptibility to SARS-CoV-2, we reran the 2020 simulations, varying the duration of immunity parameter between 365 days and 3285 days. All other parameters were kept constant and the same samples were used as in the original analysis. Figure S8 shows the results. In all simulations, complete cross-protection resulted in a lower age susceptibility for children, however if the immunity was less than 2 years, the pattern of immunity was different. The simulations were not able to account for the reduced susceptibility in children in any scenario.



Appendix C Figure S9: Age-specific serology. Simulated age-specific serology rates for SARS-CoV-2 by the end of May 2020. Each facet was run with a different duration of protection, displayed in the facet title, in days.

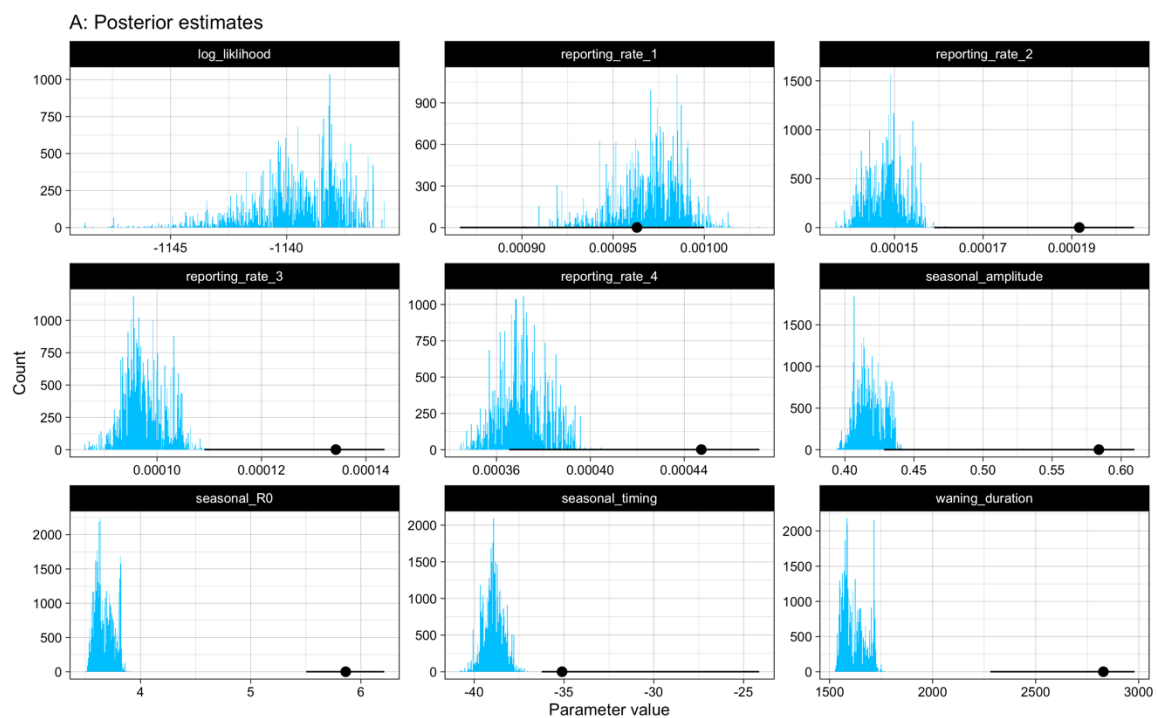
C.9 Sensitivity - Excluding 2014 season

As the 2014/15 season has a lower epidemic peak than the other seasons, we ran a sensitivity analysis by excluding data before August 2015. This is to take into account potential reduced testing in the first season. As previously, we ran the parallel tempering algorithm and removed 50,000 samples as burn in, resulting in 50,000 samples. The posterior parameter estimates differed slightly compared to the main model (Table S4), although both the estimate of the R_0 and the waning parameter were still substantially higher than previous estimates. As before, we took samples from the posterior (in this case 50), and modelled the impact on age-susceptibility to SARS-CoV-2, with varying degrees of cross-protection. The conclusions remained the same as in the main paper, where cross-protection was unable to explain the reduced susceptibility of children.

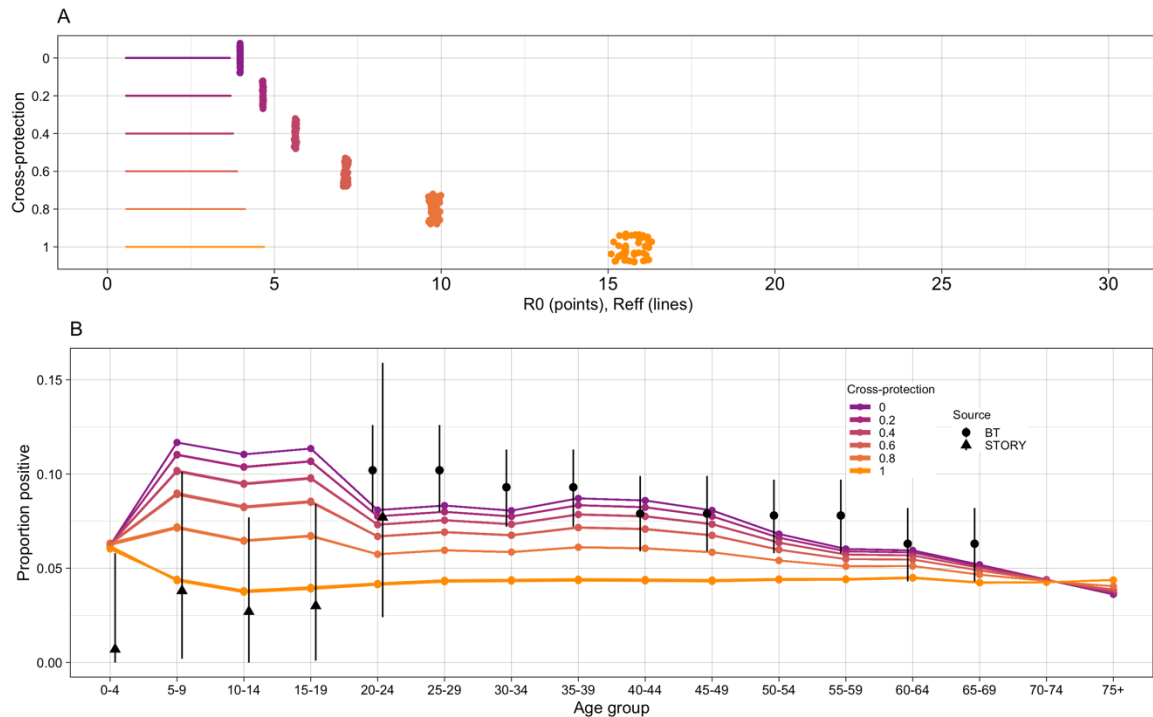
Appendix C Table S 4: Posterior parameter estimates for the sensitivity analysis excluding all data before August 2015.

Parameter	Symbol	Median (95% CrI) - excluding 2014/15	Median (95% CrI) - main model
Basic Reproduction number	$R_{0,HCoV}$	3.7 (3.6 - 3.8)	5.9 (5.5-6.2)
Immunity duration	ω	4.4 (4.3 - 4.6)	7.8 (6.3 - 8.2)
Age-specific reporting proportion 0-4	$\mu_{HCoV,i}$	0.00097 (0.00094 - 0.0010)	0.00096 (0.00087 - 0.00100)

Age-specific reporting proportion 5 - 14, 45-64	$\mu_{HCov,i}$	0.00015 (0.00014 - 0.00015)	0.00019 (0.00016 - 0.00020)
Age-specific reporting proportion 15-44	$\mu_{HCov,i}$	0.000097 (0.000092 - 0.00010)	0.00013 (0.00011 - 0.00014)
Age-specific reporting proportion 65+	$\mu_{HCov,i}$	0.00037 (0.00036 - 0.00038)	0.00058 (0.00043 - 0.00061)
Seasonal forcing amplitude	A	0.42 (0.040 - 0.43)	0.58 (0.42 - 0.61)
Seasonal forcing timing	ϕ	-39 (-39 - -38)	-35.1 (-36.2 - -24.1)



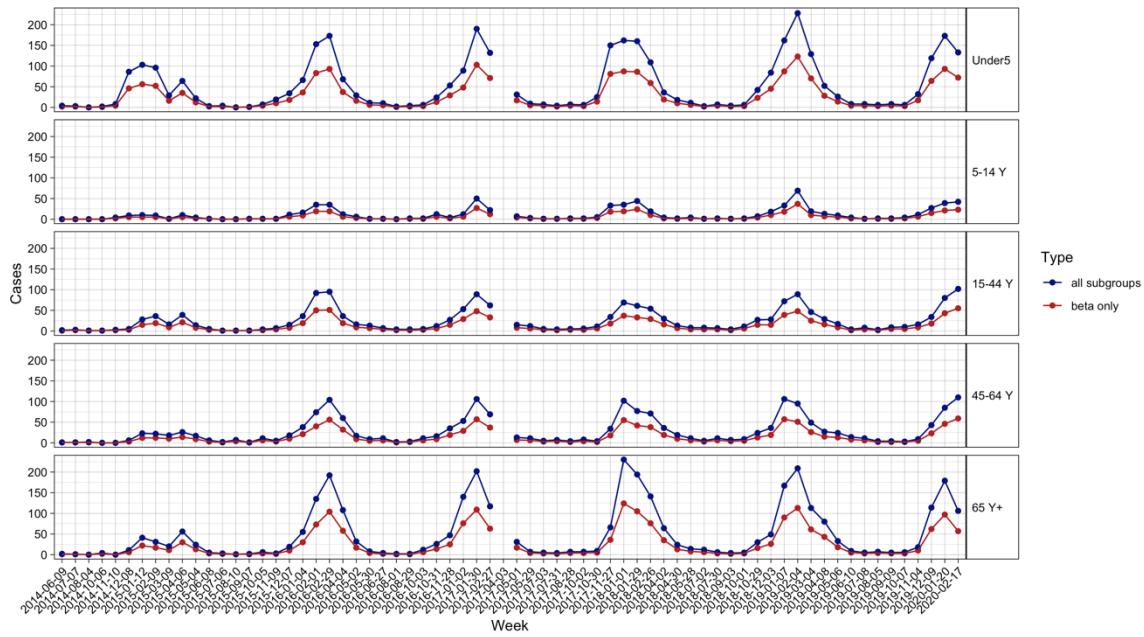
Appendix C Figure S10: Posteriors from sensitivity analysis excluding 2014/2015 season. A) Histogram of posterior estimates from the beta-coronavirus only sensitivity analysis. Black lines show the median and 95% CrI from the main model.



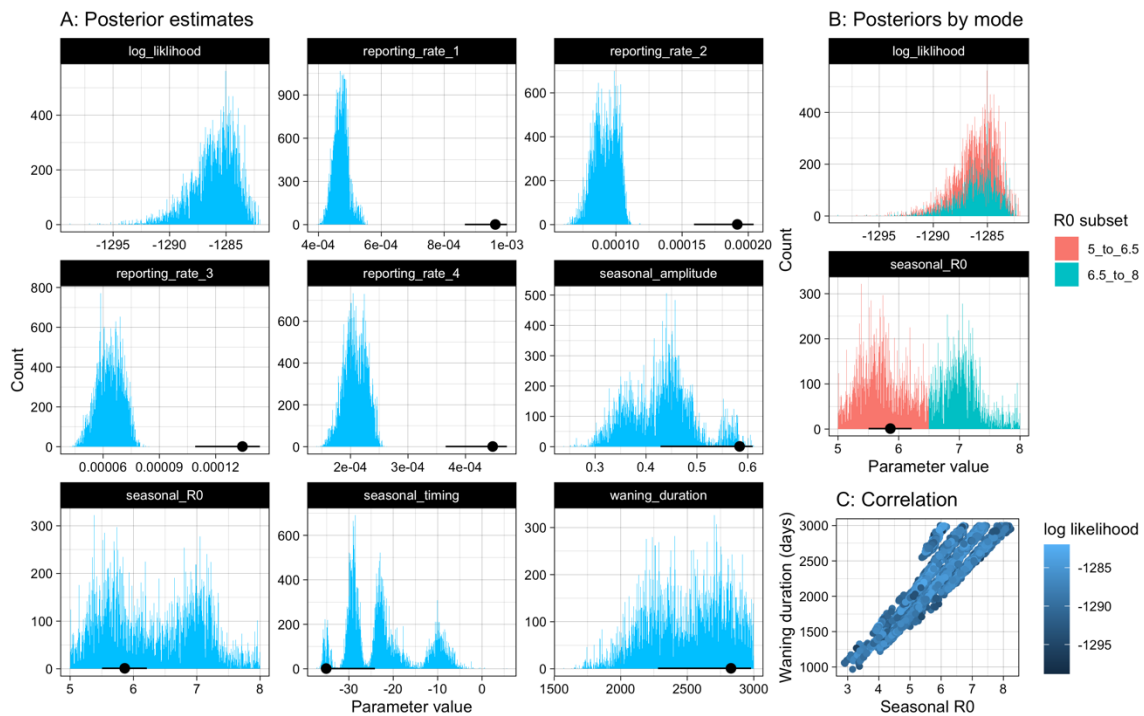
Appendix C Figure S11: Simulations excluding 2014/15 season. A) Estimated R_0 values for SARS-CoV-2 with different strengths of cross-protection. Points display the $R_{0, C19}$ and lines show the range of $R_{eff, C19}$ during the simulation. B) Simulated age-specific serology rates for SARS-CoV-2 by the end of May 2020.

C.10 Sensitivity - Only beta-coronaviruses

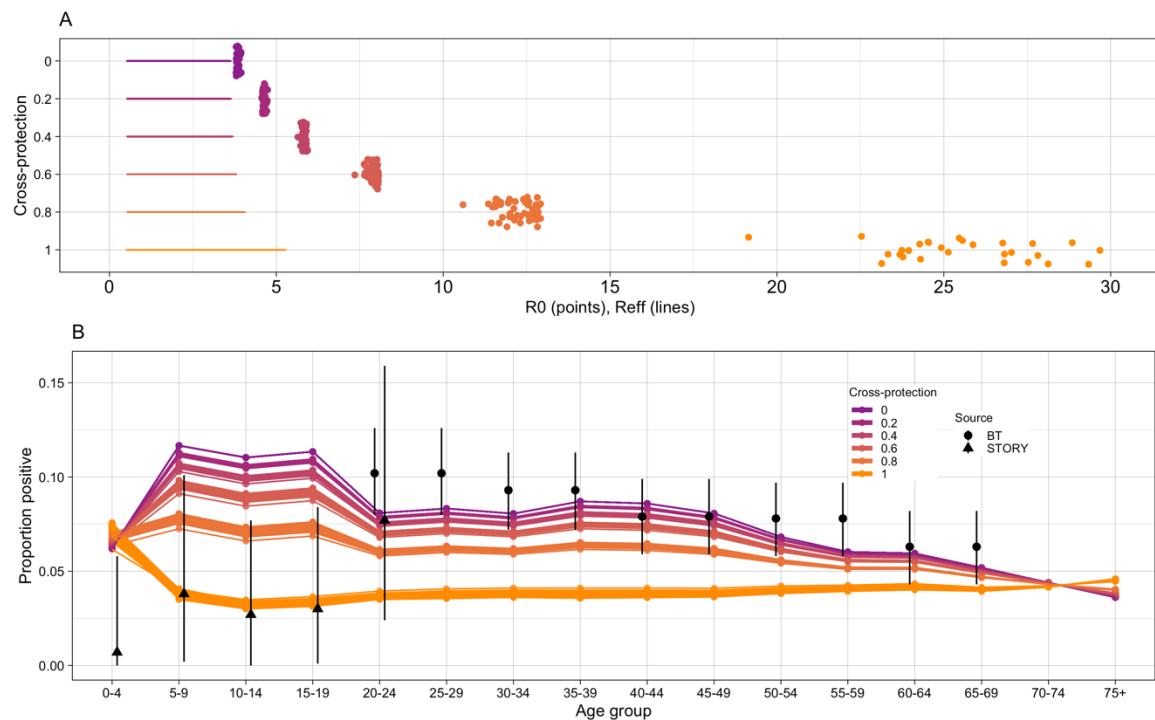
Due to the complexities of cross-subtype immunity, we ran a sensitivity analysis including only beta-coronaviruses. We fixed the number of beta-coronaviruses at 54% of the overall number of coronaviruses each month, based on subtype-specific surveillance data from 2005-2017 in Glasgow¹⁴. Case numbers were rounded to the nearest full number. We reran the model fit with parallel tempering (50'000 burn-in, 50'000 samples), and the estimated posterior parameters are shown in Figure S10A. The key parameters of the seasonal HCoV R_0 and the duration of immunity overlapped with estimates from the main model (Figure S12). However in this sensitivity analysis parameters, especially the R_0 , appear bimodal. Figure S10B shows that these two modes have equivalent likelihood, with one mode coinciding with the estimated posterior R_0 from the main analysis. We ran the SARS-CoV-2 simulations with 50 samples from these new posteriors and found the same message: cross-protection was unable to explain the reduced susceptibility of children. (Figure S11).



Appendix C Figure S12: Beta-coronavirus only data. Blue shows the original data including all subtypes, red shows the data following our assumption that only 54% of cases are beta-coronavirus cases.



Appendix C Figure S13: Posteriors from beta-coronavirus sensitivity analysis. A) Histogram of posterior estimates from the beta-coronavirus only sensitivity analysis. Black lines show the median and 95% CrI from the main model. B) Subset of parameters showing histograms of the posterior distribution split by R_0 mode. Black line shows the median and 95% CrI from the main model. C) Correlation between posterior samples of Seasonal HCoV R_0 and the waning duration.



Appendix C Figure S14: Simulations excluding alpha-coronaviruses. A) Estimated R_0 values for SARS-CoV-2 with different strengths of cross-protection. Points display the $R_{0, C19}$ and lines show the range of $R_{eff, C19}$ during the simulation. B) Simulated age-specific serology rates for SARS-CoV-2 by the end of May 2020.

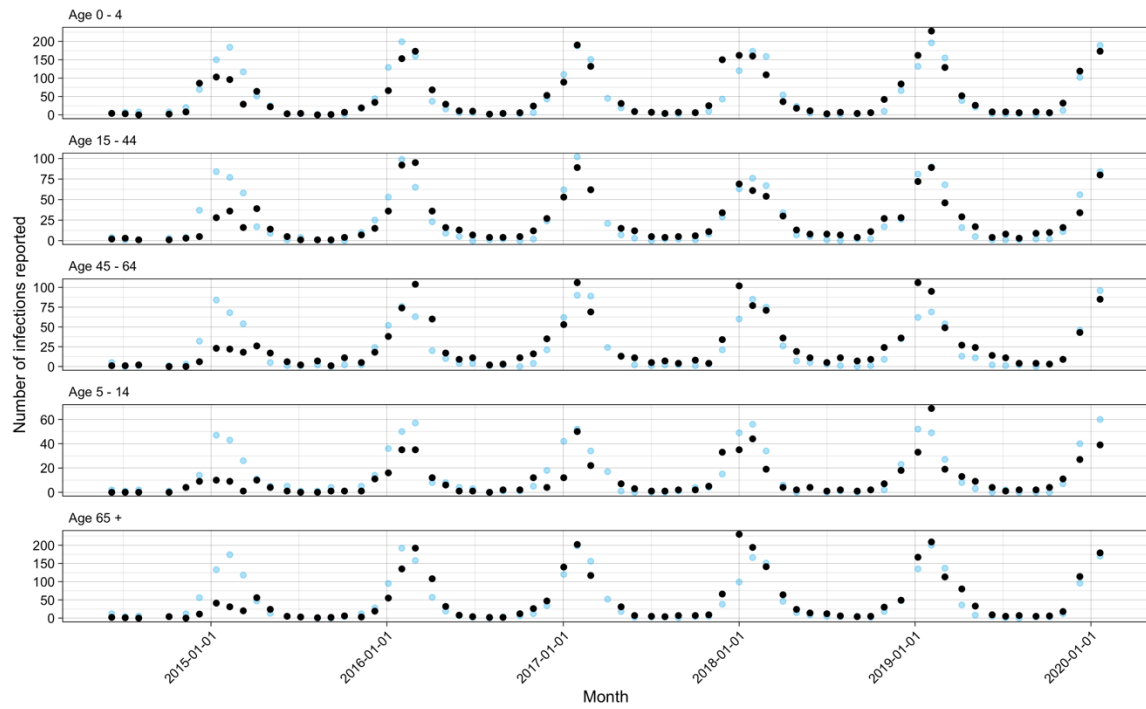
C.11 Comparison with existing estimates

As our estimate of the duration of immunity is longer than other estimates, we compared it to parameters estimated in the 2020 Kissler et al. paper¹. While the states are the same in the two model, there are some key differences including:

- Kissler et al. only model beta-coronaviruses, whereas we model all seasonal coronaviruses
- Kissler et al. model the two coronaviruses separately and estimate the cross-protection between them. We are instead modelling all coronaviruses together, thereby implicitly assuming complete cross-protection.
- The Kissler et al. model is not age structured
- The latency period in the Kissler et al. model is slightly longer (3 days instead of 2 days).

We investigated the impact of using their estimated parameter values in our model. We fixed their estimated values of R_0 (2), waning (45 weeks) and seasonality parameters, as well as changing our model to match their longer latency period. We then fit the reporting rates using Maximum Likelihood Estimation (L-BFGS-B optimisation) to fit the seasonal coronavirus, using the same

likelihood as in the main paper. While the model still produced what looked like a good fit (See Fig S4), the log likelihood values were significantly lower (-2235 vs -1905).



Appendix C Figure S15: Model fit for seasonal HCoV, using the immunity and R_0 parameters from Kissler et al. 2020.

1. Kissler, S. M. Projecting the transmission dynamics of SARS-CoV-2 through the postpandemic period | Science. <https://science.sciencemag.org/content/368/6493/860>.
2. Liu, Z., Chu, R., Gong, L., Su, B. & Wu, J. The assessment of transmission efficiency and latent infection period in asymptomatic carriers of SARS-CoV-2 infection. *Int. J. Infect. Dis. IJID Off. Publ. Int. Soc. Infect. Dis.* **99**, 325–327 (2020).
3. Tyrrell, D. A., Cohen, S. & Schlarb, J. E. Signs and symptoms in common colds. *Epidemiol. Infect.* **111**, 143–156 (1993).
4. Birrell, P. J. *et al.* Forecasting the 2017/2018 seasonal influenza epidemic in England using multiple dynamic transmission models: a case study. *BMC Public Health* **20**, (2020).
5. Davies, N. G. *et al.* Estimated transmissibility and impact of SARS-CoV-2 lineage B.1.1.7 in England. *Science* (2021) doi:10.1126/science.abg3055.
6. Byrne, A. W. *et al.* Inferred duration of infectious period of SARS-CoV-2: rapid scoping review and analysis of available evidence for asymptomatic and symptomatic COVID-19 cases. *BMJ Open* **10**, e039856 (2020).
7. Levin, A. T., Cochran, K. B. & Walsh, S. P. Assessing the Age Specificity of Infection Fatality Rates for COVID-19: Meta-Analysis & Public Policy Implications. *medRxiv* 2020.07.23.20160895-2020.07.23.20160895 (2020) doi:10.1101/2020.07.23.20160895.
8. ONS. Births in England and Wales: 2019.
9. Estimates of the population for the UK, England and Wales, Scotland and Northern Ireland - Office for National Statistics.
<https://www.ons.gov.uk/peoplepopulationandcommunity/populationandmigration/populationestimates/datasets/populationestimatesforukenglandandwalesscotlandandnorthernireland>.
10. Mossong, J. *et al.* Social contacts and mixing patterns relevant to the spread of infectious diseases. *PLoS Med.* **5**, 0381–0391 (2008).
11. Diekmann, O., Heesterbeek, J. A. P. & Roberts, M. G. The construction of next-generation matrices for compartmental epidemic models. *J. R. Soc. Interface* **7**, 873–85 (2010).
12. Vousden, W. D., Farr, W. M. & Mandel, I. Dynamic temperature selection for parallel tempering in Markov chain Monte Carlo simulations. *Mon. Not. R. Astron. Soc.* **455**, 1919–1937 (2016).
13. Vats, D. & Knudson, C. Revisiting the Gelman-Rubin Diagnostic. (2018).
14. Nickbakhsh, S. *et al.* Epidemiology of Seasonal Coronaviruses: Establishing the Context for the Emergence of Coronavirus Disease 2019. *J. Infect. Dis.* **222**, 17–25 (2020).

London School of Hygiene & Tropical Medicine

Keppel Street, London WC1E 7HT

United Kingdom

Switchboard: +44 (0)20 7636 8636

www.lshtm.ac.ukLONDON
SCHOOL of
HYGIENE
& TROPICAL
MEDICINE**Observational / Interventions Research Ethics Committee**Miss Naomi Walker
LSHTM

7 March 2019

Dear Naomi,

Study Title: PhD Project: Modelling the interaction of influenza and RSV**LSHTM Ethics Ref:** 16166

Thank you for responding to the Observational Committee's request for further information on the above research and submitting revised documentation.

The further information has been considered on behalf of the Committee by the Chair.

Confirmation of ethical opinion

On behalf of the Committee, I am pleased to confirm a favourable ethical opinion for the above research on the basis described in the application form, protocol and supporting documentation as revised, subject to the conditions specified below.

Conditions of the favourable opinion

Approval is dependent on local ethical approval having been received, where relevant.

Approved documents

The final list of documents reviewed and approved by the Committee is as follows:

Document Type	File Name	Date	Version
Investigator CV	CV - Naomi R Walker	24/10/2018	1
Consent form	Annex1. Text Verbal Informed Consent-KHGH-HSB-edit-2016Aug	23/11/2018	1
Local Approval	IRBapproval-2ndphase	23/11/2018	1
Protocol / Proposal	Study_Protocol_NRW	23/11/2018	1
Covering Letter	Cover Letter	28/02/2019	1

After ethical review

The Chief Investigator (CI) or delegate is responsible for informing the ethics committee of any subsequent changes to the application. These must be submitted to the Committee for review using an Amendment form. Amendments must not be initiated before receipt of written favourable opinion from the committee.

The CI or delegate is also required to notify the ethics committee of any protocol violations and/or Suspected Unexpected Serious Adverse Reactions (SUSARs) which occur during the project by submitting a Serious Adverse Event form.

An annual report should be submitted to the committee using an Annual Report form on the anniversary of the approval of the study during the lifetime of the study.

At the end of the study, the CI or delegate must notify the committee using an End of Study form.

All aforementioned forms are available on the ethics online applications website and can only be submitted to the committee via the website at: <http://leo.lshtm.ac.uk>Additional information is available at: www.lshtm.ac.uk/ethics

Yours sincerely,

Professor John DH Porter
Chair



NATIONAL INSTITUTE OF HYGIENE AND EPIDEMIOLOGY

1 Yersin Street, Hai Ba Trung District, Hanoi 10,000 Vietnam
Tel: (84-4) 3 9716 356 /3 821 3241 ; Fax: (84-4) 3 821 0853
Email: nihe@hn.vnn.vn; website: <http://www.nihe.org.vn>

January 18, 2011
No: 15 IRB

Research proposal: "Collaborative study on Emerging and Re-emerging infectious diseases in Vietnam: Enhancement of research capacity"

Funding source **Japan**

Principal Investigator of project Ass. Prof. NGUYEN TRAN HIEN, MD, PhD
National Institute of Hygiene and Epidemiology
No 1 Yersin street, Hanoi, Vietnam

The Institutional Review Board of National Institute of Hygiene and Epidemiology has reviewed and approved the extension of Dr. NGUYEN TRAN HIEN's application for the above project, which involves human subjects research.

We consider this to be a minimal risk study. Thus, this project was approved to carry out from the approved date to December 2015.

Prof. Hoang Thuy Long
IRB Chair, National Institute of Hygiene and Epidemiology
Hanoi, Vietnam



Lặng Đức Anh

Appendix F LSHTM Ethics for coronaviruses

London School of Hygiene & Tropical Medicine

Keppel Street, London WC1E 7HT
United Kingdom
Switchboard: +44 (0)20 7636 8636
www.lshtm.ac.uk



Observational / Interventions Research Ethics Committee

Mrs Naomi Waterlow
LSHTM

22 March 2021

Dear Mrs Naomi Waterlow

Study Title: Duration of immunity to seasonal coronaviruses: implications for COVID-19

LSHTM Ethics Ref: 25706

Thank you for your application for the above research project which has now been considered by the Observational Committee via Chair's Action.

Confirmation of ethical opinion

On behalf of the Committee, I am pleased to confirm a favourable ethical opinion for the above research on the basis described in the application form, protocol and supporting documentation, subject to the conditions specified below.

Conditions of the favourable opinion

Approval is dependent on local ethical approval having been received, where relevant.

Approved documents

The final list of documents reviewed and approved is as follows:

Document Type	File Name	Date	Version
Protocol / Proposal	Study_Protocol_Corona_Immunity	15/03/2021	1
Investigator CV	CV - NRW	16/03/2021	1
Other	citiBasic_NRW	16/03/2021	1
Other	citiGCPC_NRW	16/03/2021	1
Other	citiRCR_NRW	16/03/2021	1

After ethical review

The Chief Investigator (CI) or delegate is responsible for informing the ethics committee of any subsequent changes to the application. These must be submitted to the committee for review using an Amendment form. Amendments must not be initiated before receipt of written favourable opinion from the committee.

The CI or delegate is also required to notify the ethics committee of any protocol violations and/or Suspected Unexpected Serious Adverse Reactions (SUSARs) which occur during the project by submitting a Serious Adverse Event form.

An annual report should be submitted to the committee using an Annual Report form on the anniversary of the approval of the study during the lifetime of the study.

At the end of the study, the CI or delegate must notify the committee using the End of Study form.

All aforementioned forms are available on the ethics online applications website and can only be submitted to the committee via the website at: <http://leo.lshtm.ac.uk>.

Further information is available at: www.lshtm.ac.uk/ethics.

Yours sincerely,



Professor Jimmy Whitworth
Chair

ethics@lshtm.ac.uk
<http://www.lshtm.ac.uk/ethics/>